Floodplain wetland-river flow synergy in the White Volta River basin, Ghana

Dissertation

zur

Erlangung des Doktorgrades (Dr. rer. nat)

der

Mathematisch-Naturwissenschaftlichen Fakultät

der

Rheinischen Friedrich-Wilhelms-Universität Bonn

vorgelegt von

Benjamin Kofi Nyarko

aus

Sovie, Ghana

Bonn 2007

1. Referent: Prof. Dr. B. Diekkrüger

2. Referent: Prof. Dr. B. Reichert

Tag der Promotion: 20.09.2007

Erscheinungsjahr: 2007

Diese Dissertation ist auf dem Hochschulschriftenserver der ULB Bonn
http://hss.ulb.uni-bonn.de/diss_online elektronisch publiziert

ABSTRACT

The Upper East Region of Ghana is characterized by an unreliable mono-modal rainfall pattern making rain-fed agriculture a risky business. Therefore, farmers along the White Volta River cultivate on the floodplain to make use of residual moisture. This has prompted the Government of Ghana through the Ministry of Food and Agriculture to encourage dry season floodplain wetland cultivation, using pumped river water as a source of irrigation. The increasing use of floodplains for dry season cultivation has placed pressures on land allocation practices and floodplain wetlands resources. To ensure good management and sustainable water resource use, the role of floodplain-wetlands in regulating stream flow needs to be recognized, understood and taken into account when modeling hydrological processes within the basin. This study examines floodplain wetland-river flow synergy within the White Volta River basin. The methods applied in this study involve generating a floodplain wetland probability map and selection of floodplain wetlands, the use of HYDRUS-1D to model floodplain hydrodynamics, the result served as an input into the MODFLOW model to simulate interaction between floodplain wetland and the White Volta River; and applying isotopic tracers $\delta^{18}O$ and $\delta^{2}H$ to derive a water balance. The mapping process used a combination of geographic information system, remote sensing and statistical techniques. Logistic regression, a statistical technique used within the GIS platform, identified distance, texture, log transformation of ETM- band4 and evapotranspiration as the parameters having the greatest predictive power in wetland mapping, at 95 per cent confidence level. The map generated enabled the selection of Pwalugu and Tindama wetland sites as suitable for detailed hydrological analysis. Applied to the Pwalugu floodplain wetland as a test site, the HYDRUS-1D model indicated that the infiltration contribution to sub-surface storage over 16 months was 444 mm. The period of highest contribution occurred between July and September. In addition, the estimated vertical gradient indicates a low upwelling of sub-surface water in areas close to the river. The results of the isotope analysis of $\delta^{18}O$ and $\delta^{2}H$ showed that the trajectory of the tropical continental and tropical maritime air masses influenced isotopic composition of the rainfall over the Pwalugu and Tindama wetlands. Using the Rayleigh equation, evaporative fractions from Pwalugu wetland and Tindama were estimated to be 53.25% and 16.79%. However, to verify surface and sub-surface water interaction for the Pwalugu wetland, within August and September, the isotope signatures showed a similar ratio and plot around the local meteoric water line indicating some form of interaction. To determine wetland-river flow interaction, HYDRUS-1D bottom flux was used as groundwater recharge, an input into PW-WIN (MODFLOW). The PW-WIN (MODFLOW) simulation showed a systematic variation in hydraulic head of the wetland to changes in rainfall pattern, the observed interaction between floodplain wetlands and the White Volta River was bidirectional in terms of horizontal direction. Sensitivity analysis was performed using the dimensionless and dimension scaled methods, and model outputs were found to be highly sensitive to the parameters such as horizontal hydraulic conductivity, specific storage and specific yield. The study assisted to understand the relationship between recurrent spatial and temporal patterns of water table response within the floodplain and their controlling factors. Additionally, the study showed that a combination of methods such as tracers and hydrological models can be successful used to understand the dynamics of floodplain wetlands in White Volta River basin.

Wechselwirkung zwischen einem Feuchtgebiet und dem Flusssystem im White Volta River basin, Ghana

ZUSAMMENFASSUNG

Ghanas Upper East Region ist durch ein unzuverlässiges monomodales Regenfallmuster gekennzeichnet, das Regenfeldbau zu einem riskanten Unternehmen macht. Darum kultivieren Bauern Felder in den Auengebieten entlang des White Volta Flusses, um von deren Bodenfeuchte zu profitieren. Dies bewog die Ghanaische Regierung, repräsentiert durch das Ministry of Food and Agriculture, den Feldbau in Auengebieten durch gepumptes Flusswasser während der Trockenzeit zu fördern. Die verstärkte Nutzung der Feuchtgebiete in der Trockenzeit hatte Auswirkungen auf Praktiken der Landvergabe sowie anderer Ressourcen dieser Feuchtgebiete. Um ein gutes Management und die nachhaltige Wassernutzung sicherzustellen, bedarf es der Anerkennung und des Verständnisses der Rolle der Feuchtgebiete für die Regulation des Abflusses, um hydrologische Prozesse im Volta Flussbecken modellieren zu können. Diese Studie befasst sich mit der der Synergie von Feuchtgebieten und Abfluss innerhalb des Becken des White Volta. Zu den angewandten Methoden zählen die Erstellung einer Auenwahrscheinlichkeitskarte und die Auswahl von Feuchtgebieten sowie die Nutzung des HYDRUS_1D zur Modellierung der Hydrodynamik des Feuchtgebietes. Das Ergebnis dient als Input für das MODFLOW-Modell zur Simulierung der Interaktion zwischen Feuchtgebiet und dem White Volta Fluss. Die isotopischen Tracer δ18O und δ2H wurden angewandt, um die Wasserbilanz zu ermitteln. Die Kartierung basierte auf einer Kombination von GIS (*geographic information system*), Fernerkundung und statistischen Techniken. Eine logistische Regression, eine im GIS verwendete Technik, identifiziert Distanzen, B4-Beschaffenheit, die logistische Transformation von ETM-band4 und Evapotranspiration als Parameter, die die größte Vorhersagekraft für Feuchtgebietskartierung haben, bei einem Konfidenzintervall von 95%. Die erhaltene Karte ermöglicht die Selektion der Orte Pwalugu und Tindama, deren Feuchtgebiete detailliert untersucht und hydrologisch analysiert wurden. Auf das Pwalugu Feuchtgebiet angewandt, zeigte das HYDRUS-1D-Modell, dass die Infiltration in 16 Monaten zu 444mm unterirdischer Speicherung beitrug. Der höchste Beitrag wurde zwischen Juli und September gemessen. Außerdem zeigt der geschätzte vertikale Gradient einen geringen Auftrieb des Grundwassers in flussnahen Gebieten. Das Ergebnis der Isotopenanalyse mit den Tracern δ18O und δ2H zeigt, dass die Bewegung der tropischen, kontinentalen sowie tropischen maritimen Luftmassen die isotopische Zusammensetzung des Regenfalls über den Feuchtgebieten von Pwalugu und Tindama beeinflussten. Unter Verwendung der Rayleigh- Gleichung wird der evaporative Anteil der Feuchtgebiete von Pwalugu und Tindama auf 53,25% und 16,79% geschätzt. Um die Interaktion von Oberflächen- und Grundwasser in Pwalugu während August und September zu verifizieren, zeigen die isotopischen signatures eine ähnliches ratio und plot um die meteorische Wasserlinie, was auf eine Interaktion hindeutet. Um diese Interaktion zu bestimmen, wurde HYDRUS -1D bottom flux für Grundwasserrecharge, ein Input für PW-WIN (MODFLOW, genutzt). Die PW-WIN (MODFLOW)– Simulation zeigt eine systematische Variation der Piezometerhöhe des Feuchtgebietes aufgrund von Änderungen im Regelfallmuster an. Die beobachtete Interaktion zwischen Feuchtgebiet und White Volta verlief horizontal bidirektional. Eine Sensitivitätsanalyse wurde ausgeführt, in der dimensionslose sowie die durch Dimensionen skalierte Methoden genutzt wurden. Die modellierten Ergebnisse waren sehr sensitiv im Hinblick auf die Parameter horizontale hydraulische Durchlässigkeit, spezifischer Speicher und spezifisches Wasserdargebot. Die Studie trägt zum Verständnis der Beziehung zwischen periodischen, räumlichen und zeitlichen Mustern des Grundwasserstandes in Abhängigkeit zu den Feuchtgebieten und den sie bestimmenden Faktoren bei. Außerdem belegt die Studie, dass eine Kombination von Methoden, wie Tracern und hydrologischen Modelle, erfolgreich eingesetzt werden können, um die Dynamik der Feuchtgebiete des White Volta Becken zu verstehen.

TABLE OF CONTENTS

1 INTRODUCTION

1.1 Background and statement of problem

Wetlands occupy about 6% of the earth surface and vary according to origin, geographical location, hydro-period, chemistry and plant species around the wetlands. Farmers along the White Volta River in the Upper East Region of Ghana practice floodplain cultivation as a form of supplementary irrigation. This region is characterized by a mono-modal rainy season, although uncertain precipitation patterns make rain fed agriculture risky. As rain fed cultivation often fails to provide adequate food security for the region's residents, farmers are exploring alternative methods of cultivation, including the cropping of areas that are often seasonally inundated. The Government of Ghana through the Ministry of Food and Agriculture is actively encouraging floodplain cultivation, which can be practiced in the dry season using pumped river water as a source of irrigation. The increasing use of floodplains for dry season cultivation has placed pressures on land allocation, however; and has decreased the average distance from the margin of cultivated land to the main river from 30.7m to 5.3 m. Tillage close to the river channel as observed during the 2004 and 2005 fieldwork has resulted in high silt delivery levels.

Due to the importance of wetlands they are included as waters and sites for preservation in most countries in the world, and policies have been fashioned out to govern their use. In 1999, the government of Ghana through its agency, Ministry of Lands and Forestry outlined strategies for managing wetlands (MLF 1999). The USA, included wetlands as water bodies in the Federal regulations (40 CFR 122.2, 40 CFR 230.3, and 40 CFR 232.2) implementing the Clean Water Act [Section 502(7)] (U.S. EPA 1996, 1998). Wetlands have important functions: they serve as infiltration basins, route floods, and store water which they release gradually to adjacent streams, thereby influencing runoff in a catchment.

Therefore runoff, a component of the hydrological cycle, is considered an important process in the study of hydrology. Knowledge about runoff components (surface and channel flow) under changing climatic and vegetation condition in the White Volta River catchments is limited. Studies commissioned by the Center for Development Research, Bonn (GLOWA-VOLTA Project 2000-2009) seeks to

understand the spatial and temporal distribution of runoff components as a contribution to understanding the behavior of the catchment. Information about catchment behavior (response to rainfall input) is fundamental to the understanding of the overall hydrological processes in the Volta basin. For instance, runoff contributing to stream flow from all parts of the catchment is an important factor in meeting its water volume standards in the main Volta River and Akosombo dam. Hence changes in the hydrological regime in the basin as a result of changes in climate and vegetation have an influence on infiltration and base flow contributing to the sustenance of flow within the Volta River.

Runoff being water flowing over the land surface within the White Volta River catchment reaches the main stream through different pathways (Carey and Woo 2000), which affect both timing and magnitude of its response to rainfall. But an important factor within the catchment worth considering is its initial storage, which is influenced by floodplain wetland status, through heterogeneity in time and space influences water movement into streams/rivers. In addition, antecedent wetland conditions as well as volume and intensity of rainfall governs the processes by which streams/rivers respond to rainfall inputs (Beven 2001). However, changes in soil hydraulic parameters of wetlands and adjacent land also contributes to changes in preferred pathways of storm runoff, which in turn have ramifications on stream flow. In this instance, researchers are challenged to model adequately and understand the contribution of wetlands to stream flow processes in the hydrological meso-macro scale in order to meet the demands of stream/river flow (Bonel and Balek 1993).

Brian (1962), Ayibotele (1999), Andreini and Van de Giesen (2001) and many other researchers have noted that the White Volta River catchment is experiencing climatic, hydrologic and vegetation changes through its continual usage. Therefore, in the face of environmental changes, coupled with uncertain impacts, an evolving adaptive strategy seems a necessary condition for sustainable water resource management. In order, to ensure good management and sustainable level of water resource usage, it is essential that the role of floodplain wetlands in stream flow are recognized, understood and taken into account when modeling hydrological processes within the White Volta basin. In addition, there is a need to examine how changes in floodplain-wetland characteristics have ramifications on surface water flow.

1.2 Objectives

The main objective of the study is to examine wetland-river flow synergy within the White Volta River catchment. Specifically the study will:

i. Map floodplain wetlands in the catchment area
ii. Assess the hydro-geomorphology of floodplain wetland
iii. Examine floodplain wetland hydrodynamic using environmental isotopes
iv. Determine the form of interaction between floodplain wetlands and stream flow

1.3 Rationale

The Volta lake behind Akosombo dam experiences periodic water shortage and therefore the need to conserve its environment has been of concern to the government, hydrologists and planners alike. Yet no detailed database has been complied and analyzed to enable a thorough understanding of the factors contributing to such periodic water shortage. This study is thus aimed at providing further information to help close the existing gap.

Farmers along the White Volta River in the Upper East Region of Ghana practice floodplain cultivation as a form of supplementary irrigation. The increasing use of floodplains for dry season cultivation has placed pressures on land allocation, however; and has decreased the average distance from the margin of cultivated land to the main river from 5.3 to 30.7m (Nyarko et al. 2006). It is hoped that through the use of hydrological models, geographic information system and remote sensing tools, areas that contribute effectively to the sustenance of floodplain and the river will be identified, mapped and protected by the appropriate agencies.

The results of this study will be communicated to such institutions as the Hydro Division of A.E.S.C., Water Resources Institute of CSIR, Volta River Authority and NGO's to sensitize the communities to the need for improved basin management. The results of the study should also provide the basis for policy formulation and strategy for development, particularly in the preparation of educational material that will address the public attitude towards preventing the occurrence of catchment degradation. The study has the potential of encouraging further research in hydrology, geomorphology, and the environment of related catchment areas.

1.4 Expected output

The data analysis will be targeted towards the specific management needs of the Volta River Basin. The study will:

- Map the probable floodplain wetland areas along the White Volta River.
- Provide a detailed description of the hydrological characteristic of the wetlands in the catchment area.
- Characterize the flow paths from the wetlands to discharge into the stream.
- Develop a water budget for the floodplain wetland using isotopes technique.

1.5 Chapter organization

This thesis is divided into 9 chapters. Chapter 1 captures the introduction, statement of the problem, also spelling out objective of the research and its justification. Chapter 2 describes the study area. Chapter 3 reviews the recent developments in floodplain wetland river flow interaction research. Chapter 4 discusses the materials and methods used to conduct the research and models used are explained in this section. Chapter 5 presents results of floodplain wetland mapping. Chapter 6, here results relating to the hydrodynamics of Pwalugu and Tindama wetlands are discussed by looking at soil colour and sub-surface water interaction, spatial and temporal variation of hydraulic conductivity, unsaturated and saturated dynamics using the HYDRUS-1D model, last sub surface ground water level monitoring. Chapter 7 discusses the use of isotope to model floodplain wetland dynamics. Chapter 8 dwells on the results from the MODFLOW for establishing an interaction between wetland and river flow, while Chapter 9 is the summary and conclusion of the major research findings.

2 STUDY AREA

2.1 Location

The two main floodplain wetland sites at Pwalugu and Tindama, located along the White Volta River, were selected for the detailed study (Figure 2.1, Table 2.1). The Pwalugu site is located within the UTM coordinates 735861N and 738621N, and 1100905.666W and 1103725.666W; it covers an area of 7.78km^2. The Tindama research site, covering an area of 7.88km^2, is located within the UTM coordinates 717811.410N and 722191.410N, and 1164658.915W and 1166458.915W. Pwalugu site has a longitudinal stretch of 2.82km, Tindama a stretch of 4.38km.

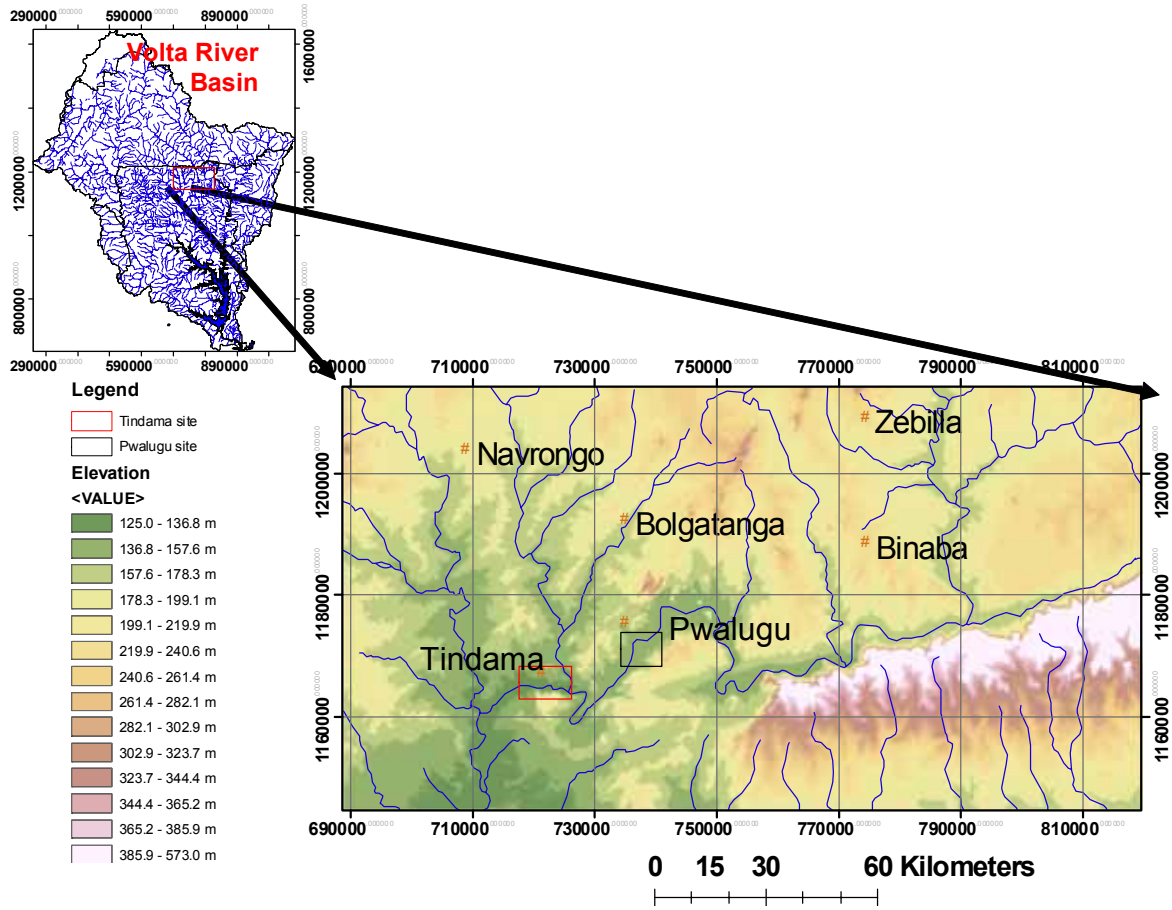

Figure 2.1 Map of the study areas in the White Volta River catchment,Ghana

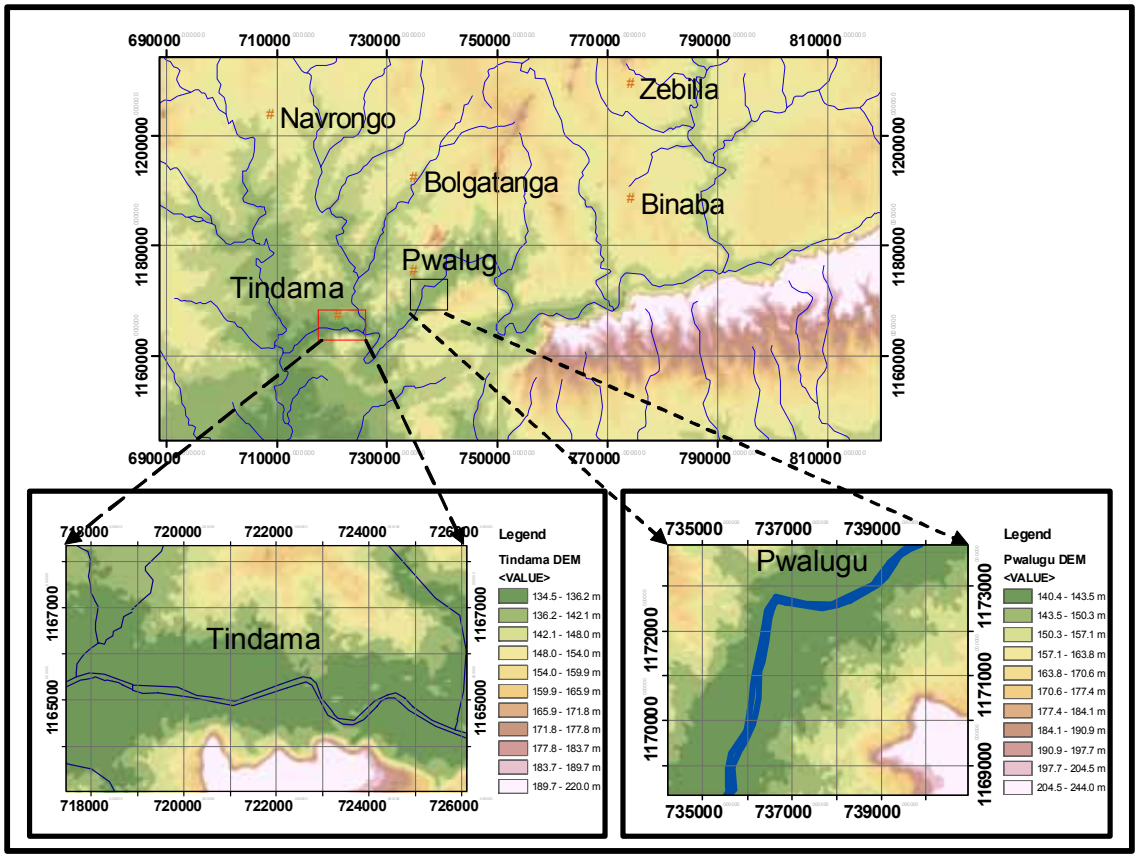

Figure 2.1 continued

Table 2.1 Characteristics of the study sites in Pwalugu and Tindama

	Pwalugu	**Tindama**
Northern (UTM)	735861N	717811.410N
Eastern (UTM)	1100905.666W	1164658.915W
Climate	Tropical savanna	Tropical savanna
Total annual Rainfall	1000 mm	1000 mm
Mean Temp	25^{o}C	25 ^{o}C
Geology	Voltaian sandstone	Voltaian sandstone, Phylitic, weathered schist
Soil	Breyanese and Kuapela Series	Kuapela Series
Vegetation	Savanna	Savanna
Human activities	Farming, Fishing, trading, Quarry, Manufacturing	Farming, Fishing

The description of the Pwalugu and Tindama floodplain wetland sites are outlined in Table 2.1 These sites were selected because they exhibit different geological conditions and different position along the main White Volta River. The Pwalugu wetland has a general slope of 3^{o} and lies at the foot for the Gambaga ridge, while the

Tindama wetland has virtually flat topography of a slope of 1°. They are therefore representative of the basin so that, insight could be generalized.

2.2 Climate

The climate of the study site (Pwalugu and Tindama) can be characterized as semi-arid type that is influenced by three air masses Eastern continental (E), Tropical maritime (mT) and Tropical continental (cT) air masses. Climate of the study site is defined by an annual estimated mean rainfall of 1100mm (Figure 2.2). Rainfall in this region begins in May with highest recording of about 250mm within the month of August and September. The interaction of these air masses depends on the oscillation of the inter-tropical convergence zone (ITCZ). The sole influence of mT or cT determines the characteristics of the weather at that particular point in time. The cT winds are dusty and dry mostly experienced in the dry seasons from November to April, temperature within these periods ranges from 20°C to 34°C. The mT is highly moisture laden, is felt mostly in the wet season between March and October, exhibiting a high rate of humidity. Humidity is variable and ranges from 60% to 90% at 0600hrs and 77% to 78% at 1500hrs. In a semi-arid climate the annual potential evaporation is estimated to be exceeds precipitation in 6-9 months.

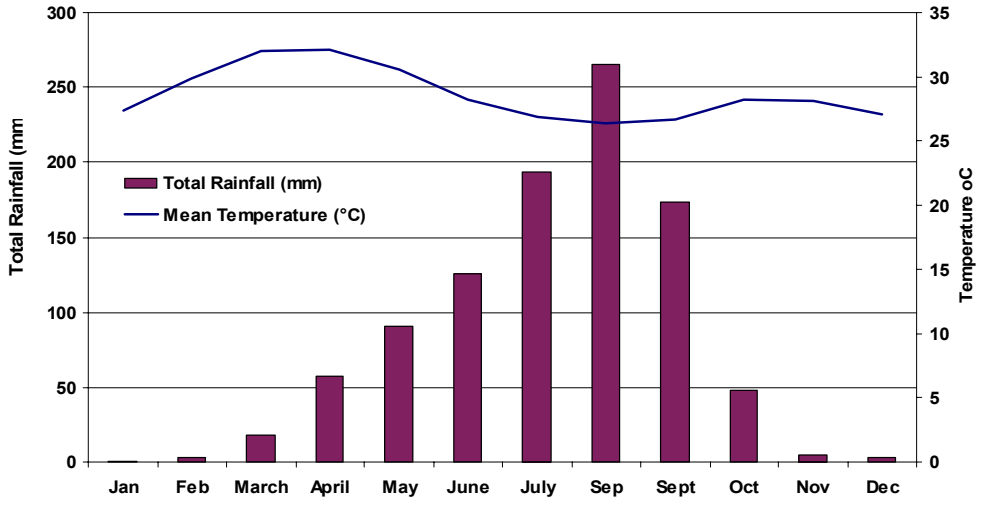

Figure 2.2 Monthly mean temperature and rainfall measurement at Navrongo climatic synoptic station (1961-1990). Source: Ghana Meteorological Agency

2.3 Rainfall trend and general climatic circulation over the Volta River basin

The semi-arid climatic zone presents a striking contrast relative to the surrounding areas due to low annual rainfall. This region of reduced rainfall often is denoted as Togo Gap, meaning the dry sequence along the coast of Ghana and Togo. The part of the dry zone extending inland in Benin, Ghana and Togo is called Dahomey Gap or Ghana Dry Zone. The causes for these dry zones are summarized and discussed in detail in Vollmert et al. (2003) and are a good example of the complexity of the climate system within the region of interest. For the coastal dry zone, the dominating influence is found in its divergence anomaly which induces subsidence. This anomaly is induced by differing averting of the coastal parallel monsoonal winds due to friction. Furthermore an up-welling of cold water along the coast intensifies the effect in stabilizing the lower troposphere. This upwelling is, on one hand due to the Ekman drift, orthogonal to the coastal parallel winds. On the other hand it is reinforced by coastal Kelvin waves that transport the signal of an oceanic flow divergence with origin in the western Atlantic to the Gulf of Guinea. For dry spells reaching further inland in Benin, three major influences are found. First, a velocity divergence can be found near the monsoon low of Lake Tschad. Moreover a lee effect is apparent in the northern region east of the Togo Mountains. Forced ascent of air masses on the western side of the mountains leads to high rainfall amounts there, leaving air masses with reduced amounts of perceptible water for the eastern side of the mountain range. A third reason lies in squall lines that originate from mountainous regions, with a maximum of generation in the Nigerian plateaus of Jos and Bauchi, that reach the Dahomey gap in a state of dissolution without a reinforcement, due to the flatness of the terrain.

2.4 Large scale dynamics

Within the semi-arid climate the general climate characteristics and its annual cycle of meteorological variables, and their spatial distribution are determined primarily by large scale atmospheric dynamics. The large scale atmospheric dynamics (global circulation system) induced a consequence of the latitudinal dependence of solar insulation and the subsequent permanent thermal deficit in Polar Regions. Within this global circulation, the Hadley circulation, which is the mean meridional circulation in lower latitudes and the Walker circulation which is the mean zonal circulation along the meteorological

equator are the dominating factors determining West African dynamics and its variability. The Hadley cell is a thermally driven, direct circulation cell with a rising of warm, light air at the meteorological equator, and rapidly descending colder, heavier air in the subtropics, associated with a production of kinetic energy.

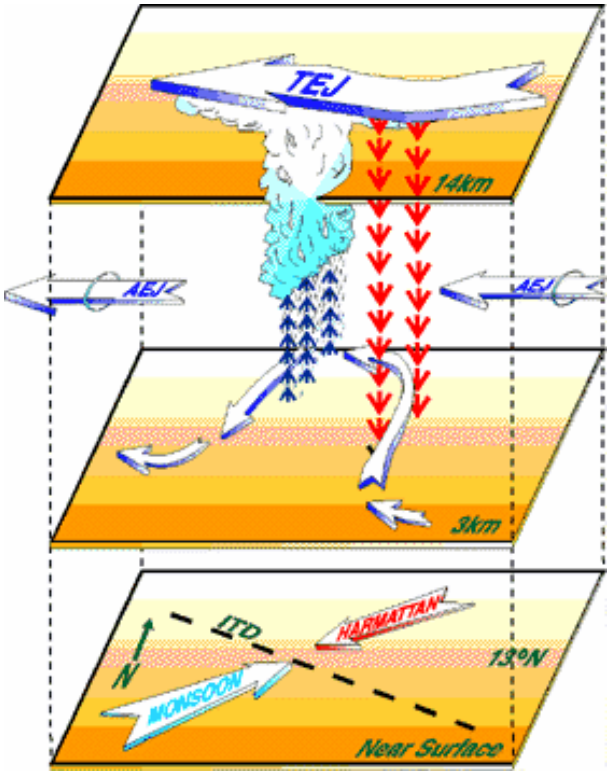

Figure 2.3 Schematic U-shaped AWD is shown at the middle of three levels in the atmosphere. Arrows indicate winds at different altitudes. TEJ = Tropical Easterly Jet; AEJ = African Easterly Jet;AWD= Africa wave disturbance; ITD = Intertropical Discontinuity, where monsoon winds from the ocean meet dry Saharan harmattan winds (Source: http://www.giss.nasa.gov/research/briefs/druyan_01)

Navrongo (Figure 2.4) is positioned at a point within the landscape of Ghana were its climate is influenced by Hadley circulation which in different weather zones (A-D) throughout the course of the year. These weather zone designated A-D associated with different weather phenomena, these are Harmathan in zone A, thunderstorms in zone B, squall line in zone C and monsoonal rains in zone D. As indicated in (Figure 2.4) for a period of four months from November to March, Navrongo is under the influence of zone A weather. During this period the ITCZ is in the southern hemisphere, hence the northeastern trade winds dominate. The trade winds influence is as a result of

pressure differences induced by temperature. From March to May zone B weather generated due to intense heating triggering convection of air mass in an unstable atmosphere resulting in the formation of convectional rainfall, in this situation there is localized thunder storm. The influence of Zone D is felt when the movement of ITCZ from the southern towards the north. This movement causes moisture laden air mass moving inland to deposit some it moisture in the form as rain on it way northwards. Rainfall from this zone may last for few minutes to several days and is due to convergence of air masses. Zone C is generated as a result of squall lines and occurs for about four months from May to early August, then August to mid October.

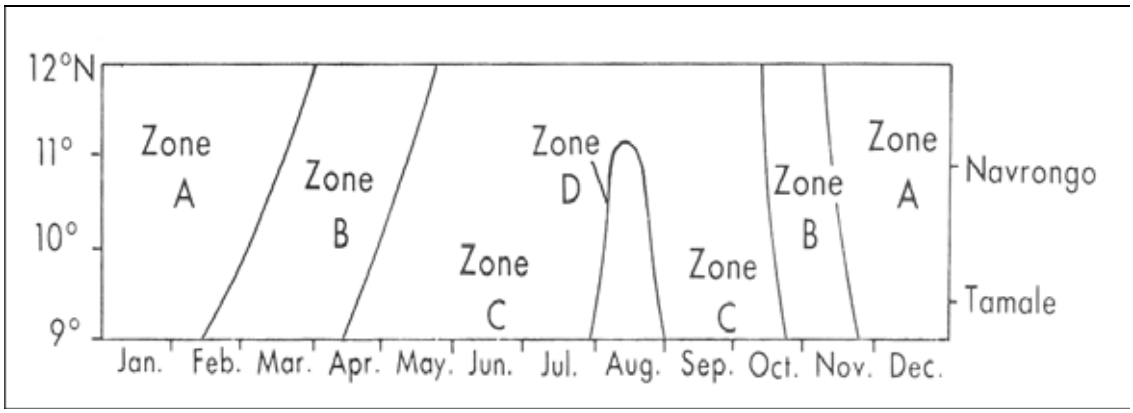

Figure 2.4 Navrongo's membership to different weather zones in the course of a year. Zone A: little clouds, low rainfall and dry air; Harmattan. Zone B: low rainfall but humid air; Thunderstorms. Zone C: rainfall in heavy showers, humid air; Squall lines. Zone D: cloudy/overcast, frequent, persistent rainfalls; Monsoon (adpoted from: Weischet and Endlicher 2000, p. 263)

Along the meteorological equator referred to as the Inter Tropical Discontinuity (ITD), Hayward and Oguntoyinbo (1987) is the point where two air masses converge. In the lower troposphere air masses from higher latitudes flow southwards. The discontinuity that is separating the subsident air masses of the Hadley circulation from this low level, southward moving cooler air masses is the trade inversion. Only within the range of the ITD, the trade inversion vanishes due to the intense lifting of air masses. The upbranch of the Hadley circulation is adjacent to the northern edge of the monsoon circulation (Vizy and Cook 2002) that controls moisture transport to the continent. The north-eastern, lower tropospheric trade winds floating from the subtropics equatorwards form the lower branch of the Hadley circulation (Peixoto and Oort 1992). In the subtropics, above the downwards directed branch of the

Hadley cell, at around 200 hPa, the Subtropical Jet stream (STJ), which spans around the entire globe. Though the STJ affects large scale convection in the lower troposphere, for West Africa it plays a role of minor importance.

Most flow characteristics in West Africa are connected with the ITD. The ITD separates humid maritime monsoon air masses from dry, continental air masses from the Sahara. Within an annual cycle the ITD moves northwards, up to 30°N in summer and southwards in winter as far down as to the (geographical) equator, triggered by the position of the sun. As a consequence of the northward movement of the ITD the cross-equatorial moist cool monsoonal air masses from the Gulf of Guinea penetrate deep into the continent during the rainy season. In the dry season the dominating flow is the Harmattan, originating from the Sahara desert.

In addition the Africa Easterly Jet (AEJ) that is found in 600-700 hPa, and the Tropical Easterly Jet (TEJ) in 200 hPa are related to the ITD. The formation of both of these jet streams depends on barotropic as well as baroclinic instabilities in regions of high temperature and moisture gradients along the discontinuity. Cook (1999) stated that the horizontal soil moisture gradient is the major player in the formation of the AEJ. Due to the existence of these easterly jet streams over West Africa the circulation system is not explainable solely through the idealized Hadley circulation, but zonal contributions to the flow are also important. Strength and location of both, the AEJ as well as the TEJ influence the climatic conditions of the region. Instabilities of the AEJ are responsible for the formation of African Wave Disturbances (AWD), or African Easterly Waves (AEW). Most important for the generation of the kinetic energy of these waves is the horizontal shearing within the AEJ. The waves in turn trigger the formation of squall lines and mesoscale convective complexes. The greatest share of precipitation in Navrongo is associated with either one of these convective systems, and so AEWs play a key role modulating convection and rainfall over the Volta basin.

2.5 Runoff

The production of runoff within the catchment as part of the entire hydrological cycle is being influenced by effective rainfall and losses. The loss comprises of infiltration, soil moisture and depression storage, additionally losses occur through percolation and evaporation. As observed by Opoko-Ankomah (1986), rainfall within the Volta River

catchment generates about 39.8 x $10^9 m^3$/day of runoff that contributes to stream flow. Ayibotele (1999) estimated an annual mean runoff yield on the main Volta River of 24.79 x 10^6 m^3/day, with the lower Volta having a runoff yield of 12.10 x $10^6 m^3$/day.

Runoff may reach the main White Volta River through channel transport and overland flow, but not all areas within the catchment produce runoff at the onset of the rains. The flow mechanisms indentified to occur in the basin include infiltration-excess, overland flow, saturation overland flow and subsurface storm flow (Ayibotele 1999). An additional mechanism is return flow, resulting from subsurface storm flow constrained to flow out of the soil as ex-filtration contributing to overland flow.

2.6 Hydro-geological units

The catchment area is underlain by the Voltaian system, Birimian and Granitiods (Figure 2.5). Voltaian system consists of quartzite, shale, sandstone, limestone, conglomerate and arkose. Kesse (1985) noted that the Voltaian system has a total thickness of between 3000 and 4000 meters, as determined by Shell Oil Company during an oil exploration exercise. The average dip of the Voltarian rocks is 5^o, and the systems are gently folded. The Birimian system consists of metamorphosed lava, pyroclastic rock, schist, tuff and greywacke. These rocks have a dip of about 30^o - 90^o along a NE-SW axis. Faulting in this system tends to follow the folds. Joints in the rocks have different orientation but are mostly parallel to the folds. The Granitiods are mostly of the Bongo and Cape Coast series. The Bongo Granitiods consist of prophyritic hornblende, microdine granite and the Cape Coast series has potash rich muscovite-biotite granite. Consequently, rocks within the study area have different thermal capacities, giving an indication that heat can be stored in these rocks which eventually affects the rate of soil evaporation and soil moisture content when highly exposed.

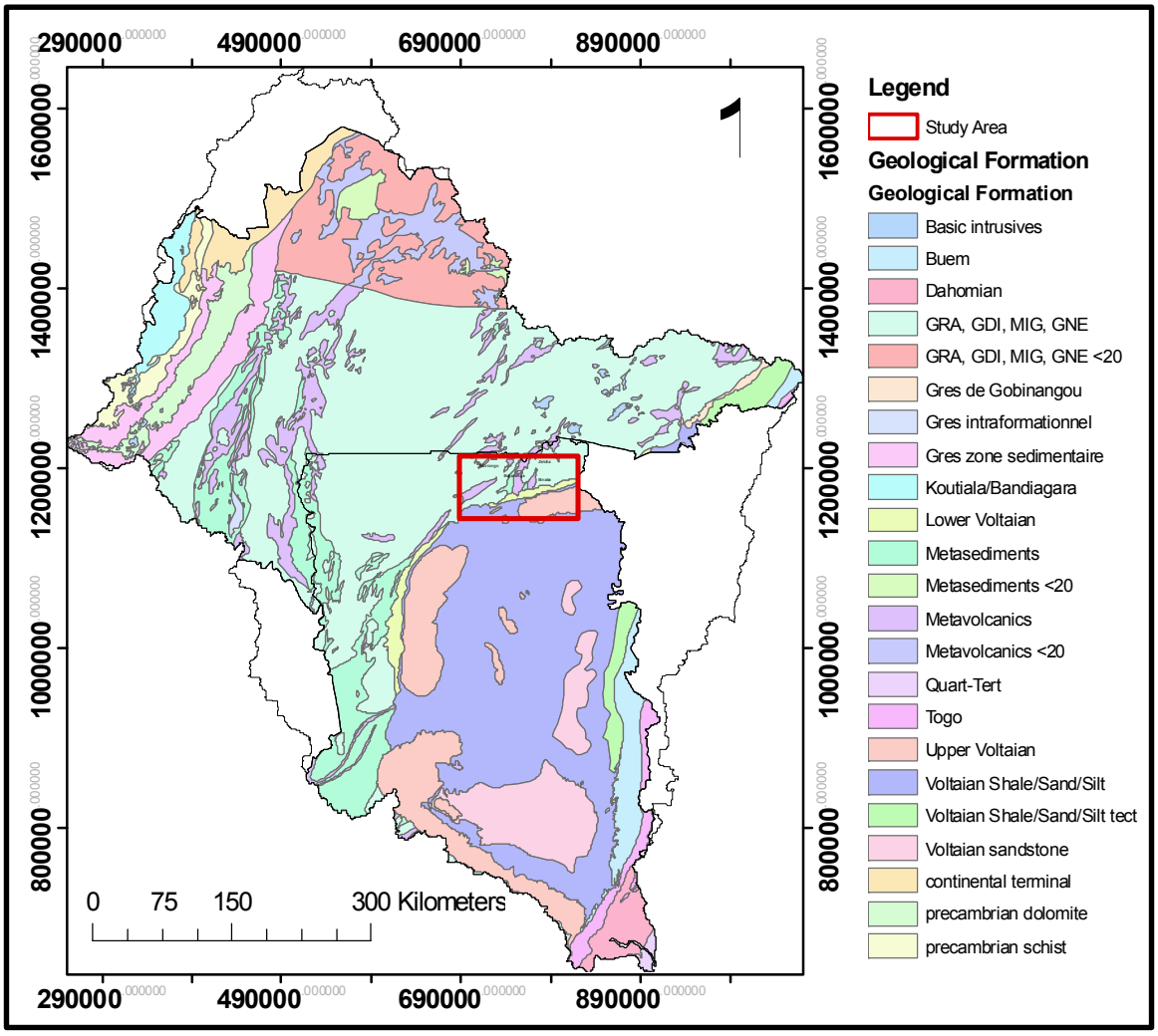

Figure 2.5 Hydrogeology of the Volta River basin

The Birimian system rocks are strongly jointed and foliated, where they come out on to the surface, sufficient water percolate. Boreholes dug to an average depth of 35 m gave a yield of 450 to 23,625 liters per hour in the Upper East and Northern Region. The Voltaian systems are well consolidated and are not inherently permeable except in a few areas. A borehole at a depth of 100 m in the Northern Region and Kete Krachi has an average yield ranging from 800 to 16,380 liters per hour.

2.7 Soil

Soils found within the Volta River catchment are grouped as those derived from granites, sandstones, alluvial materials, greenstone, andesite, schist and amphibolities. Specifically the soils are Eutric Fluvisol, Gleyic Lixisols, Eutric Gleysols and Lithic Leptosols (Figure 2.6). These soils exhibit different hydraulic properties in terms of

infiltration, transmission and water holding capacity. Bonsu and Laryea (1989) attempted to provide a single hydraulic conductivity value for alfisol for the catchment area but it varied with the texture of the soil. In alfisol, the clay and sand content shows hydraulic conductivity at varied gravel content. For instance the total sample of clay in alfisol presents a hydraulic conductivity of 7.2 x 10^{-6} ms^{-1} as compared to 6.4 x 10^{-6} ms^{-1} in sand.

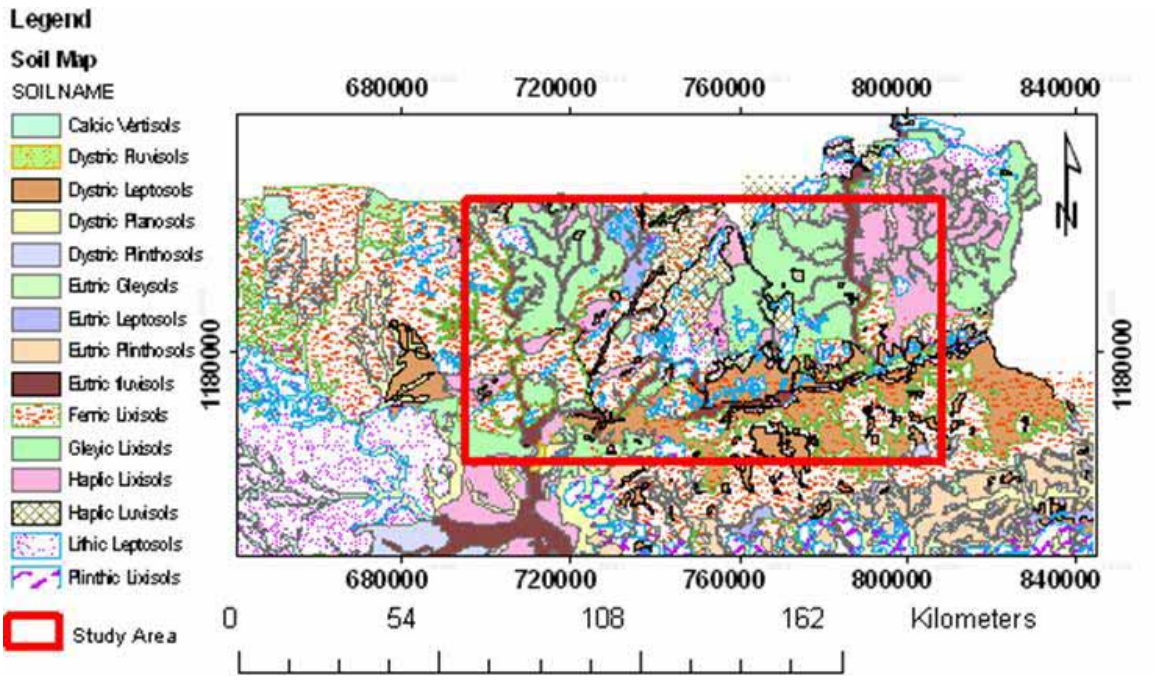

Figure 2.6 Soils Map of Upper East Region of Ghana

2.8 Vegetation

Ghana has two main vegetation patterns, tropical forest occupies the southern portion, and savanna the northern and some parts of southeastern Ghana. Taxonomically the two are very distinct and very few plant species occur naturally in both ecosystem. A few tree species which can be found in both vegetation zones, are *Afzelia africana* and *Diospyros mespilliformis*. *Leptaspis cochleata* and *Olyra latifolia* are some of the grasses found in the high forest but not in the savanna. The vegetation of the savanna region in Ghana is discussed in detailed in the work of Bagamsah (2005). The Pwalugu and Tindama floodplain wetlands have predominantly elephant grass (*Pennisetum sp.*)

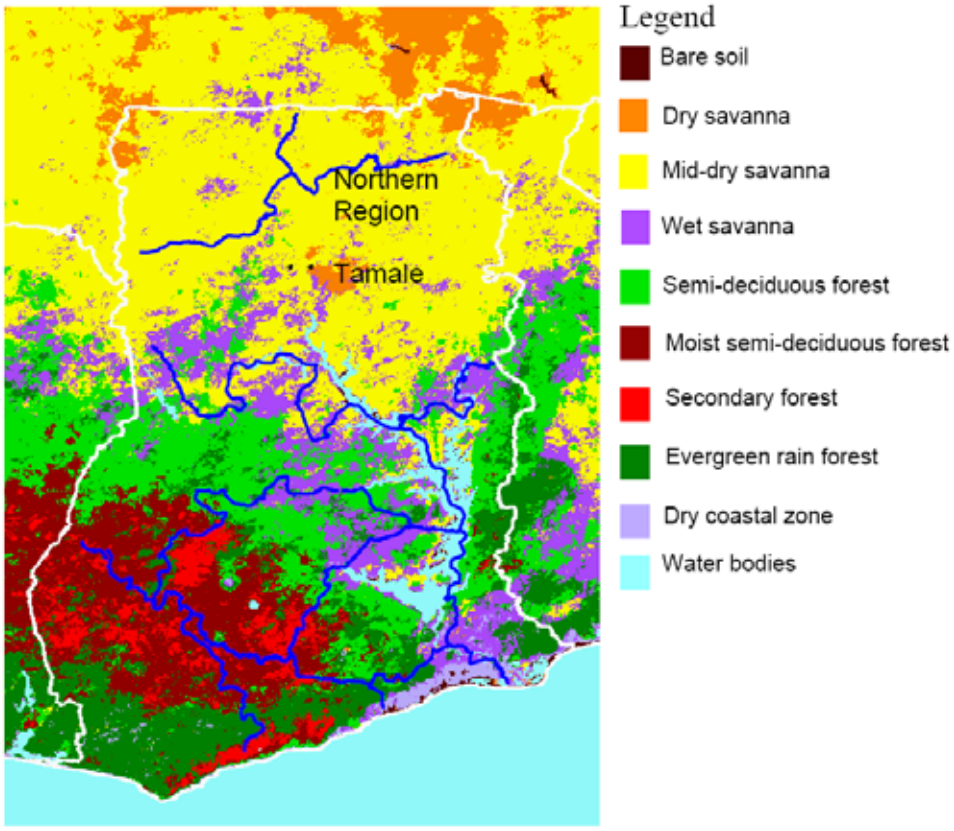

Figure 2.7 Vegetation map of Ghana (Source: Menz and Bethke 2000)

Vegetation in the Pwalugu and Tindama study site is characterized by interior wooded savanna (mid-dry savanna and wet savanna) and Guinea savanna (dry savanna) (Figure 2.7). The interior wooded savanna vegetation of this area can be classified into mid-dry savanna and wet savanna woodland. The mid-dry woodland savanna has two main structures based on the growth forms. In one aspect, vegetation cover is very low, woody plants contribute about 32 % coverage with a height between 2-4 m. The herb stratum reaches up to 1.5 m in height and contributes about 8% coverage and interspersed by bare soil surfaces and scattered trees. This vegetation type occurs in most parts of Northern Ghana. The wet savanna woodland cover varies between 3 – 65%; woody plant cover is about 64% and up to 6 m in height. The herb stratum is sparse and about 12% and up to 1.5 m in height. Wood exploitation in the wet savanna is not as intense as in the mid-dry savanna woodland but is always found in association with the mid-dry savanna woodland. Wet savanna woodland has a vegetation cover of this woody plant cover of about 80% and up to 7 m and above. The herb stratum is about 12% and 1.5 m in height. This vegetation type is mostly found in restricted

reserved lands, especially forest reserves and sacred groves. The dry savanna has different vegetation structure coverage range from 8-76%. The woody plant cover is very sparse and about 12% with a height up to 7 m. The herb stratum (dominated by grass) is dense with coverage of about 65% and up to 2.5 m in height. Trees such as baobab, dawadawa, acacias, sheanuts, and ebony have adapted to this environment. Grass growth can reach a height of 3 meters or more. Trees in this zone shed their leaves mostly within dry seasons and bloom in the rainy season.

2.9 Vegetation dynamics

The vegetation of the study area has changed over the years as a result of human activities, giving it a heterogeneous cover characteristic. This can be attributed to annual burning, cropping and grazing. During cultivation, trees and shrubs are cut down. The prolonged sequences of farming periods with shorter bush fallow have led to a considerable decrease in trees. Those that remain are largely confined to trees considered to be useful or restricted to sacred groves and wildlife reserves. Livestock density is high leading to overgrazing in some areas and the reduction of vegetation cover a factor leading to soil erosion. Bush fires in the dry season leave trees and shrubs leafless with charcoal-blackened barks. Fire severely damages many of the woody plants; some fire resistant species, however; survive. Cutting of wood for fuel is a common practice and has led not only to changes in species composition but also to changes in vegetation structure and deterioration of the vegetation.

3 LITERATURE REVIEW

3.1 Introduction

Studies of wetlands in Africa with respect to hydrology, status of appropriate databases and analytical techniques are yet to be consolidated. This is frequently hampered by the lack of reliable hydrological records (Bonell and Balek 1993), and to date there have been little or no attempts to collate and integrate findings of those few existing studies in a comprehensive manner. However, efforts are being made by the Center for Africa wetlands located at the University of Ghana to collate studies on African wetlands as a first step in creating appropriate databases. These studies can be put into three main categories: 1) detailed investigations of individual wetlands, 2) regional hydrological studies concerned with the relationships between wetland extent and river flow regimes, and 3) monitoring and modeling of internal wetland hydrology for developmental purposes. An understanding of the dynamics of floodplain wetland hydrology in Africa is a key step toward their management.

3.2 Studies on African wetlands

Different countries in Africa have different definitions for wetland. In the Water Act of South Africa, a wetland is defined as "a land which is transitional between terrestrial and aquatic systems, where the water table is usually at the surface or the land is periodically covered with shallow water, and which land in normal circumstances supports or would support vegetation typically adapted to life in saturated soil" (South Africa National Water Act 36 of 1998). In the report of FAO (1999), the Okavango Delta, the Sudd in the Upper Nile, Lake Victoria basin and Lake Chad basin, and the floodplains and deltas of the Congo, Niger and Zambezi rivers are some of the largest wetlands in Africa. Most of these wetlands found in Africa are concentrated within latitudes 15ºN and 20ºS (Hails 1996). Outside these latitudes, significant wetlands are linked to inland oasis, wadis and chotts in North-West Africa, the Oualidia and Sidi Moussa lagoons in Morocco, the Limpopo river floodplain in South Africa, the Banc d'Arguin of Mauritania, and the St. Lucia wetlands in South Africa.

In studying the hydrological aspects of Africa wetlands, Von der Heyden and New (2003) examined the role dambo plays in the hydrology of the river network in

north-western Zambia. In their studies, they used hydro-chemical data to explore hydrological processes and discussed the role wetlands in the catchment play in the catchment evapotranspiration budget. In attempt to examine the potential use and method of conserving Africa wetland, FAO and world conservation monitoring center, have generated approximation of wetlands in located in Africa (Figure 3.1). The map shows Ramsar sites, and as a proxy variable, location of dams, to indicate the potential of changed hydrological regimes. (FAO 1999)

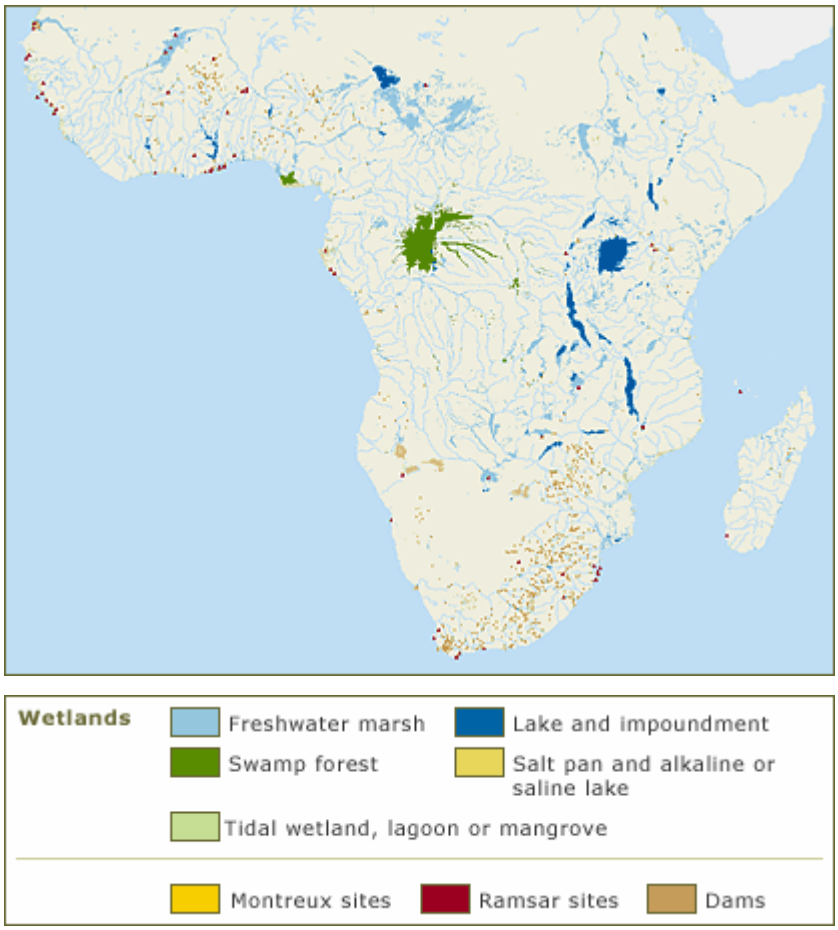

Figure 3.1 Map showing wetlands, dams, and Ramsar sites in Africa (FAO 1999)

3.3 Definition and importance of wetland

Wetlands are lands where saturation with water is the dominant factor determining the nature of soil development and the types of plant and animal communities living in the soil and on its surface (Cowardin et al. 1979). Wetland is also a general term used to describe areas that are neither fully terrestrial nor fully aquatic. These areas range in character from the majestic cypress swamps of southern USA to shallow, unimpressive

depressions that hold water at the most only a few weeks of the year (US EPA 1998). A wetland can be described as an area that has permanent water or is synonymous to swamp, and two main distinct types of wetlands can be distinguished, namely, coastal and inland wetlands (Buckle 1978). Coastal wetlands are primarily associated with the coastal environment, while the inland wetlands are either associated with a river system such as floodplain or isolated from the main drainage system. Wetlands can take different forms and shapes; they can be longitudinal, circular or amorphous.

As natural systems it is extremely difficult to ascribe monetary value to the functions of wetlands. More often than not, estimates of land value are more a reflection of the assessor's values than any intrinsic quality of the land. Wetlands have been given the lowest estimate in terms of value, because land is assessed based on the potential benefits it could provide to the purchaser. In most cases, wetlands are seen as land unfit for both farming and building. Their appraised value would probably be very nearly nothing. However, in the 1970's, the National Wildlife Federation of the USA defined a value per acre of wetland between $50,000 and $80,000 (Sullivan 1976). Estimates such as this attempt to look beyond benefits reaped by the purchaser and take into account the often hidden "environmental services" such wetlands are likely to provide to the larger community. These include flood prevention, sediment accumulation, purification of groundwater and surface water as well as the production of commercially and recreationally important species of fish and waterfowl (Sullivan 1976; Cowardin et al. 1979; Adams 1993; Brinson 1993; Thompson and Gerts 2000).

3.4 Delineation and indicators of floodplain wetland

The geomorphic structure of a floodplain wetland is a template within which hydrologic function evolves and on which biodiversity depends. The morphology of floodplain wetlands determines the patterns of surface water flow, which in turn influences its seasonal sustenance (Poole et al. 2002).

The USA federal system for defining and delineating wetlands is based on specific hydrology, soils and vegetation criteria (Brinson 1993). Such a system of delineation is difficult to apply, because wetlands have high seasonal hydrology, indistinct hydric soil indicators, small ephemeral wet-season plants, and ambiguity about subspecies and wetland status of dominant shrubs (Clausniter and Huddleston

2002). Therefore, wetland hydrology in any setting requires periodic or permanent inundation of the soil surface or saturation at a shallow depth below the surface, which must occur within the root zone of the prevalent vegetation. In other words, inundation and saturation must be continuous for at least the greater part of the growing season with a high probability of occurrence in any year (Dewey et al. 2006; Atkinson 1993; Brinson 1993). The presence of hydric soil (soil formed under conditions of saturation) and hydrophetic vegetation throughout the duration of inundation and survival under anaerobic condition serve as indications of the presence of wetland (Brinson 1993). Using hydrophetic vegetation presence as a wetland indicator, it was noted that dry season soil observation (as within the White Volta Basin), would not reveal the hydric status of the soils, and vegetation presence would always be nil (Fletcher, unpublished).

Clausniter and Huddleston (2002) used hydric soils and vegetation indicators to characterize and determine if the Oregon Vernel pool-USA meet the standard for wetland classification, by describing soil samples, their morphological characteristics and by monitoring soil saturation with piezometers at varied depths. The interpretation of hydrologic criteria was ambiguous, because wells sited in clayey soil might provide misleading measurements of saturation, for the reason that water may flow through an unsaturated macro-pores matrix. The classification of soil by Fletcher (unpublished) provides a powerful tool for assessing the soil-water state throughout the year, and is useful for delineating floodplain wetlands. using soil morphology to delineate floodplain wetlands is often more difficult, since soil mottling in some textured soils is typically less distinct and not as gray in color as in other soils.

However, fluctuations in groundwater levels of floodplain wetland can be estimated using soil color. Gray colors are associated with saturated and chemically reducing soil environments, while yellowish-brown colors are related to generally aerobic and chemically oxidizing conditions (Hunt and Carlisle 2001; Veprakas 2001). Soils without any excess water during the year are usually aerated and yellowish-brown-colored. Soils with high water tables during some part of the growing season exhibit gray coloration at the depth of the high water mark and below. The wet period has a more distinct grayer soil. Many soils exhibit both gray and yellowish-brown colors, reflecting the presence of an elevated water table in the rainy season and a drier, more aerated condition during the dry season when the water table subsides. The occurrence

of gray colors at a particular depth marks the presence of elevated groundwater levels at that depth during part of the year. The grayish colors at these sites are not formed rapidly but as a result of many cycles of soil saturation. Those colours are not easily obliterated but serve as a permanent marker of the mean groundwater elevation at a site. The gray colours do not indicate the duration of the anaerobic event, but provide evidence of the existence of a water table during part of the year. Low chroma colors in the vertical column of the soil are a result of reduction / oxidation cycles that have occurred over many seasons.

During drainage, some areas around pores, cracks, and root channels become dry and aerated more quickly than the matrix soil, leading to the precipitation of ferric iron, which forms reddish-brown spots. During the alternating wet and dry seasons, ferrous iron is not entirely transferred out of the soil profile, but moves over short distances and precipitates during the drying phase (Vepraskas 2001). Such conditions are characterized by blotches of gray and reddish-brown colors occurring at the same depth. The longer the saturation period, the more pronounced the reduction process, and the grayer the soil becomes.

3.5 Mapping of wetlands

Determining the boundary of a wetland is the most difficult part of mapping. Normally, transitions are found at the boundary from upland vegetation to wetland vegetation, from nonhydric to hydric (wetland) soils, and from land that is not flooded to areas that are subject to flooding or saturation. On color-infrared photographs, water generally shows as a distinctive black and blue-black color because of its lack of reflectance. Wetlands that have canopy openings and contain standing water exhibit this signature along with assorted wetland-vegetation signatures. Baghdadi et al. (2001) in their evaluation of synthetic aperture radar (SAR) data for wetland mapping adopted an approach in which for each surface type, several training sites and test sites were selected based on field observations for incidence angles from 20° to 60°. In addition, they investigated the backscattering coefficients for each training site in both co- and cross-polarizations: σ^{o}_{HH}, σ^{o}_{vv} and σ^{o}_{cross} (mean of HV and VH). They also studied separability between classes for all images in order to identify the best configuration period and polarization to discriminate the different surface types in a wetland setting.

In remote sensing application, features are said to be well separated if the distance between the class mean values are large compared to the standard deviations (Cumming and Van Zyl 1989). The statistical analyses of normalized backscattering coefficients at HH, cross and VV polarizations show that open water is easily discriminated from the other categories by its low returns. The measurements of backscattering signatures of wetlands indicate good capabilities for mapping wetlands areas at C-band frequencies. Therefore, using multi-polarization data (HH, cross, VV) and a decision tree model, wetland regions can be classified (Hess et al. 1995). Van de Giesen (2000) used Shuttle Imaging Radar (SIR-C) imagery for the dry and wet season to map floodplains in West Africa. During the process, features such as gallery forests, open water, water with reeds, and non-flooded areas were easily classified. The overall evaluation of the use of this imaging approach suggests that it works best for mapping in environments with high cloud cover.

In other words, microwave signatures of various surface types have been studied as a function of incidence angle, and discrimination between different classes is always clear. With the use of synthetic aperture radar (SAR), statistical analyses of signatures indicate that multi-polarization data are necessary for accurate classification of cover types present in an area. The separation between classes is greatest with cross-polarization, which proved more suitable for discriminating between classes. McCarthy et al. (2003) noted that to discriminate between class areas have to be based on similarity in contextual juxtaposition as compared to dry areas with a similar flooding pattern. However, the lack of evaluation data for the regions under study prevents researchers from evaluating the success of their approaches, and furthermore, most errors in rule-based classification are to a great extent due to definition problems. For instance, boundaries between grasslands and floodplains, and floodplains and permanent swamp communities are not always clearly defined. A second source of error is the adjacency and positional accuracy of the classes, because, for example, the majority of errors related to water is due to the generalization and positional accuracy problem.

Earley (2000) developed a wetland suitability index to determine wetland loss in the Richmond catchment, UK. This involved a wetland extent model based on an

analytical model, which is a combination of multi-attribute data modeling, drainage proximity, and flow accumulation modeling.

3.6 Classification of wetland

Classification is the process of systematic arrangement of objects or phenomena into classes according to criteria and the schemes developed, which can be used to provide a common framework for implementation or studying a phenomenon. A number of wetland classification systems have been developed to classify wetlands, include hydro-geomorphic (HGM), hydrogeology and landscape systems.

The hydro-geomorphic classification (HGM) scheme for wetland classification is based on the premise that wetland structure and functions are expressions of geomorphic setting, water source and hydrodynamics. In addition, hydro-geomorphic classification describes the broad pattern of functional diversity of wetland in a region, which can be used as a standard to make and assess management decisions (Gwin et al. 1999; Bedford 1996). Brinson (1993) listed hydrogeomorphic wetland classes that are distinguishable at the content scale (Table 3.1). Additionally, Gwin et al. (1999) defined four classifications of wetlands for naturally occurring wetlands. These are depression, lacustrine fringe, riverine, and slope.

Table 3.1 Hydrogeomorphic wetland classes at the continental scale

Hydro-geomorphic classification **Wetland Class**	**Definition**
Depression	Depression wetlands occur in topographic depressions (i.e., closed elevation contours) that allow the accumulation of surface water. Potential water sources are precipitation, overland flow, streams, or groundwater/interflow from adjacent uplands. The predominant direction of flow is from the higher elevations toward the center of the depression.

Table 3.1 continued

Tidal fringe	Tidal fringe wetlands occur along coasts and estuaries and are under the influence of sea level. They intergrade landward with riverine wetlands where tidal current diminishes and river flow becomes the dominant water source. Additional water sources may be groundwater discharge and precipitation.
Lacustrine fringe	Lacustrine fringe wetlands are adjacent to lakes where the water elevation of the lake maintains the water table in the wetland. In some cases, these wetlands consist of a floating mat attached to land. Additional sources of water are precipitation and groundwater discharge, the latter dominating where lacustrine fringe wetlands intergrade with uplands or slope uplands.
Slope	Slope wetlands are found in association with the discharge of groundwater to the land surface or sites with saturated overflow with no channel formation. They normally occur on sloping land ranging from slight to steep. The predominant source of water is groundwater or interflow discharging at the land surface. Precipitation is often a secondary contributing source of water. Hydrodynamics are dominated by downslope unidirectional water flow. Slope wetlands can occur in nearly flat landscapes if groundwater discharge is a dominant source to the wetland surface.
Mineral soil flats	Mineral soil flats are most common on interfluves, extensive relic lake bottoms, or large floodplain terraces where the main source of water is precipitation. They receive virtually no groundwater discharge, which distinguishes them from depressions and slopes.
Organic soil flats	Organic soil flats, or extensive peatlands, differ from mineral soil flats in part because their elevation and topography are controlled by vertical accretion of organic matter. They occur commonly on flat interfluves, but may also be located where depressions have become filled with peat to form a relatively large flat surface. Water source is dominated by precipitation, while water loss is by overland flow and seepage to underlying groundwater.
Riverine	Riverine wetlands occur in floodplains and riparian corridors in association with stream channels. Dominant water sources are overbank flow from the channel or subsurface hydraulic connections between the stream channel and wetlands. Additional sources may be interflow, overland flow from adjacent uplands, tributary inflow, and precipitation.

Source: Brinson (1993)

Hydro-geomorphic classification has become an appropriate approach for wetland landscape scale analysis, because it has an intrinsic link between hydrology and geomorphic setting and could also augment other wetland classification systems (Brinson 1993). This method of wetland classification is inexpensive, because readily available existing mapped data in combination with rapid non-destructive field

verification is used. Bedford (1996) proposed the use of landscape profiles to describe the number and kind of wetlands in the landscape using classes defined in terms of hydro-geomorphic factors that cause a specific type of wetland to form and support their functions.

Tiner (2003) also proposed the use of hydrogeology to classify wetlands (Figure 3.2). Many wetlands have developed in shallow water or floodplains associated with estuaries, rivers, lake and streams. Others have become established in poorly drained depressions, at times surrounded by upland, traditionally referred to as isolated wetlands. Isolated wetland can be defined from the geographic, hydrologic and ecological perspective.

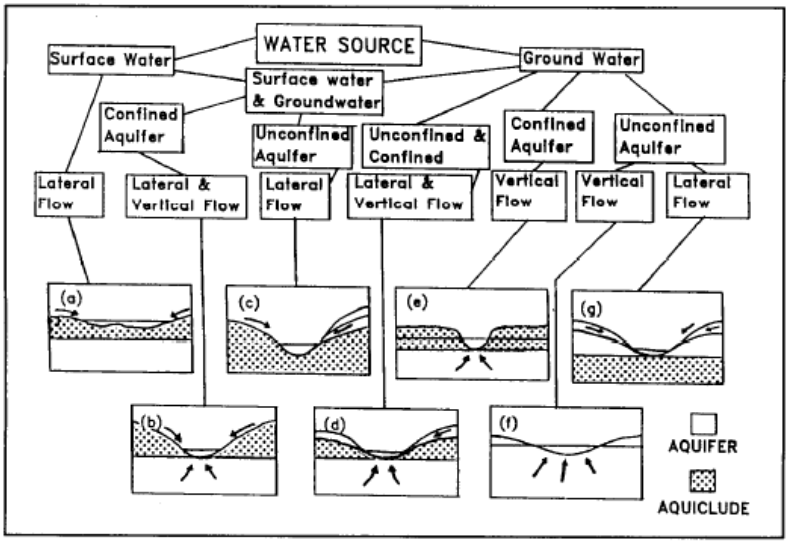

Figure 3.2 Hydrogeologic classifications of wetlands. Description of wetland classes are as follows: (a) those fed by surface water runoff and wetlands that receive river flooding, (b) those receiving aquifer discharge in addition to some surface water, (c) those fed by surficial groundwater in addition to some surface water, (d) those receiving both surficial groundwater and aquifer discharge, (e) those fed predominately by aquifer discharge with minor surface water input, (f) those fed by unconfined main aquifer, and (g) those receiving total surficial groundwater. Precipitation inputs are assumed similar (Brinson 1993)

In addition, four commonly occurring wetland systems have been identified. These are surface water depression wetlands, groundwater slope wetlands, groundwater depression wetlands, and surface water slope wetlands (Novitski 1979; Brinson 1993). Wetlands that receive water primarily from rainfall have been classified as surface water

depressional wetlands. Wetlands for which groundwater is the predominant source of water are classified as groundwater slope or groundwater depressional wetlands. Wetlands that are dependent upon surface water inflow are classified as either riverine or fringe wetlands along existing bodies of open water.

Andriesse (1986) identified four categories of wetland occurring in Africa: coastal wetlands, inland basins, inland valleys, and river floodplains; the latter form large and distinct physiographic units in the landscape. Inland valleys, however, are small and relatively inconspicuous. Inland valleys also are varied: internally, where they comprise such different elements as valley bottoms, slopes and crests as well as externally, where they have a characteristically high spatial variability due to differences in parent material, physiography and climate and as a result, hydrology and soils. Inland valleys, therefore, have a very high variability in actual and potential uses.

3.7 Soil water flow in floodplain wetlands

Water movement in the soils of floodplain wetlands is generally conceptualized as occurring in the three stages infiltration, redistribution, and drainage or deep percolation (Figure 3.3) (Ravi et al. 1998). Infiltration is the initial process of water entering the soil. During this process, capillary forces, or matric potentials, are dominant. Redistribution occurs as the next stage, where the infiltrated water is redistributed within the soil profile after the cessation of water application to the soil surface. The final stage of water movement, termed deep percolation or recharge, occurs when the wetting front reaches the water table.

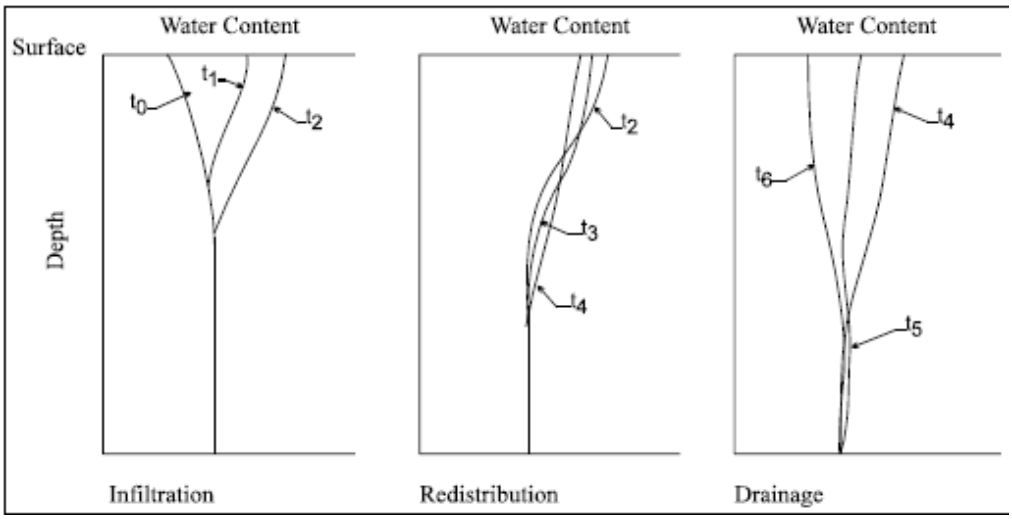

Figure 3.3 Conceptualization of water content profiles during infiltration, redistribution, and drainage (deep percolation) (Ravi et al. 1998)

Infiltration refers to the movement of water into the soil layer, and the rate of this movement is called infiltration rate (Ravi et al. 1998). There are various factors that have been identified to affect infiltration (Fox et al. 1998), including the rate and duration of water application, soil physical properties, slope, vegetation, and surface roughness. Generally, whenever water is ponded over the soil surface, the rate of water input exceeds the soil infiltration capacity. On the other hand, if water is applied slowly, the infiltration rate may be smaller than the soil infiltration capacity, and the supply rate becomes a determining factor for the infiltration rate; this type of infiltration is termed supply controlled (Dingman 2002; Beven 2000; Hillel 1982). Generally, soil water infiltration has a high rate in the beginning, decreasing rapidly, then slowly decreases until infiltration approaches a constant rate. It will eventually become steady and approach the value of the saturated hydraulic conductivity (Ravi et al. 1998; Wu et al. 1999).

There are numerous methods for modeling infiltration (Table 3.2) which are based on different principles, including conservation of mass and Darcy's law as used in Richard's, and Green and Ampt models (Beven 2000; Dingman 2002). Infiltration models can be classified as simple infiltration equations, analytical or quasi-analytical and numerical models. Empirical methods are usually in the form of simple equations, the parameters of which are derived by curve-fitting the equation to actual measurements of cumulative water infiltration.

Table 3.2 Infiltration equations

Author	**Infiltration Equation**	**Remarks**
Richards equation	$\frac{\partial\theta}{\partial t}=\frac{\partial}{\partial z}(K(h)\frac{\partial h}{\partial z}+1)$	Richards equation for vertical flow
Philip 1957	$Y=T^{1/2}+T\lambda$	
Philip 1969	$Y=\frac{1}{4}\left[2T^{1/2}\exp\left(-T/\pi+2T+\pi\right)erf\left[\left(T/\pi\right)^{1/2}+2T\right]\right]$	
Parlange 1975	$2Y-\left[1-\exp\left(-2T^{1/2}\right)\right]=2T$	
Green Ampt	$F_{t+\Delta t}=F_t+K\Delta t+\psi\Delta\theta\ln[\frac{F_{t+\Delta t}+\psi\Delta\theta}{F_t+\psi\Delta\theta}]$	
Mezencev	$i(t)=i_f t+\alpha t^{-\beta}$ and $I=i_f t+\frac{\alpha}{1-\beta}t^{(1-\beta)}$	

T is time (hr), f_t is the infiltration rate, cm/hr; ψ is the initial matric potential of the soil, cm; $\Delta\theta$ is the difference of soil water content after infiltration with initial water content, cm^3/cm^3; K is the hydraulic conductivity, cm/hr; F_t is the cumulative infiltration at time t, cm; $F_{t+\Delta t}$ is the cumulative infiltration at time t+ Δt , cm; Δt is the time incremental, hr; θ is the soil water content, cm^3/cm^3; h is the initial matric potential of the soil, cm; and $K(h)$ is the hydraulic conductivity at h, cm/hr.

The Green and Ampt (1911) model is a physically based equation describing the infiltration of water into a soil (Figure 3.4). This model has been the choice model of infiltration estimation in physically based hydrologic models owing to its simplicity and satisfactory performance for a variety of hydrological problems (Wesley et al. 1992).

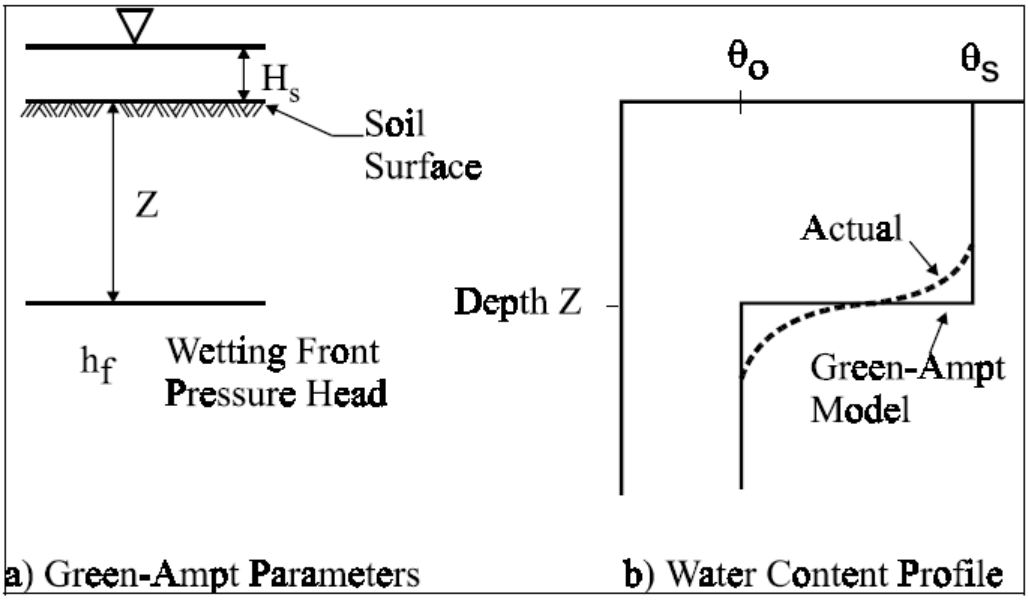

Figure 3.4 Green-Ampt parameters and conceptualized water content profile, which demonstrates the sharp wetting front

Richard's model, which combines Darcy's law for vertical unsaturated flow with conservation of mass, is the basic theoretical equation for infiltration into a homogenous porous medium. This equation is nonlinear, hence there is no closed form analytical solution except specifying boundary conditions are applied (Swartzendruber 1997; Ross 1990). Though Richard's equation almost exclusively deals with absorption and infiltration problems, relatively little work have been done on redistribution and drainage problems. Philip (1991) gives three reasons for this relative paucity of mathematical-physical studies of redistribution. First, the initial conditions for the redistribution process tend to be complicated. Second, various mathematical techniques useful in the infiltration context do not, generally, carry over to redistribution problems. Third, redistribution processes involve the very considerable complication of capillary hysteresis. Therefore, the analyses of redistribution and drainage processes using the Richards model almost totally rely upon numerical techniques. Depending on the simplicity (or complexity) of these input parameters, the Richards equation can be solved analytically or numerically.

Notably, the two basic soil hydraulic characteristics identified to be controlling soil water flow in floodplain wetlands are soil water retention θ(h) and unsaturated hydraulic conductivity k(h) (Joris and Feyers 2003; Fox et al. 1998). The physical processes that controlled outflow within a soil column are entrapment of water, pore

water blockage, air entrapment, air entry effect and dynamic angle effect (Wildenschild et al. 2001). Wu et al. (1999), pointed out that air entrapment has the potential of decreasing water retention in the soil and is more plausible if air permeability is low at high water saturation. In most soils, trapped air effectively decreases both cumulative drainage and drainage rate. The resulting effect is the reduction in unsaturated hydraulic conductivity values near saturation (Fox et al. 1998). Morin (2006) in his research to verify the relationship between porosity and hydraulic conductivity in sand and gravel aquifers in Cape Cod, Massachusetts, USA, based on multivariate analysis (factor analysis) noted a consistently bipolar relationship which he defined as a negative relationship. But he concluded that the relationship being either positive or negative relates to the interplay between a fluid winding through a mass of particles at different microscope velocities, and to the shapes and sizes of pores. Modeling the movement of moisture through unsaturated porous media has many field applications as is in the case of floodplain wetlands, but these are subject to appropriate boundary and initial conditions (Sanford 2002).

Processes that link surface and sub-surface waters are important in wetland hydrodynamics. Water movement into unsaturated soil generally occurs under the combined influence of suction and gravity gradients. As the water percolates, it lengthens the wetted part of the soil profile, the average suction gradient decreases, and thereby the overall difference in pressure head (between the saturated soil surface and the unwetted soil inside the profile) divides itself along an increasing distance (Jaramillo et al. 2000). The suction gradient in the upper part of the profile eventually becomes negligible; this makes gravitational gradient the only remaining force moving water downward. Hence, the gravitational head gradient has the value of unity (the gravitational head decreasing at the rate of 1 cm with each centimeter of vertical depth below the surface), making the flux approach the hydraulic conductivity as a limiting value (Wu et al. 1998). In a uniform soil (without crust) under prolonged ponding, the water content of the wetted zone approaches saturation (Fox et al. 1998).

3.8 Climate and wetland

Climatic influence on floodplain wetlands is important, because it affects the periodic inundation or soil saturation within 30 cm of the surface for a stipulated period

(Moorhead 2003). According to IPCC 2007 report (Meehl et al. 2007), climate change scenarios have indicated an equilibrium climate sensitivity for the 21st is projected to lie in the range 2^{o}C to 4.5^{o}C. Temperature increase within this range will affect the distribution and function of wetlands throughout the world. For instance, changes in climate with high rainfall will put pressure on some wetlands, leading to frequent flooding, e.g., in Brazil, Bolivia and Paraguay. The drying of wetlands will result in a significant release of carbon dioxide thus losing their function as a point for carbon sequestration. Additionally, some in land wetlands will experience a decrease in rainfall which will affect wildlife, e.g., in the Zimbabwe Kariba National Park and the Okavango National Park in Botswana.

Poiani and Johnson (1993), using a rule-based simulation model, attempted to assess the effects of greenhouse-gas-induced global climate change on the hydrology of wetlands. They concluded that wetlands will be severely impacted by increases in temperature and changes in rainfall. In another study, Kroes and Brinson (2004) used the potential evapotranspiration (PET) ratio (potential evapotranspiration divided by precipitation) to define the occurrence of riverine floodplain wetlands along a humid and semi-arid climatic continuum. They found that streams with a PET ratio greater than 0.98 did not have associated wetlands therefore, the role of climate in the sustenance of wetland need not be underrated. Lott and Hunt (2001) noted that inaccuracies in wetland water balances are a result of the difficulties in accurately calculating wetland evapotranspiration. Hence, within the Wilton wetland complex along the Kickapoo River in Monroe County, southwestern Wisconsin, USA, they compared a commonly used meteorological estimate of evapotranspiration with direct measurement of evapotranspiration (lysimeter and water table fluctuation) and root zone geochemistry. They found that lysimeter and water table combination underestimated the evapotranspiration because of the heterogeneity of the surface, while stable isotopes elucidated the qualitative differences in evapotranspiration methods.

The influence of climate on the spatial and temporal variability of wetlands has been noted in a number of studies (Poaini et al. 1995 and 1996, LaBaugh et al. 1996). However, understanding the interactions of the wetland complexes with their neighboring uplands and the climate system is a key issue spelt out by scientist in fields related to wetland studies. Wetlands store precipitation and surface water and slowly

release the water into associated surface water resources, groundwater, and the atmosphere (Kebede et al. 2006).

3.9 Water balance

Wetland types differ with regard to water balance based on a number of physical and biological characteristics including: landscape position, soil saturation, fiber content/degree of decomposition of the organic soils, vegetation density and type of vegetation (Taylor et al. 1990). Wetlands play a critical role in regulating the movement of water within watersheds as well as in the global water cycle (Richardson 1994; Mitsch and Gosselink 1993). Wetlands, by definition, are characterized by water saturation in the root zone or above the soil surface for a certain amount of time during the year. This fluctuation of the water table (hydroperiod) above the soil surface is unique to each wetland type.

According to Mitsch and Gosselink (2000), the wetland hydrologic budget has the typical inputs and withdrawals that apply to other ecosystems. These inputs include direct rainfall, overland flow, channel and overbank flow, groundwater discharge, and tidal flow. Withdrawals include evaporation and transpiration, groundwater recharge, and overland, channel, and tidal flows. Temporary storage within the wetland includes channel and overbank storage as well as groundwater storage. At wetland boundaries, wetland hydrologic budget and corresponding flow rates are easy to calculate with conventional methods, but difficulties arise when modeling hydrodynamic flow that occurs within a wetland. Though the underlying concepts of continuity and conservation of momentum apply to modeling wetlands, adjustments to numerical models need to be made to account for the hydrodynamic processes that occur within wetlands.

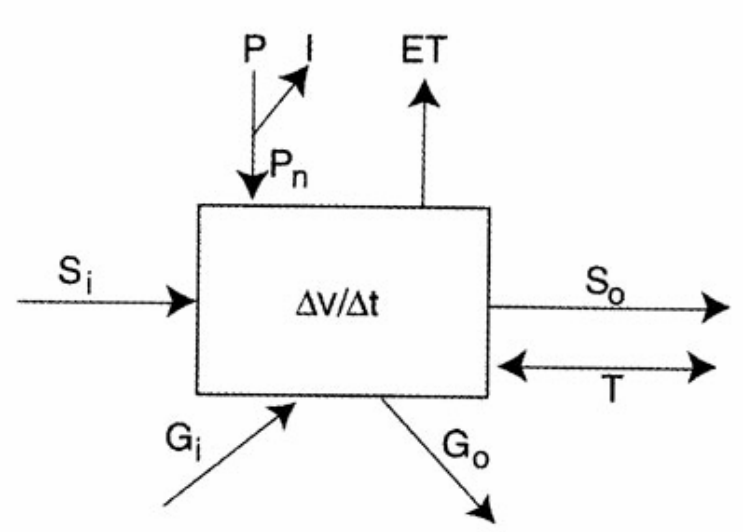

Figure 3.5 Water balance, where P=precipitation, Pn=net precipitation, ET=evapotranspiration, I=Interception, Si=surface water inflow, So=surface water outflow, Gi= groundwater inflow, Go=groundwater outflow, T= Tide, V=change in storage, and t=time (Mitsch and Gosselink 2000)

In the dynamics of wetland hydrology (Figure 3.5), water may come to the wetland from the upstream drainage area or directly via rainfall, and once in the wetland it remains in soil storage, leaves by evaporation or drains away. The wetland water balance is strongly affected by groundwater processes as well as by the interaction between groundwater and surface water, hence the consideration of surface water alone is not suitable for characterization of process boundaries (Krause and Bronstert 2005). Krause and Bronstert (2005) noted that it is possible to simulate the hydrologic characteristics of floodplain wetlands reflecting the water balance and the groundwater processes. Models should have the capabilities of integrated modeling of water balance and groundwater dynamics of floodplains. The dynamics of groundwater exfiltration and surface water infiltration have been used to prove the importance of groundwater-surface water interaction for floodplain water balances (Matos et al. 2002).

Conceptual wetland models have been developed to describe the interactions between a wetland, the surrounding catchment and local groundwater. Numerical evaluation of a wetland water balance can be achieved by applying a bucket model, which requires little calibration, and uses physically based catchment properties and recorded climatic data sets (Krasnostein and Oldham 2004). In the study, the model

enabled differentiation between groundwater components. Flow paths were separated into groundwater inflows and outflows, and an overflow mechanism connecting the wetland to the nearby cave system was identified. Results from this study show that the bucket model can be used to isolate dominant hydrological processes of a wetland system, focus field studies of wetland hydrology, or facilitate management of the system.

In addition, landscape-scale or catchment-scale water budget approaches are appropriate for the analysis of wetland hydrodynamics and hydro-periods. The use of soil water content as a method to evaluate the hydrologic water balance has been proposed by Or and Wraith (2002). This is based on the concept of conversation of mass, under a typical condition, change in water content is significant over a short term (weeks to months) or zero over one to several years.

3.10 Evaporation estimation

Accurate estimation of evaporation is important in water balance modeling. Evaporation is required for a variety of climatological, hydrological and ecological problems but is very difficult to obtain. Results estimated from studies are often inconclusive or conflicting. Evaporation in wetlands is often determined as the residual in water balance studies or measured at a spatial scale inconsistent with other measurements (Souch et al. 1998). There are a range of wetland types in the world, ranging from open-water dominated wetlands, where evaporation is not constrained by water availability, to those where the water table is frequently below the surface, and water availability for evaporation is controlled by vegetation factors (Reikerk and Korhnak 2000). Most conventional techniques for monitoring evapotranspiration efficiently using point measurements are representative only of local areas and cannot be extended to large areas because of the dynamic nature and regional variation of evapotranspiration. Remote sensing has proven to be a suitable approach for areal estimation of evapotranspiration, because it is the only technology that can provide and combine representative parameters such as radiometric surface temperature, albedo, and vegetation index in a globally consistent and economically feasible manner (Compaore 2005).

Physical analytical approaches based on the Penman–Monteith resistance model and surface energy balance equations are the most common methods of potential evaporation estimation. When combined with a remote sensing approach, radiometric surface temperature is used to calculate sensible heat flux and to evaluate the terms of the energy balance equation to obtain potential evapotranspiration. Radiometric surface temperature is also used to calculate crop water stress index to obtain evapotranspiration. However, using radiometric surface temperature as a substitute for the aerodynamic temperature as used in the original Penman–Monteith model, can lead to substantial errors, especially over partial vegetation cover, because the radiometric surface temperature is the composite temperature of soil and vegetation. This error can be reduced by introducing an extra resistance (Kustas et al. 1989, 1996), resulting in a two-source model, using more complicated multilayer models (Choudhury and Monteith 1988; Lhomme et al. 1994; Norman et al. 1995) or by developing an empirical formula to estimate the aerodynamic temperature (Huang et al. 1993), and by incorporating a vegetation index within the model (Moran et al. 1994 , 1996).

The existence of extra-resistance, soil-adjusted vegetation index and two-source resistance models highlight the limitations of these models when air temperature is not measured or if it varies substantially over a region (Kustas et al. 1989, 1996). For regional scale applications, it may be difficult to use these approaches in areas where there is a very sparse network of air temperature and wind speed observations. The application of single-source approaches over various landscapes will be tenuous and will be affected not only by the aerodynamic properties of the surface but also by sensible heat.

3.11 Wetland river interaction

The review of the literature reveals that little or no research has been conducted on horizontal floodplain wetland river flow interaction. Most research has been on the vertical interaction of surface and groundwater. For instance, Nield et al. (1994) used a numerical model to examine groundwater flow in vertical sections near surface water bodies, such as lakes, wetlands, ponds, rivers, canals, and drainage and irrigation channels. They distinguished different flow regimes by noting the presence and nature of groundwater mounds or depressions near the edges of a surface water body and by

corresponding stagnation points. But the increasing anisotropy or sediment resistance and decreasing length of a water body relative to aquifer thickness have effects on flow geometry. Therefore, decreasing anisotropy and sediment resistance and increasing water body length tend to affect the flow-through behavior. Matos et al. (2002) examined aquifer heterogeneity and channel pattern on flow interactions between stream and groundwater systems. They used MODFLOW, a numerical model, to evaluate the magnitude, direction and spatial distribution of stream-subsurface exchange flows. After intense runoff-producing rainfall events, the soil textural composition enhances infiltration of the surface runoff waters. The underlying sediments act as an aquifer resulting in groundwater flow. The infiltrating water moves along the hydraulic gradient until it reaches an impeding layer of fine clay and silt, which has a lower hydraulic conductivity; hence less water is transmitted per unit time. Stratigraphy and topography with wells and piezometer log data have been used to characterize water conditions in all types of landscapes (Richardson et al. 2001). FLOWNET or other numerical models have been used to plot and visualize equal hydraulic heads and groundwater flow paths and mostly consist of equipotential lines and flow stream lines.

3.12 Tracer application in wetland studies (environmental isotope)

Environmental isotopes now contribute to groundwater investigations, complementing other methods used in hydrological studies in wetland settings. Isotopes serve as tracers of water flow paths, assist in estimating recharge and provide information on forms of interaction occurring within the hydrological landscape. Isotopes such as oxygen-18 (^{18}O) and deuterium (^{2}H) have been used to study wetland processes in many parts of the world.

Tobias et al. (2001) used Darcy's law, salt balance and Br-tracer in an attempt to estimate the seasonal variation in groundwater discharge at the fringes of an estuarine wetland. Their finding indicate that Darcy's law and salt balance revealed similar patterns at the scale of seasonal variation, but showed some differences in the magnitude of discharge in a 10 order of magnitude. The Br-tracer estimates were nearly equal to the salt balance. The authors concluded that Darcy's law performed well during low flows, while the salt balance estimated a more accurate value for groundwater discharge in high flow conditions.

Harvey et al. (2006) used three main approaches to quantify surface and groundwater interaction in the central Everglades in south Florida. These are Darcy's flux calculation based on measurements of the vertical gradient in the hydraulic head, and the hydraulic conductivity in the wetland to calculate vertical flux between surface and groundwater. In addition, Radium and Tritium were used to verify flow within the wetland and the results compared to those obtained by methods based on the magnitude of vertical exchanges within the wetland. They concluded that each method has a unique time scale of averaging, depending on the frequency and location of measurements and whether the measurements are made in peat pores, water or in underlying groundwater. According to Brown et al. (2003), when modeling flows in wetlands, the incorporation of spatially distributed storage state variables may give misleading results when the origin of flow within the watershed is of interest. In other words, as the hydraulic properties of soils differ spatially, fluid flow becomes more pronounced in inter-aggregate pores reducing the possibility of obtaining an equilibrated pore water pressure profile.

Gilbert et al. (1999) explored the effectiveness of the environmental isotopes oxygen-18 (^{18}O) and deuterium (^{2}H) in tracing water circulation and mixing of isotopically depleted river water and isotopically enriched wetland water during pumping events in wetland cells. The results of the pumping test indicate that ^{18}O values at the sampling point closest to the inflow were isotopically depleted by river water. The rising water levels had no significant effect on the isotopic concentration in stations farthest away from the inflow during the period of their study. The isotope data suggest that river water is only present in the areas closest to the inflow, and that river water and wetland water mix in the central part of the cell while river water never reaches areas farthest from the inflow. It appears that wetland water is displaced by the pumped river water and is forced by hydrostatic pressure into areas farthest from the inflow.

Clay et al. (2004) used stable isotopes in water to identify spatial and temporal changes in the source of recharge to a lowland headwater wetland within the River Tern in UK. They found that groundwater appears to be the main source of water to the wetland, but stable isotope ratios enable identification of seasonal variations in the contribution of precipitation, which indicates the extent of precipitation storage within the wetland. Wang and Yakir (2000) used stable isotopes to estimate evapotranspiration

flux from vegetated areas and to partition evapotranspiration into components of soil evaporation and leaf evapotranspiration. A combination of local meteorological (Bowen ratio estimates) data and isotope data has the potential for partitioning evapotranspiration into soil evaporation and plant transpiration.

The use of hydrology as a criterion to delineate floodplain wetlands has been practiced for a long time, but the importance of the groundwater contribution to the system is poorly understood, specifically, how groundwater flows into and out of wetland. A distinction can be made as to the contribution of groundwater to wetland flow by noting the content of isotopes carried by groundwater, which is higher than that of surface water (Hunt et al. 1999; Bradford and Acreman 2003). Although sub-surface wetland water is very difficult to characterize, the use of traditional aquifer tests have had limited success in elucidating the effects of groundwater on physical and chemical hydrology of wetlands (Joris and Feyen 2003). The recent developments, in the use of chemical and isotopic composition of wetland aquifer are gaining importance. As noted by Hunt et al. (1999), wetland hydrologists have difficulty in developing methods to characterize groundwater data as well as in demonstrating how important groundwater flow affects the physical and biogeochemical composition of wetlands.

3.13 Models used in studying wetlands

Wetland importance worldwide cannot be overemphasized. However, low perception and poor management is threatening their life span. Therefore, the urgent need to find the best solution and practice in sustaining the role that wetlands plays in our environment has led to the use of models. In wetland studies, model applications are considered to be an option to understand the role the wetlands play and ascribe the appropriate management procedure or application. Numerous wetland models exist, but scientists have not been able to come to a consensus as to which model is the best to apply to specific problems (Janssen and Hemke 2004). Within the wetland scientist community, among the numerous models two main models for studying wetlands can be distinguished. These are models based on data and models based on processes.

Models based on data are generally known as stochastic models. They are also considered as a black box system that uses mathematical and statistical techniques to link model inputs to outputs. Common techniques are regression, transfer function and

neural networks. In this case, wetlands are treated as a black box, where time series of input data are related to outputs. The internal processes and controls are not made reference to; it is only the overall behaviour that is considered. Wetlands themselves are superb simplifiers, converting a spatial complexity of patterns and processes into a relatively simple and well understood output like a hydrograph (Mulligan 2004).

Models based on process description, commonly called deterministic models, can be sub divided into single event models and continuous simulation models. This type of model represents physical processes observed in the wetland, and typically contains representations of surface runoff, evapotranspiration, and sub-surface flow. However, the use of this kind of model can be complicated, due to the large number of parameters that usually are required to be estimated from limited data input-output observation (Young 2001). Application of models in this category require very good understanding of the nature of the system and internal working of and connection and interaction between its subsystems and components of the subsystem, together with knowledge of the physical laws governing the processes occurring in the system to formulate (Dooge 2003).

In most studies, finite difference models describe floodplain wetland as a series of cross sections perpendicular to the flow direction in wetlands and require detailed field work to collect data. Models such as MIKE11, FLUCOM and HEC-RAS fall into this category. As noted by Bardford and Acreman (2003), physical-based, process-oriented, spatially distributed models such as MIKE-SHE, MIKE-BASIN, have seldom been applied to study wetlands, as they are complex to operate and require a level of data that is seldom available in the developing world.

MODFLOW, a physical based numerical groundwater flow model, has been applied in many aspects of wetland hydrology research because it can represent a wide range of drainage situations, geometry, configurations and different hydraulic settings. Restropo et al. (1998) developed a wetland package for MODFLOW in which the physics of flow processes and the mathematical basis of various features in wetland hydrodynamics were considered. Bradford and Acreman (2003) used MODFLOW to examine water table variations in wetlands.

To model the local wetland hydrology within a landscape, Mansell et al. (2000) used a multidimensional numerical model WETLAND to simulate and describe water

flow in variable saturated soil and estimated evapotranspiration. The model provided a linkage between pond water, groundwater and unsaturated soil zones. WETTRAN, a model that focuses on the consistent description of hydrological inflow and outflow pathways in a simple mathematical form has been applied to the study of wetland in Germany (Trepel and Kluge 2004). The model is based on the path transformation concept where wetlands are hydrologically connected with their surrounding drainage basin and detected by the morphology and geohydrology of the wetland and its surrounding basin. However, Brown et al. (2003), in attempting to quantify lateral flow into wetlands, used DEMON, a stream tube flow routing model and compared the results with those of the model D8 (a model that uses DEM to define flow directions). They found that D8 produced unrealistic results, while DEMON incorporated with storage term predicted observed changes from storage-dominated flow to catchment-topography-dominated flow as rainfall increased.

The unsaturated water content in wetlands was modeled using UNSAT1, a Hermitian finite element model, to simulate one-dimensional non-homogeneous soil profiles (Bradley and Gilver 2000). However, an accurate description of wetland substrates and near-surface water flux and expressing them in two dimensions is important. Joris and Feyen (2003) used HYDRUS-2D to model the water flow and seasonal soil moisture dynamics in groundwater-fed wetlands. They were able to assess the effect of changes in floodplain depressions and hydrological boundary conditions on vegetation-related groundwater parameters. The distributed wetland model FLATWOOD was applied to one-dimensional unsaturated flow in the vadose zone of wetlands. Its limitation is that surface water and groundwater interaction are not explicit (Sun et al. 1998).

Maggio (1998), in an attempt to delineate floodplain wetland boundaries, developed a new approach by integrating GIS with hydrological/hydraulic modeling via a loose coupling approach. The approach involved the use of a GIS package (ArcInfo) and a hydrological modeling programme HEC. The model has a four phase approach, namely, database creation, hydrological modeling using HEC -1 (rainfall-runoff), hydraulic modeling using HEC-2 (water surface calculation) and floodplain mapping.

Most recently, two-dimensional finite difference and finite element models have been developed that overcome the limitations of one-dimensional models (Bates

and De Roo, 2000). The model TELEMAC-2D, compared with low resolution satellite imagery and measured water level, provides a higher order representation of topography, which requires no secondary processing steps to determine floodplain wetland inundation. One major drawback in the use of this model is its operational cost in acquiring data. The use of a digital elevation model (DEM) enhances the capabilities of 2-D models in its landscape simulation process (Bates and De Roo 2000).

From the above review, there are a wide range of models that researchers can select to simulate wetland processes. However the choice of a model should be preceded by answering the following questions (Beven 2001):

- Is the model readily available or could it be made available if time and money were invested?
- Does the model predict the variables required by the aims of a particular project?
- Are the assumptions required by the model likely to be limiting in terms of what one wants to model?
- Can all input requirements for specification of flow domain, boundary condition, initial conditions, and parameters be provided within the time and cost constraint of a project?

4 MATERIALS AND METHODS

4.1 Data identification and source

Data collected for the study are based on field measurement, field observation and laboratory analysis. The field data collection involved measurement of soil infiltration, hydraulic conductivity, river cross sections and water sampling in streams/wetlands to determine level of isotopic tracers within the catchment. Field observations were undertaken to attain a level of generality by locating common factors such as vegetation density, water logging and other topographic parameters. This was carried out for quick and appropriate predictions in areas where detailed installation of equipment is not required (De Vans 1993; Molenaar 1998; Mitchell 1973). In addition, field observation techniques assisted in cross checking predictions derived from models based on data obtained from measurements and secondary sources. Laboratory analysis was carried out for chemical and physical properties at the Soil Research Institute, Kumasi, and at the Ghana Highways Authority Laboratory in Bolgatanga. In addition, Geographic information system and remote sensing tools were used to analyse SRTM-DEM (cell size of 90 m resampled to 30 m) and ETM-LandSat images to identify and incorporate spatial data into the proposed hydrological models for simulation and analysis. Data collected were used to describe the hydro-dynamics of the wetlands that served as input into the HYDRUS and MODFLOW models for this study.

4.2 Wetland mapping

Floodplain wetlands were mapped for an initial assessment to determine the feasibility of the study and to aid in site selection for field observation/measurements. A cloud free Landsat image (30/10/2002-194/53) and a preprocessed digital elevation model (STRM-DEM) were used as the main input data. The hydrotope approach was used to define a set of elementary units, which assisted in derivation of a floodplain wetland map. Hydrotopes are distinct hydrological units that behave in a hydrologically uniform way (Krysanova et al. 2000). They are natural spatial units defined depending on the objective of the research, which are based on the character of the environment. Modeling the hydrological processes of wetlands is challenging because of the complex interactions between soil water, groundwater and surface water. Therefore, to maximize

the application of spatial data in the process of wetland modeling, zones of similar hydrological response (hydrotopes) were derived. These zones are the expression of the spatial distribution of parameters influencing wetland hydrodynamics and, they also save computation time and data demand. Hydrotopes were aggregated to ensure statistically sound spatial validation in the process of mapping. Hydrotope identification relied on detailed knowledge of environmental processes, and free globally available datasets from the United States Geological Services (USGS). Based on extensive knowledge of the local hydrology of the Volta Basin, hydrotopes were generated see (chapter 5) using SRTM-DEM and landsat-ETM of 30th October 2000 (Table 4.1). The choice of this image was based on its clarity in terms of absence of clouds.

Table 4.1 Description of identified hydrotopes

ID	**Description**
LogB4	Logarithm Transformation of Band 4 of 30 October 2000 satellite image [-]
Cover	Land cover classes derived from 30 October 2000 satellite image
Distance	Distance from the main river [m]
Evapo	Evapotranspiration data calculated using SEBAL [mm/day]
Power	Stream Power Index [-]
Height	Elevation data derived from the SRTM-DEM [m]
Internal	Internal relief [m/km^2]
Ndvi	Normalized Density Vegetation index [-]
Wetness	Zone of Saturation [-]
Texture	Pattern of pixel brightness [-]
Slope	Slope in degrees [degree]
Shape	Shape of topography (Convex, Concave or straight) [-]
Savi	Soil adjust vegetation index [-]

For cover class extraction, spectral bands of the landsat-ETM were combined to give a vivid image differentiating between wetlands and other environmental variables and thereby defining a training data set for supervised classification. Classification was based on the maximum likelihood method within the ENVI 4.0 program platform, commonly used for digital spectral classification. This classification

was found to give better results than visual classification. Supervised classification was used to obtain the final land-cover classes.

4.3 Site selection and data sampling

On the basis of the land cover map, the Pwalugu and Tindama floodplain-wetland sites, 85km apart within the White Volta River basin, were selected. The selection of these two sites was based on accessibility, heterogeneity of their geological formation and the occurrence of subsurface water. The purposive sampling technique was used to select points (Figure 4.1) for soil sampling, infiltration and hydraulic conductivity measurements. Using either the stratified or the simple random sampling methods was not suitable, because these methods require a sample frame, which was difficult to compile (de Vans 1993). Moreover, using the simple random method, areas to be selected may be rocky or waterlogged and thus not suitable for any form of measurement.

Using the purposive sampling technique, the sites selected for data collection was chosen based on the interest of the researcher and on background knowledge, hence no sampling frame was needed. The sampling method was purely for convenience and did not demand proportionate representation of samples. It thus permitted observation and measurement of cases in any unit that was judged important in the study (Shaw and Wheeler 1985). Regardless of its advantages, purposive sampling techniques make generalization from selected sampled sites problematic (de Vans 1993).

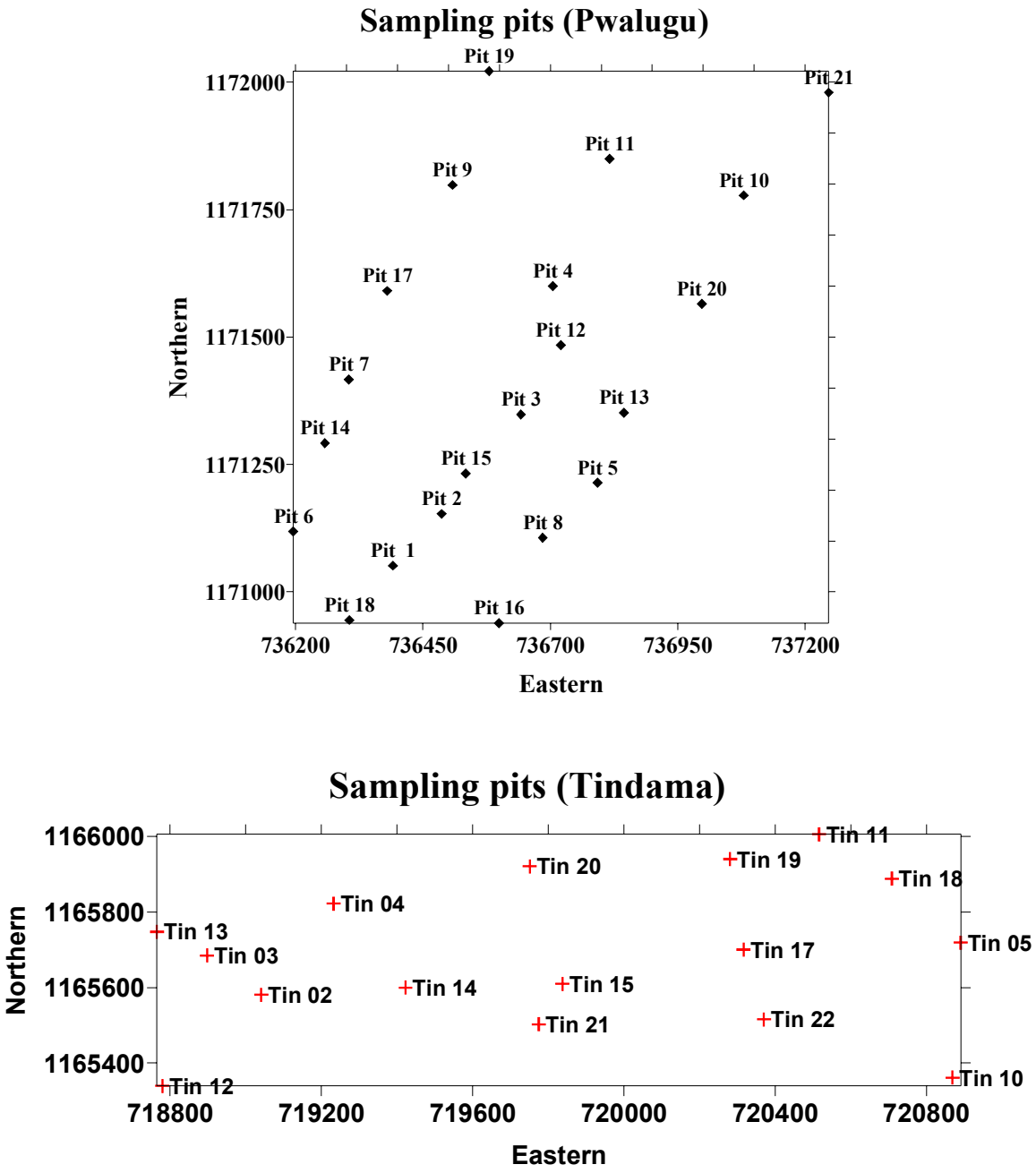

Figure 4.1 Location for pits for soil sampling at the Pwalugu and Tindama floodplain wetland sites

4.4 Installation of monitoring wells

Wetland subsurface water levels were monitored at the Pwalugu sites using eight piezometer wells consisting of 3 cm diameter pipes ranging from 3 m to 6.6 m in depth. These piezometers were installed using a hand auger. The piezometers were back-filled with sand, and then cement was placed on the top to prevent surface water entry. The depth of free water was measured by inserting a tape down into the wells and observing

when it encountered the water surface. The elevation of the piezometers were surveyed to benchmarks to allow adjusting the water levels in the wells to the local datum of the White Volta River at the Pwalugu gauging station.

4.5 Soil properties

Bulk density, total porosity; effective porosity water content, soil texture, organic carbon, hydraulic conductivity and infiltration were measured. The soil data are used to describe the hydrodynamics of the Pwalugu and Tindama wetland sites. In addition, they serve as input parameters into the HYDRUS-1D and MODFLOW models.

4.5.1 Bulk density

Soil bulk density refers to the weight (mass) of soil per unit volume. This relates primarily to the physical ability of the soil to hold water and sustain plant growth. Bulk density was measured through extracting a soil sample of known volume. The mass was obtained after oven-drying the soil overnight at 105^{o}C, and dividing by the volume of the cylinder that was used to collect the sample. The following equation was used to estimate bulk density:

$$\rho_b = \frac{M_s}{V_s} \tag{4.1}$$

Where ρ_b [g/cm^3] represents bulk density, M_s [g] mass of sample, V_s [cm^3] is the Volume of sample.

4.5.2 Total and effective porosity

The number of pores and their size distribution (as reflected in estimates of total pore space, coarse porosity and air-filled porosity) are general indicators of the physical condition of the soil. However, the tortuosity and continuity of soil pores are important features influencing aeration, water movement and root penetration. Total porosity can be estimated from bulk density and particle density as specified in the following equation:

$$Porosity = \left(1 - \frac{\rho_b}{\rho_s}\right) * 100 \quad (4.2)$$

Where ρ_b [g/cm^3] is bulk density and ρ_s is particle density (2.65g/cm^3)

Effective porosity is that part of the pore system that can contain immobile or partly immobile fluids. Normally, the effective porosity is smaller than the total porosity with respect to flow. Transport models to calculate average velocity of flow through a porous medium use the effective porosity.

$$P_e = \frac{V_{mw}}{V_T} \quad (4.3)$$

P_e is effective porosity, V_{mw} represents volume of mobile water pores in the pores and V_T is the total volume of sample

4.5.3 Water content

Water content is a measure of the ratio of water volume to soil volume. The soil sample was collected by coring into the soil with a ring volume of 100 cm^3. The sample was weighed for its initial wetness and later dried in the oven at 105^{o}C for 24 to 48 hours to remove inter-particle absorbed water, but not structural water trapped within the soil lattices known as crystallization water. The difference between the wet and the dry weights is the mass of water held in the initial sample:

$$\theta = \frac{M_w - M_d}{\rho_w V_s} \quad (4.4)$$

θ [cm^3/cm^3] represents water content, M_w [g] is mass of wet sample, M_d [g] is mass of dried sample, and ρ_w is density of water [g/cm^3]

4.5.4 Soil texture

Soil texture describes the mass proportions of the various sizes of the soil particles. The three major groups of soil particles are sand, silt and clay. Soil texture is an important

physical property, as the size distribution of particles in the soil greatly influences the physical and chemical properties of the soil such as pH and cation exchange capacity (CEC). There are different ways of analyzing soil texture, namely sieving, pipette and the hydrometer methods. In this study, the hydrometric method was used. This involved the removal of organic matter by adding a chemical dispersing agent (sodium hexametaphosphate) after which the sample was mechanically agitated through shaking overnight for complete dispersion of soil floccules. The bouyoucos hydrometer was then used to determine the density of the solution at timed settling increments. The density of the soil solution was used to determine the concentration percentages for sand and clay particles. For the determination of sand and clay size fractions, Stokes´ Law relationship between the diameter of suspended particles and their rate of settlement in liquid at constant temperature was used. The hydrometer procedure uses higher concentration of soils and is less accurate than the pipette method.

4.5.5 Soil organic carbon (organic matter)

Measurement of soil organic carbon gives an estimate of the amount of organic matter in a soil as a percentage by weight. The level of organic matter in the soil is a broad indicator of soil condition. Its concentration in the soil is largely determined by the addition of surface litter (fallen leaves, manure and dead organisms), root material and the rate at which microbes break down organic compounds. Organic matter is important, since it binds soil particles together into stable aggregates, which are necessary for soil structural stability and significantly influence soil water holding capacity, especially in sandy soils. The Walkley Black procedure was used to obtain organic carbon. To obtain % organic matter content, the organic carbon content is multiplied by the van Bemmelen factor of 1.724 (Duguy et al. 2007).

4.6 Soil colour and sub-surface water indication

Soil colour gives an indication of the chemical and physical processes that have occurred within the soil column. Soil colour serves as a proxy to indicate the presence or absence of organic matter and the level of water table fluctuation taking place in the soil. The description of soil colour in the Pwalugu and Tindama sites follows the standardized Munsell colour system, quantifying soil colour of the wetlands in a

standard reproducible manner. The Munsell colour chart considers 3 aspects of colour: Hue, Value and Chroma. Hue describes the quality of pigmentation, value the lightness or darkness of the colour and chroma describes the richness of pigmentation expressing how pale or bright the colour is.

4.7 Hydraulic conductivity

Saturated hydraulic conductivity (K_{sat}=LT^{-1}) is the rate at which water can pass through unit cross-section area of a soil in unit time. Measurement were undertaken to compare the conductivity rates of different soil horizons, which serve as a guide to water movement within the soil profile. In addition, the measurements were used to compute the velocity of water movement from the floodplain wetlands toward the river or into the water table. Hydraulic conductivity of water in soil (or the intrinsic permeability of the soil) was measured using both field and laboratory experiments. The experimental measurements assisted in the estimation of K_{sat}, a numerical value used in Darcy's equation. The methods used for the determination of K_{sat} in the laboratory and field experiments were based on the following procedures.

4.7.1 Laboratory measurement (falling-head method)

The saturated hydraulic conductivity (K_{sat}) measurements were made on core samples with a length of 10.0 cm and diameter of 8.3 cm in the laboratory (Figure 4.1) using the falling head method developed by Klute and Dirksen (1986). This method operates according to Darcy's law with a one-dimensional, saturated column of soil with a uniform cross-sectional area. The falling-head method differs from the constant-head method in that the water that percolates through the saturated column is kept at an unsteady-state flow regime in which both the head and the discharged volume vary during the test. The soil in the core is held in place by a fine nylon cloth tied with a rubber band and soaked in water until it was saturated. The soaked soil is fitted with another cylinder of the same diameter but of 40 cm of length at the top of the core to allow imposition of a hydraulic head. A large metallic box and plastic with a perforated bottom is filled with gravel (<2 cm). A fast filtration filter paper is place between the soil core and the reservoir. With the core placed on the gravel box, water is gently added to the core to give a hydraulic head in the extended reservoir. The water then flows

through the soil and is collected in the box and drained off by plastic pipe tubing. The fall of the hydraulic head at the soil surface is measured as a function of time using a water manometer with a meter scale. However, time was allowed for water to flow through the soil to ensure uniform flow. The saturated hydraulic conductivity of the soil samples was calculated by the equation:

$$K_{sat} = \left(\frac{AL}{At}\right)\ln\left(\frac{H_1}{H_2}\right) \tag{4.5}$$

K_{sat} is the hydraulic conductivity (LT^{-1}), A is the cross-sectional area of the sample (L^2), H_1/H_2 is the difference in the hydraulic head between the upgradient end of the sample and the down gradient end, L is the length of the sample or the distance over which the head is lost, and t is time.

A problem encountered in using the falling-head method is related to the degree of saturation achieved within the soil samples before and during the test. The presence of air bubbles in the system alters the results, because air bubbles are usually trapped within the pore space, and they tend to disappear slowly by dissolving into the deaerated water. Therefore, after using these instruments to measure K_{sat}, it is always recommended that the degree of saturation of the sample be verified by measuring the volumetric water content of the sample and comparing the results with the total porosity calculated from the particle density. For a more accurate laboratory measurement of K_{sat} in soil samples in which the presence of air bubbles becomes critical, the conductivity test with back pressure is recommended (Radcliffe and Rasmussen 2002). With this method, additional pressure (back pressure) is applied to the pore fluid of the soil sample, which reduces the size of the gas bubbles in the pores, and consequently increases the degree of water saturation.

Figure 4.2 Setup of hydraulic conductivity measurements

4.7.2 Field methods

Method of in-situ determination of saturated hydraulic conductivity of soils can be separated into two groups: (1) methods that are applicable to sites near or below a shallow water table, and (2) methods that are applicable to sites well above a deep water table or in the absence of a water table. More specifically, these groups are applicable to sites located, respectively, in the saturated and unsaturated zones of the soil. In either group (similar to the laboratory methods), the determination of K is obtained from Darcy's law after measuring the gradient of the hydraulic head at the site and the resulting soil water flux.

Many in-situ methods have been developed for determining the saturated hydraulic conductivity of saturated soils within a groundwater formation under unconfined and confined conditions. These methods include (1) the auger-hole and piezometer methods, which are used in unconfined shallow water table conditions (Amoozegar and Warrick 1986), and 2) well-pumping tests, which were primarily developed for the determination of aquifer properties used in the development of confined and unconfined groundwater systems.

The auger-hole method (Porchet method) was used for in-situ determination of the saturated hydraulic conductivity of soils in the Pwalugu and Tindama sites. A hole of 70cm depth with a diameter of 4.5 cm was bored with a hand augur while

maintaining a minimal disturbance of the soil. After preparation of the cavity, water was poured into the augured hole and allowed to drain, and its rate of movement was monitored using a tape measure and a stopwatch until a point of constant movement was reached. Due to the swelling properties of the soil, hydraulic conductivity measurements were performed immediately after the infiltration test, or the ground had been soaked for some hours, or some hours after rainfall. Due to the three-dimensional aspect of the flow pattern of the water near the cavity, there is no simple equation for accurately determining the conductivity. Numerous available semi-empirical expressions that can be used to approximate the hydraulic conductivity for different soil types (Amoozegar and Warrick 1986). However, hydraulic conductivity was estimated on the assumption that the hydraulic gradient is approximately 1, then according to Darcy's law the rate of flow is given by:

$$K = \frac{1.15r\left[\log(h(t_1) + r/2) - \log(h(t_n) + r/2)\right]}{t_n - t_i} \tag{4.6}$$

K represents hydraulic conductivity (length/time), r is radius of the auger hole (length), h is water level in the hole (length) at time t_i initial time and t_n is final time and.

This method is applicable to areas above the water table within homogeneous soil. It provides an estimate of the average horizontal component of the hydraulic conductivity of the soil. Enhanced variations of the method have been developed to account for layered soils and for the determination of either horizontal or vertical components of hydraulic conductivity. Results obtained by the auger-hole method are not reliable for cases in which (1) the water table is above the soil surface, (2) artesian conditions exist, (3) the soil structure is extensively layered, or (4) highly permeable small strata occur.

4.7 Infiltration measurement

Understanding water movement into and through the unsaturated zone of floodplain wetlands is of exceptional importance for the assessment of contaminant fate and transport, the management of agricultural lands, and natural resource protection. The process of water movement is very dynamic, changing dramatically over time and

space. Knowledge of the infiltration process is a prerequisite for understanding and managing soil water flux.

Numerous techniques exist for the estimation of water movement through the vadose zone. API (1996) provides a good review of such techniques, identified as: 1) soil-water balance, 2) lysimeter measurements, 3) Darcy flux method, 4) plane of zero flux method, 5) soil temperature methods, 6) electromagnetic methods, 7) groundwater basin outflow method, 8) water-level fluctuations, 9) stream gauging, 10) chemical tracers and isotopes, 11) chloride mass balance, 12) water balance models, and 13) numerical models based on the Richards equation. However, none of these methods outlined by API (1996) offers a quick and easy way to obtain an estimate of the infiltration rate for the purpose of preliminary analysis and decision-making. Infiltration measurement was done using a doubled ring infiltrometer to reduce the lateral movement of water. The use of two concentric rings reduces the problem of overestimating infiltration in the field due to three-dimensional flows. The measurement was done with each monitor filling the inner and outer rings with water. To minimize lateral flow from the inner ring, the outer ring was constantly filled with water at a constant head. The outer ring supplied water, which contribute to lateral flow so that the inner ring contributed to downward flow. After infiltration measurement, the sharp wetting front at each point of measurement was verified by auguring down to a point where the moisture content is very low.

4.8 Water balance

Application of the water balance approach included quantifying the inputs and outputs of water and storage in the Tindama and Pwalugu floodplain wetlands. The main input of water was from rainfall, and outputs included evapo-transpiration, groundwater and river seepage. Water balance for the wetland and sub-surface of the study area was determined using a simplified open-lake water-balance model (Kedebe et al. 2006) of the form:

$$\text{STORAGE} = \text{INPUTS} - \text{OUTPUTS} \quad (4.7)$$

$$\Delta H = P(t) - E(t) + \left(\frac{R_{in}(t) - R_{out}(t) + G_{net}(t)}{A(h)} \right) + \varepsilon_t \qquad (4.8)$$

Where H is the water level of the wetland [mm], A is the depth-dependent surface area of the wetland [mm], P is the rate of rainfall over the wetland [mm/day], E is evaporation [mm/day], t is time, R_{in} and R_{out} are surface water inflow and outflow [mm/day], G_{net} is the net groundwater flux [mm/day] and ε_i is the error term

4.8.1 Penmann- Monteith method to estimate evapotranspiration.

Evaporation from the wetland is an important component of the water balance model and its accurate determination is important for a reasonable water balance estimate. The Penman-Monteith method has been shown to be suitable for estimating evaporation under a wide range of climatic conditions and time scales (Allen et al. 1998; pg 24). This method combines evaporation as a diffusive process and energy that can be expressed in terms of mass. The assumption is that water advection energy, change in stored energy over time, heat exchange by conduction between the wetlands, and underlying sediments are assumed to be negligible.

$$ET_o = \frac{0.408\Delta(R_n - G) + \gamma \frac{900}{T + 273} u_2 (e_s - e_a)}{\Delta + \gamma(1 + 0.34u_2)} \qquad (4.9)$$

where R_n is the net radiation (MJ m^{-2} day^{-1}), G is the soil heat flux (MJ m^{-2} day^{-1}), (e_s-e_a) represents the vapour pressure deficit of the air (kPa), e_s is saturated vapour pressure (kPa), e_a is actual vapour pressure (kPa), T is the specific heat of the air at 2 m height (k), Δ represents the slope of the saturation vapour pressure temperature relationship, γ is the psychrometric constant (kPa $^oC^{-1}$), and u^2 is wind speed at 2 m height (ms^{-1}).

The Penman-Monteith approach as formulated above includes all parameters that govern energy exchange and corresponding latent heat flux (evapotranspiration) from uniform expanses of vegetation. Most of the parameters are measured or can be readily calculated from weather data. The equation can be used for the direct calculation

of any plant evapotranspiration as the surface and aerodynamic resistances are plant specific.

The transfer of heat and water vapour from the evaporating surface into the air above the canopy is influenced by the aerodynamic resistance:

$$r_a = \frac{\ln\left[\frac{z_m - d}{z_{om}}\right]\ln\left[\frac{z_h - d}{z_{oh}}\right]}{k^2 u_z} \qquad (4.10)$$

Where: r_a aerodynamic resistance [s m^{-1}], z_m height of wind measurements [m], z_h height of humidity measurements [m], d zero plane displacement height [m], z_{om} roughness length governing momentum transfer [m], z_{oh} roughness length governing transfer of heat and vapour [m], k von Karman's constant, 0.41 [-], and u_z wind speed at height z [m s^{-1}].

The equation is restricted for neutral stability conditions, that is, where temperature, atmospheric pressure, and wind velocity distributions follow nearly adiabatic conditions (no heat exchange). The application of the equation for short time periods (hourly or less) may require the inclusion of corrections for stability. However, when predicting potential evapotranspiration (ET_o) in the well-watered reference surface, heat exchanged is small, and therefore stability correction is normally not required (Allen et al. 1998).

4.9 Terrain parameter extraction and preprocessing

A digital elevation model (DEM) is defined as the digital representation of the continuous variation of relief over space (Burrough 1986). Elevation data can be represented digitally in many ways, including a gridded model where elevation is estimated for each cell in a regular grid, a triangular irregular network, and contours. Representation of the DEM as a grid is quite common and lends itself well to automated computations. The DEM, being a mathematical representation of the earth's surface, provides a base data set from which topographic parameters can be extracted digitally (Wood 1996).

DEM data, like other spatial data sets, are subject to errors that are elusive and constitute uncertainty. DEM errors are often not evaluated by DEM users, but incorporated into elevation and derived topographic parameters that affect results of analyses. In fact, any pit that departs from its "true" value will be an error; however, pits (local minima) and peaks (spikes) create problems in topographic analysis.

For the DEM to be hydrologically sound enough to be used for analysis, erroneous depressions should be filled and all pixels should have a defined flow direction. DEMs often have many local minima (pits), many of which are the result of errors in the DEM production process. These erroneous minima cause difficulties for algorithms that simulate water flowing across the landscape, hence the SAGA software was used for removing the pits. The first step in removing the pits was that all depressions were located, after which an algorithm was applied to eliminate all remaining false depressions. The process of removing spurious minima is commonly referred to as pit filling and is the process of changing the relative elevation of the DEM for an area that does not easily route flow. In other words, the elevations of the pixels within a pit were increased until they matched the elevation of the lowest boundary pixel to enable easy flow routing. For instance, routing of water over a surface is closely tied to surface form, therefore, hydrological features such as, slope, flow direction, drainage density, wetness index, flow direction and river network were extracted.

4.10 Statistical analysis

To understand the factors that determine the hydrodynamics of the Pwlaugu and Tindama floodplain wetland, factor analysis was employed to decompose data collected into various factors. Factor analysis is used to study the patterns of relationships among many dependent variables, with the goal of discovering the nature of the independent variables that affect them, even though these independent variables are not measured directly. Insights obtained by factor analysis are necessarily more hypothetical and tentative than is true when independent variables are observed directly. The inferred independent variables are called factors.

Another challenge in conducting factor analysis comes from the presence of competing techniques such as cluster analysis and multidimensional scaling. While factor analysis is typically applied on the basis of correlation matrix, the other methods

can be applied to any sort of matrix of similarity measures, such as ratings of the similarity of faces. But unlike factor analysis, those methods cannot cope with certain unique properties of correlation matrices, such as reflections of variables. For instance, if the scoring direction of a measure is reflected or reversed, such reflections would completely change the output of a cluster analysis or multidimensional scaling. Factor analysis recognizes the reflections for what they are; the reflections would change the signs of the "factor loadings" of any reflected variables, but would not change anything else in the factor analysis output.

The principal components are oriented to provide the maximum separation amongst the observation, implying that the first component is a linear function of the original variables having the maximum variance. The second component has its axis oriented orthogonally to the first component and explains the maximum amount of the residual variance of the sample. Each successive component is independent of the former and explains the residual variance. The unexplained variance gets smaller as subsequent components are added. This gives a likely indication that the dimensionality of samples is less than the number of variables currently being analysed. The principal component is not independent of the scale of the original varieties. The use of correlation matrix standardizes all variables to zero mean and unit variance.

4.11 Models and conceptual framework

The research on floodplain wetlands and river flow interaction was carried out within a framework of hydrological and geographic information system models. The models used were able to recognise the morphological controls on water pathways either theoretically or by experimental processes to enable lateral flow of water to occur widely at different parts of the catchment (Zaslavsky and Sana 1981; Beven 1978). Two models were adopted for the study, namely PMWIN-MODFLOW (Chiang and Kinzelbach 1998) and HYDRUS-1D (McDonald and Harbaugh 1988). These models are capable of simulating the exchange of water between floodplain wetland and stream flow, and within wetlands. These models used were able to fulfill conditions required to conduct a hydrological study in the White Volta basin setting;

- To describe water and hydrological exchange and transformation of wetlands consistent with the geo-hydrology setting of the wetland

- To include all essential inflow and outflows
- To be applicable with commonly available data within a short time

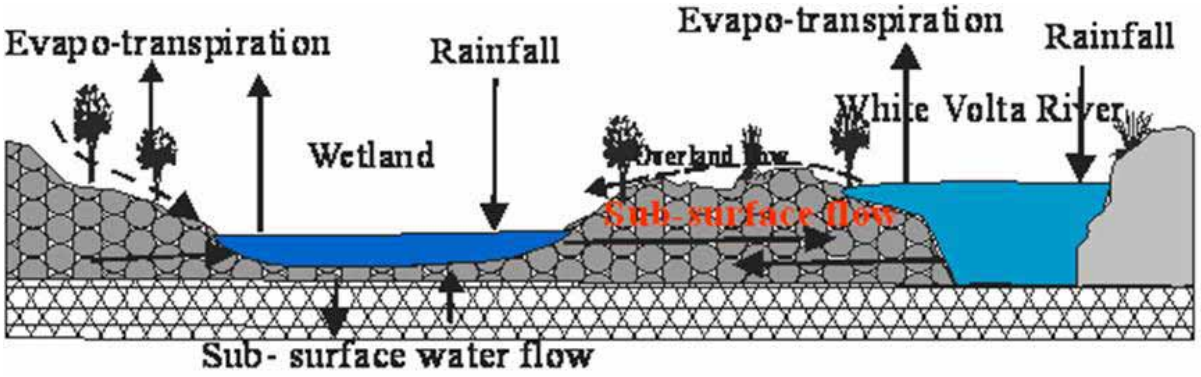

Figure 4.3 Conceptual diagram of floodplain wetland dynamics in the White Volta basin

Conceptually, the inflow pathways within the Pwalugu and Tindama floodplain wetlands in the White Volta basin (Figure 4.3) differ both in the amount of water and in isotope concentrations, which depend on their respective origin (rainfall, surface runoff, over bank flow and groundwater flow) and the processes (evapotranspiration) occurring within the system. In addition, the variation in the volume of inflowing water sources depends on the landscape position of the wetland. Additionally, the morphological and hydrological-geological features determine the flow pattern from the surrounding basin to the wetland. However, the flow pattern inside the wetland is controlled by (1) the thickness and physical parameters of the soil layer, (2) the occurrence of underlying aquifers, and (3) the occurrence of impermeable intercalated layers such as clay, silt or organic mud. The isotope retention results from several biogeochemical and physical processes occurring within the wetland.

4.12 Unsaturated zone -HYDRUS-1D

The unsaturated zone is an integral part of the hydrological cycle and plays a role in many aspects of hydrology such as infiltration, soil moisture storage, evaporation, groundwater recharge, runoff and plant water uptake. HYDRUS-1D was used to describe the hydrodynamics of the unsaturated zones of the wetlands. This is a finite element model that solves Richard's equation for saturated and unsaturated water flow. The model simulates water movement in unsaturated, partially saturated or fully

saturated porous media, which may be either uniform or non-uniform. The main equation used in the model is Richard's equation:

$$\frac{\partial \theta}{\partial t} = \frac{\partial}{\partial z}\left[K(h)\frac{\partial h}{\partial z} + K(h) \right] - S(h) \qquad (4.11)$$

where θ is the volumetric soil water content [cm^3 cm^{-3}], t is time [d], h is the soil-water pressure head [cm], z is the gravitational head and the vertical coordinate [cm] (upwards is positive), $K(h)$ is the unsaturated hydraulic conductivity [cm/d^{-1}], and S is the soil water extraction rate by plant roots [cm^3 /cm^{-3} d^{-1}].

The classical Richards-flow theory (Richards 1931), upon which most simulation models are based, holds for stable flow conditions only. Yet instability of flow has been observed under a wide variety of circumstances such as abrupt and gradual increases of hydraulic conductivity with depth, compression of air ahead of the wetting front and water repellency of the solid phase. Another example of non-Richards type flow is the preferential flow through non-capillary macropores. Classical flow theories may therefore underestimate the velocity and depth of infiltrating water.

4.12.1 Soil hydraulic properties

HYDRUS-1D solve Richards equation by establishing relationships between soil water retention θ(h) and hydraulic conductivity K(h) which are nonlinear functions of pressure head and water content. However, HYDRUS-1D permits the use of four alternative analytical models for determining soil hydraulic properties, namely: Brooks and Corey, Van Genuchten-Mualem, Kosugi and modified Van Genuchten.

In modeling the unsaturated flow in the floodplain wetlands, the van Genuchten-Mualem, an analytical model, was used to predict and describe the soil water retention parameters expressed as:

$$\theta(h) = \begin{cases} \theta_r + \dfrac{\theta_s - \theta_r}{\left[1 + |\alpha h|^n\right]^m} & for\ h <= 0 \\ \theta_s & for\ h >= 0 \end{cases} \qquad (4.12)$$

The relationships between water retention and pressure head as expressed above have five parameters that define the shape of the function, θ_s saturated porosity of the soil, θ_r residual moisture content, K_s saturated hydraulic conductivity, α the inverse of the air entry value (or bubbling potential), and, n a pore size distribution index.

The hydraulic conductivity function in HYDRUS-1D is described by the van Genuchten-Mualem pore size distribution model in which the relationship is expressed as:

$$k(h) = K_s S_e^l \left[1 - \left(1 - S_e^{1/m}\right)^m\right]^2 \tag{4.13}$$

where

$$m = 1 - \frac{1}{n}; \qquad S_e = \frac{\theta - \theta_r}{\theta_s - \theta_r} \tag{4.14}$$

S_e is effective saturation, and l is pore connectivity parameter estimated to an average of 0.5 for most soils.

4.12.2 Initial conditions

To model the transient soil water flow, initial soil moisture contents were defined at each nodal point within the soil profile. The values of matric head or soil water content at each nodal point within the soil profile are required. However, when these data are not available, water contents at field capacity or those in equilibrium with the groundwater table were assumed as initial values.

4.12.3 Upper boundary conditions

The upper boundary condition of the soil depends on atmospheric conditions and the actual flux through the soil surface is limited by the ability of the soil matrix to transport water. Similarly, if the potential rate of infiltration exceeds the infiltration capacity of the soil, part of the water runs off, since the actual flux through the top layer is limited by moisture conditions in the soil. However, the exact boundary conditions at the soil surface cannot be estimated a priori, and solutions must be found by maximizing the absolute flux. The minimum allowed pressure head at the soil surface was estimated from the equilibrium conditions between soil water and atmospheric vapour. In case of ponding, the height of the ponded water as a function of time is usually given. However, when the soil surface is at saturation, then the problem is to define the depth in the soil

profile where the transition from saturation to partial saturation occurs. In this case, the prescribed pressure head was assigned on the assumption that the pressure head at the soil surface is at equilibrium with the atmosphere.

4.12.4 Lower boundary conditions

At the lower boundary, three different types of conditions can be defined: (1) Dirichlet condition in which the pressure head is specified, (2) Neumann condition in which the flux is specified, and (3) Cauchy condition. The phreatic surface is usually taken as the lower boundary of the unsaturated zone in the case where recorded water table fluctuations are known a priori. Then the flux through the bottom of the system can be calculated.

A flux at lower boundary condition is usually applied in cases where one can identify a no-flow boundary (e.g., an impermeable layer) or a free drainage case. In the latter case, the flux is always directed downward and the gradient $dh/dz = 1$, so the Darcian flux is equal to the hydraulic conductivity at the lower boundary. In regions with a very deep groundwater table, a Neumann type of boundary condition is used.

4.12.5 Required input data

Simulation of water dynamics in the unsaturated zones requires input data concerning the model parameters, the geometry of the system, the boundary conditions and, when simulating transient flow, initial conditions. The dimensions of the problem domain are defined via geometry parameters. The physical properties of the system under consideration are described via the physical parameters. With respect to the unsaturated zone, these include the soil water characteristic, $\theta(h)$, and the hydraulic conductivity, $K(h)$. For a proper description of the unsaturated flow, a correct description of the two hydraulic functions, $K(h)$ and $\theta(h)$, is important. The hydraulic conductivity, decreases strongly as the moisture content decreases from saturation. The experimental procedure for measuring $K(h)$ at different moisture contents is rather difficult and not very reliable. Alternative procedures have been suggested to derive the $K(h)$ function from more easily measurable properties characterizing the soil. In many studies, the hydraulic conductivity of the unsaturated soil is defined as a product of a nonlinear function of the effective saturation and hydraulic conductivity at saturation.

4.13 Processing MODFLOW (PM-WIN)

MODFLOW is a quasi-three-dimensional finite-difference groundwater model, which has a modular structure that allows easy modification to adapt to a particular application. PM-WIN simulates steady and nonsteady flow in an irregularly shaped flow system in which aquifer layers can be confined, unconfined, or a combination of confined and unconfined. Flow from external stresses, such as flow to wells, areal recharge, evapotranspiration, and flow through river beds or walls can be simulated. Hydraulic conductivities or transmissivities for any layer may differ spatially and may be anisotropic (restricted to having the principal directions aligned with the grid axes), and the storage coefficient may be heterogeneous. Specified head and specified flux boundaries can be simulated as a head-dependent flux across the model's outer boundary, which allows water to be supplied to a boundary block in the modeled area at a rate proportional to the current head difference between a source of water outside the modeled area and the boundary block. The layer type depends on the Block-Centered-Flow formulated numerically to describe groundwater flow. Two layer types for this study were defined, namely:

- Type 1 The layer is strictly unconfined. The option is valid for the first layer only. Specific yield is used to calculate the rate of change in storage for this layer type. During a flow simulation, transmissivity of each cell varies with the saturated thickness of the aquifer.
- Type 3 A layer of this type is fully convertible between confined and unconfined. Confined storage coefficient (specific storage × layer thickness) is used to calculate the rate of change in storage if the layer is fully saturated, otherwise specific yield will be used. During a flow simulation, transmissivity of each cell varies with the saturated thickness of the aquifer. Vertical leakage from above is limited if the layer desaturates.

4.13.1 Horizontal hydraulic conductivity and transmissivity

The horizontal hydraulic conductivity is the hydraulic conductivity along model rows multiplied by an anisotropy factor specified in the layer option to obtain hydraulic conductivity along the model columns. Transmissivity is calculated as follows;

$$\text{Transmissivity} = K_s \times m \quad (4.15)$$

K_s is horizontal hydraulic conductivity [L/T] and m is layer thickness [L]

Transmissivity is calculated if the horizontal hydraulic conductivity and the elevations of the top and bottom of each layer is specified. However, it can be specified manually by the modeler.

4.13.2 Vertical hydraulic conductivity and vertical leakance

This is used when more than one model layer is used. MODFLOW requires the input of the vertical conductance term, known as vertical leakance (VCONT), between two model layers. The vertical leakance between layers is required for the bottom layer; the model assumes that the bottom layer is underlain by semi-permeable material.

In most cases, VCONT needs to be calculated manually, because the model represents resistance to flow in a low hydraulic conductivity unit by lumping the vertical hydraulic conductivity and thickness of the confining unit into a vertical leakance term between the adjacent layers. These kinds of models are often called quasi three-dimensional models, because semi-confining units are not explicitly included and simulated.

4.13.3 Specific storage, storage coefficient and specific yield

For transient flow simulations, MODFLOW requires dimensionless storage terms specified for each layer. In a confined layer, the storage term is given by storativity or confined storage coefficient (=specific storage [1/L] × layer thickness [L]). The storativiy is a function of the compressibility of the water and the elastic property of the soil matrix. The specific storage or specific storativity is defined as the volume of water that a unit column of aquifer releases from storage under a unit decline in hydraulic head. The specific storage ranges in value from 3.3×10^{-6} [1/m] of rock to 2.0×10^{-2} [1/m] of plastic clay (Domenico 1972).

PM-WIN uses specific storage and the layer thickness to calculate the confined storage coefficient. In a phreatic (an unconfined) layer, the storage term is given by specific yield or drainable porosity. Specific yield is defined as the volume of water that an unconfined aquifer releases from storage per unit surface area of aquifer

per unit decline in the water table. Specific yield is a function of porosity and is not necessarily equal to porosity, because a certain amount of water is held in the solid matrix and cannot be removed by gravity drainage.

4.13.4 Boundary condition

In MODFLOW, boundary conditions need to be specified, and there is an array of codes for each cell. In the boundary condition (IBOUND), a positive value in the array defines an active cell (the hydraulic head is computed), a negative value defines a fixed-head cell (the hydraulic head is kept fixed at a given value), and the value 0 defines an inactive cell (no flow takes place within the cell). Specifying a boundary condition, the use of 1 implies active cells, 0 inactive cells and -1 fixed-head cells. If a fixed-head cell is specified, the initial hydraulic head remains the same throughout the simulation. A fixed-head boundary supplies a continuous amount of water and is specified whenever an aquifer is in direct hydraulic contact with a river, or a reservoir (wetland) if the water level is known.

4.14 Application of isotopes in wetlands studies

Isotope tracers have been the most useful in terms of providing new insights into hydrologic processes, because they integrate small-scale variability to give an effective indication of catchment-scale processes (Kendell and McDonnell 1998). In particular, oxygen-18 ($\delta^{18}O$) and deuterium ($\delta^{2}H$) are integral parts of natural water molecules that fall as rain each year over a watershed and, consequently, are ideal tracers of water. The application of isotope tracers is to study wetland-river-flow interaction by using varying behaviors of isotopes during phase changes (Clark and Fritz 1997). During phase changes (evaporation and condensation) the accumulation of heavier isotope $\delta^{18}O$ and $\delta^{2}H$ in the liquid phase rather than the vapour phase is caused by fractionation.

Isotopic concentrations are generally reported and expressed as the difference between the measured ratios of the sample and reference over the measured ratio of the reference. This is expressed using (δ) notation:

$$\delta = \frac{\left({}^{18}O/{}^{16}O\right)_{sample} - \left({}^{18}O/{}^{16}O\right)_{reference}}{\left({}^{18}O/{}^{16}O\right)_{reference}} \tag{4.16}$$

During the process of isotopic fractionation it does not impart huge variations in isotope concentrations; hence δ-values are expressed as part per thousand or per mil (‰)

$$\delta^{18}O_{sample} = \left[\frac{\left({}^{18}O/{}^{16}O\right)_{sample}}{\left({}^{18}O/{}^{16}O\right)_{reference}} - 1\right] * 1000‰ \text{ VSMOW} \tag{4.17}$$

Isotope fractionation is a natural physical phenomenon that causes changes in the relative abundance of isotopes due to their differences in mass (Clark and Fritz 1997; Mook 2000). Hydrogen and oxygen isotopes of water vary through the process of fractionation in the atmosphere, rivers and wetland reservoirs in time and space. The fractionation process is accompanied by phase change, transportation, diffusion, reduction, oxidation, chemical reaction and biological metamorphism. Isotope fractionation can occur by either equilibrium or kinetic fractionation during atmospheric circulation.

Isotope fractionation occurs in any thermodynamic reaction due to differences in the rate of reaction for different molecular species. The result is a disproportionate concentration of one isotope over the other on one side of the reaction (Clark and Fritz 1997; Mook 2000). This is expressed by the fractionation factor α which is the ratio of the isotope ratios for the reactant and the product (Clark and Fritz 1997; Mook 2000):

$$\alpha_{l-v} = \frac{R_{reactant}}{R_{product}} \tag{4.18}$$

$$\text{e.g. } \alpha^{18}O_{l-v} = \frac{\left({}^{18}O/{}^{16}O\right)_l}{\left({}^{18}O/{}^{16}O\right)_v} \tag{4.19}$$

The value of α is always close to one and can be expressed in the form of 10^3 ln α.

$$10^3 \ln \alpha_{l-v} = 10^3 \ln \frac{1+\delta_{vap} \times 10^{-3}}{1+\delta_{liq} \times 10^{-3}} \quad (4.20)$$

The enrichment factor, ε, is another way to express fractionation and is express as ‰ values. The ε-factor is defined by the formula below (Clark and Fritz 1997):

$$\varepsilon_{l-v} = \left(\frac{R_X}{R_Y} - 1 \right).10^3 = (\alpha - 1).10^3 \quad (4.21)$$

$\varepsilon_{l\text{-}v}$ is enrichment factor from liquid to vapour phase

4.14.1 Kinetic fractionation

Kinetic fractionation occurs when one isotope reacts more rapidly than the other in an irreversible system, in other words the reactants are swept away from each other before they have an opportunity to come to equilibrium. This is an irreversible physical or chemical process. Processes such as evaporation, chemical dissociation reactions, biological mediated reactions and diffusion are a few of the kinetic fractionation process that are unidirectional (Clark and Fritz 1997). This can be defined as:

$$K = \frac{R_{X'}}{R_Y} = \alpha_{X-Y} \quad (4.22)$$

K is the thermodynamic constant of the partition ratio, R_X is isotope ratio in the sample and R_Y is the standard isotope ratio in Vienna Standard Mean Ocean Sea Water (VSMOSW)

4.14.2 Temperature effect

Temperature within any environment is an important controlling factor on the isotopic composition of rainfall or water stored in rivers and wetlands. Temperature changes do affect the enrichment in heavier isotopes, but in a linear relationship (Clark and Fritz

1997). Temperature is noted to affect fractionation at a rate of approximately 5‰ for every 100 ^{o}C for oxygen (Clark and Fritz 1997). In addition, similar effects are experience with increasing elevation and increased distance from the equator (both of which correspond to lower temperature). To understand and verify the effect of temperature on isotope fractionation on $\delta^{18}O$ and $\delta^{2}H$ the following equation can be used (Majoube 1971).

$$10^3 \ln\alpha^2 H_{l-v} = 24.844\left(10^6/T^2\right) - 76.248\left(10^3/T\right) + 52.612 \quad (4.23)$$

$$10^3 \ln\alpha^{18} O_{l-v} = 1.137\left(10^6/T^2\right) - 0.4156\left(10^3/T\right) - 2.0667 \quad (4.24)$$

T represents temperature (Kelvin)

4.14.3 Meteoric water line

Within the process of the hydrological cycle and at each step, $\delta^{18}O$ and $\delta^{2}H$ has been noted to behave in a predictable manner (Clark and Fritz 1997). Craig (1961) noted that $\delta^{18}O$ and $\delta^{2}H$ correlate on the global scale thereby this relationship is defined by the Global Meteoric Water Line (GMWL) is expressed using the equation stated:

$$\delta^2 H = 8 * \delta^{18} O + 10 \quad (4.25)$$

The slope of 8 is due to cloud condensation at 100 % relative humidity, while the intercept of 10 – called the Deuterium excess – is caused by an average 10% kinetic enrichment of Deuterium during evaporation from the ocean surface (Kendall and McDonnell 1998; Clark and Fritz 1997). The meteoric water line averages many local or regional meteoric water lines, which show some variance from the GMWL. The regional and local meteoric waterlines differ from the GMWL in both slope and deuterium excesses; this is as a result of climatic difference and other geographical factors such as altitude and distance from the sea.

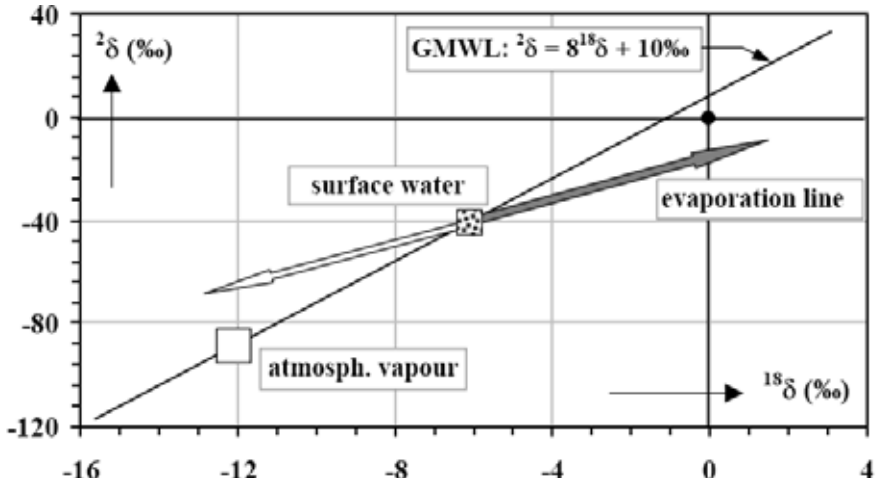

Figure 4.4 Relation between the $\delta^{18}O$ and $\delta^{2}H$ values of meteoric water which undergoes evaporation, the vapour leaving the water and the residual water following evaporation, described by the evaporation line, compared with the relationship between atmospheric water and precipitation described by the meteoric water line. The relatively "light" (depleted) water vapour leaves the water reservoir (open arrow) causing the residual water to become enriched (grey arrow) (www.iaea.org)

4.14.4 Evaporation of water

The rate of evaporation limits vapour-water exchange and the degree of isotopic equilibrium. Evaporation from wetland and river surface fractionates the isotopes of hydrogen and oxygen in a manner, which depends on mostly atmospheric humidity (Kendall and Caldwell 1998). A higher humidity does have a change in $\delta^{18}O$ and $\delta^{2}H$ during evaporation processes. Therefore, the slope of evaporation line is less than eight (8) when $\delta^{18}O$ is plotted against $\delta^{2}H$, in other words, data from evaporated surface water falls below the Global meteoric water line (GMWL) but intersect the GMWL at the composition of the original water (Figure 4.4).

The principal observation is that during evaporation water becomes progressively enriched in both $\delta^{18}O$ and $\delta^{2}H$, but it is affected by relative humidity (Clark and Fritz 1997). If there is no exchange with the vapour phase as humidity remains close to 0% the enrichment follows a Rayleigh distillation. Rayleigh distillation is an exponential function that describes the progressive partitioning of heavy isotopes into the wetlands and rivers, as they diminish in size and volume because of seasonal variation (Clark and Fritz 1997).

$$R = R_o f^{(a-1)} \tag{4.26}$$

$$\delta^{18}O_{final} = \delta^{18}O_{initial} - \varepsilon^{18}O_{l-v}.\ln f \tag{4.27}$$

with

$$\varepsilon_{l-v} = \varepsilon^{*}{}_{l-v} + \Delta\varepsilon_{l-v} \tag{4.28}$$

R is isotopic ratio in a diminishing reservoir which is a function of R_o, the initial isotopic ratio of water; *f* is the remaining fraction of that reservoir and α the equilibrium fractionation factor. $\varepsilon^*_{l\text{-}v}$ is equilibrium enrichment factor for a system when relative humidity is 100%.

Hence, the interface between water surface and air produce a balance between these two opposing water fluxes, with an upward movement from the water surface and downward movement of atmospheric moisture. In an environment with a high humidity of near saturation, the upward and downward physical fluxes can become equivalent and their isotopic compositions may then reach equilibrium. Therefore, a net evaporative flux is produced when air humidity is under saturated (h < 100%). The rate that determines the evaporation step is the diffusion of water vapor across the air boundary layer, this occurs in response to the humidity gradient between the surface and the fully turbulent ambient air (Clark and Fritz 1997). Kinetic effect (Figure 4.5) can be described in terms of humidity with the following relationship (Clark and Fritz 1997):

$$\varepsilon^{18}0_{bl-v} = 14.2(1-h)‰ \tag{4.29}$$

$$\varepsilon^{2}H_{bl-v} = 12.5(1-h)‰ \tag{4.30}$$

ε-kinetic fractionation factor, h-humidity.

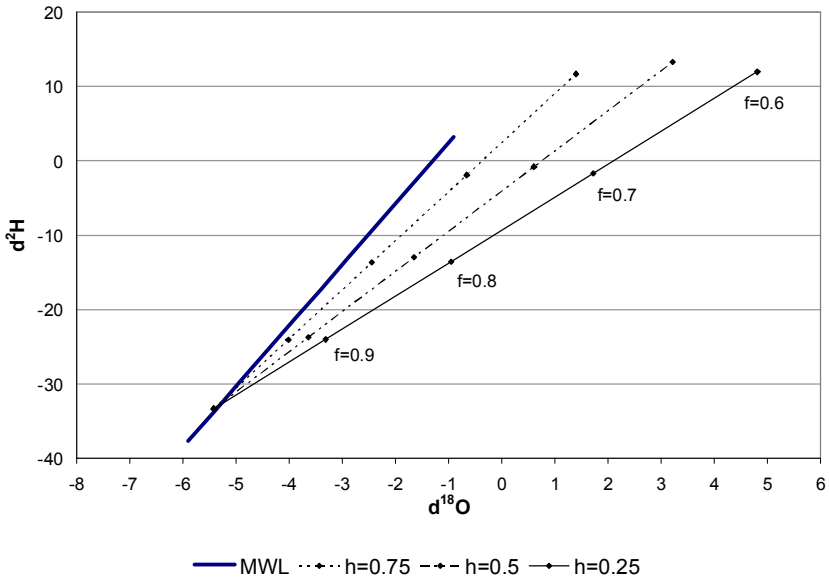

Figure 4.5 Kinetic isotopic enrichment during evaporation at different humidity's in Atankwidi catchment, White Volta, Ghana (Martins 2005).

4.15 Model evaluation

The root mean squared error was used to evaluate the predictive ability of the model. The root mean squared error (RMSE) quantifies the error or difference between the observed and predicted values. This difference helps in deriving useful information about the nature of the error. The RMSE has the same units as the predicted and observed values. The root mean square error estimator is expressed as:

$$RMSE = \sqrt{\frac{\sum_{i=1}^{n}(P_i - O_i)^2}{N}} \tag{4.31}$$

where N is the number of paired observations, P is the predicted value, and O is the observed value.

Another model diagnostic is the index of agreement (d) (Mulligan and Wainwright 2004). This is a dimensionless value that gives an overall assessment of the prediction accuracy by describing the degree to which O is approached by P. The index of agreement is calculated as:

$$d = 1 - \left[\frac{\sum_{i=1}^{N} |P_i - O_i|}{\sum_{i-1}^{N} \left[\left(P_i - \overline{O} \right) + \left(O_i - \overline{O} \right) \right]} \right] \tag{4.32}$$

where the resulting d has a value ranging from 0.0 to 1.0 (0.0 signifies no agreement, and 1.0 means a perfect fit between the observed and predicted values).

5 FLOODPLAIN-WETLAND MAPPING WITHIN THE WHITE VOLTA RIVER BASIN

5.1 Introduction

From visual inspection of 1967 aerial photographs of the Upper East Region of Ghana, wetlands in the White Volta basin vary in shape, size and accessibility. Hence, an inventory of floodplain wetlands in the basin and determining their characteristics are important for modeling environmental flows and assessing their contribution to the livelihood of the communities within the catchment. The use of remote sensing techniques for a quick inventory and to determine the characteristics of wetlands are well developed, but to some extent are not operational within the sub-Saharan Africa region (Smith 1997; Mejerink 2002). However, the increase in satellite orbital precision and the availability of multi-temporal satellite data have enabled the estimation of land area, river stage and discharge from space in most developed parts of the world (Lyon 1995; Smith 1997; Jain et al. 2001). Three general approaches have emerged in the use of aerospace techniques for wetland studies:

- Direct measurement of water surface elevation from radar altimeter waveform data;
- Determination of water surface elevations at their point of contact with the land surface using high-resolution satellite imagery and topographic data; and
- Correlation of satellite-derived water surface areas with ground measurements of stage or discharge.

Modeling floodplain wetlands and determining their location has been enhanced with the advent of remote sensing imagery and GIS capabilities (Van de Giesen 2001; Mejerink 2002). These techniques in earth sciences have made it possible to formulate and execute different methods that assist in predicting and getting an overview of floodplain wetland present in the White Volta basin. This chapter discusses the method used to map floodplain wetlands within the White Volta basin. For wetland mapping within the White Volta basin three (3) main stages were adopted; 1) extraction of hydrotopes, 2) points sampling, and 3) floodplain wetland extraction using logistic regression analysis.

5.2 Hydrotope identification and predictors extraction

The concept of hydrotopes was applied to enable the maximization of the application of remote sensing and geographic information system in the process of floodplain wetland mapping. The data sets were derived on the basis of image processing and related to other derived mapping outputs. The assumption here is to conceptually derive zones of similar hydrological response units. The zones derived are expressions of the spatial distribution of parameters influencing floodplain wetlands within the White Volta basin. Different hydrotope data sets that related spatially were identified (Table 5.1) and incorporated into the process of modeling and mapping of floodplain wetlands in the White Volta basin.

Table 5.1 Description of hydrotopes used for floodplain wetland mapping

	ID	Description
Topographic	Slope	Slope in degrees [degree]
	Shape	Shape of the topography (convex, concave or straight) [-]
	Wetness	Zone of saturation [-]
	Power	Stream power index [-]
	Height	Elevation data derived from the SRTM-DEM [m]
	Internal	Internal relief [m/km^2]
Environmental	Ndvi	Normalized Difference Vegetation index [-]
	Savi	Soil Adjusted Vegetation Index [-]
Climatic	Evapo	Evapotranspiration calculated by SEBAL [mm/day]
Image	Texture	Pattern in pixel brightness [-]
	LogB4	Logarithm Transformation of Band 4 of 30 October, 2000, satellite image [-]
Spatial	Distance	Distance estimated from the main river [m]

Within the White Volta basin, variables that could assist in predicting the location of wetlands were not very clear, but there was a need for a quick inventory to

select sites for detailed study. Therefore, variables that are likely to play a role in establishing a trend in which wetlands location can be determined were assembled. Five main predictor groups were identified, and within these groups 12 predictors (Table 5.1) and a dependent were selected to assist in maximizing the predicting power of the logistic regression model.

5.2.1 Topographic predictors

Most of the topographic variables such as slope, topographic wetness, stream power index, shape (concave, convex or straight), internal relief and height were derived from the SRTM-DEM, which were re-sampled to 30m resolution within the ENVI 4.0 and ILWIS 3.3 software environment. Many hydrologic processes are related to topographic surface parameters such as elevation, slope, wetness index, topographic shape, stream power index and internal relief. In the absence of detailed topography survey data and accurate DEM from the Ghana Survey Department, the alternative SRTM-DEM from USGS was the only reliable source for topographic extraction of the Upper East Region within the Volta basin. Like any other spatial data, SRTM-DEM was taken as a true representation of the topography in the basin after it was corrected with ground truth data collected using differential GPS. Soil and geological map components of the defined topographic layer were acquired from the Soil Research Institute and Geological Survey Service in Ghana. Surface topography, which controls the flow sources, flow direction and soil moisture concentration are important parameters indicating the presence of wetlands. Stream power index is the product of catchment area and slope used to identify areas where surface runoff is concentrated. The stream power index was transformed into different data sets using the logarithm method. This transformation was necessary because of high variances within the data. Internal relief and topographic wetness are defined below:

- Internal relief explains the maximum elevation changes within a km^2 of land.
- Topographic wetness is the spatial distribution and zones of saturation or variable sources for runoff generation.

5.2.2 Environmental predictors

Environmental predictors are vegetation-based indices extracted from the mosaic Landsat-ETM scene. The indices are Normalized Difference Vegetation Index (NDVI) and Soil Adjusted Vegetation Index (SAVI). NDVI was calculated (equation 5.1) from the ratio between TM bands 4 and 3, while SAVI was calculated (equation 5.2) to minimize the effect of soil background on vegetation signal by incorporating a constant into the NDVI equation. The constant 0.5 was chosen because an intermediate density of vegetation in the study area was observed in the field during the period of October 2005. SAVI (Figure 5.1) exhibits a greater sensitivity to partial ground cover than NDVI.

$$NDVI = \frac{IR - RED}{IR + RED} \tag{5.1}$$

$$SAVI = \frac{IR - RED}{IR + RED} * (1 + L) \tag{5.2}$$

IR = near infra-red; RED = the red channel, L = soil adjustment factor

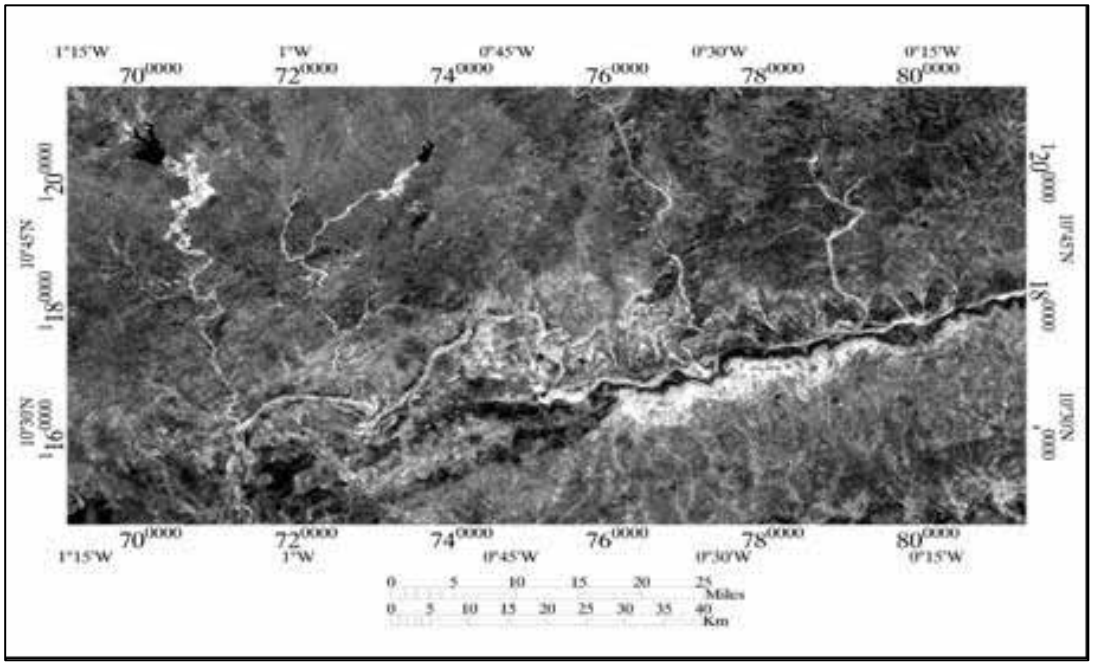

Figure 5.1 Soil adjusted vegetation index of 30 October 2002 image to reduce the effect of soil background on vegetation

5.2.3 Image predictors

Image predictors were derived from digital images of Landsat-ETM of 30 October 2002. This image was used because it was clearest image after the rainy season in which wet conditions could be captured. The spectral band 4 ETM satellite image was selected because of its high potential for delineating water bodies and discriminating soil moisture. This was transformed into $\log_{10}$ to reduce the variance in the image and sharpen it to clearly show the likely moist areas (Figure 5.2). Texture occurrence measure filters were applied to the satellite image. Texture is the spatial distribution of the intensity values in the image, which contains information regarding contrast uniformity, rugosity and regularity (Lillesand and Kiefer 2000). The adoption of texture in this process is because each band accentuates certain characteristics of the data that could contribute to floodplain wetland mapping. The variance of the texture band 4 was selected as part of the variables for analysis (Figure 5.3).

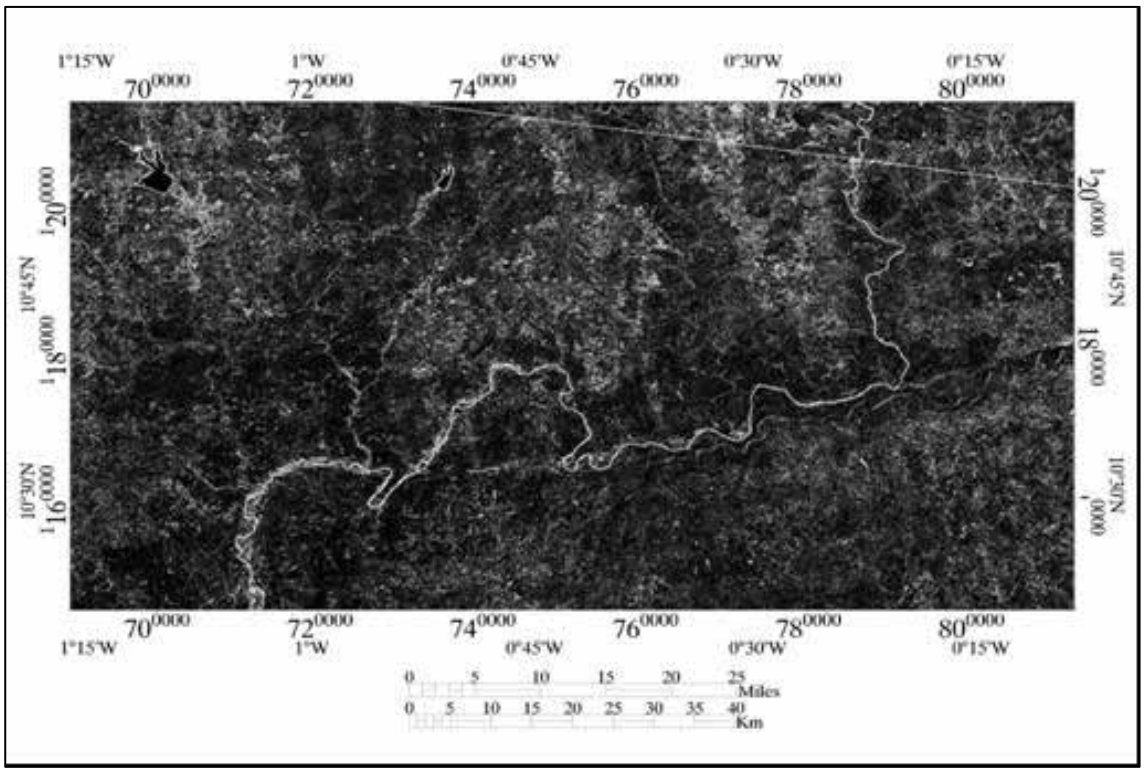

Figure 5.2 Logarithm transformation of spectral band 4 of 30 October 2002 ETM image to reduce variance and sharpened to clearly show moist areas

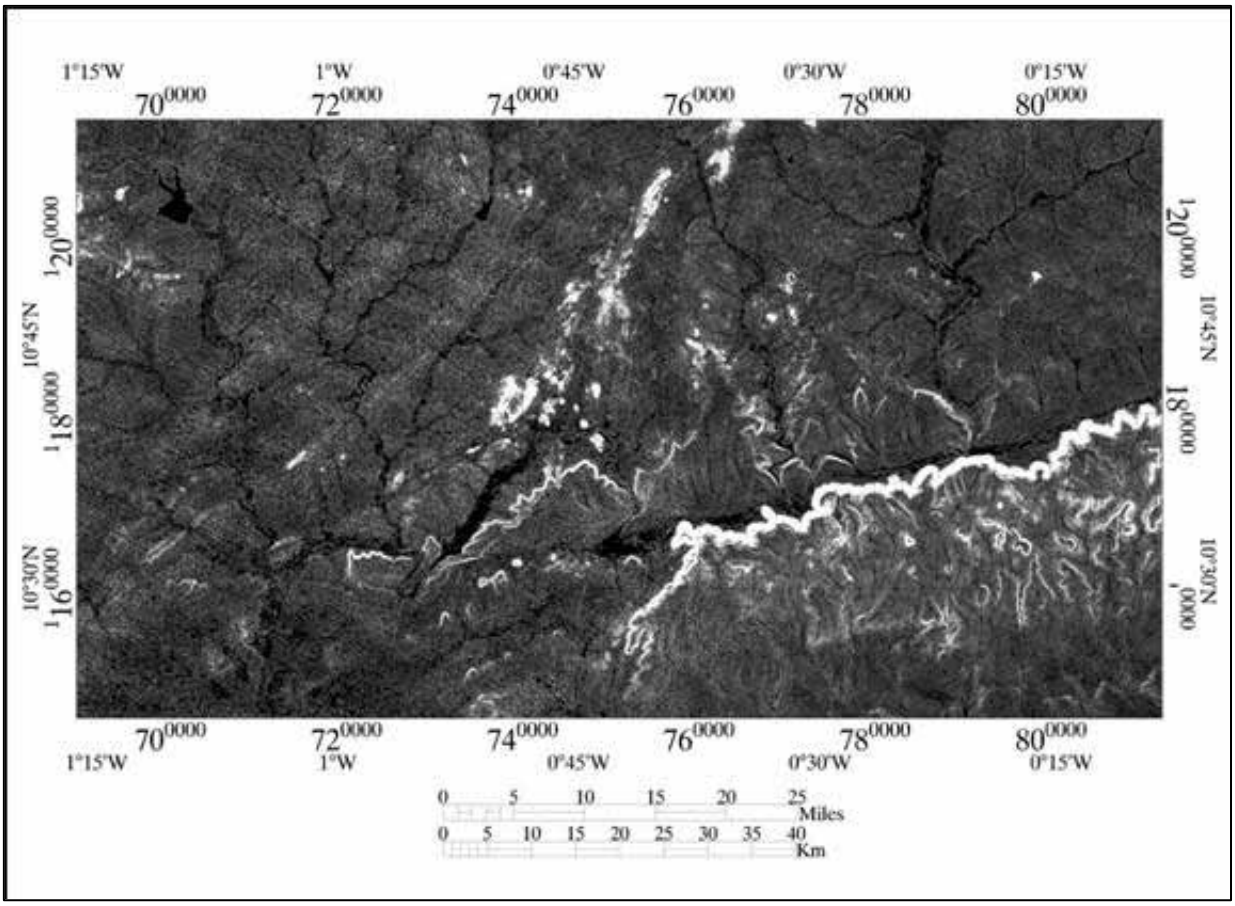

Figure 5.3 Texture filter applied to ETM band 4 to accentuate uniformity, rugosity and regularity in the image

5.2.4 Climatic predictor

The main climatic predictor used in the automated identification of wetland areas was the 30 October 2002 evapotranspiration map of the Upper East region (Figure 5.4). This climatic predictor was extracted from Compaore (2005), who calculated it using the surface energy balance algorithms (SEBAL). Wetland sites with high moisture and vegetation indicated high evapotranspiration value as compared to low vegetative areas. In the floodplain wetland areas, high rates of evapotranspiration are possible due to advection of heat and dry air from the surrounding dry land, which enhances rate of water loss.

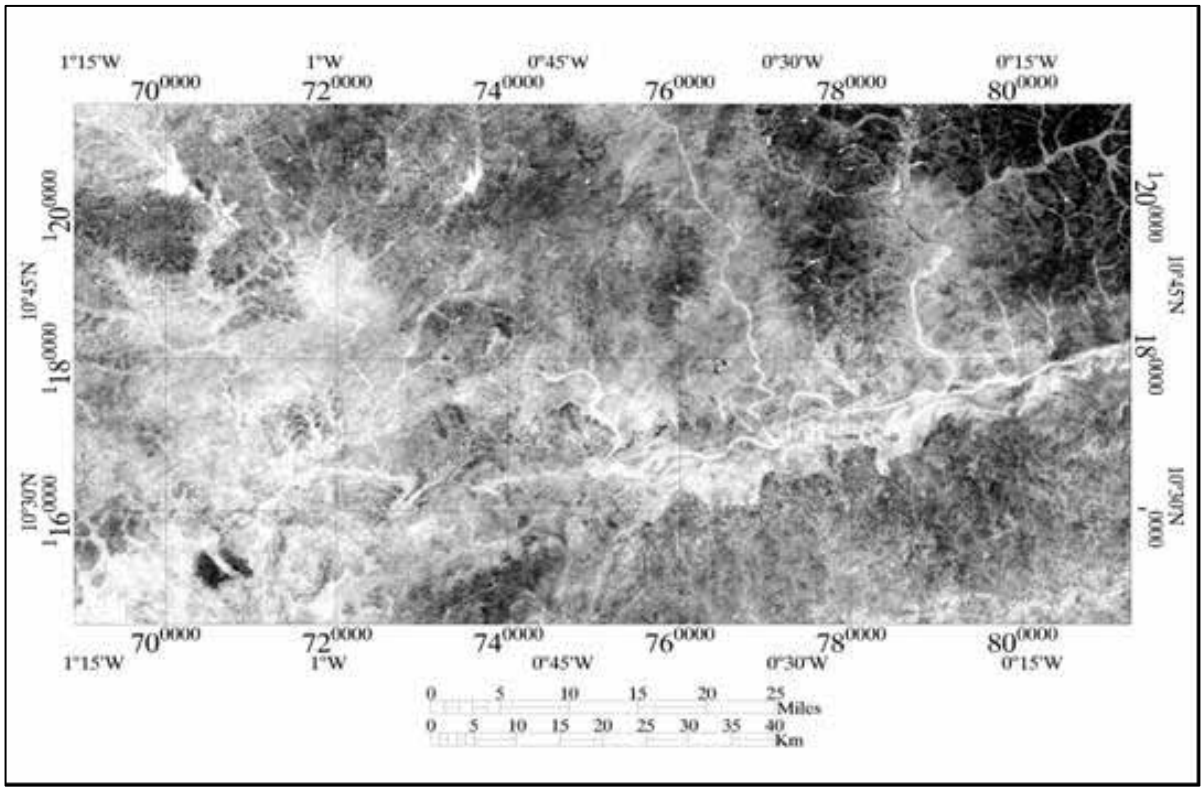

Figure 5.4 Evapotranspiration image of study area derived using the SEBAL algorithm for 30 October 2002 (Compaore 2005)

5.3 Spatial metric

Location and occurrence of floodplain wetlands from the main river, play an important role in its classification. Floodplain wetlands by definition occur along the margins of main river channels, the search domain was further limited by identifying all areas within a pre-selected distance from perennial river courses within the study area. Using the river network of the study area, a distance map was created; pixels were assigned values representing distance. The distance filter in ILWIS 3.3 was used to calculate distance.

5.4 Land cover classes extraction

The extraction of the land cover classes of the White Volta basin was part of the process of providing information to describe and interpret the landscape. Knowledge gained through the extraction gave a momentum for modeling and predicting processes to locate floodplain wetlands in the basin. Therefore, a combination of contextual and knowledge methods was used, which offered a strong platform for conceiving and

defining rules based on the data characteristics and the inherent spatial relationships for modeling the location of the floodplain wetland.

The first activity in the land cover class extraction using 30th October 2002 image was to become familiar with features in the basin. Unsupervised classification, using the ISOCLASS algorithm (Lillesand and Kiefer 2000), was performed for exploring the cover types. However, with this process, there was no control over the nature of the classes, the final classes were relatively homogeneous but did not correspond to any useful land cover classes. Using ground-based knowledge after a detailed field survey during 2004 and 2005, a supervised classification was performed using the maximum likelihood classifier on the selected satellite data sets, which resulted in eight classes in the region (Figure 5.5). The maximum likelihood estimates method was applied to extract land cover classes by generating a correlation matrix for training sample pixel from a multivariate normal pixel distribution. Using the maximum likelihood method, variable correlation was weighted by the inverse of the uniqueness of the variables, hence an iterative algorithm was employed to generate cover classes.

The maximum likelihood method has an advantage over other methods because of its probability theory (Lillesand and Kiefer 2000). However, in using such a method, the following was taken into consideration:

- Sufficient ground truth data need to be sampled for estimating the mean vector and the variance-covariance matrix of population.
- The inverse matrix of the variance-covariance matrix becomes unstable in the case where very high correlation between two bands or the ground truth data are very homogeneous. In such cases, a number of new variables were created using principal component analysis.
- The maximum likelihood method is not applicable to situations where population distribution is not normally distributed.

The accuracy assessments of the classes were evaluated in the field to verify how close the classification conformed to the real situation on the ground. The results of land cover class classification gave an overall accuracy of 96.79%. The overall accuracy assessment gives credence to the fact that the classes specified were easily distinguishable.

The Kappa coefficient (K) has a maximum of 1 and a minimum of 0 computed as:

$$K = \frac{P_{correct} - P_{chance}}{1 - P_{chance}} \quad (5.3)$$

$P_{correct}$ is the proportion of correctly classified pixels and P_{chance} is the proportion of sampled pixels to be classified correctly by chance.

A kappa coefficient of 0.96 indicated a high probability of the proportion of pixels that were classified correctly by assigning classes and also by chance. The producer accuracy of over 91% enabled verifying how well areas within the White Volta River basin could be mapped (Table 5.2). The user accuracy of 89.60% and above indicated how well pixels representing a feature or cover class could be found on the ground.

Table 5.2 Producer and user accuracy assessment of land cover classification

Cover class	Producer accuracy %	User accuracy %	Producer accuracy (Pixels)
Wetlands	91.05	89.60	1577/1732
Waterbody	96.95	98.75	4487/4628
River	94.96	89.08	791/833
Forest reserve	98.87	97.77	2103/2127
Bareland	97.92	97.86	5167/5277
Open woodland	96.00	95.55	3840/4000
Cliff vegetation	98.40	95.69	1043/1060
Mixture of grass/shrubs and scattered tress	97.11	98.31	5947/6124

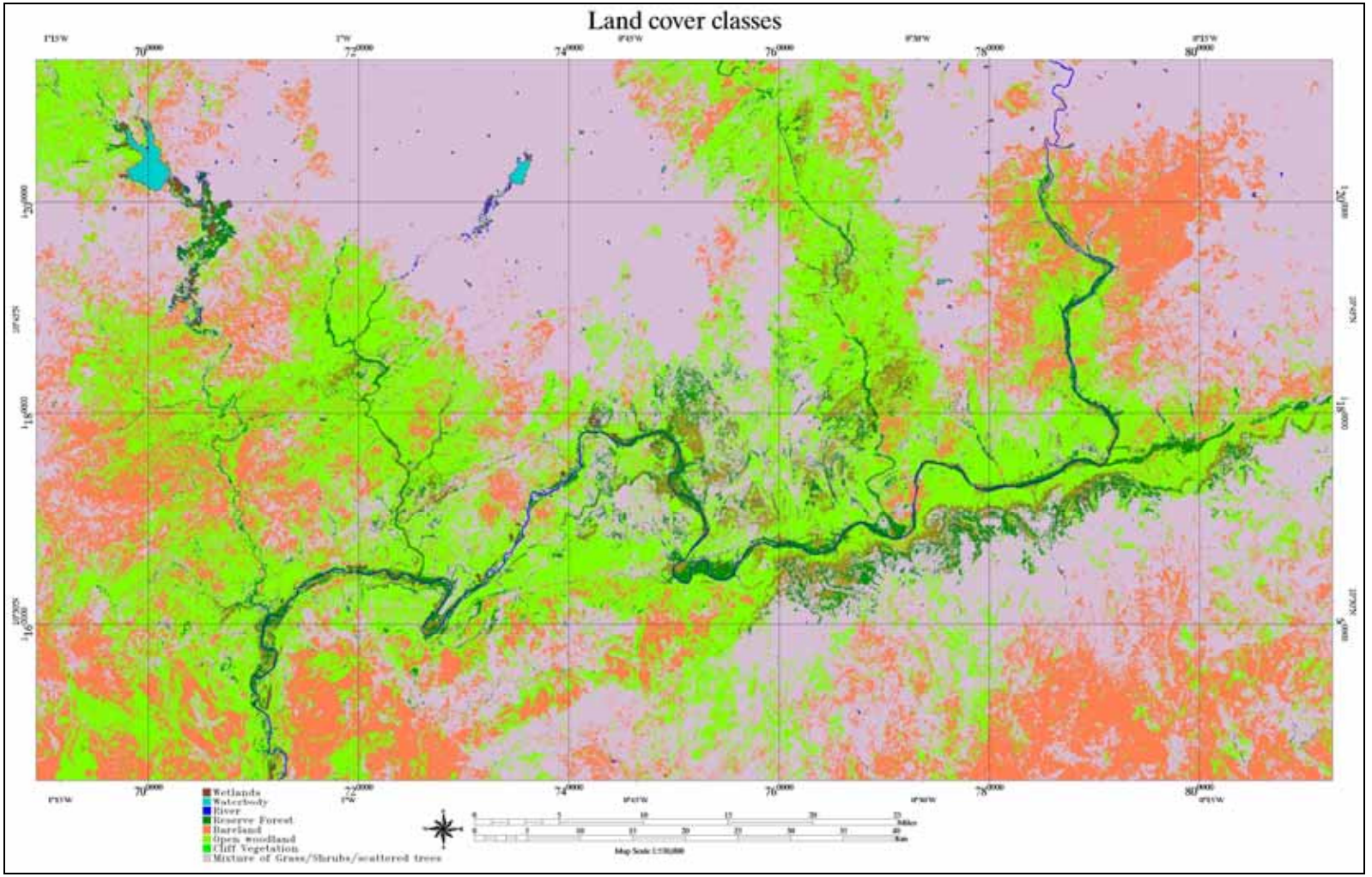

Figure 5.5 Land cover classes of the study area in Upper East Region, Ghana

5.5 Wetland prediction

The prediction of the location of floodplain wetlands was modeled by sampling pixels on the hydrotope data and exported into STATA 9.2 statistical software for logistic and simple linear regression analysis. The area to be modeled covered an area of about 8409.87 km^2 containing 9,362,580 pixels. Part of the study site, containing 2,683,080 pixels, was selected as a test site for predicting wetlands in the basin. Using the simple random sampling method, 23,796 pixels were sampled from the test site for detailed study (Table 5.3). In predicting floodplain wetlands in the White Volta basin, the effectiveness of the logistic regression model was tested.

Table 5.3 Descriptive statistics of wetland predicting parameters

	Pixel Parameters	Min	Max	Mean	Std. Error of Mean	Std. Deviation	Variance	Skewness	Kurtosis
Topographic	Slope	0	16.82	1.49	0.0075	1.15	1.33	1.52	7.66
	Shape	-1.8	2.60	0.0018	0.0023	0.33	0.11	0.03	1.07
	Power	0.19	8.27	1.85	0.0053	0.82	0.67	1.44	4.91
	Height	125	264	163.58	0.139	21.37	456.65	0.47	-0.04
	Internal	0	46	3.26	0.014	2.16	4.66	2.95	28.19
	Wetness	8.23	28.60	12.17	0.015	2.30	5.31	1.61	3.71
Environmental	NDVI	-0.47	0.04	-0.25	0.0002	0.03	0.000956	0.16	13.62
	SAVI	0	594	7.53	0.301	46.74	2184.24	10.94	127.85
Climatic	Evapo	-0.71	5.51	3.02	0.005	0.81	0.66	-0.58	0.28
Image	Texture	0	217.1	3.83	0.055	8.46	71.49	10.62	159.69
	LogB4	3.37	4.73	4.32	0.001	0.15	0.022	-0.62	4.89
Spatial	Distance	0	15281	2663.82	16.13	2488.35	6191896	1.72	3.47

Due to the high number of independent predictors used in the logistic regression method, a procedure to select variables was performed using significance level and multi-colinearity. Data sampled were examined to see whether colinearity

existed between the independent variables. Colinearity is the situation where one independent variable is a linear function of other independent variables. During the process of iteration, colinearity variables are not always included, as this affects the predicting power of the model. To diagnose for colinearity, tolerance and variance inflation factor (VIF) are the two important indices recommended for this purpose. Tolerance is the percentage of variance in a predictor that cannot be explained by other prediction. A small tolerance shows that 70% to 90% of variance in a given predictor can be explained by another prediction in the model. Therefore, high multi-colinearity exists if tolerance is close to zero. In this case, the standard error of the regression coefficient becomes inflated. The variance inflation factor expresses the degree to which colinearity of predictors degrades the precision of a regression coefficient estimate.

5.6 Logistic regression

The selection and use of the logistic regression model in the prediction of floodplain wetlands in the White Volta basin was to analyse the relationship between the probability of the response being a success and the explanatory variables rather than to analyze the relationships. The dependent variable is dichotomous, which takes a binary form of 1 and 0, and has a nonlinear relationship with the independent predictors. The land cover classes was transformed to 1 and 0, that is, identified wetland presence is labeled 1 and 0 is areas that have no wetlands, this served as the dependent variable (covbin) for delineation of the wetland. To test and predict the relationship between the wetland and independent predictors within the White Volta basin, an assumption of the probability that the dependent predictor takes the value of 1 can be estimated by:

$$P = \frac{e^{\beta_o + \sum_{j=1}^{k} \beta_j x_{ij}}}{1 + e^{\beta_o + \sum_{j=1}^{K} \beta_j x_{ij}}} \tag{5.4}$$

where P is defined as the dependent predictor expressing the probability that y=1, β_0 is the intercept, β_j is the j^{th} coefficient for the i^{th} case, and x_{ij} is the j^{th} predictor for the i^{th} case.

In the application of the logistic regression, the dichotomous data needs to be logit transformed, thereby producing a resultant layer containing real series from zero to one. In other words, logistic transformation of the system effectively linearises the model so that dependent predictors of the regression are continuous with a probability range of 0-1, which is the response of the value of the predictors. For predicting floodplain wetland presence, y=1 represents wetland and y=0 represents no wetland. The logistic regression equation used in the prediction process can be expressed as:

$$Logit(P) = \ln\left(\frac{P}{1-P}\right) = \beta_0 + \sum_{j=1}^{k} \beta_j x_{ij} + \varepsilon \qquad (5.5)$$

where P is defined as the dependent predictor expressing the probability that y=1, β_0 is the intercept, β_j is the j^{th} coefficient for the i^{th} case, and x_{ij} is the j^{th} predictor for the i^{th} case.

The prediction function as stated in equation 5.4 takes a fitted model object and returns a vector corresponding to the predicted response. Therefore, the relationship between the dependent and independent predictors follows a logistic curve (Figure 5.6).

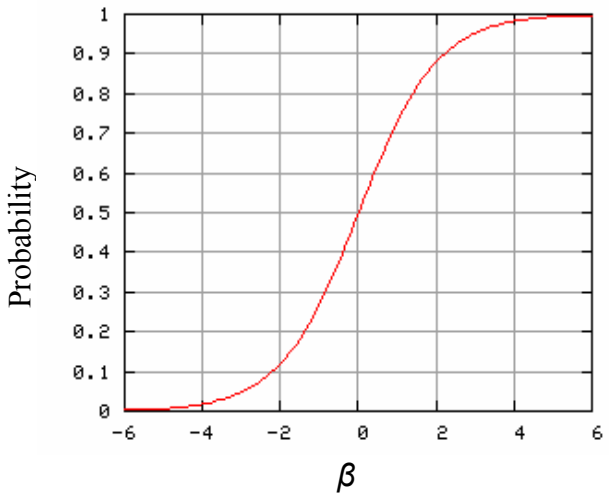

Figure 5.6 Model for probability of wetland identification.

The logistic regression estimates the probability of a pixel being a wetland. Therefore, this will be enhanced if it is validated by selecting or masking pixels that are wetlands and verify if the specification made correspond with ground truth.

Nevertheless, the significance of the explanatory variable in a logistic regression model cannot be tested in the same way as in linear regression, since variables in logistic regression are Bernoulli distributed, other forms of test such as Log likelihood and Psuedo R^2 are used. To explain the likelihood that a pixel belongs to a floodplain wetland or not, the odds ratio plays an important role. The odds ratio of a pixel is defined as the ratio of the probability that a pixel will be classified as a floodplain wetland to the probability that it fails to be classified as a floodplain wetland.

In probabilities the occurrence of events are constrained to lie between 0 and 1, with 0.5 as a neutral value for which both outcomes are equally likely. The constraints at 0 and 1 make it impossible to construct a linear equation for predicting probabilities. The odds ratio lies between 0 and $+\infty$, with 1 as a neutral value for which both outcomes are equally likely. A higher odds ratio signifies that a pixel has a better chance of being classified as a floodplain wetland.

For the application of a logistic regression model for predicting floodplain wetlands in the White Volta basin, the study site was divided into two subsets of pixels: one set for modeling and the other set for testing. The logistic regression result obtained from the analysis (Table 5.4) is discussed in accordance to the essential and important role they play in explaining the predictors. The result indicates 4 significant predictors out of 12 that have a high probability in explaining floodplain wetland location.

Table 5.4 Logistic regression results

	β	S.E$_\beta$	P
LogB4	-5.31090	0.4240	0.000
Distance	-0.00068	0.0001	0.000
Evapo	-0.37779	0.1286	0.003
Power	0.19117	0.1186	0.107
Height	-0.00444	0.0049	0.372
Internal	-0.00907	0.0678	0.894
Wetness	-0.06997	0.0498	0.160
Texture	0.02915	0.0024	0.000
Slope	-0.12957	0.1326	0.329
Shape	0.19420	0.2878	0.500
savi	-0.00456	0.0115	0.692
Constant	20.78	2.5409	0.000
Number of obs	23796		
LR chi^2(11)	454.3		
Prob > chi^2	0		
Pseudo R^2	0.2526		

The logistic regression model assisted in determining important predictors that had the highest probabilities of modeling floodplain wetland, and this was identified by using the significance value (P-value). The smaller the p-value, the stronger is the confidence attached to the predictors as having an influence in floodplain modeling. The four (4) significant predictors LogB4, distance, texture and evapo showed the highest predictive power at a 95% significant level. Hence the final model generated by the logistic regression function is:

$$Logit(P)=\left(\frac{P}{1-P}\right)=20.78+(0.0291*texture)-(5.311*\log B4)-(0.0007*distance)-(0.378*evapo) \quad (5.6)$$

With 12 predictors of which 4 were significant, the Pseudo $R^2 = 0.25$ shows that the independent predictors to some extent explain the dependent predictor. The 4 predicting variables are Logb4, Evapo, texture and distances were significant at $p< 0.05$. However, other predictors that were not classified as significant were not discarded but assisted in explaining the occurrence of wetland at the modeled location. The pseudo R^2 of 0.25 is unlike the R^2 found in ordinary linear regression, where R^2 measures the proportion of variance explained by the model. The pseudo R^2 is not measured in terms of variance, since in logistic regression the variance is fixed as the variance of the standard logistic distribution. Therefore, the Likelihood Ratio Chi-Square test of whether all regression coefficients predictors in the model are simultaneously zero was used test model fit. A LR of 454.3 computed with the Prob > chi2 = 0 indicates a good model fit and none of the predictors was equal to zero.

The reduction of variable is to verify how the model can perform within the data limited environment as in the case of Ghana and other developing countries. The map computed using equation 5.6, shows the probability of floodplain wetland occurrence within the White Volta basin (Figure 5.7). Areas marked with brown color along the White Volta River and its tributaries have the highest probability of wetland occurrence, whereas not mark with brown color are areas with a low probability; the greater the distance from the main river course, the less the probabilities of wetland.

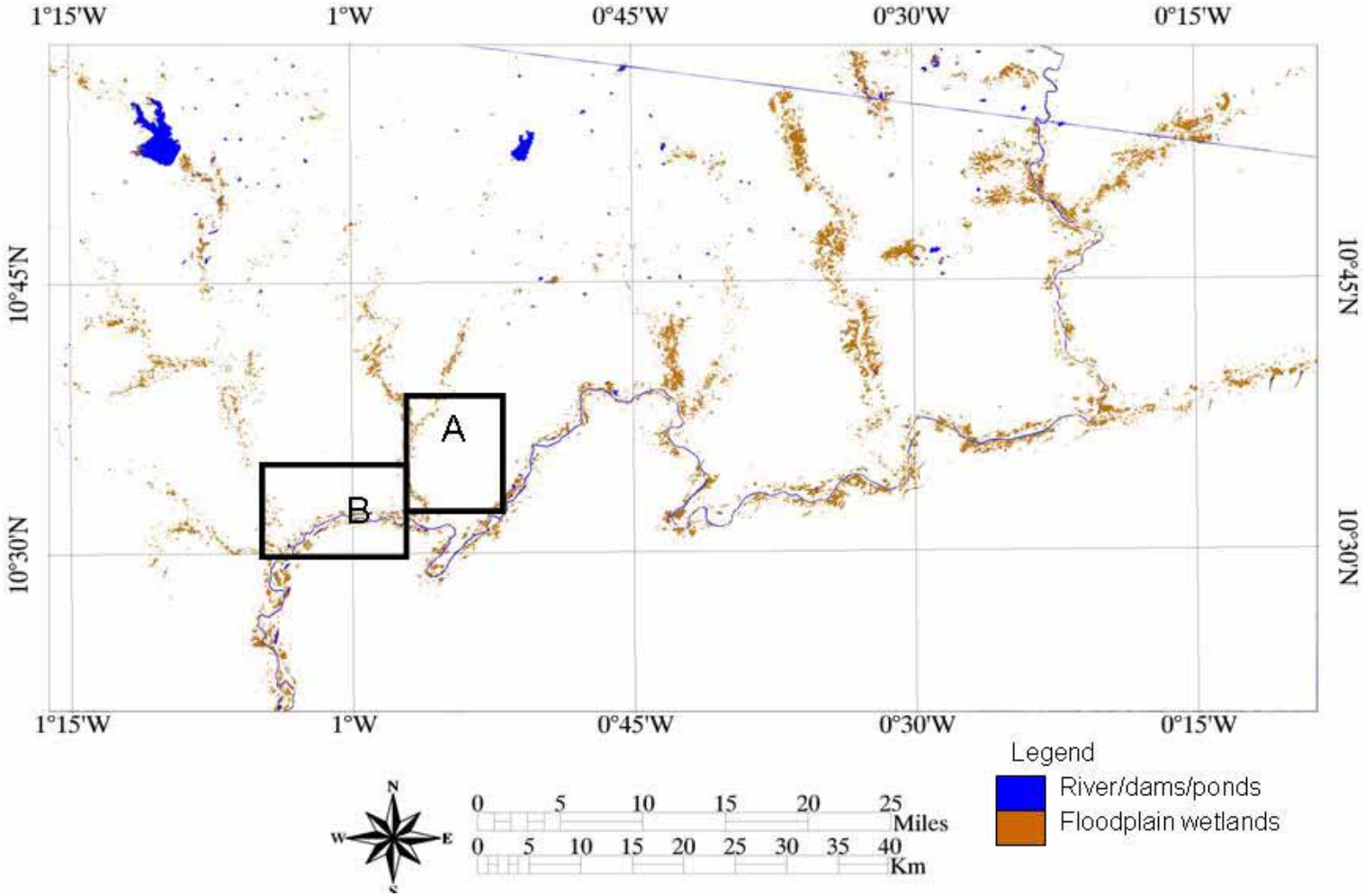

Figure 5.7 Floodplain wetland probability map of the White Volta basin, Ghana

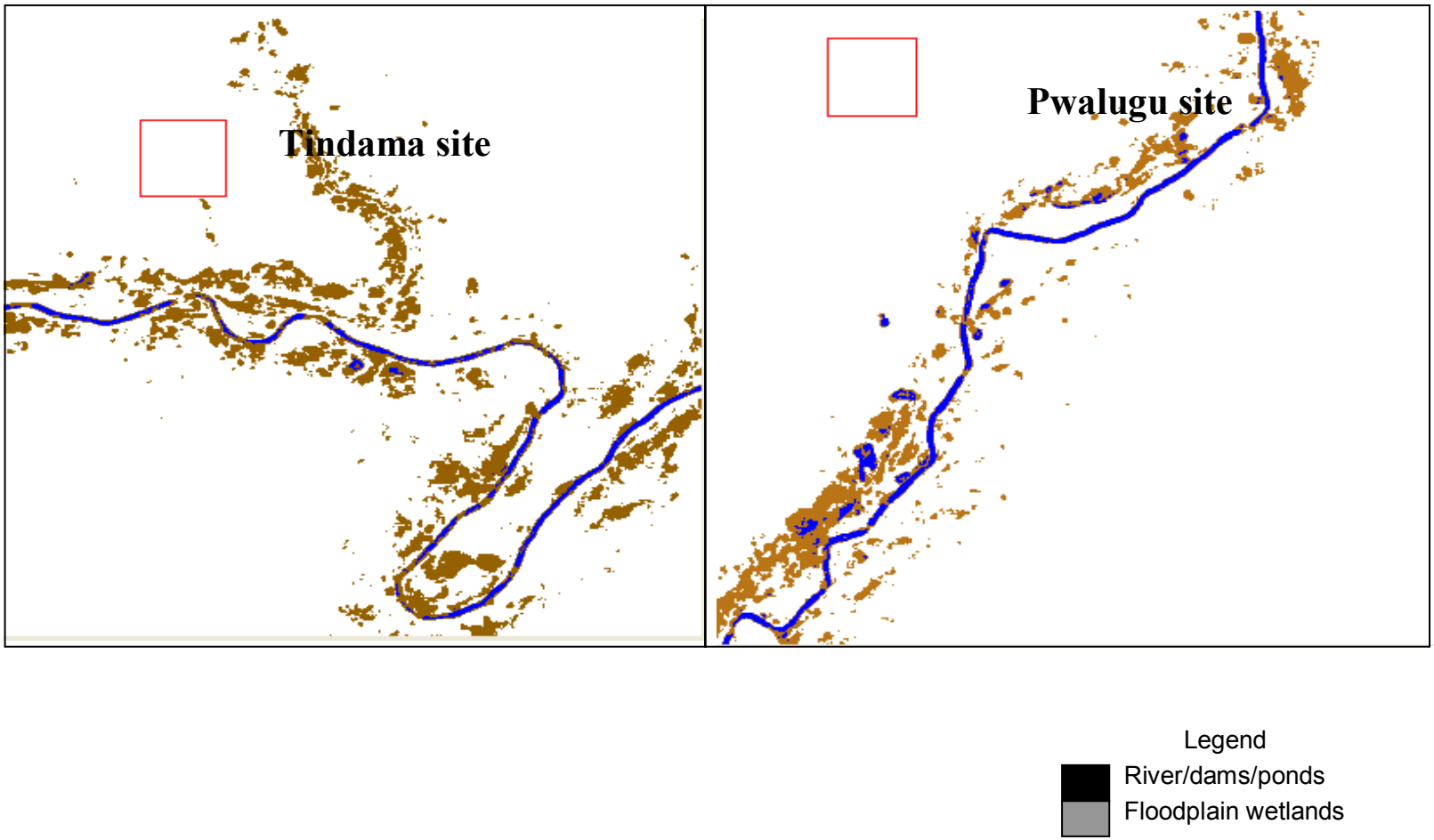

Figure 5.8 Floodplain wetland probability map of selected sites along the White Volta River, Ghana

Distance from the main river channel on either side of the bank has a negative relation with wetland presence; a change in distance of 0.7 km away from the river course dwindles efforts in encountering floodplain wetlands. In other words, the probability of encountering a floodplain is reduced with increasing distance from the river system, as floodplain wetlands are fed occasionally by overbank flow and foot-slope recharge.

Evapotranspiration has a negative influence on the odds ratio with an estimated coefficient value of -0.38 ($P<0.05$). It is an important component in the hydrological cycle and is the result of processes of energy and water exchange between wetland, its surroundings and the atmosphere. Evapotranspiration of 0.37 mm/day influences the sustenance of wetlands, because it means a high water extraction rate within the study sites. Water supply, heat conditions, air humidity, intensity of air turbulence, barometric pressure and the material composition of the underlying surface control the evapotranspiration of underlying surface. The difference between marsh and evaporation of water surface are that both of them are well supplied with water. The evapotranspiration from wetlands includes the transpiration of plants and the evaporation occurring from the water surface between individual plants. From field observations, areas with high vegetation density in October have a high probability of being associated with a floodplain wetland, as crops are harvested thus exposing the bare land.

The Texture predictor has a high predictive power for floodplain wetland identification, having a significance of 0.029 ($p<0.05$). This predictor has a high probability of separating wetland pixels from non-wetland pixels, and hence a change in the roughness of texture by 0.03% enhances its contribution to the classification of wetland in the White Volta basin. The image predictor the logB4, which is the logarithm transformation of the landsat band 4 of the October 2000 image of the basin has a high power for discriminating vegetation and water bodies. During this period of the year where vegetation is reduced, it has less power to discriminate between water bodies and vegetation. It may not contribute to the mapping of the entire basin, but only to a fraction of the landscape where vegetation and water is present. Though significant, it has a negative relationship of -5.311 ($p<0.05$).

Within the study area of of 8409.87km^2, using the logistic regression within the GIS platform, a total of 259.45km2 of the land mass is estimated as wetlands. Greater part of the wetlands are associated with the White Volta River network, while wetlands can found in isolated patches and close to reservoirs and irrigated sites.

6 HYDRO-GEOMORPHOLOGY OF THE WHITE VOLTA RIVER BASIN

6.1 Introduction

Fluvial geomorphology and hydrological principles provide the ideal starting points from which structure and function of a river catchment can be assessed. Without a geomorphological and hydrological understanding of the distribution of physical processes within the White Volta Basin, specifically, processes that determine river structure and approaches employed to determine environmental flow requirements; sustainable catchment management is unlikely to succeed over the longterm. The White Volta Basin is a complex system that has diverse topographic orientations, geological formations and soil series, which indicate different ways of processing overland flow. Knowledge about this variability will enable the effective and sustainable management of the White Volta Basin. To reveal the pattern of floodplain wetland and river system functions, analysis within the catchment based on hydro-geomorphology is important. In addition, the differences in the flow regimes throughout a catchment, especially in floodplain wetlands, are manifested by changes in the catchment morphology. This chapter discusses the hydro-geomorphology of the Tindama and Pwalugu wetlands, looking specifically at their water sources and hydrodynamics.

6.2 Soil horizons

Soils in the wetlands are an important part of the geological cycle, and their characteristics are determined by parent material, topography, climate, weathering and time over which soils in these wetlands developed. These factors produce distinct soils that show temporally and spatially variation. Soils in the Pwalugu and Tindama wetlands site have distinct horizons. These horizons have distinctive characteristics, which are revealed when a particular profile is exposed (Table 6.1 and Table 6.2). The upper one meter was analyzed at both sites. The reason being that during the period of pit excavation at Pwalugu wetland site, sub-surface inflow of water was encountered, while in Tindama, soils below the first 0.75 m were very hard to dig.

Table 6.1 Soil horizon description at Pwalugu wetland site

Horizon	Depth (cm)	Colour	Field texture	Structure	Concretion	Mottle	Mottle colour	Root density
Pit 4 Kuapela Series Eutric Gleysol								
A	13	Dark grey	Silty Clay	Moderate sub-angular block	-	-	-	Common
AB	32	Grey	Clay Loam	Weak sub-angular block	-	common	Brownish yellow	Many
1	51	Grey	Clay	Weak sub-angular block	-	common	Brownish yellow	Few
B2	72	Grey	Sandy clay	Medium sub-angular block	-	abundant	Yellowish brown	Very few
B3	100	Whitish grey	Gritty Clay	Medium sub-angular block	Few Femm concretion	common	Yellowish brown	Very few
Pit 6 Cultivated soil Kuapela Series								
AP	12	Dark brown	Silty clay	Weak and medium sub-angular block	-	-	-	Abundant coarse root
A1	23	Dark brown	Loamy clay	strong and medium sub-angular block	-	-	-	Many roots
AB	36	Dark brownish yellow	Loamy clay	strong and medium sub-angular block	-	-	-	Common
B1	60	Dark brownish yellow	Clay	Moderate and medium sub-angular block	-	-	-	Common
B2	84	Brownish yellow	Clay	Moderate and medium sub-angular block	-	-	-	Many

Table 6.1 continued

Pit 8 Breyanese soil Series								
A	15	Dark brown	Loam	Weak sub-angular block	-	-		Abundant coarse root
AB	31	Dark brown	Sandy loam	Weak sub-angular block	-	Many	Dark yellowish brown	Few coarse root and many small roots
B1	50	Brownish grey	Sandy clay	Medium sub-angular block	-	Many	Yellowish Brown	Few coarse
B2	71	Greyish brown	Sandy clay	Moderate sub-angular block	-	Abundant	Yellow brown	Very few
B3	100	Grey	Sandy clay	Moderate sub-angular block	-	Abundant	Reddish brown	Very few
A	15	Dark brown	Loam	Weak sub-angular block	-	-		Abundant coarse root
Pit 9 Kuapela Series								
A	12	Dark Brown	Silty clay loam	strong and medium sub-angular block	-	-		Abundant coarse and few fine
AB	29	Dark greyish brown	Clay	strong and medium sub-angular block	-	-		Abundant fine and Few coarse
B1	46	Dark greyish brown	Clay	Moderate and medium sub-angular block	-	Few	Dark brownish grey	Few fine roots
B2	67	Yellowish Brown	Sandy clay	Weak and medium sub-angular block	-	Common	Dark brown	Few fine roots
B3	100	Brown	Sandy clay	Weak and medium sub-angular block	-	Common	Dark brown	-

Table 6.2 Soil horizon description at Tindama wetland site

Horizon	Depth	Color	Field texture	Structure	Concretion	Mottle	Mottel color	Root Density
TP2 Kuapela Series								
A	20	Very dark grayish brown	Clay	Strong and medium angular block	-	-	-	Very few fine roots
AB	50	Dark grayish brown	Clay loam	Medium angular block	-	-	-	few
B1	80	Grayish brown	Clay	Strong and medium angular block	-	-	-	-
B2	100	Light brownish gray	Clay	Strong and Medium angular block	-	-	-	-
TP3 Kuapela Series								
A	20	Very dark grayish brown	Silty loam	Strong and medium angular block	-	-	-	Abundant
B1	50	Dark yellowish brown	Clay	Strong and medium angular block	-	**Few**	-	common
B2	80	Yellowish brown	Clay loam	Strong and medium angular block	-	**Few**	-	Very few
B2	100	Brownish yellow	Clay loam	Strong and medium angular block	-	-	-	-
TP 4 Kuapela Series								
A	20	Dark brown	Clay	Strong and medium angular block	-	-	-	Abundant
B1	50	Yellowish brown	Clay loam	Strong and medium angular block	-	**Trace**	-	Very few
B2	80	Yellowish brown	Sandy clay	Strong and medium angular block	-	**Trace**	-	-
B3	100	Strong brown	Loam	Strong and medium angular block	-	-	-	-

Table 6.2 continued

TP 5 Kuapela Series								
A	20	Dark yellowish brown	Silty clay loam	Strong and medium angular block	-	-	-	Abundant coarse and small root
B1	50	Yellowish brown	Silty clay	Strong and medium angular block	-	-	-	Few fine roots
B2	80	Yellowish brown	Clay	Strong and medium angular block	-	-	-	Very few
B3	100	Strong brown	Sandy clay loam	Strong and medium angular block	-	-	-	-

The soils in these wetlands sites can be distinguished on the basis of the types of horizons and their properties. To differentiate horizons, morphological properties such as texture, structure, concretion, colour, mottle and root density were used. Four 100 cm pits were selected of out of 20, of which was examined in-situ. At the Pwalugu wetland site, two main soil horizons were detected. In Tindama, 4 out of 10 pits were also selected randomly and examined. Soil texture at Pwalugu is mostly clay, silty clay, loamy clay or sandy clay. In Pit 8, the B-horizon is mostly of a sandy clay texture type, the structure of the soil is a medium to moderate sub angular block. Pit 6 belongs to the Kuapela soil series; this has high clay content in the B-horizon. Concretion is absent in all sites except Pit 4 of the Kuapela soil series, which had a few iron (Fe) concretions.

The B-horizons of the sampled soils show signs of illuviation, revealed through brighter colour than in the A-horizon. The A-horizon is at the surface, and has high organic matter accumulation from decomposing vegetal matter. The activities of organism such as ants, earthworm, and termites are prevalent, creating preferential pathways for rainfall infiltration. Kuapela series is the most common soil series in the Tindama floodplain wetlands site. The textural composition of the soil has high clay content; structurally they have strong angular blocks with no concretion. In addition, the rooting depth is up to 25 cm and a few signs of mottling were found in some pits.

6.3 Soil colour and sub-surface water

Soils at the Pwalugu and Tindama sites showed distinct. In some parts of the Pwalugu wetland, most of the soil profiles showed predominant mottles, a sign of water logging or hydric soil (Table 6.1). Soils in the Pwalugu and Tindama floodplain wetlands are saturated during the rainy season from flooding events or high groundwater levels as in Pwalugu wetlands, which reduces the oxygen level in the soil system, creating anaerobic conditions. The longer the duration of saturation, the greater the oxygen deficiency. Basic requirements for this reduction process are absence of oxygen, as induced by saturated soil conditions, and presence of organic matter.

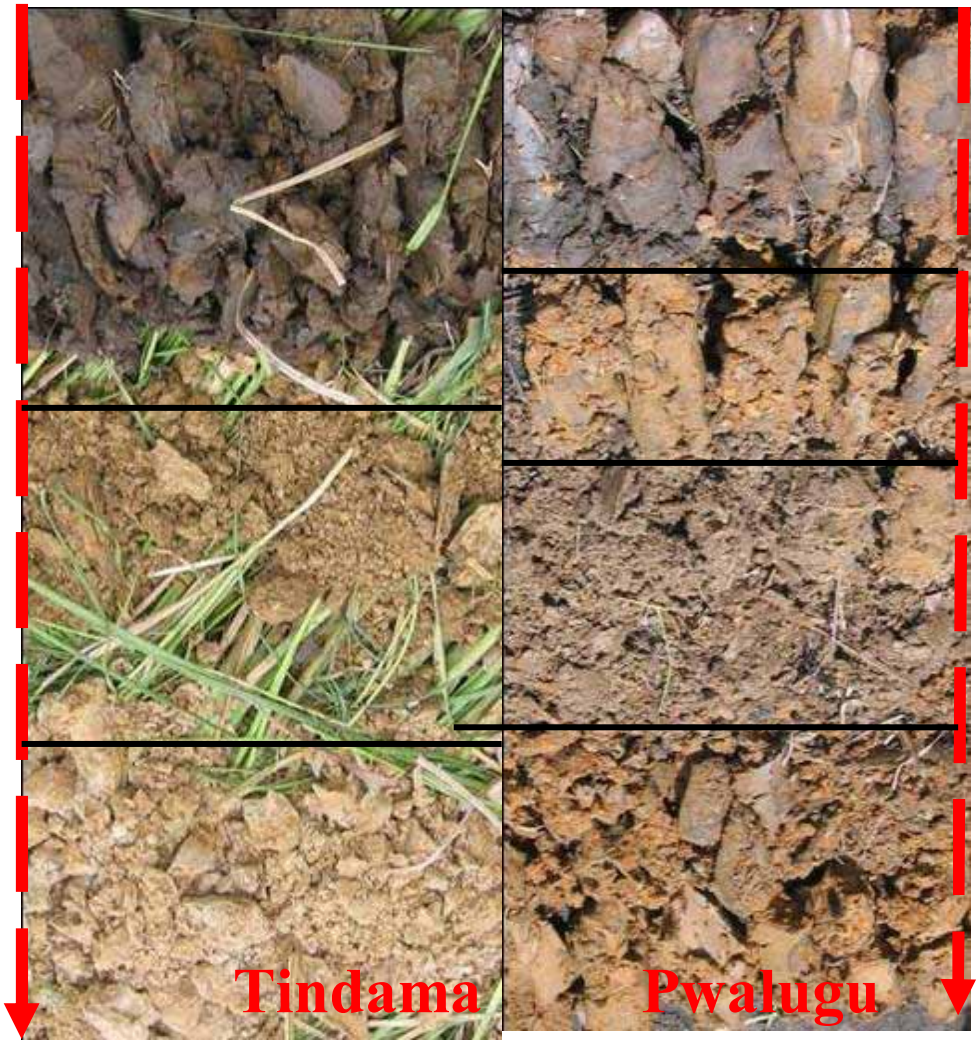

Figure 6.1 A) Augured soil at 150 cm depth showing 3 layers of soil profile at Tindama wetland site. B) augured soil at 300 cm depth showing 4 layers of soil profile at Pwalugu wetland site

Prolonged soil saturation in these wetlands occurs between July and October, resulting in anaerobiosis, which leads to the formation of mobile ferrous iron (Figure 6.2). The migrating subsurface water in the Pwalugu wetland redistributes the iron throughout the soil profile. The subsequent drainage restores aerobic conditions, although some iron coatings on the soil particles are not entirely removed, but leave a grayish surface on the mineral grains exposed.

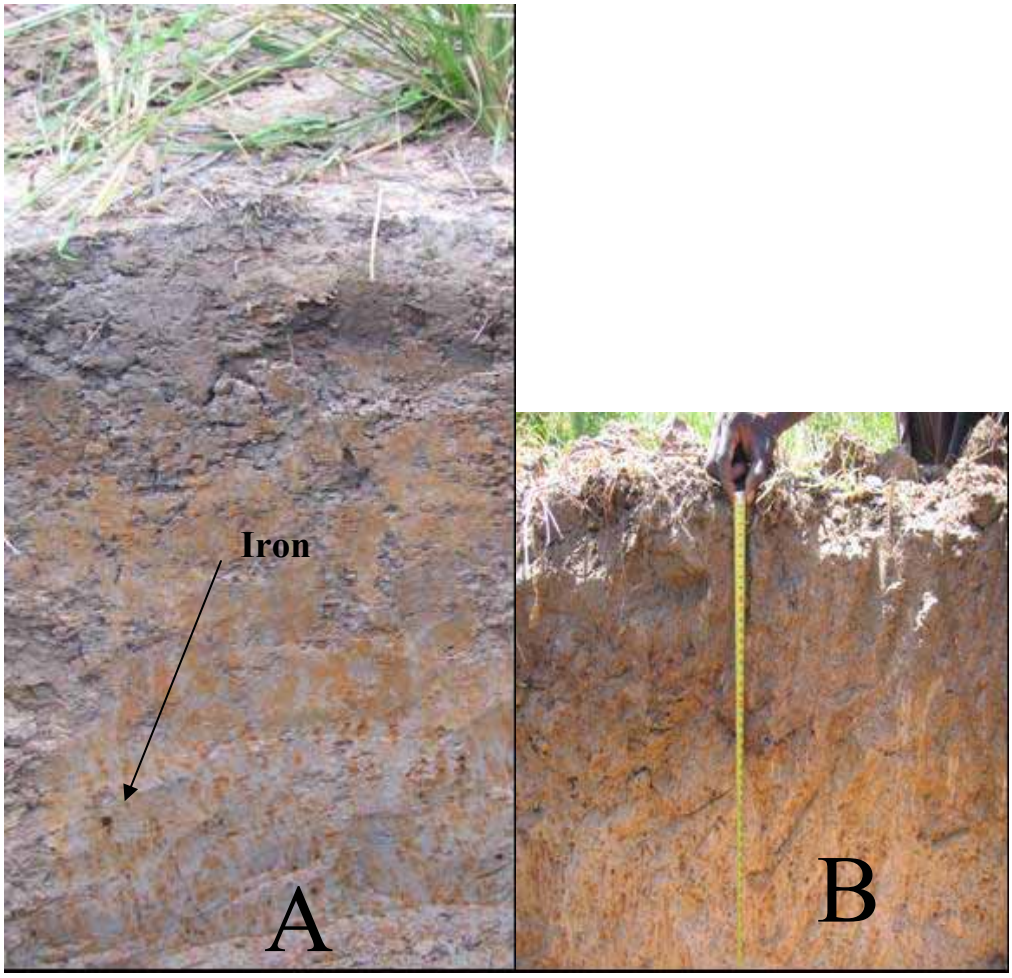

Figure 6.2 Soil profile colour distinctions between Pwalugu (A) and Tindama (B) sites. Pwalugu profile shows iron strips and matrix of gray

Low chroma colors of between one and four present in most of the soils indicate distinct periods of saturation. The yellowish colored soils in Pwalugu and Tindama wetlands do not have such high iron contents that low chroma mottles are masked. However, using gray clayey layers to indicate continuous total saturation is misleading since most part of the year the water table is deeper than indicated by low

chroma colours. In such situations, the presence of the yellowish-brown-colored sandy layers shows that the drainage of that soil is much better. In parts of Tindama and Pwalugu wetlands, some soils have a gray-coloured layer directly below the topsoil. The incomplete breakdown of soil organic matter in the topsoil results in the formation of low molecular-weight organic acids, which causes extensive leaching in underlying soil layers unrelated to anaerobic soil conditions. The iron is stripped (Figure 6.2) from the sand grains by the process of chemical complexation resulting in gray colors. This process is termed podzolization, and the brownish-colored underlying soil layers constitute a better indicator of the actual hydrology than the grayish-colored, leached layer. Other situations in which wet soil conditions do not necessarily cause distinct low chroma colors occur in soils with organic matter distributed throughout the soil profile, such as in frequently flooded fluvial soils.

Soils in the Pwalugu and Tindama sites exhibiting low chroma colors might not result from seasonal anaerobic conditions. Soils high in dark-colored phyllitic minerals inherited low chroma colors from their geologic parent materials, and soil formation in the past years in the region has not released sufficient iron to give the soil a uniform brown appearance. Soil morphology, therefore, cannot be said to be a reliable indicator of mean water level in drained soils (Vepraskas 2001), since colors and patterns develop due to a fluctuating seasonal high water table, leaving a permanent marker within a soil. This morphology persists even when these soils have been drained for many years, hence the altered hydrology may be misinterpreted.

The division of soils in the Pwalugu and Tindama study sites into drainage classes depends on the frequency and duration of periods of saturation or partial saturation during soil formation. Excessively and somewhat excessively drained soils typically have sandy and gravelly textures within the subsoil and substratum. They have bright colors (strong brown to yellowish brown) in the subsoil that fade gradually with depth. Well-drained soils of the Kuapela series (Figure 6.2) have bright colors in the subsoil that fade gradually with depth; they are free of mottling to depths of 5 m. The Kuapela series, are moderately drained soils, have bright colors in the upper portion of the subsoil and are mottled beneath the soil surface. Additionally, these soils are grayish with a chroma of 3 or 4 at the subsoil's. Measurement of water level in installed

piezometers confirms that within August and September these soil series experiences high groundwater table and ponding.

The Tindama wetland soils are poorly drained and have a blackish surface layer (Figure 6.1) underlain by gray subsoil that has little or no mottle. These soils have no water table at or near the surface for a significant part of the year, but rather ponded water on the surface. Soils at this site are very poorly drained and can be divided into those that developed in mineral deposits and those that developed in organic material. Tindama soils have poorly drained organic soils developed in thick, dark (often black) deposits of partially or well decomposed organic matter, and have black topsoil and subsoil.

6.4 Multivariate analysis of soil parameters

The accuracy of in-situ field investigations of soil hydraulic properties at the Pwalugu and Tindama floodplain wetland sites are very difficult to ascertain (Marriot 1996), thus laboratory analysis was used. Soil samples were collected from the Pwalugu and Tindama floodplains at a depth of 100 cm. This depth was chosen because during the period of pit digging at Pwalugu, water was encountered at a depth of 110 cm and at the Tindama site, it was very hard to dig because the soils were extremely compact. Soil texture and other parameters at the Pwalugu and Tindama wetland sites control the amount of water that soils in floodplain wetlands can absorb, retain and transmit. Moreover, the temporal and spatial variability of soil texture makes it difficult to generalize soil water content over a wide area. Using correlation analysis, some form of relationship was found to exist between soil properties in the study sites, but most important is to determine how effectively they affect each either directly or indirectly (Appendix B).

Soils in the Pwalugu floodplain wetland, the field capacity (FC) and the permanent wilting point (PWP) are extremely influenced by clay, sand, cation exchange capacity (CEC), organic matter (OrgM), but the influence of clay is higher than that of the other soil properties. However, effective porosity (EP) defined as that part of total porosity occupied by pore fluid, showed a negative relationship (-0.75) with moisture content but an indirect effect through clay content. Organic matter showed a significant influence on CEC (0.68), and effectively influences water holding capacity. On the

other hand the effect of CEC on wilting point (67.8%) was lower than that on field capacity (68.1%). Clay content has been noted to play important roles in the adsorption and desorption of water molecules. The surface adsorptive forces of clay minerals greatly affect water retention because of the permanent negative charge of clay mineral particles and the polar nature of water. Clay showed a positive relation with FC (0.92), PWP (0.99), CEC (0.68) and OrgM (0.61), but it is negatively related to the estimated saturated conductivity (-0.67). Additionally, CEC and OrgM showed significant positive relations with pF at $p<0.05$ level. Furthermore, the indirect effects of OrgM on the soil moisture is through bulk density, bulk density decreases with increasing OrgM (Bauer and Black 1992), though there should be a correlation between the two, the correlation value of (-0.47). Soil organic matter influences water retention (PWP-0.62, FC-0.63) because of its hydrophilic character and its influence on soil structure and bulk density (Klute 1986), thereby it increases plant available water holding capacity (Kern 1995).

As bulk density decreases with increasing clay content in soil, it is expected that water retention is also increased with decreasing bulk density. According to Skopp (2002), as bulk density decreases and total porosity increases, water retention will be affected but this was not the case in the soil samples that were analysed. The CEC in the soil depends on the kind of colloids present, i.e. whether clay or organic matter. Therefore CEC present indicated a significant relationship with clay (0.68), OrgM (0.68) and FC (0.68).

The particle size distribution of low clay content in soils might behave similar to coarse fractions of soil texture. Macropores as a result of high coarse texture proportion are important recharge pathways for water but are eventually plugged due to accumulation of fine clay particles (Stephens 1996). Therefore increasing fine sediment content may be the reason of decreased water retention due to the decreasing macropores at the Pwalugu and Tindama sites. Moisture content (MC) showed low correlations with CEC (0.26) and OrgM (0.009), though OrgM content does influence CEC. A high CEC is a result of high OrgM content which improves soil conditions by increasing soil water holding capacities and infiltration. Clay content was positively correlated with all pF value, but negatively with saturated hydraulic conductivity (-0.67). However, the indirect role of soil properties in influencing pF can be seen in the

soil texture, but percentage of clay and sand are the most significant soil properties that influence soil pF.

An understanding of the relationships between soil properties and hydraulic conductivity is essential in identifying factors that influence the hydrodynamics of water holding capacity and distribution in the soils in the Pwalugu and Tindama wetlands. The water holding capacity of the soil controls the rate of removal of water from the soil by drainage or evapotranspiration and rate of storage change when water input is by rainfall or irrigation. Soil water retention is the basic soil property that reflects soil physical and chemical properties needed for the study of plant available water, infiltration, drainage, hydraulic conductivity, irrigation and solute movements. The soils in Pwalugu and Tindama displayed varied optimum soil water retention capacities. When the soil water retention is kept near the field capacity, the wetland in Pwalugu contributes effectively to the sustenance of the main river in the low rainfall season (Brady 1974). The average water retention at field capacity for Tindama and Pwalugu was 36.04% and 28.53%, respectively, though they exhibited a similar porosity of 40.65% and 43.92%, respectively. A weak correlation of 0.09 between water retention at field capacity and total and effective porosity was estimated, the latter being the part of the pore system that stores immobile water.

6.5 Spatial and temporal vertical hydraulic conductivity

The saturated hydraulic conductivity (K_s), is the quantitative measure of a saturated soil ability to transmit water when subjected to a hydraulic gradient. This parameter (K_s) can be understood as the ease with which pores of a saturated soil permit water movement. At the Pwalugu and Tindama wetland sites K_s was measured using Darcy's law. According to Park and Smucker (2005), depending on the aggregate density and pore continuity of soils, K_s can be 4 orders of magnitude lower in single aggregates than in bulk soil except where the aggregate contains mostly sand or has a high pore ratio. The volume of water passing through the soil per unit cross-sectional area (perpendicular to the flow) per unit time (water flux density) in floodplain wetlands reflects differences in hydraulic properties of soils, because as fluid flow increases, inter-aggregate pores reduce the possibility of obtaining equilibrated pore water pressure profiles (Park and Smucker 2005). Hence, macropore continuity and the more tortuous pore system found

at the edge of the Pwalugu and Tindama wetlands where root systems dominated enable preferential flow particularly at saturation, thereby giving high conductivity values (Figure 6.3 and 6.4). The interpolation of the conductivity value was done using the ordinary krigging method within the SURFER 8.0 software. Ordinary krigging is a regression technique for estimation and is designed to give a best linear unbiased estimate of measurements at an unsampled location. Ordinary krigging was used to obtain a regional overview of the field measurements, because it smoothes out the local variability by calculating a moving spatial average.

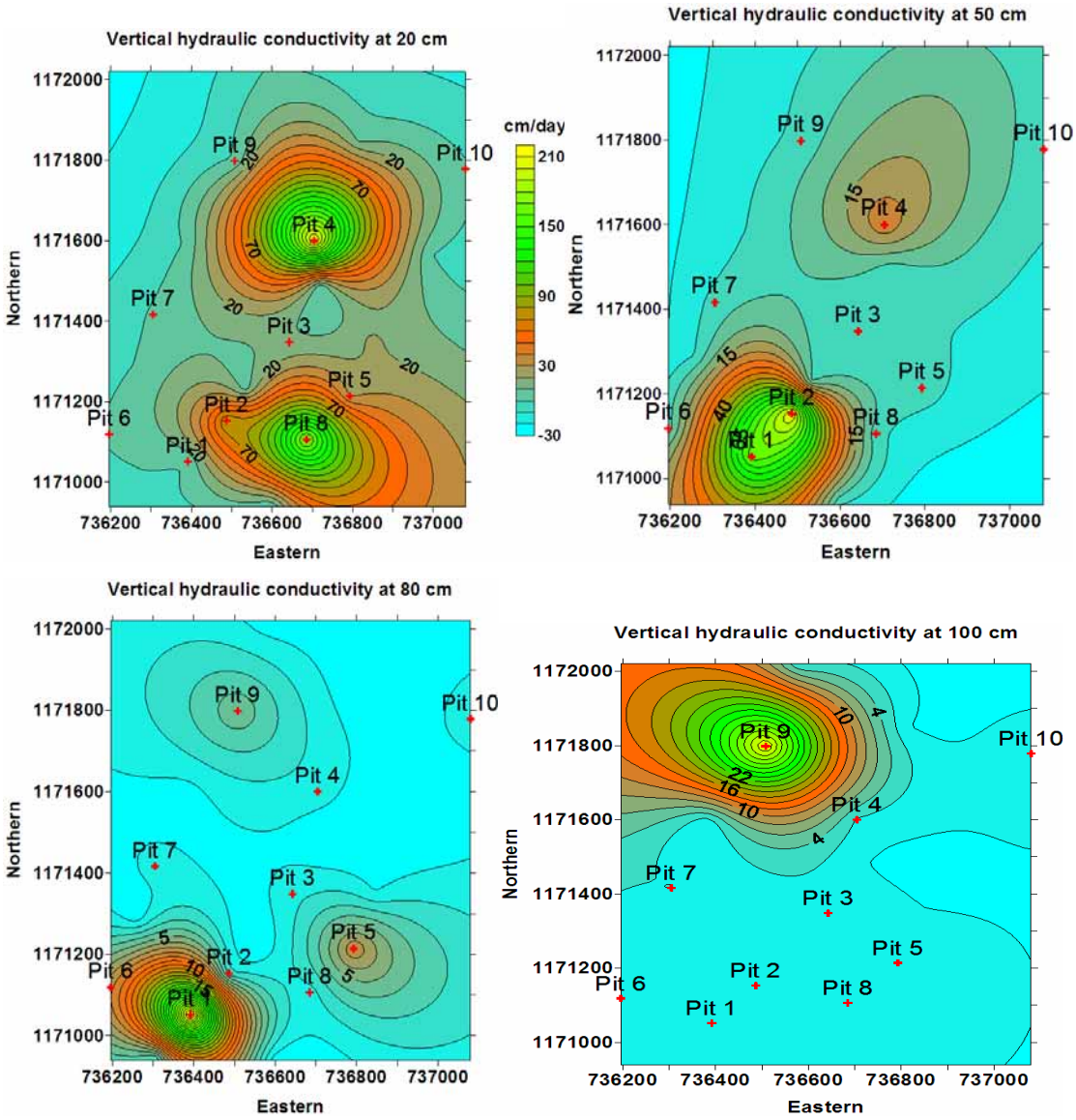

Figure 6.3 Spatial interpolation of vertical hydraulic conductivity at Pwalugu wetland site

The vertical K_s measured in Pwalugu and Tindama sites were not the same for each depth of sample collected. Conductivity tests on the four soil horizons of the Pwalugu wetland reveal that K_s varied spatially (Figure 6.3) within the landscape, and that each layer possess different conductivity values. For instance, over the first 20 cm of depth, K_s ranged from 0.01 cm/day to 0.15 cm/day and in the lower depth of 100 cm between 0.002 cm/day and 0.022 cm/day. The vertical flow direction within layers was likely to be different, because layers show marked differences in vertical hydraulic conductivity. The Pwalugu site is unsaturated during the dry season, but at the onset of rainfall, gravitational potential induces drainage. The same cannot be said about the Tindama wetland, since lateral drainage is unfavorable due to the nature of the lithology. The site showed vertical K_s averaging 0.09 cm/day, and the highest was towards the north-western corner of the site. The lithology in Tindama is mostly of weathered shale and schist.

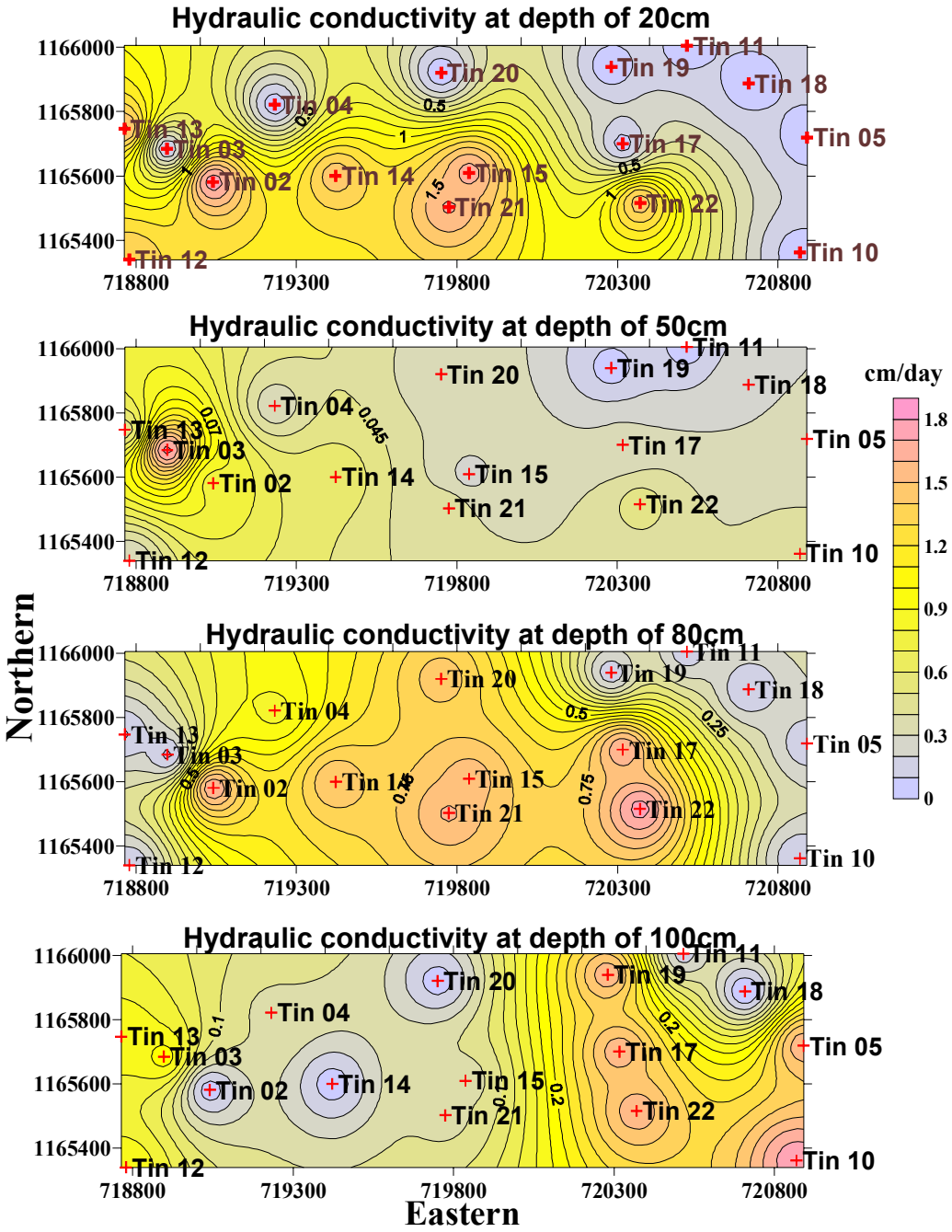

Figure 6.4 Spatial interpolation of vertical hydraulic conductivity at Tindama wetland site

The measured K_s at Tindama wetland (Figure 6.4) also showed spatial and depth variation, with the edges of the wetland (where trees or vegetation with extensive root density existed) having high K_s values.

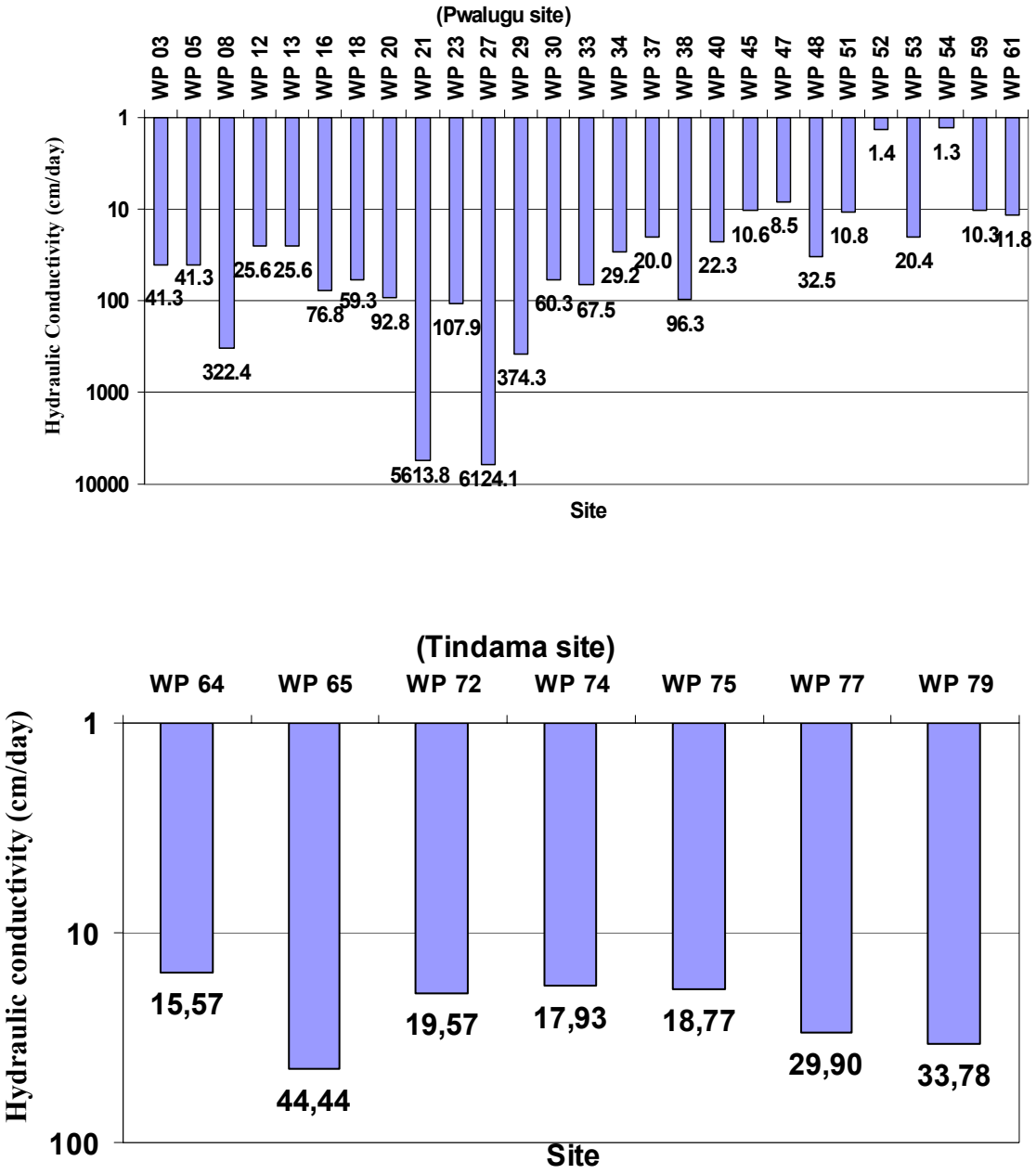

Figure 6.5 Inverse auger hole method of field estimates of hydraulic conductivity in Pwalugu and Tindama wetland sites (results are presented in logarithm format due to low values)

Inverse auger involves auguring a hole to the desired depth and measuring the flow rate of water in the hole. Inverse auger estimates (Figure 6.5) of K_s at a depth of 70 cm displayed little variability at the Tindama site, where values ranged between 15.57 cm/day and 44.43 cm/day. The K_s values at Pwalugu ranged between 1.28 cm/day and

96.29 cm/day, though there were outliers of 6124.14 cm/day and 5613.79 cm/day. These high values were at places where pipes and cracks existed at the time of measurement. The flow in the unsaturated soil at the study sites is more complicated than flow through a continuously saturated pore space. Within unsaturated soils, macropores are filled with air leaving the finer pores to accommodate water movement. Therefore, gravity does not dictate the movement of water through the soil but rather differences in metric potential.

The auger hole method resulted in higher values than the laboratory measurements. This is due to the near destructive nature of the auguring method and to roots sticking out in the pits.

6.6 Porosity and hydraulic conductivity

Investigations reveal that grain size is a fundamental independent parameter that controls hydraulic conductivity. Grain packing models used in the works of Marion et al. (1992) demonstrated that porosity of granular material varies with the volume fractions of fine materials. Hydraulic conductivity reaches its minimum value when the porosity of fine-grained particles equals the porosity of the coarse-grained particles. In some circumstances, porosity and hydraulic conductivity may be consistently bipolar, thereby defining a negative relationship (Morin 2006). However, the relationship between porosity and hydraulic conductivity at the Pwalugu and Tindama wetland sites relates to the interplay between water moving through pores at different velocities, which in effect is influenced by pore size and discontinuity as a result of fine sediment accumulation, especially during the rainfall season (May and October).

Soil structure notably influences soil porosity, an important parameter in characterizing hydraulic behavior in the macropore flow areas of the Pwalugu and Tindama wetlands. In reality, macroporosity is deficit in organic matter and weak in bulk density, this indirectly affects some soil water parameters. For instance, the low OrgM of 0.03% in some parts of the Pwalugu wetland site influenced the effective moisture and porosity of these parts. Depending on the dominant flow type, estimation of soil hydraulic parameters requires a combination of different morphometric properties, and no single morphometric property provides adequate estimation. In defining the relationship between saturated hydraulic conductivity and porosity, Park

and Smucker (2005) proposed a power law relationship between hydraulic conductivity and porosity in soil without tillage, but not in cultivated soil. Statistically, porosity and hydraulic conductivity showed no relationship in either Pwalugu or Tindama wetlands, where correlation was 0.22 and 0.17, respectively. Given the soil structure of the Pwalugu wetlands with weak to moderate sub-angular blocks, deep cracks (Figure 6.10) and high plant root density, opportunities exist for preferential flow process. This allows macropore flow to influence infiltration and hydraulic conductivity. Regression analysis (Figure 6.6 and 6.7) indicates no power law relationship between porosity and hydraulic conductivity for Pwalugu wetland r = 0.20, but Tindama indicates some what high correlation coefficient r = 0.44. The exponential fit gave an r value of 0.19 for Pwalugu and 0. 49 for Tindama.

Within the Pwalugu and Tindama wetland sites, there are mixtures of large and small narrowly connected pores, hence the high Ks values measured depend not only on porosity but also on factors such as surface tension and antecedent moisture. In addition, there are differences in the interconnected porosities that are narrow or sealed with finer particles at points down the pore.

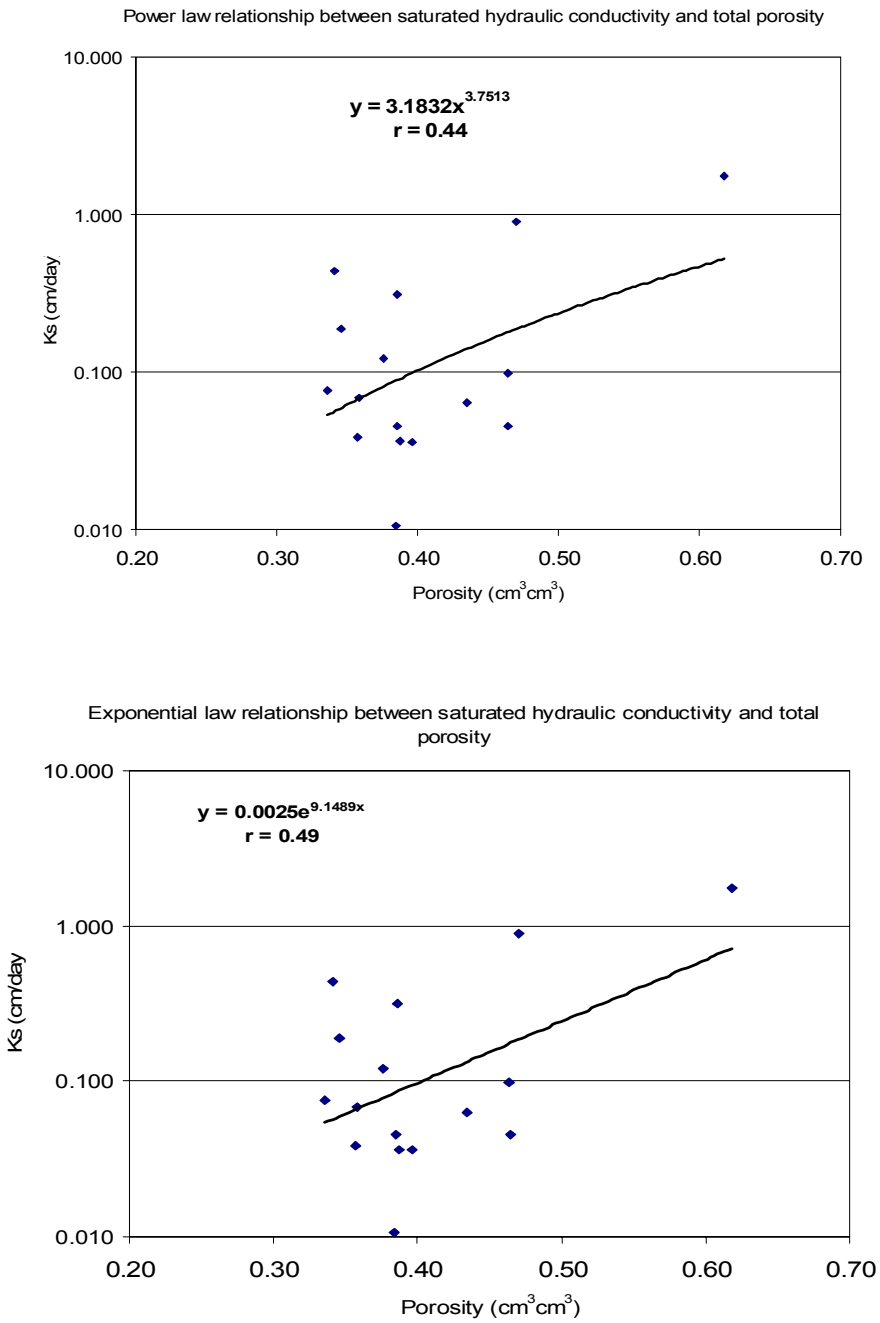

Figure 6.6 Relationship between saturated hydraulic conductivity and total porosity in the Tindama floodplain wetland

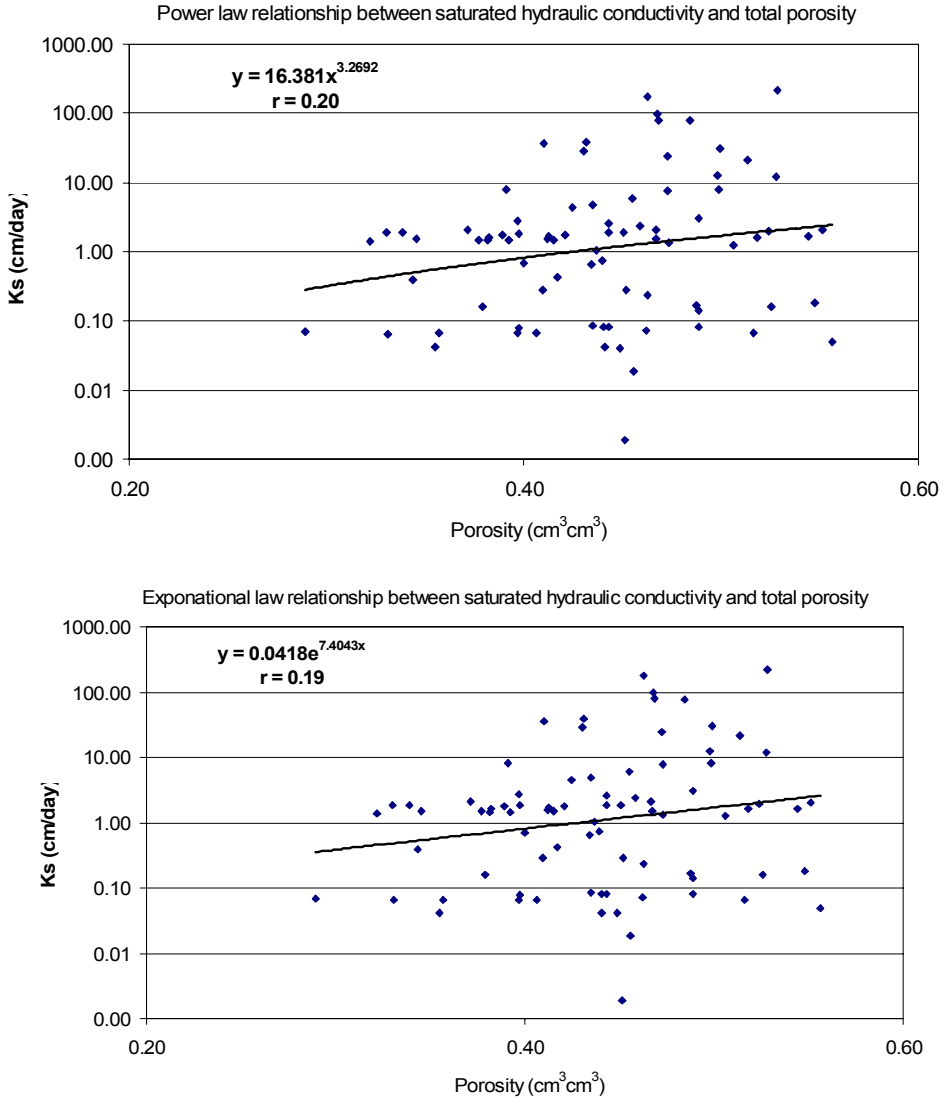

Figure 6.7 Power and exponential law relationship between saturated hydraulic conductivity and total porosity in the Pwalugu floodplain wetland

6.7 Infiltration

The ease or difficulty with which water can pass into and through the soil profiles of Pwalugu and Tindama wetlands is important and influences surface compaction and structure decline. Infiltration processes represent a wide range of mechanisms of vertical water movement in the soil in Tindama and Pwalugu under gravity and capillary forces. To understand soil water movement at these sites, infiltration was measured using double-ring infiltrometers. Philip's two-term infiltration model, which is a truncated form of the Taylor power series, was used to extrapolate the instantaneous infiltration results to a steady state (Figure 6.8 and 6.9). Before measuring the infiltration process,

the soil was wetted to obtain uniform water content and reduce the soil hydro-phobicity. Each point presented different infiltration rates that decreased with time for any given point.

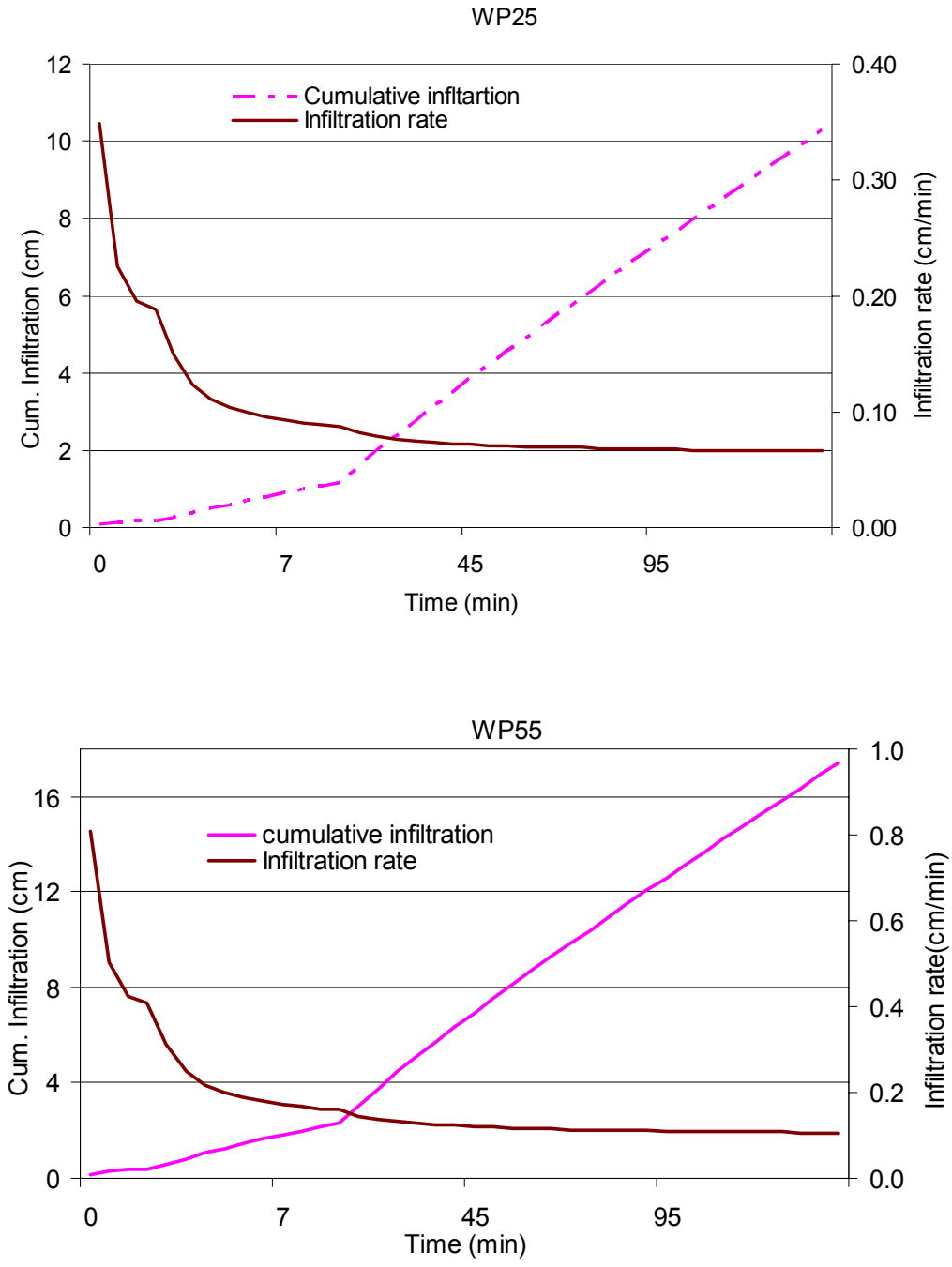

Figure 6.8 Infiltration in Pwalugu wetland site

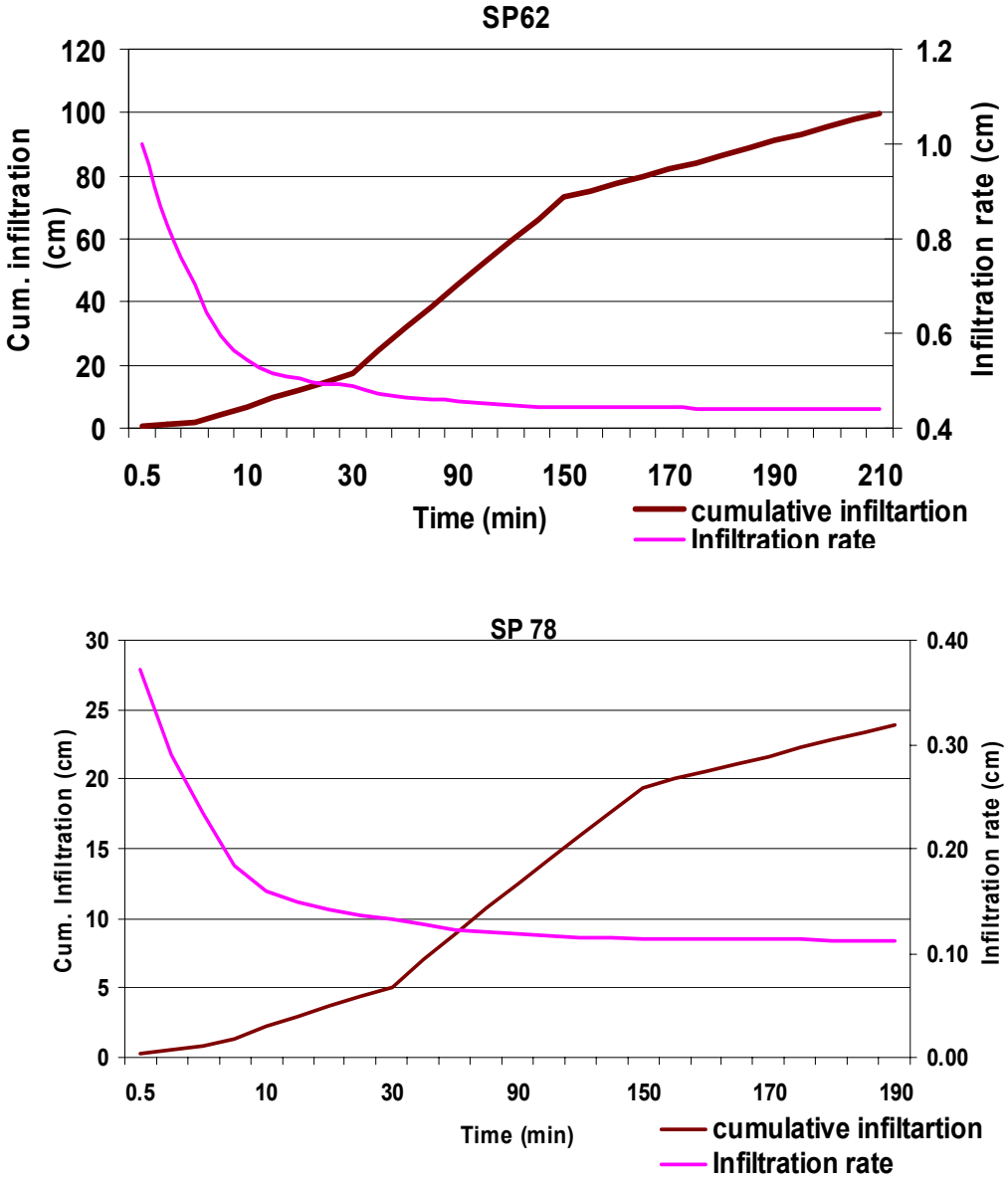

Figure 6.9 Infiltration in Tindama wetland site

Though infiltration at the Pwalugu and Tindama sites is an important process in water movement into the subsurface, cracks of 30 mm width formed on the soil surface during the dry season (Figure 6.11), and roots of both living and dead plants allow preferential flow during the onset of rainfall. The preferential flow process leads to quick water storage in the unsaturated zone and recharge into the groundwater system. Surface sealing is a common occurrence at the onset of the rainy season (Figure 6.11) as a result of aggregate breaks down and coalescence under raindrop impact. This

reduces soil porosity in the upper soil layer which eventually forms a structural crust, thereby preventing infiltration.

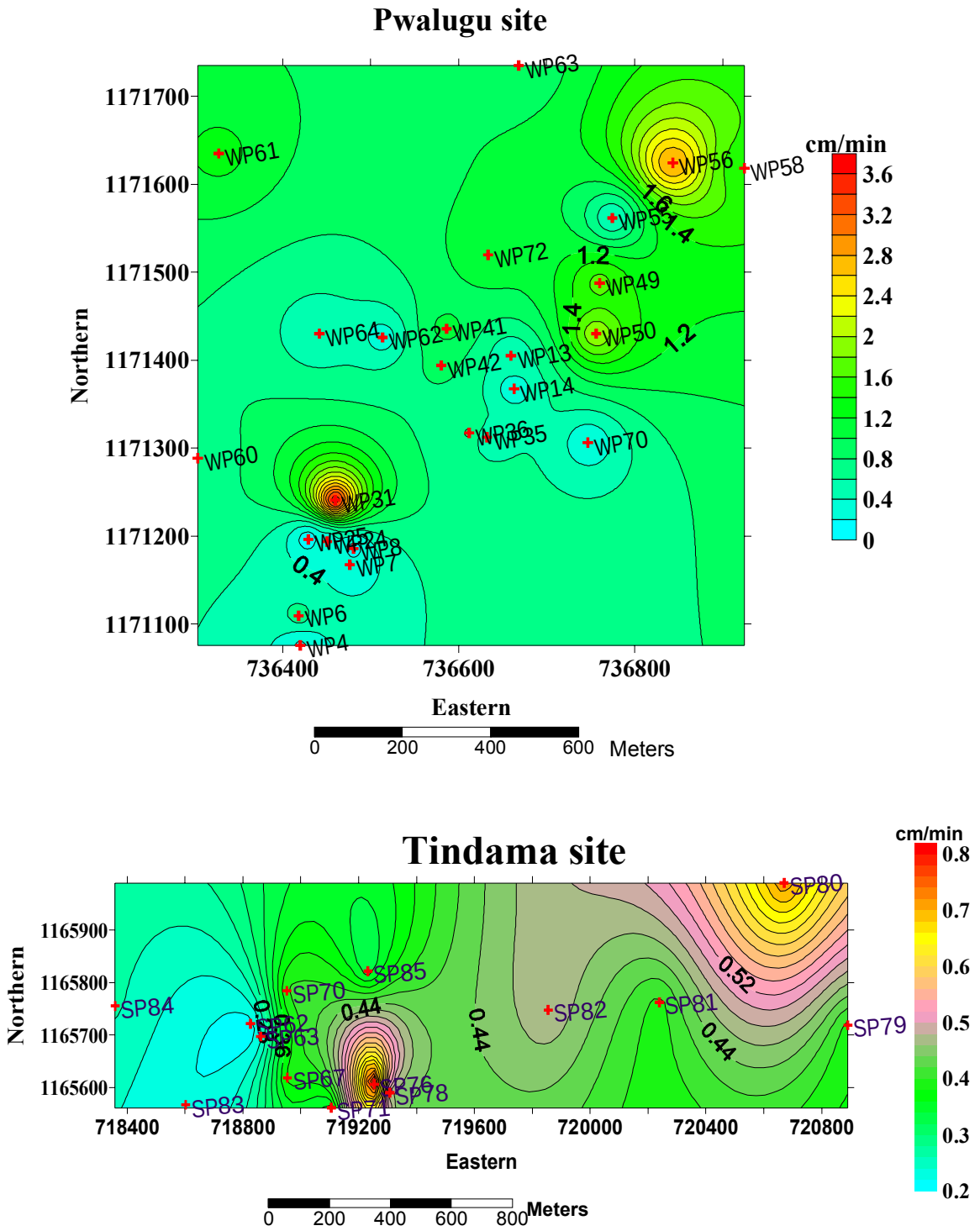

Figure 6.10 Spatial variation of infiltration rate in Pwalugu and Tindama wetland sites (Interpolated using ordinary kriging in SURFER-8)

Variation in rate of infiltration at the study sites occurred because the experimental condition was not an accurate reflection of the real condition with rainfall or when irrigation water is applied. Some common problems were noted and are those likely to affect the results obtained. These include inadequate pre-wetting, trapping of air, soil disturbance by the infiltration ring, irregular wetting effect and variability in the nature of water flow in the soil.

The infiltration experiment conducted at the Tindama and Pwalugu wetland sites (Figure 6.10) mostly a high infiltration rate at the start of the measurement, which declined gradually over time, but there were exceptions (Beven 2001) due to the break down of the surface crust or reduction in the hydro-phobicity. This resulted in an increasing infiltration rate over time. A high infiltration rate of 2 to 4 cm/min was mostly found at the fringes of the wetlands in Pwalugu, where the vegetation cover was high. The same applies to the Tindama wetland with a rate of 0.65 to 0.9 cm/min; the middle part of the wetlands these showed an infiltration rate of about 0.4 cm/min. The initially high rate in the Pwalugu and Tindama wetlands is usually due to the capillary potential drawing water into the dry soil, and the effect of gravity. However, at these sites, the rate of water input, i.e., the intensity and duration of rainfall can be a factor limiting infiltration. In addition, the soil characteristics at a point in time limit infiltration rate once saturation and time to ponding is reached. Other issues worth considering are that after a long period of water input, the wetting fronts i.e., the depth of water penetration after infiltration have moved deeper into the soil, making the effect of the capillary potential very low, hence the gravity potential dominates here. The depth of penetration for Pwalugu ranged from 15.4 cm to 92 cm, and 16.5 cm to 38 cm for the Tindama site, all in a period of 150 minutes. At the end of infiltration experiment, depending on the location and time, the depth the water penetration varies (Table 6.3).

Table 6.3 Infiltration characteristics at Pwalugu and Tindama wetland sites

Infiltration characteristic of Pwalugu wetland site			
Site	**Infiltration rate (cm/min)**	**Depth of penetration**	**Infiltration (cm/10 min)**
WP4	0.174	80	0.52
WP6	0.653	92	0.2
WP7	0.194	80	0.4
WP8	0.133	48	0.12
WP13	0.438	82	1.24
WP14	0.266	81.5	0.16
WP24	0.262	89.5	0.87
WP25	0.073	15.4	0.09
WP31	3.531	68	0.48
WP35	0.448	19	0.2
WP36	0.819	37.5	0.14
WP41	1.079	23.5	0.11
WP42	0.839	28.5	0.21
WP49	1.652	26.5	0.29
WP50	1.942	62.5	0.34
WP55	0.447	50	0.21
WP56	2.800	42	0.28
WP58	1.489	37.5	0.04
WP60	0.696	40.5	0.37
Infiltration characteristic of Tindama wetland site			
SP62	0.2100	38	0.28
SP63	0.2300	34.5	0.96
SP67	0.3911	39	1.33
SP70	0.4033	16.5	1.83
SP71	0.3311	29.3	0.52
SP76	0.8156	38	2.29
SP78	0.4600	29.7	0.54

Infiltration measurement at the two sites revealed different rates in the first 10 minutes. The higher rate of initial infiltration of 0.2 to 2.29 cm/10min at the Tindama

wetland site could be attributed to a high surface tension of the soil as compared to the Pwalugu wetland site, where 0.2 to 1.24 cm/10min was recorded.

Table 6.4 Infiltration categories

Class	Infiltration category	Infiltration rate (cm min^{-1})
1	Very slow	< 0.1
2	Slow	0.1 - 0.5
3	Moderately slow	0.5 - 2.0
4	Moderate	2.0 - 6.0
5	Moderately rapid	6.0 - 12.5
6	Rapid	12.5 - 25.0
7	Very rapid	>25.0

Source: Dingman(2002)

Rainfall storm varies spatially with intensity and duration, and has an effect on the infiltration capacities of the Pwalugu and Tindama wetland sites, thereby affecting the redistribution within the soil profile. Infiltration processes at the Pwalugu and Tindama sites have the potential to rapidly change the negative capillary pressure head in the capillary fringe to a positive pressure, which is likely to change the water table gradient, forcing pre-event water out. This process produces a rise in the nearby stream water table, which can form a seep zone where subsurface water discharges onto the land surface, thereby discharging into the main White Volta River.

The aerial infiltration rate (Figure 6.10) is important for spatial hydrological modeling, but these processes are often simplified by using local classical infiltration equation such as Green-Ampt, Philip and other models. Additionally, while assumptions about spatial homogeneity in soils are always made, these assumptions are hardly valid for the natural settings where heterogeneity in hydraulic properties prevails. Therefore, the heterogeneity in the soils at the Pwalugu and Tindama sites influences the aerial infiltration rate with a spatial uniform rainfall rate.

01-05-05 28-6-05

Figure 6.11 Surface crack before rainfall (A) and surface sealing after rainfall (B)

6.8 Saturated and unsaturated dynamics

The flow within the unsaturated zone of the Pwalugu and Tindama wetlands is controlled by two basic soil characteristics, i.e., retention factors and unsaturated hydraulic conductivity characteristics. Comparatively, the Tindama wetland soil is less well drained than that of Pwalugu, though its occurrence is not concurrently, this process can aid soil water retention, but the decrease in unsaturated hydraulic conductivity is influenced by the decrease in effective moisture that is the mobile portion of soil water. Some parts of the wetlands experience high flow rates which occur mostly in areas with very coarse soil texture (Park and Smucker 2005), where water entrapment is more prevalent at the onset of rainfall and water input but declines with time. The pore water blockage affects flow rate, and this depends on the extent of pressure applied to isolate the conductive flow path; this process is seen in soils with uniform pore size distribution. The Tindama wetland sites have high clay content and a uniform fine pore system where, when water flow rates within a cross section of the soil are high, a disconnection of flow paths occurs leading to entrapment of water in the end of the pore space, thereby increasing the depth of ponding.

Studies of wetlands have focused on determining wetland water budgets and how individual wetlands depend on rainfall, evaporation, surface and sub-surface flow and outflows (Bradley and Gilvear 2000). The determination of wetland water budgets and the description of hydro-periods neglect the importance of the unsaturated zone in wetlands. The unsaturated zones in Pwalugu and Tindama have a marked spatial

variability of water inflows and outflows. The White Volta basin floodplain wetland systems (Pwalugu and Tindama sites) are seasonal in nature, and only a fraction of the entire system (Figure 6.12) is saturated throughout the year; this condition depends on the nature of the previous seasonal rainfall. Most of the year, the water table in Pwalugu is always below the surface and the unsaturated zone takes up a significant part of the rainfall after infiltration and then redistributes it into the groundwater. The response of the Pwalugu and Tindama wetlands to rainfall events is a reflection of the textural composition, hydraulic conductivity, moisture retention and evapo-transpiration of the unsaturated zone.

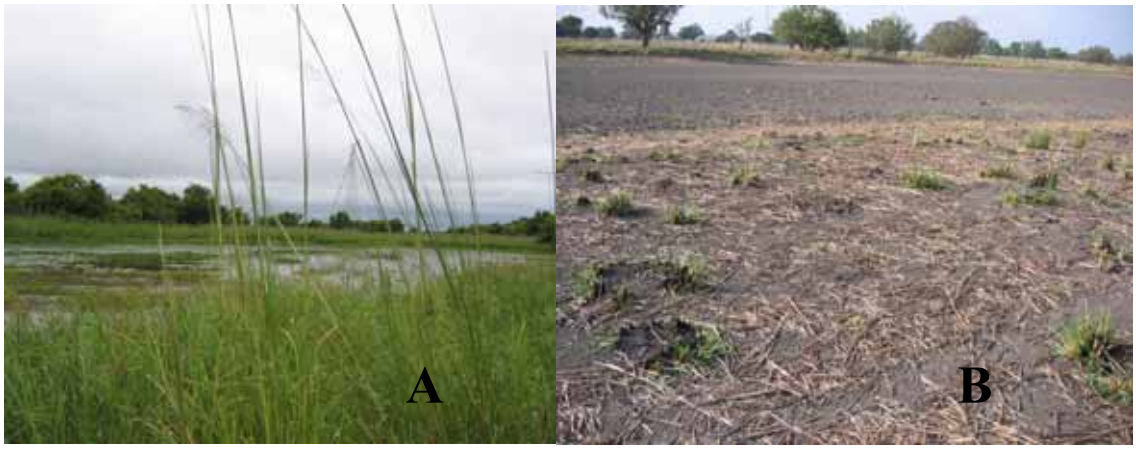

Figure 6.12 Seasonal nature of wetlands in the White Volta basin (A) 11 August 2004 (B) 01 May 2005

Since the unsaturated zone is very difficult to measure, and only limited data are available, HYDRUS-1D was used to model the redistribution of rainfall input, deal with hydrological complexities of the Pwalugu wetland system and derive water budgets and estimate fluxes. The model was not applied to the Tindama wetland site, because the geological formation does not support appreciable sub-surface water that can contribute to stream flow.

6.8.1 Input parameters

For modeling the Pwalugu floodplain wetland site, the HYDRUS-1D model needs the input data number of layers in the soil profile, initial water table depth, residual and saturated water contents of each soil layer, parameters α and n (coefficient and exponent respectively in the soil water retention function) and saturated hydraulic conductivity of each soil layer. The van Genuchten parameters (Table 6.5) residual soil water content (**Θr**), saturated soil water content (**Θs**), parameter in the soil water retention function (α) [L^{-1}] and parameter (n) in the soil water retention function were estimated using the Rossetta program and the measured soil parameters, while the K_s was measured in the laboratory using the falling head method.

Table 6.5 Saturated soil water content (Θ_s), residual soil water content (Θ_r) coefficient α and exponent n for soil water retention function, and saturated hydraulic conductivity (Pwalugu wetland)

Site	Depth (cm)	Θ_s (cm^3/cm^3)	Θ_r (cm^3/cm^3)	α (1/cm)	n	**K_{sat} (cm/day)**
Pit 1	0-20	0.0799	0.4829	0.0137	1.2596	1.2572
	20-50	0.0820	0.4848	0.0116	1.2348	77.2024
	50-80	0.0839	0.4943	0.0147	1.2165	30.4318
	80-100	0.0696	0.4337	0.0119	1.2694	0.7348
Pit 2	0-20	0.0776	0.4666	0.0117	1.2461	80.0460
	20-50	0.0745	0.4566	0.0065	1.3319	95.9068
	50-80	0.0685	0.4390	0.0088	1.3288	2.3418
	80-100	0.0599	0.4045	0.0093	1.3280	1.7405
Pit 3	0-20	0.0687	0.4684	0.0085	1.3859	12.0089
	20-50	0.0509	0.3978	0.0121	1.3643	1.8557
	50-80	0.0626	0.4016	0.0262	1.2805	1.6901
	80-100	0.0429	0.3613	0.0221	1.3449	1.8321
Pit 4	0-20	0.0531	0.4424	0.0129	1.4069	216.4252
	20-50	0.0449	0.4056	0.0052	1.4406	24.4840
	50-80	0.0605	0.4033	0.0071	1.3374	1.5534
	80-100	0.0522	0.3759	0.0086	1.3320	1.7427
Pit 5	0-20	0.0626	0.4078	0.0319	1.2949	28.7747
	20-50	0.0343	0.3487	0.0355	1.3773	2.7344
	50-80	0.0419	0.3582	0.0435	1.3902	8.0096
	80-100	0.0443	0.3587	0.0507	1.4077	1.6005
Pit 6	0-20	0.0280	0.4108	0.0110	1.4648	1.6447
	20-50	0.0442	0.3885	0.0094	1.3962	2.5616
	50-80	0.0528	0.4137	0.0155	1.3642	7.7770
	80-100	0.0431	0.3713	0.0123	1.3615	1.4746
Pit 7	0-20	0.0574	0.4400	0.0213	1.3564	1.6081
	20-50	0.0347	0.3780	0.0077	1.4262	1.8674
	50-80	0.0487	0.4072	0.0104	1.3983	1.4969
	80-100	0.0532	0.4070	0.0348	1.3423	2.0852
Pit 8	0-20	0.0329	0.3751	0.0494	1.3889	176.9292
	20-50	0.0244	0.3204	0.0135	1.3588	2.0749
	50-80	0.0441	0.3420	0.0332	1.3617	1.5216
	80-100	0.0424	0.3286	0.0239	1.3291	1.3797
Pit 9	0-20	0.0511	0.4517	0.0095	1.4324	2.0501
	20-50	0.0413	0.3516	0.0146	1.3386	1.4392
	50-80	0.0386	0.3715	0.0373	1.3751	4.8721
	80-100	0.0409	0.3749	0.0159	1.3668	38.5936
Pit 10	0-20	0.0230	0.3645	0.0223	1.3962	1.3412
	20-50	0.0363	0.3216	0.0083	1.3248	1.8674
	50-80	0.0441	0.3541	0.0173	1.3299	1.4649
	80-100	0.0406	0.3590	0.0067	1.3808	1.4356

6.8.2 Boundary conditions

Boundary conditions specified for running the model are the atmospheric boundary condition with surface layer and free drainage for the lower boundary. The initial conditions were selected so as to accurately represent the topography and substrate to be modeled. The initial textural characteristics for the soil profiles remained constant, and the maximum height of ponding at the soil surface was set at 50 cm.

The atmospheric boundary conditions with surface layer allow the build-up of water on the surface, which is influenced by rainfall, evaporation and infiltration. The upper boundary condition represents the daily rainfall measured using the HOBO tipping bucket rain gauge, while the actual evapotranspiration was estimated using the Penmann-Monteith algorithm (Allen et al. 1998) based on data from the synoptic weather station located in Navrongo about 45 km away.

The bottom condition was specified as free drainage, because most of the time groundwater level in the wetland is between 0.25 m and 15 m below the surface; this varies spatially within the wetland. Soil hydraulic properties were specified in four layers for the top 100 cm of the soil. This specification allowed the data to be fitted into the finite element difference scheme used by the model to simulate flow processes. For each layer, the hydraulic properties and the van Genunchten parameters were specified.

The model was run for 457 days starting from August 2004 to October 2005 during the study period when groundwater level measurements were performed. Since the measurement of actual flux, bottom flux, volume of storage and level of ponding was difficult; the HYDRUS-1D model enabled the reproduction of the seasonal variation of these factors at the different study points in relation to the potential flux of water input (rainfall and evapotranspiration).

Water flowing through the cross section of the soil travel to add up to already water stored in the soil. In the simulation, soil properties were seen to vary spatially, which had a bearing on the volume of water stored. The sample pits had a volume of 1 m^3 with an average total porosity of 44% and effective porosity of 23%. The volume of water stored by the pits in the Pwalugu floodplain wetland ranged between 0.25m^3 and 0.48m^3. The rate of water input as inflow and withdrawal as outflow influences the volume of storage, hence the intensity of actual flux between the July and October contributed to the volume of water stored in the system. The volume of storage has a

significant effect on the contribution of water from the floodplain wetland to the sustenance of the main White Volta River as base flow in the wet and dry seasons. In September 2005, the volume of storage in Pit 1, Pit 2, Pit 4 and Pit 7 was 0.48 m^3, 0.40 m^3, 0.38 m^3 and 0.39 m^3, respectively; these values represent the highest storage points.

The contribution of water input subsurface or groundwater system recharged showed spatial variation; this is clearly indicated by the amount of bottom water discharge by the pits (Figure 6.13). In August 2006, Pit 1 discharged about 0.73 cm of water, while Pit 6, which was about 100 m away from Pit 1 close to the main river channel, discharged about 0.96 cm. The average bottom discharge of 0.29 cm in June 2005 and 1.23 cm in July 2005 contribution of discharge into the sub-surface increased the hydraulic head from 138.94 m in June to 139.30 m in July 2005, the highest discharge was within the period of highest total water input of 0.97 cm. Groundwater upwelling as a result of increased hydraulic head occurred in July and October, where recharge from the unsaturated zone was highest (see section 6.10).

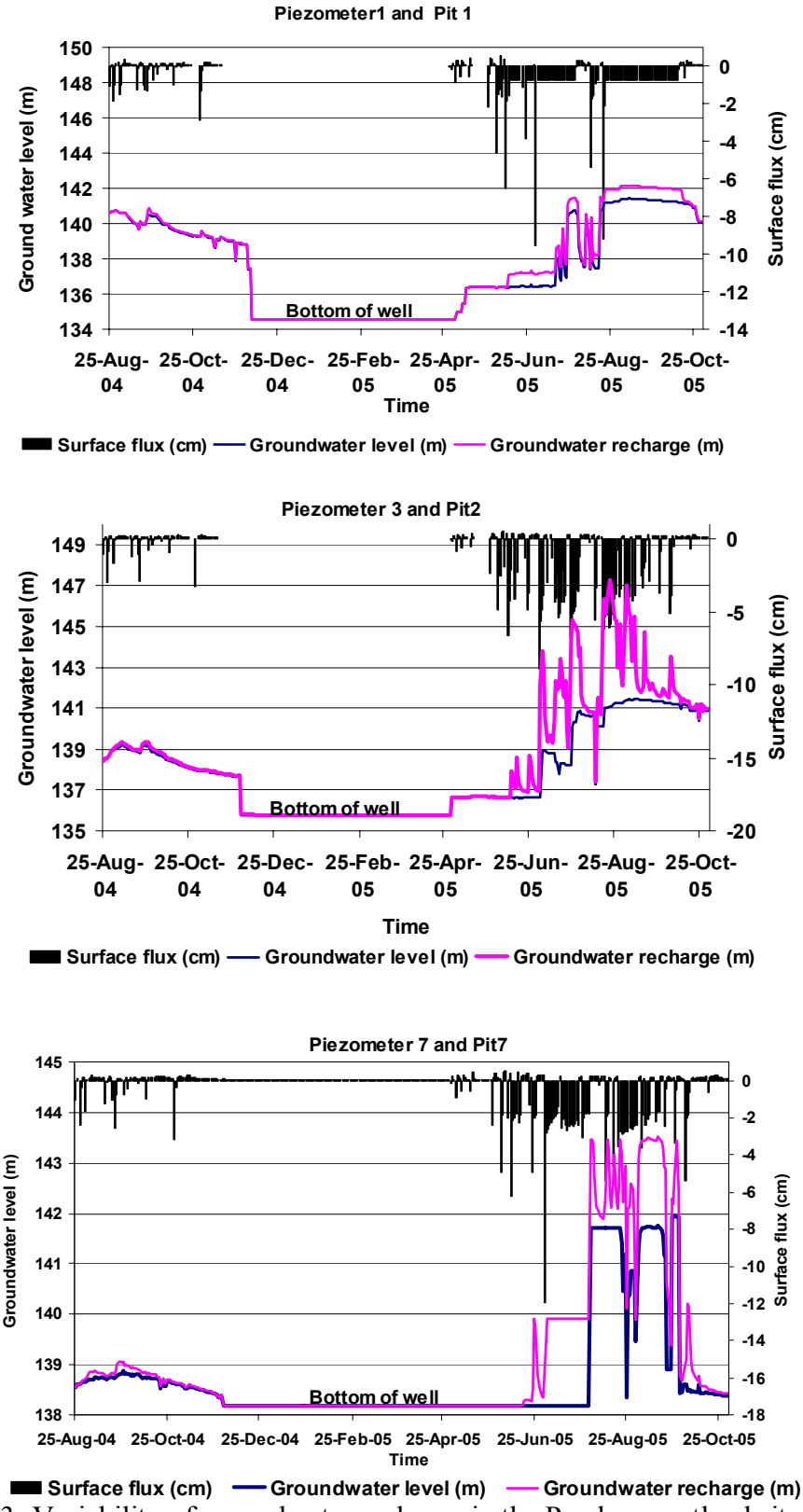

Figure 6.13 Variability of groundwater recharge in the Pwalugu wetland site

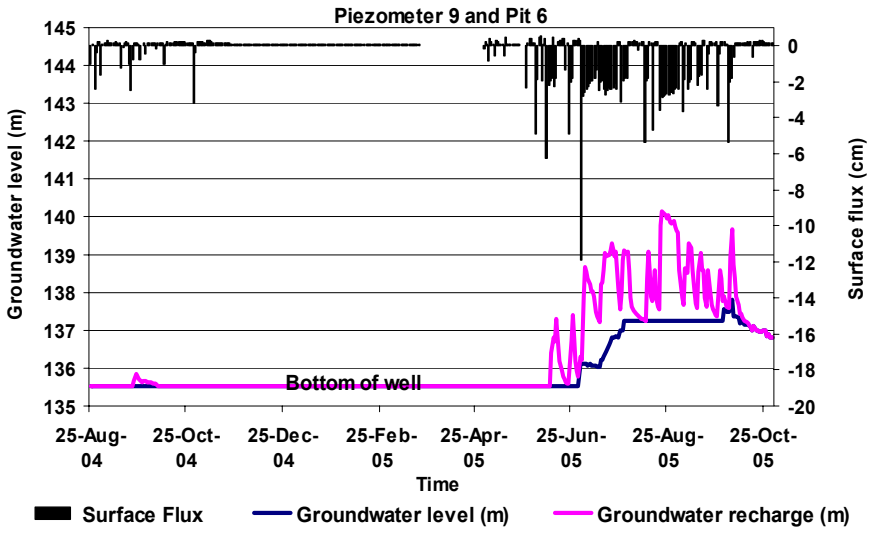

Figure 6.13 continued

The amount of water storage in the soil has a bearing on the compactness or looseness of the soil taking into consideration effective porosity. The volume of storage of each point in the wetland is different in terms of actual surface flux, bottom flux and storage capacities. However, exceeding the porosity threshold is water stored at the surface or runoff. Given the potential flux for Pwalugu wetland from August 2004 to October 2005, the actual flux for each soil point unit conducted the input differently. Therefore, due to the seasonal variability of water input and output, a recharge into the groundwater is at different rates.

The accuracy of the HYDRUS-1D model depends on the simplification and assumption implicit in the model and its relationship with the conditions of the site. The model applied to the Pwalugu site assisted to partition excess soil water moving vertically, thus estimating the amount of recharge into the groundwater.

6.8.3 Water balance

Water flowing within the floodplain wetlands in the White Volta basin are rarely quantified, for floodplain water management to sustain the proposed floodplain agriculture by the Ghana Ministry of Food and Agriculture. In order to quantify water flow in the unsaturated zone and identify sustainable management options, the water balance was estimated for the Pwalugu floodplain wetland for the period from September 2004 to December 2005 (Table 6.6).

Table 6.6 Monthly water balance at the Pwalugu wetland site

Time	Inflow of water [mm/month]	Potential evapotranspiration [mm/month]	Actual surface flux [mm/month]	Groundwater recharge [mm/month]
September 2004	107.99	47.91	56.30	48.06
November 2004	66.79	108.61	26.50	39.45
May 2005	21.03	169.72	11.68	8.44
July 2005	21.15	74.18	13.97	6.38
September 2005	101.99	57.29	53.30	47.03
November 2005	51.91	122.39	36.51	11.30

Table 6.7 Annual water balance for soil profile in the Pwalugu wetland

Time	Inflow of water [mm]	Potential evapotranspiration [mm]	Actual surface flux [mm]	Groundwater recharge [mm]
2004	352.09	342.18	174.42	168.56
2005	379.17	1093.37	627.17	276.15
	731.26	1435.55	452.75	444.71

The amount of water storage varied with seasons (Table 6.6). The volume of water in the entire wetland is a reflection of inflows relating to actual surface flux and groundwater recharge contributing to subsurface water. The contribution of water into the subsurface water vary seasonally, and its within the rainy season, where September 2004 within this period contributes a total of 48.06 mm whiles September 2005 contributes 47.03 mm. The inflow simulated by HYDRUS-1D was 107.99 mm and 101.99 mm for September 2004 and September 2005 respectively. Drainage i.e., groundwater recharge is beyond 6 mm is associated with significant amount of water input beyond. During the dry period of the climatic year between November and May, high evaporative values are recorded, little contribution to the subsurface water system is simulated. The annual contribution to deep drainage or groundwater recharge as calculated from the water balance averaged 168.57 mm for the year 2004, while 276.16 mm was calculated for 2005 (Table 6.7).

6.9 Electromagnetic profiling

To locate piezometers for monitoring water dynamics in Pwalugu and Tindama floodplain wetlands, a reconnaissance survey was undertaken. The electromagnetic profiling technique (EMP) was used to detect the presence and depth of sub-surface water in the Voltaian formation that underlies the study area. The Voltaian sandstone is

an old sedimentary formation of the Paleozoic era and behaves like a hard rock, which is mostly non-porous with low permeability. The technique can detect variations in subsurface conductivity in the Voltaian formation, i.e., large extensive fractures with thick weathered materials that may contain groundwater.

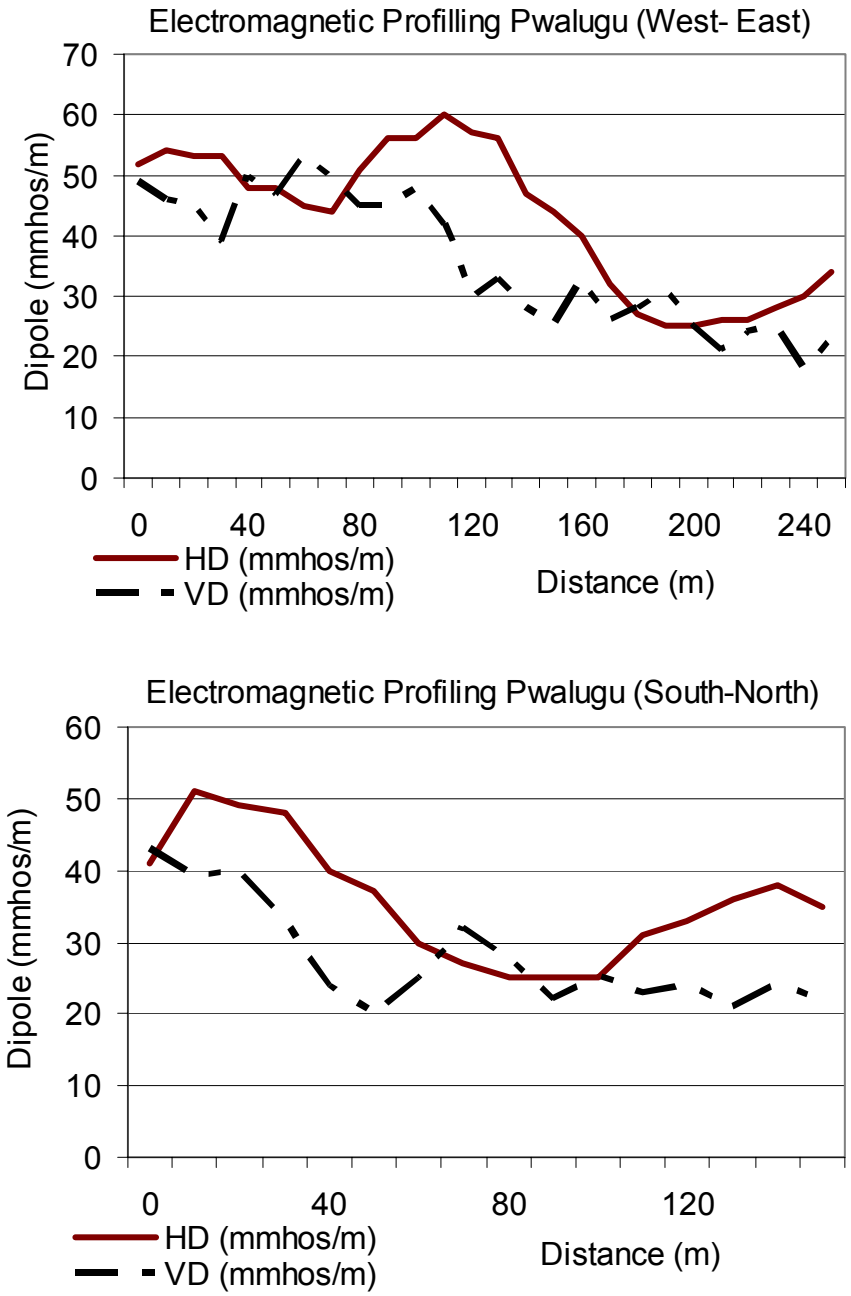

Figure 6.14 Electromagnetic profile curves for Pwalugu wetland (HD-horizontal dipole, VD-vertical dipole)

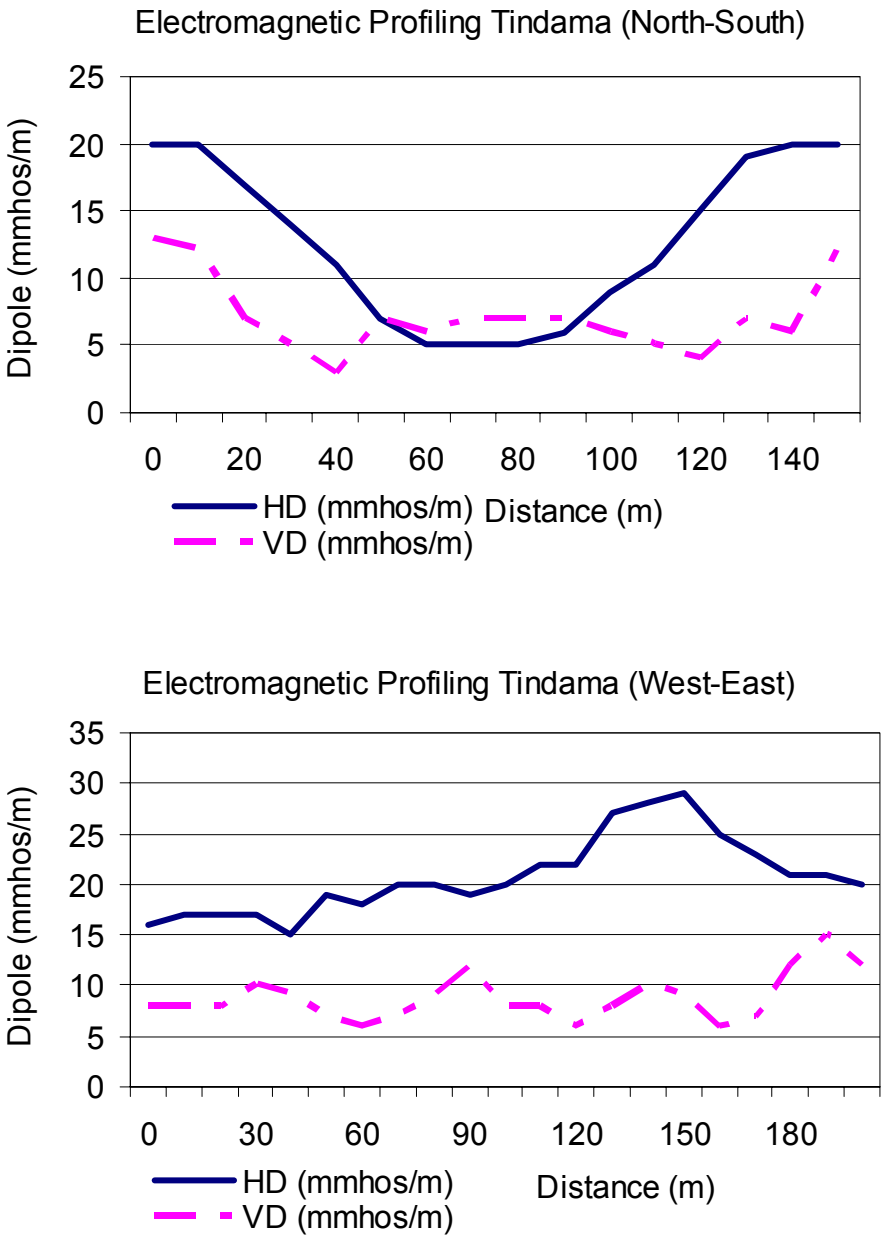

Figure 6.15 Electromagnetic profile curves for Tindama wetland (HD-horizontal dipole, VD-vertical dipole)

Electromagnetic profiling makes use of a time-varying electromagnetic field (primary field) to induce eddy currents within subsurface conductors. These currents result in a secondary magnetic field that is measured together with the original transmitted signal, using a receiver coil on the EMP instrument. The depth of penetration attained is dependent on a number of factors including ground conductivity, loop spacing and orientation of the primary field (dipole orientation). The electromagnetic sounding curve (Figure 6.14 and 15) at each transect of the wetlands

matched to the stratigraphy of the area provides an estimate of the depth to sub-surface water. The Tindama transect A showed a horizontal dipole conductivity of 20 mmhos/m and a vertical dipole of 16 mmhos/m. For transect B, the HD was 29 mmhos/m and the VD 15 mmhos/m. At the Pwalugu wetland site, values were high for the transect A with a HD of 60 mmhos/m and a VD of 52 mmhos/m. Pwalugu transect B the HD was 52 mmhos/m and the VD of 43 mmhos/m. The high conductivity values at Pwalugu wetland site indicate accumulation of highly weathered material that contains an appreciable amount of subsurface water as compared to Tindama with its low conductivity values.

6.10 Water table monitoring

Floodplain wetlands in the White Volta basin have many complexities in the water flow, both overland and subsurface, hence there is a need to monitor them. Pwalugu and other wetlands have different hydroperiod that defines the seasonal pattern of groundwater upwelling. This is an important indicator in the water budget of wetlands and links the input with outputs. Therefore, seasonal changes in subsurface water level may be the result of external factors. At the Pwalugu wetland 8 piezometers were installed to give a general picture of fluctuation of the groundwater level.

Figure 6.16 Water ponded on the surface at the Pwalugu wetland site

Wetland subsurface water levels were monitored at the Pwalugu wetland using 8 piezometers consisting of 3 cm diameter pipe ranging from 3 m to 6.6 m in depth. The locations of the piezometers (Figure 6.17) were selected to represent different aspects of the floodplain wetland to give an overview of the subsurface water situation. Vertical and horizontal hydraulic gradient and variance were calculated for the piezometers. From the piezometers measurement it could be seen that the groundwater level declined after the rainy season due to the absence of rainfall input. Between 11 and 16 September 2004, a total rainfall input of 15.99 cm the response rate for most of the piezometers started from 20th September, 2004. The decline rate in the site varied, and PZ08 and PZ09 closer to the main river, experienced a fast decline, while PZ01 at the toe of the wetland slope was the last to empty.

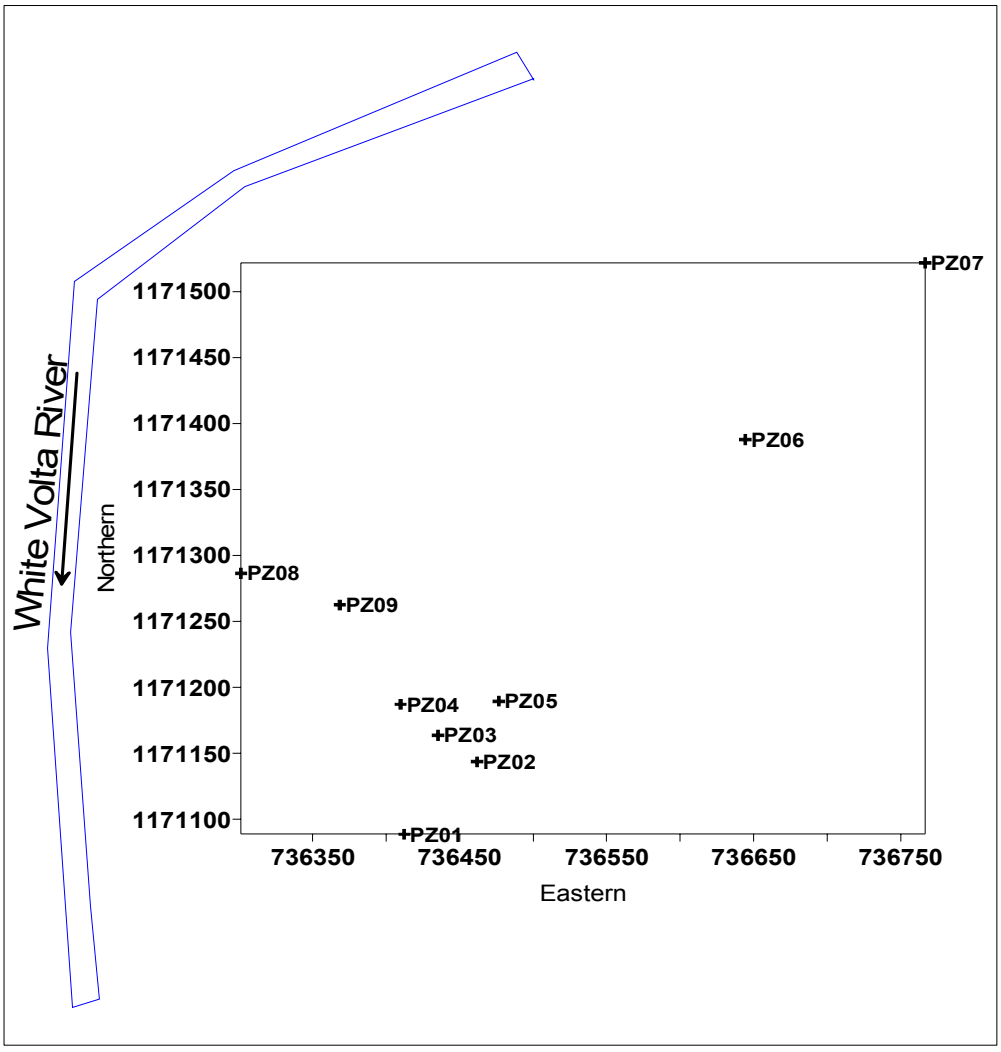

Figure 6.17 A map showing the location of piezometers at the Pwalugu floodplain wetland site along the main White Volta River

Table 6.8 Analysis of variance for groundwater monitoring for the Pwalugu Wetland site

	PZ01	PZ02	PZ03	PZ05	PZ06	PZ07	PZ08	PZ09
Mean	137.501	139.557	137.822	137.324	138.386	138.725	36.813	135.956
Median	136.477	138.733	137.635	136.888	137.478	138.163	136.497	135.523
Std Error	0.128	0.059	0.098	0.075	0.070	0.053	0.041	0.035
Std Dev.	2.654	1.220	2.049	1.555	1.447	1.099	0.845	0.723
Variance	7.044	1.489	4.198	2.418	2.095	1.209	0.715	0.523
Coeff. Var.	1.930	0.874	1.487	1.132	1.046	0.792	0.618	0.532
Skewness	0.164	0.837	0.550	0.197	1.237	2.171	3.518	1.181

For most of the wells, August to September showed a high response rate and at PZ01, water ponded at the surface to a depth of 44.63 cm; this piezometer was located at the lowest point of the wetland. Ponding was found in PZ02, PZ03, PZ05 and PZ06, while the other piezometers experienced a rise in water level. However, the level of ponding was not uniform but varied from point to point within the wetland, since the topography is uneven.

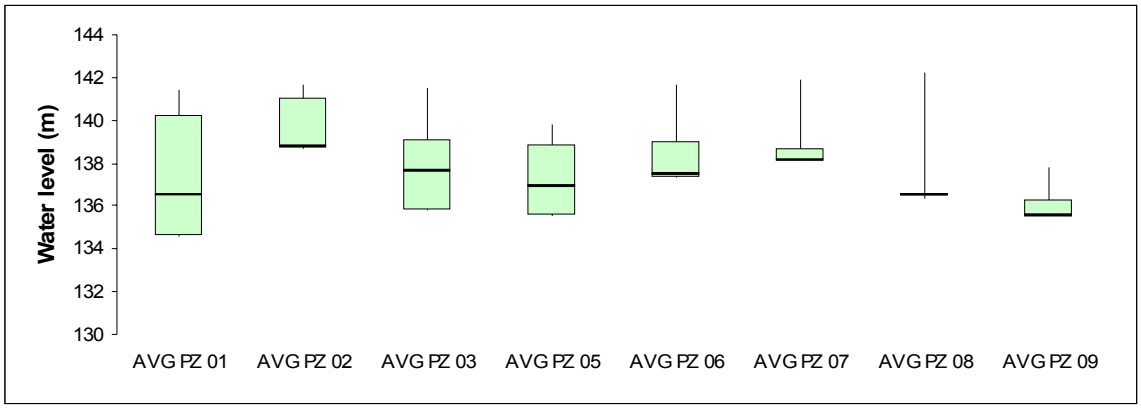

Figure 6.18 Box plot showing groundwater level fluctuation at the Pwalugu floodplain wetland site. Median are shown as the thick line in the box and the whiskers are the 10th and the 90th percentiles

To verify the level of variation or dispersion between and among wells, the box plots of the groundwater levels (Figure 6.18) were compared to the median of water level ranged from 135.5 m to 138.73 m over the 433 days of the study period. The absolute water level fluctuation ranged between 2.285 m and 6.87 m. The difference in fluctuation could be seen in their rate of which they respond to rainfall input. The box

plot of the median indicates that fluctuation in Pwalugu floodplain wetland was high. The analysis of variance (Table 6.8) showed variability in water level in different parts of the wetland, PZ01 with a variance of 7.04 and coefficient of variation of 1.93 had a high level of response rate than PZ08 that is close to the main White Volta river channel, which had a variance of 0.72 and coefficient of variation of 0.62. The water level in the piezometers are skewed towards the rainfall event, except PZ01 and PZ05 having a skewness on 0.16 and 0.19 indicating that these wells had some level of water throughout the year.

The vertical hydraulic gradient (VHG) was calculated as the difference between hydraulic head divided by the depth to the piezometer screen. A positive VHG indicates upwelling, a negative indicates draw down.

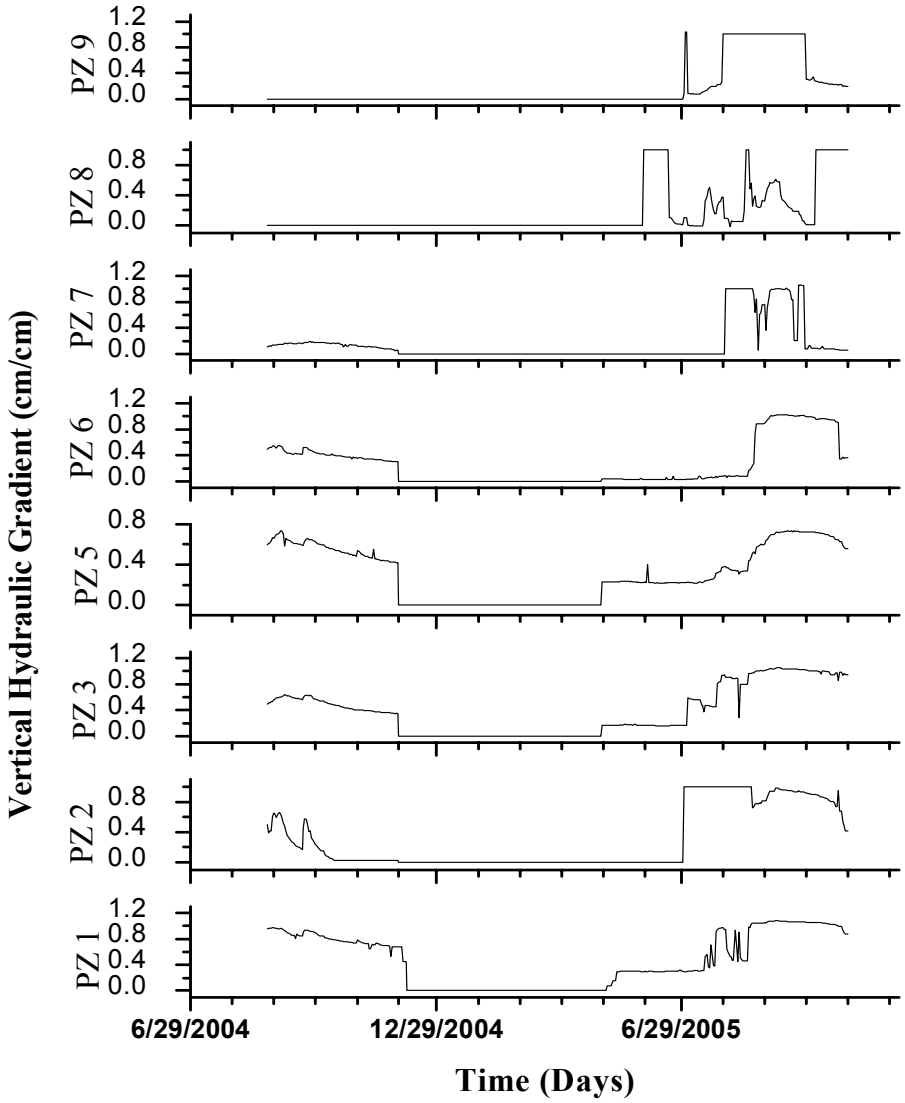

Figure 6.19 Vertical hydraulic gradient in Pwalugu wetland site

The groundwater level at the Pwalugu wetland site showed a distinct and regular seasonal fluctuation (Figure 6.19). In general, the water table declines gradually from November and becomes empty in May for most part of the wetland. The VHG showed down welling in the dry season and most of the wells had little or no water. The level of groundwater dislocated deep beneath. From July till November in every year, upwelling was observed in all piezometers. A VHG of 0.4 and above is a good indicator of subsurface water rising up. The Tindama wetland site has a geological formation that is not a good aquifer, therefore; no piezometer was installed in there. The piezometers installed at the Pwalugu site enabled the identification of hydraulic heads and the

quantification of the direction of groundwater flow. The temporally measurement of the hydraulic head gives an idea about the variability of water fluxes. But the variation in topography contributes to the local differences and redistribution of water within the study site.

6.10.1 Horizontal hydraulic gradient

To determine the flow direction of groundwater (Horizontal Hydraulic Gradient), the hydraulic heads of piezometers were used, which were installed at different points in the wetland. As noted before, the position of these wells in relation to the water table is used to relate groundwater discharge as a component of the wetland water balance. Topographically, the Pwalugu wetland site has a gentle slope making it very difficult to determine the direction of flow of groundwater when considering the overall landscape.

The horizontal hydraulic gradient (H_x) is the change in hydraulic head per unit of distance of the groundwater flow in a given direction. The horizontal hydraulic gradient, H_x, in the flow direction X, is expressed as follows:

$$H_x = \frac{H_2 - H_1}{X} \tag{6.1}$$

where H_1 represents the down-gradient hydraulic head and H_2 the up gradient hydraulic head, and X is the distance between these two points.

Mathematically, the hydraulic gradient is a vector that can be expressed as gradient (h). The norm of the vector represents the maximum slope of the hydraulic gradient; its orientation represents the direction along the maximum slope. The hydraulic gradient is a dimensionless parameter, usually represented as a fraction rather than as a percentage.

Table 6.3 Horizontal hydraulic gradient between selected piezometers in Pwalugu wetland site

Date	PZ07 & PZ01	PZ07 & PZ05	PZ05 & PZ01	PZ03 & PZ01	PZ06 & PZ01	PZ06 & PZ05	PZ07 & PZ09
Aug-04	0.00125	0.00368	-0.00778	-0.01398	0.00227	0.00700	0.01049
Sep-04	0.00210	0.00375	-0.00409	-0.00449	0.00264	0.00581	0.01057
Oct-04	0.00350	0.00501	-0.00227	-0.00313	0.00386	0.00677	0.01068
Nov-04	0.00409	0.00563	-0.00179	-0.00299	0.00458	0.00760	0.01029
Dec-04	0.01157	0.01083	0.01363	0.02723	0.01271	0.01241	0.00970
May-05	0.00907	0.00788	0.01298	0.02145	0.00946	0.00791	0.00970
Jun-05	0.00813	0.00789	0.00855	0.01449	0.00802	0.00786	0.00970
Jul-05	0.00588	0.00749	-0.00036	0.02462	0.00497	0.00752	0.00666
Aug-05	0.00812	0.01227	-0.00755	0.02522	0.00314	0.00817	0.01233
Sep-05	0.00464	0.00831	-0.00907	0.01191	0.00599	0.01311	0.01208
Oct-05	0.00045	0.00278	-0.00812	0.01266	0.00490	0.01105	0.00726

\+ *injection*
– *reversal flow (withdrawal)*

In an unconfined (water table) aquifer, the horizontal hydraulic gradient of groundwater flow is approximately the slope of the water table. In a confined aquifer, it represents the difference in potentiometric surfaces over a unit distance. The potentiometric surface is the elevation to which water rises in a well that taps a confined aquifer. It is an imaginary surface analogous to a water table. In general, the hydraulic gradient of groundwater flow in a highly permeable geologic material, such as sand or gravel, is far less than that in a geologic material with a low permeability, such as silt and clay. The direction of sub-surface water movement shows some variation with respect to season and the topographic position of the well (Table 6.9). In July 2005 there was an injection of water from PZ07 to PZ01 at a rate of 0.0059 m/m, indicating a down-gradient water movement. However, also in July 2005, there was a reversal flow from PZ01 to PZ05 at a rate of -0.00036 m/m. The general overview is that water flow within the sub-surface of the Pwalugu wetland is multi-directional, bring into question the slope and geological structure of the sub-surface layers in the wetland.

6.11 Factors affecting floodplain wetland hydrodynamics

To understand the hydro-dynamics (level of water fluctuation) within the Pwalugu and Tindama floodplain wetlands as an input into floodplain management, factors that affect these wetlands were determined using factor analysis. Factor analysis is a method based on principal component analysis and is used to derive correlation matrix and standardize

various parameters measured in the field. These parameters were rotated using the varimax method as the reference axis of the variables, thereby creating new dimensions. This form of standardization gives weights to variables, which are inversely proportional to their standard deviation. The procedure of standardization is important because the original variables used were measured discretely and are not of the same units, hence correlation analysis was the best beginning point for factor analysis.

Table 6.40 Explained variance in hydro-dynamics at wetland sites

Pwalugu (Eigenvalues)					
	Factor 1	Factor 2	Factor 3	Factor 4	Factor 5
Eigenvalue	7.184	3.406	3.074	1.474	1.471
% of Var.	34.208	16.219	14.640	7.018	7.005
Cum. %	34.208	50.427	65.067	72.085	79.090
Tindama (Eigenvalues)					
	Factor 1	Factor 2	Factor 3	Factor 4	Factor 5
Eigenvalue	8.412	3.476	2.637	2.323	1.246
% of Var.	40.056	16.554	12.558	11.061	5.934
Cum. %	40.056	56.609	69.168	80.228	86.163

Principal component analysis is quite effective for reducing the set of predictor variables, but results in a system of coefficients that is difficult to interpret. Hence, the principal component coefficients were rotated to maximize coefficients on the dominant variables in each factor while minimizing coefficients for all other variables, thereby making each factor easier to interpret with respect to the original variable. Five components (Table 6.10) were identified that influence the hydrodynamics of the Pwalugu wetland site, explaining 79.09% of its variability. In the Tindama wetland, five factors were also identified explaining about 86.32% of the overall variability. In addition, the correlation between variables and factors; greater than 0.50 ($p<0.05$) helped in defining the factors, the lower coefficients were not disregarded but also helped in identifying and naming factors (Table 6.11).

Table 6.5 Factor analysis for soil parameters in Pwalugu and Tindama wetlands

	Pwalugu -varimax rotated factor loadings					**Tindama -varimax rotated factor loadings**				
Variable	**Factor 1**	**Factor 2**	**Factor 3**	**Factor 4**	**Factor 5**	**Factor 1**	**Factor 2**	**Factor 3**	**Factor 4**	**Factor 5**
Depth	0.003	0.934	-0.003	0.185	-0.099	-0.195	-0.528	0.078	0.295	-0.029
pH	0.182	0.211	-0.011	0.198	0.103	-0.070	-0.087	-0.467	0.042	-0.111
% Org M.	-0.614	-0.330	0.147	-0.241	0.094	0.155	-0.081	0.149	-0.029	0.171
%C.E.C	-0.724	0.033	0.355	-0.068	0.174	0.122	0.207	0.918	0.033	0.124
Ks cm/day	0.008	-0.110	-0.105	-0.126	-0.049	0.097	0.850	0.149	-0.034	0.190
Bulk. Den. g/cm3	0.226	0.134	-0.011	0.933	-0.109	-0.209	-0.957	-0.081	0.013	0.101
Moist. Cont	-0.077	-0.034	-0.926	-0.341	0.087	0.236	0.836	0.026	-0.002	-0.466
Effective Moist	0.005	-0.004	-0.995	-0.012	0.044	0.135	0.095	-0.114	0.013	-0.956
Total porosity	-0.192	-0.135	-0.028	-0.940	0.100	0.209	0.957	0.081	-0.013	-0.101
Effective porosity or residual	-0.058	-0.062	0.935	-0.321	-0.018	0.084	0.801	0.144	-0.027	0.558
Sand	0.680	0.054	0.030	0.124	-0.706	-0.747	-0.200	-0.008	-0.046	0.077
Clay	-0.984	0.037	-0.040	-0.101	-0.024	0.967	0.157	0.081	-0.020	-0.031
Wilting Point. 1500KPa	-0.981	0.026	-0.045	-0.111	0.001	0.966	0.157	0.086	-0.023	-0.030
Field Capacity 33KPa	-0.904	-0.018	-0.079	-0.143	0.360	0.956	0.184	0.080	-0.020	-0.038
Saturation 0KPa	-0.897	-0.103	0.084	-0.138	0.256	0.909	0.214	0.053	0.023	-0.030
Plant Avail. %	-0.259	-0.100	-0.109	-0.135	0.927	-0.004	0.107	-0.020	0.012	-0.032
Sat. Cond. cm/day	0.624	-0.137	0.187	0.080	-0.388	-0.798	-0.029	-0.124	0.075	0.109
Hue	-0.046	-0.078	-0.041	0.023	0.109	0.377	0.121	-0.107	-0.010	-0.180
Value	-0.044	0.578	-0.016	0.246	-0.029	-0.114	-0.534	-0.110	0.455	-0.109
Chroma	0.182	0.233	-0.131	0.230	-0.080	-0.407	-0.520	-0.290	-0.059	0.061
Elevation	0.105	-0.003	0.003	-0.171	-0.009	0.140	0.087	0.910	-0.048	0.034

The factors were named according to their degree of influence on the hydrodynamics of the wetlands (Table 6.12). Vertical water movement in the wetland with respect to water input, either by rainfall or by irrigation, is influenced by a range of variables including clay content, organic matter, CEC and pF (positive influence on water input) and sand and saturated hydraulic conductivity (negative influence). Antecedent soil moisture is the most important factor that detects the level of hydrodynamics. For instance, factor 3 indicates a coefficient of 0.93 for moisture content and 0.99 for effective moisture explaining the amount of water present in a given pore system, while effective porosity (0.94) determines the pores that can store immobile water. Another factor deduced from the matrix is topography, this influences the nature of flow processes and is indirectly influenced by the nature of slope (concave,

convex or straight); the topographic position also plays an important role. The Tindama wetlands hydrodynamics varied, but not as much as those in the Pwalugu wetlands.

Table 6.6 Factors that Influence Hydrodynamics in Pwalugu and Tindama Wetland

	Factor re-named	
Factors	**Pwalugu wetland**	**Tindama wetland**
Factor 1	Water input (rainfall or irrigation)	Water input (rainfall or irrigation)
Factor 2	Soil potentials/antecedent Soil Moisture	Soil structure
Factor 3	Soil structure	Vegetation cover and topography
Factor 4	Vegetation cover and topography	Soil potentials/antecedent soil moisture
Factor 5	Groundwater level	Over bank flow of White Volta River

Hydraulic conductivity is an important factor in the hydrodynamics of the Pwalugu and Tindama wetlands and is basically classified as a strong, nonlinear function of the moisture content. The falling head method used in measuring K_s took a very long time in reading values of draw down. In this case, gravity was not a strong driving force in relation to the low hydraulic conductivities that characterize the condition of some soil type under unsaturated conditions. The best alternative was to use pressure techniques that bypass portions of the sample, because pressure is not a whole body force. Like gravity, it seek the path of least resistance, e.g., fractures, sandy areas and macropores, and can affect the stabilities of common minerals like calcite, clays and gypsum.

6.12 Land use and anticipated effects on wetlands

Floodplain wetlands provide a wide range of benefits to the surrounding communities and its use is linked to its seasonal pattern (Figure 6.20). Land use in the form of crop cultivation in both the main and off season in the Pwalugu and Tindama wetland catchment exposes the land to environmental hazards that will alter the wetland hydrodynamics and affect flora and fauna. The qualitative characterization of the observed cycle of land-use activities (Figure 6.20) using common set of parameters such as magnitude, frequency, areal extent, spatial distribution and predictability within and around the wetlands helps to some extent to avert land degradation.

This approach of land assessment by the local farmers permitted them to qualitatively evaluate/assess the anticipated effects of diverse activities such as crop cultivation, grazing, fuel wood harvesting, fishing and environmental restoration. The assessment showed that the uncontrolled use of land around the wetlands will pose problems for hydrological processes and water quality because of the natural storage and cleansing functions of wetlands. However, the soils are very heterogeneous due to uneven distribution of sediments, hence farmers optimize the soil resources by planting different crops on different textured soil. Based on local knowledge of soil characteristics farmers determine which soil support a certain kind of crop, e.g., groundnut, water melon in sandy soil and soya beans and okra in loamy soil. With regard to soil fertility, farmers use plants such as *Indigotera Secumdiflora* and *Chromolaena Odorata* as indicators of good soil and for low soil fertility these are *Striga Hermonthica, Striga Asiatica* and *Sida Acuta*. The use of these indicators is give farmers the impetus to cultivate crops closer the river banks and wetlands.

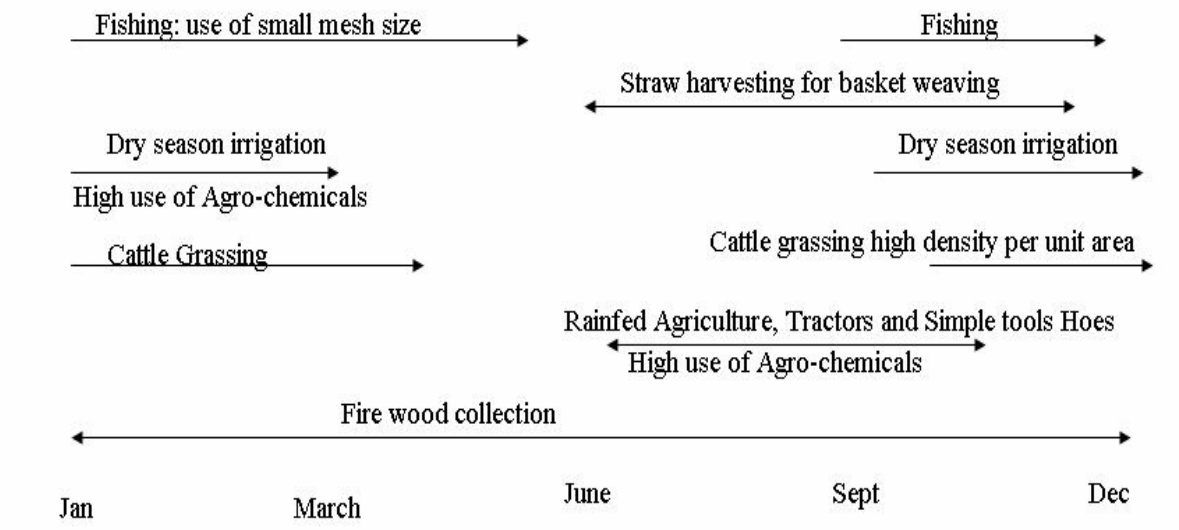

Figure 6.20 Cycle of land use in floodplain wetlands of the White Volta River (After Thompson and Polet 2000)

Water-level fluctuations in the floodplain wetlands within the basin are of concern for the potential effects they may have on sustenance of stream flow, groundwater recharge, fishing for protein, water for cattles and source of water for dry season irrigation. The increasing use of agro-chemicals such as Roundup (Gyphosate),

Karate (Lambda-Cyhalothrin) and Furadan (Carbofuran) and in some case DDT have the potential for changing species composition and entering the food chain.

Changes in land cover around the wetlands through land-use do not necessarily imply a degradation of the land. Changes by the surrounding communities are for the improvement of their livelihood, e.g., the collection of firewood, tree stumps for shelter construction and wood for fencing their gardens. Occasional tree planting is done with the best of intentions and not for harming the environment. Communities within the catchment of the wetland have seen that land-use changes around the wetland to some extent return a net profit to the land user, while the impacts of negative externalities such as sedimentation, water pollution, biodiversity loss, and increased flooding are borne by the communities. Conversely, landowners within the wetlands may not undertake activities that result in secondary benefits (or positive externalities) if direct benefits to them would not reward the costs.

Figure 6.21 Land preparation for crop cultivation and watermelon cultivation in the dry season around the wetland in Pwalugu

The concerns raised in the GLOWA-VOLTA inception workshop in Bolgatanga, Ghana, July 2005, about land degradation within the Volta Basin by the Ministry of Land and Forestry, Ministry of Food and Agriculture and Environmental Protection Agency have taken different forms. These organization now have a policy on conservation emphasizing the need for careful and efficient management to guarantee a sustained supply of productive land resources for future generations. However, the Ghana Wild life Services also have sought to protect landscape and ecosystems. All

these goals and concerns cover the varied secondary effects of land use both on land cover and on other related aspects of the global environment. A conservation programme has been initiated to restore damaged land cover by planting tree species of tress of economic value to communities within the basin. Calculating the balance of costs and benefits from the land-use and land-cover changes by communities and governmental and non-governmental agencies is extremely difficult.

7 ISOTOPE ANALYSIS OF THE WETLANDS

7.1 Introduction

The earth has abundant water in all phases that is distributed in various reservoirs; i.e., the atmosphere, oceans, groundwater, dams, wetlands and rivers. Hydrogen and oxygen isotopes of water vary among these reservoirs in time and space. The isotopic compositions of some of these reservoirs do change through exchange of water either by equilibrium or by kinetic processes (Kendall and Caldwell 1998).

Isotope tracers have the potential of providing new insights into hydrologic processes within the White Volta basin (Buttle 2003) because they integrate small-scale variability and can give an effective indication of catchment-scale processes. Isotope tracers like oxygen-18 and Deuterium are integral parts of natural water molecules that fall as rain over the White Volta basin, and thus they become ideal tracers of water sources and allow a widespread application to hydrological processes. Stable isotopes like oxygen-18 and Deuterium behave conservatively (Clay et al. 2004; Clark and Fritz 1997), as they move through the landscape and interact with oxygen and hydrogen in the organic and geologic materials. Hence, the main processes identified to dictate the oxygen and hydrogen isotopic compositions of waters in a river catchment are:

(1) Phase changes that affect the water above or near the ground surface (evaporation, condensation), and

(2) Simple mixing at or below the ground surface.

Therefore, a typical use of stable isotopes for examine the hydrological processes within the White Volta River catchment includes:

- identification of water sources in wetlands and the White Volta River
- estimation of the evaporation from wetlands
- development of a water budget model for the wetlands
- characterization of flow paths that water follow from the time rainfall reaches the ground until discharge at the stream

This chapter discusses the research findings on the application of isotope tracers (^{18}O and ^{2}H) for analysis of wetland hydrodynamics within the Pwalugu and

Tindama wetland sites. In the Pwalugu wetland site, two wetlands (wetland-B and wetland-C) were sampled for isotope analysis.

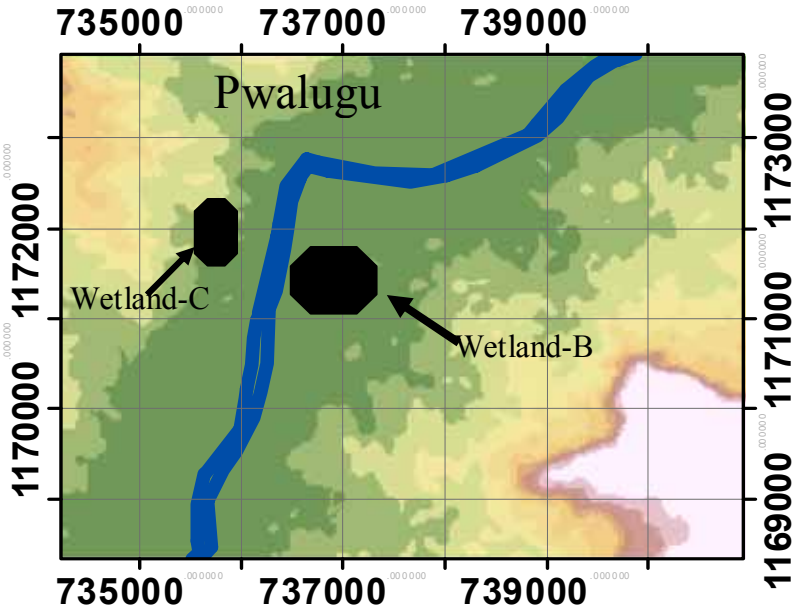

Figure 7.1 Wetland sites in Pwalugu for Isotope sampling

7.2 Results

7.2.1 Rainfall variation over the White Volta basin

Rainfall is the major source of water to the streams, rivers, reservoirs, groundwater and wetlands in the White Volta River basin. In assessing the basin water balance, rainfall amount relating to its temporal and spatial variation has to be accounted for. As water undergoes changes of state in the process of rainfall formation over the basin, the isotope molecules present in the water redistribute themselves between the phases such that the heavier molecules (^{2}H and ^{18}O) are concentrated in the condensed phase, while the lighter molecules (^{1}H and ^{16}O) are concentrated in the remaining phase, thereby making quantification of rainfall possible (Kendall and Caldwell 1998).

The interplay of several factors determines the composition of $\delta^{18}O$ and $\delta^{2}H$ in water vapor over the White Volta River Basin. The surface of the Atlantic Ocean plays a role in evaporation and in the fractionation that occurs during the change of state from liquid to vapor (Hoefs 1997). The trajectory of the tropical continental (cT) from the Sahara and maritime air masses (mT) from the Atlantic Ocean affects the isotopic composition of rainfall over the catchment (Hoefs 1997; Coplen et al. 2000). In addition

to the trajectories of cT and mT, rainfall formation through orographic or convectional processes within the White Volta basin account for differences in the isotopic composition in the Pwalugu and Tindama wetland sites (Figure 7.1 and 7.2).

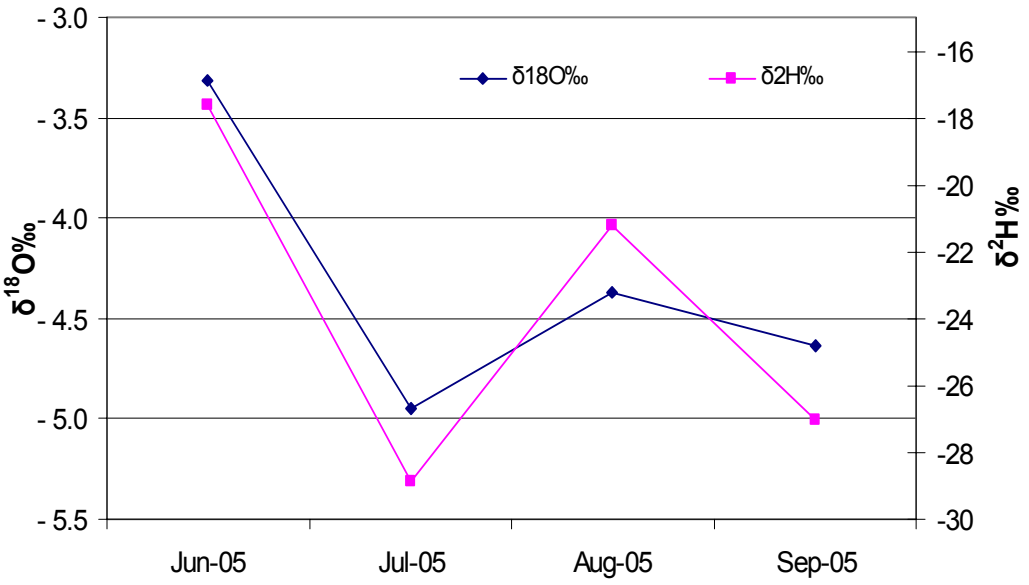

Figure 7.2 Monthly variation of $\delta^{18}O$ and $\delta^{2}H$ in rainfall in Pwalugu wetland site

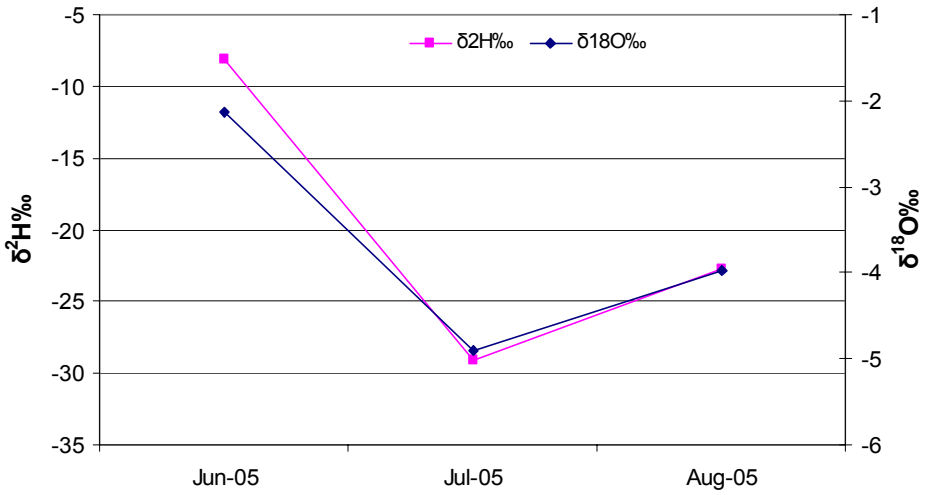

Figure 7.3 Monthly variation of $\delta^{18}O$ and $\delta^{2}H$ in rainfall in Tindama wetland site

The White Volta basin experiences seasonal variations in precipitation with peaks in June, July and September. The Navrongo synoptic weather station of the Ghana Meteorological Agency recorded a total amount of rainfall in June, July, and

September 2005 of 179 mm, 226.1 mm and 88.3 mm, respectively. As noted in the work of Mathieu and Bariac (1996), the isotopic composition at the beginning and the end of the rainy season is characterized by a low amount of rainfall with relatively enriched δ values. Hence, within the Pwalugu wetland catchment $\delta^{18}O$ measured as -3.3‰ and $\delta^{2}H$ as -17.6‰ (Figure 7.1) in June 2005, this is the beginning of the major rainy season. For July 2005, with a total monthly rainfall of 226.1 mm, the isotopic composition showed signs of depletion with values of -4.9‰ ($\delta^{18}O$) and -28.8‰ ($\delta^{2}H$).

The isotope composition of rainfall becomes enriched in August 2005 as a result of erratic rainfall pattern, September 2005, with a reduced rainfall of 88.3 mm, $\delta^{18}O$ measured -4.6‰ and $\delta^{2}H$ measured -27‰. In the Tindama wetland site, $\delta^{18}O$ measured in June was -2.1‰ and for $\delta^{2}H$ was -8.1‰ (Figure 7.2). Despite the unreliability of rainfall with isolated storm events in August 2005, at the Tindama wetland site a $\delta^{18}O$ value of -4.0‰ and $\delta^{2}H$-value of -22.7‰ were registered. A similar pattern of isotopic variation with a high depletion in the rainy season and an enrichment in the dry season is reported in the research of Martin (2005) and Acheampong and Hess (2000) in the northern and southern part of the Volta basin. The observed temporal and spatial variation in the stable isotopes composition in the rainfall in the Pwalugu and Tindama wetland sites is complicated by the systematics of the hydrological cycle, which includes evaporation, transpiration and mixing of air masses.

Kendall and Caldwell (1998) noted that during the process of surface and atmospheric interaction, part of the rained-out moisture is returned to the atmosphere by evapo-transpiration, during this process the simple Rayleigh law no longer applies. Hence, detailed of the evapo-transpiration process determines the downwind effect of the evapo-transpiration flux on isotopic composition of atmospheric moisture and precipitation. Therefore, change in isotopic composition along air-mass trajectory within the basin measures only the net loss of water from the air mass, rather than being a measure of integrated total rainout. On the other hand, during evaporation process, vapor is usually depleted in the heavy isotopic species in order to be in equilibrium with isotopic composition of atmospheric moisture. Hence the mixing of moisture derived from evaporation of wetland back into the atmospheric moisture reservoir has a somewhat smaller effect than the addition of transpired water in restoring isotopic composition of the original air mass (Hoefs 1997; Coplen et al. 2000).

7.2.2 Meteoric line

Evaporation from surface water bodies and its return via rainfall and runoff is an annual process at the local and global scale inclined to achieve some dynamic equilibrium (Dingman 2002). Periodically, there is a deviation from equilibrium, which may be due to a serious climatic shift caused by El Nino or other climatic phenomena that influence rainfall pattern, groundwater and surface water storage. Within the hydrological cycle and at each step, $\delta^{18}O$ and $\delta^{2}H$ have been noted to behave in a predictable manner (Clark and Fritz 1997), thereby a relationship can be defined at the global or local level when $\delta^{18}O$ and $\delta^{2}H$ are plotted against each other (Figure 7.3) (section 4.13.3).

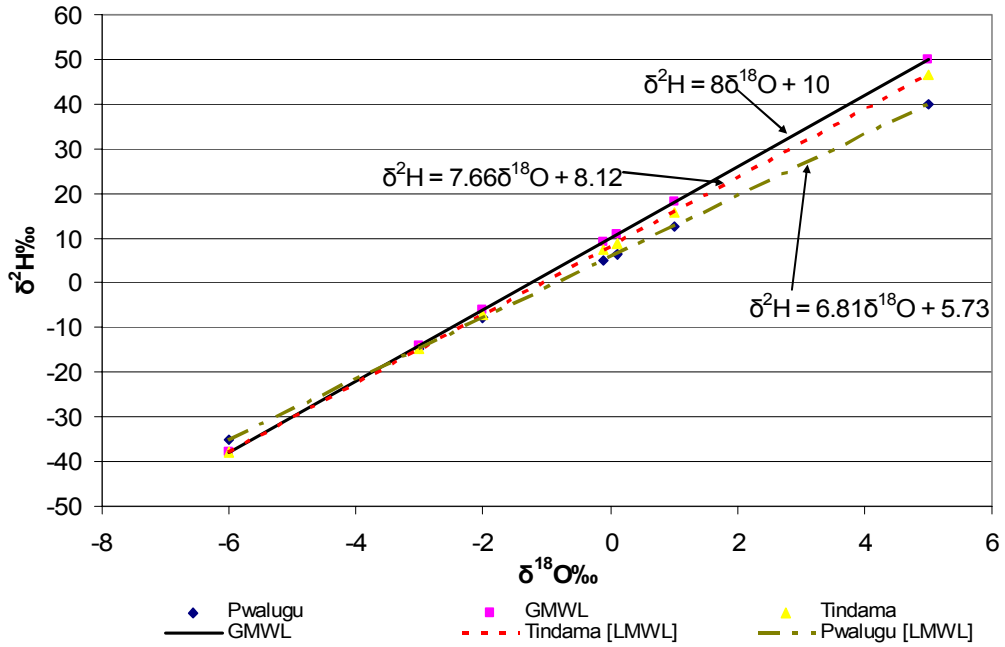

Figure 7.4 Global and local meteoric water line for Pwalugu and Tindama floodplain wetland sites

The isotope composition of rainfall in the White Volta River basin tends to follow the rainfall pattern, with isotopic depletion measured in July when total monthly rainfall is very high. However, due to topographic variation and distance (800 km) from the coast, there is a marked difference in rainfall storm events due to variation in humidity and temperature across the Volta basin (Jung 2006). In this situation, a local meteoric water line (LMWL) was computed for the Pwalugu and Tindama wetland sites by plotting $\delta^{18}O$ and $\delta^{2}H$ (Figure 7.3). For the Pwalugu wetland site, the LWML

computation yielded a δ^2H excess of 8.13 and a slope of 7.66 (r = 0.93), while a δ^2H excess of 5.73 and a slope of 6.81 (r = 94) was computed for the Tindama wetland site. The general observation is that the δ^2H values in storm events differ between the Pwalugu and the Tindama wetland sites, but show a behaviour characteristic of a tropical region (Akiti 1980). The slope and deuterium excess in the Pwalugu and Tindama sites indicate that rainfall occurred when the atmospheric humidity was less than 100% (Clark and Fritz 1997). In other words, storms events and the associated isotope enrichment at these sites are highly dependent on the humidity and temperature conditions in the evaporation region. However, the rainout effect of the storms moving over the basin determines the isotopic distribution and enrichment at the different sites.

7.2.3 Isotope variation in surface (river and wetlands) and sub-surface (piezometer) water

The Pwalugu wetland sites (wetland-B and wetland-C) derive their water from four main sources. These are direct rainfall, overland flow, occasional overbank flow of the White Volta River, and groundwater upwelling. For the Tindama wetland, the water source is limited to direct rainfall, overland flow and occasional overbank flow. There is no groundwater upwelling because the geological formation in which it occurs is a poor aquifer (Appendix A). However, the isotopic composition of these wetlands follows the seasonal (rainy and dry season) pattern, which gives information about their hydrodynamics (Figures 7.4, 7.5 and 7.6).

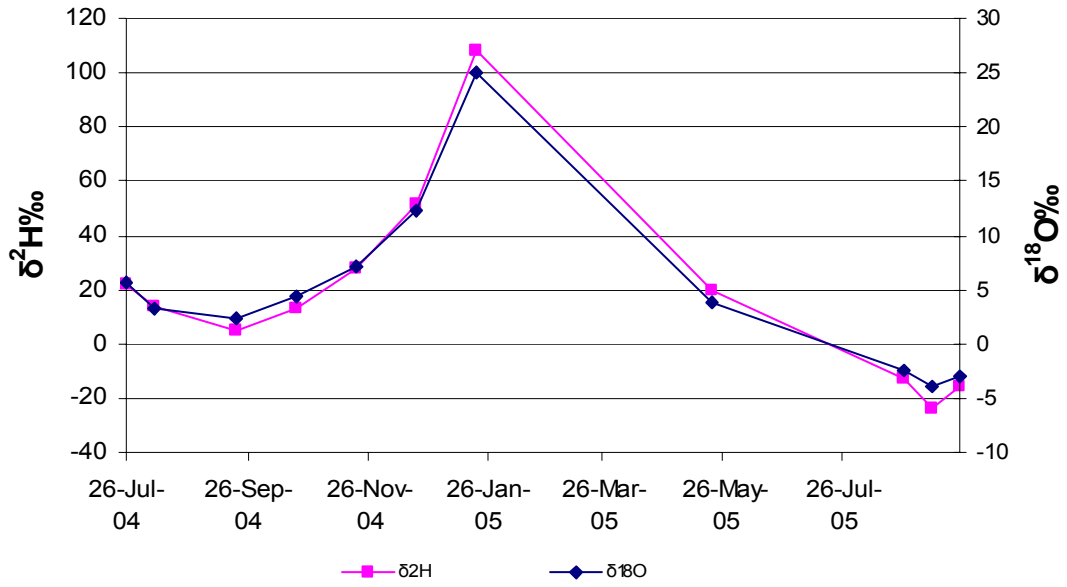

Figure 7.5 Seasonal variations of isotopic ($\delta^{18}O$ and $\delta^{2}H$) composition in Wetland-B of the Pwalugu site

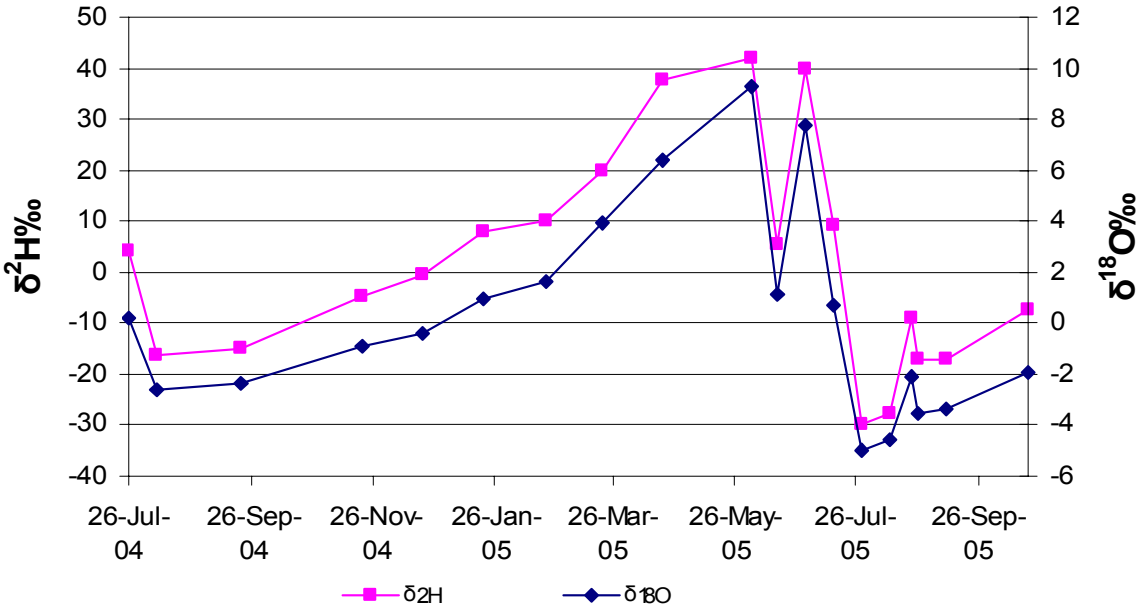

Figure 7.6 Seasonal variations of isotopic ($\delta^{18}O$ and $\delta^{2}H$) composition in Wetland-C of the Pwalugu site

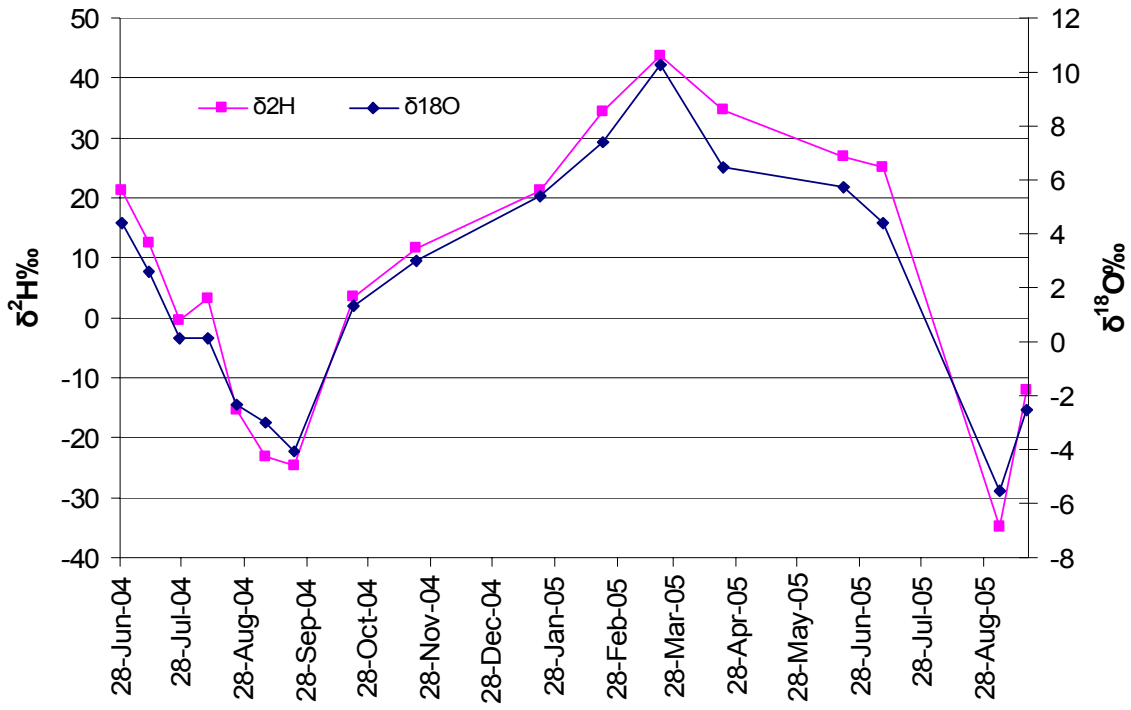

Figure 7.7 Seasonal variations of isotope ($\delta^{18}O$ and $\delta^{2}H$) composition in the Tindama wetland

To elucidate wetland hydrodynamics, $\delta^{18}O$ and $\delta^{2}H$ composition over the season in surface water and sub-surface water enabled a classification of the pattern of recharge and flow within the floodplain wetland. In other words, the seasonal dynamics of the floodplain wetlands in Pwalugu (Wetland-B and -C) and Tindama can be explained to some extent by noting the enrichment and depletion in $\delta^{18}O$ and $\delta^{2}H$ over the seasons under different atmospheric (humidity, temperature and evaporation) conditions. For instance, during the dry season in January 2005, with a mean temperature of 33°C, low humidity of 40% and potential evaporation of 50 mm/day, in the Pwalugu wetland-B site a highly enriched isotopic composition ($\delta^{18}O$ =25‰ and $\delta^{2}H$ = 108.2‰) was measured. The Tindama wetland also showed some form of enrichment ($\delta^{18}O$ = 5.4‰ and $\delta^{2}H$ = 21.3‰). During the rainy season with high rainfall, dilution is prominent and only little evaporation occurs in the system. For the period between 26 July 2005 and 9 August 2005 the rainfall values were high thereby increasing the percentage of dilution in Wetland-B and Wetland-C given by $\delta^{18}O$-values of -16.11‰ and -18.80‰, respectively. During this period, temperatures ranged

between 20°C and 28°C, humidity always above 72%, and minimal evaporation was measured.

For the White Volta River, a high isotopic enrichment is mostly recorded between November and May during the dry season, while between June and October the isotopic ratio shows signs of depletion (Figure 7.7). An exception is seen in the variation, e.g. July 2005 ($\delta^{18}O$ = -5.1‰ and $\delta^{2}H$ = –30.8‰) and September 2005 ($\delta^{18}O$ = -3.4‰ and $\delta^{2}H$ =–20.1‰) showed a high depletion ratio.

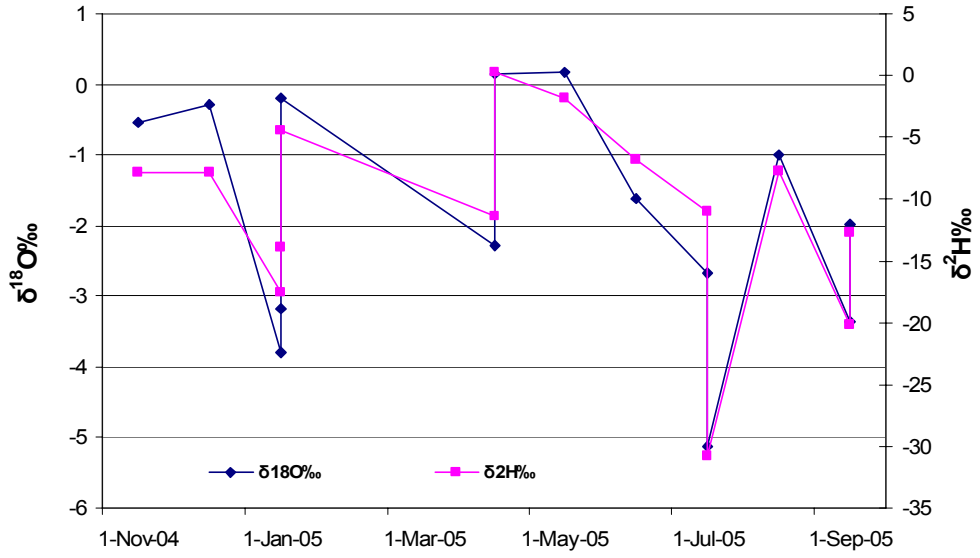

Figure 7.8 Seasonal variations of isotope ($\delta^{18}O$ and $\delta^{2}H$) composition in the White Volta River at Pwalugu gauging station

However, isotopic composition showed fractionation at all sites with significant deviations from the LMWL (Figure 7.8 and Figure 7.9). Hence, the values plot below the LMWL indicates the occurrence of evaporation. Using the Raleigh equation (equation 4.27), an estimated evaporative fraction of -9.62% was calculated for Wetland-B in August 2005 and 5.81% in September 2005. In Wetland-C, in August and September 2005, 5.9% and 8.24% were estimated respectively. For the Tindama wetland, an estimated evaporative fraction of -15.83% was calculated for August 2005 and 16.79% for September 2005.

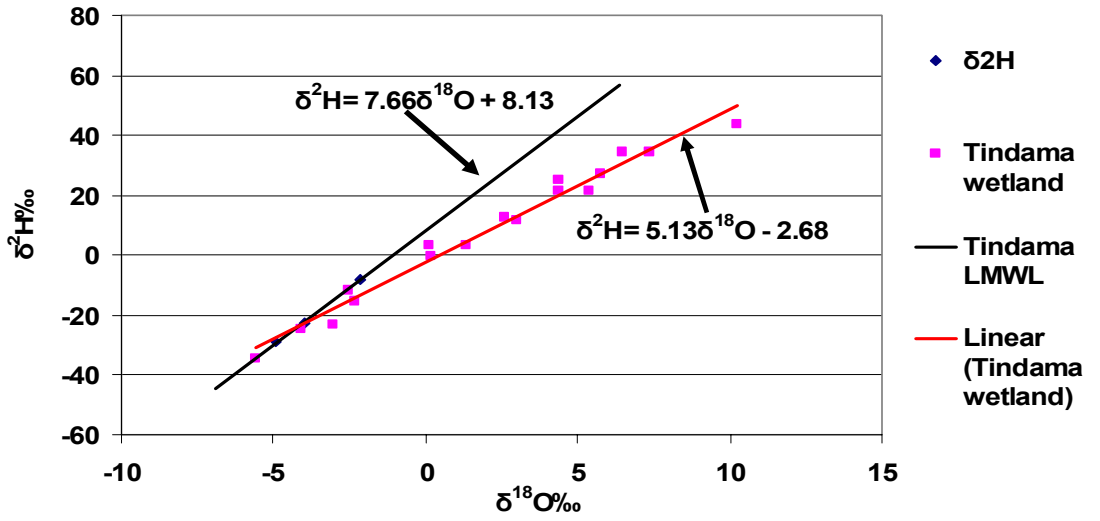

Figure 7.9 Isotopic composition of the sampled water from the Tindama wetland compared to the LMWL

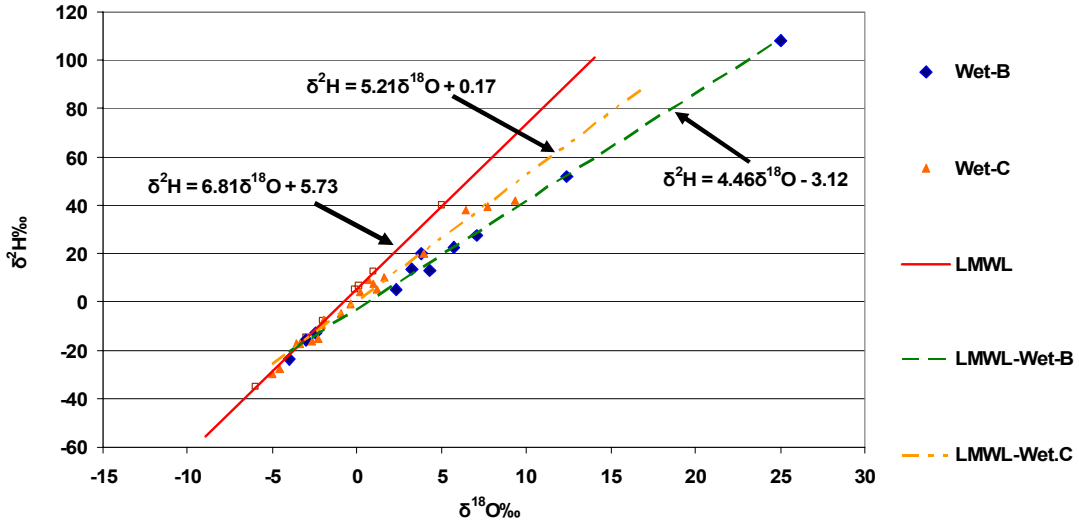

Figure 7.10 Isotopic composition of the sampled water from the Pwalugu sites (Wetland-B and Wetland-C) compared to the LMWL

Noting the isotopic composition measured in Pwalugu and Tindama, evaporation occurring within these sites shows some similarities with infinite-reservoir kinetic fractionation (Coplen 1993; Gat and Gonfiantini 1981). This is because the isotopic composition of the samples falls below their respective LMWL. Within the study period from May to December 2005 the estimated fraction of water loss from the wetlands in the form of evaporation varied from 5.81% to 53.25% for Wetland-B and

1.04% to 16.01% for Wetland-C and 9.53% and 28% for the Tindama wetland. In this situation, Wetland-B will be expected to dry up more rapidly than the other wetlands.

7.2.4 Water balance estimation

Subsurface water of the floodplain wetlands in the basin plays a vital role as it act as a major source of water for agricultural activities for the communities there. However, there is a growing concern about the sustainable use and management of this resource. In other words, an understanding and identification of floodplain wetland-river-flow interaction is necessary for viable sustainable floodplain agriculture. For any policy implication, it is important to assess how sustainable wetland water supply will be able to meet the demand of a unit area of floodplain under cultivation.

However, this is limited by lack of continuous hydrological data, making it difficult to study hydrological processes in floodplain wetlands. As an alternative means of providing hydrological data, a comparative analysis was made using 3 approaches to estimate water balance these include using open lake water budget model (equation7.1), equation 7.2 and the Raleigh equation (4.27).

The Tindama wetland and Pwalugu Wetland-B site were used for estimating the water balance. The water budget equation for open lake (Kedebe et al. 2006) and the isotope water balance model were adopted:

$$\Delta H = P(t) - E(t) + \left(\frac{R_{in}(t) - R_{out}(t) + G_{net}(t)}{A(h)} \right) + \varepsilon_t \qquad (7.1)$$

$$\Delta H = P(t)\delta_p - E(t)\delta_\varepsilon \qquad (7.2)$$

H = water level in the wetland [mm], **A** = depth dependent surface area of the wetland [mm], **P** = rainfall over the wetland [mm/month], **E** = evaporation [mm/month], t = time [month], $\mathbf{R_{in}}$ and $\mathbf{R_{out}}$ = surface water inflow and outflow [mm/month], $\mathbf{G_{net}}$ = net groundwater flux [mm/month], and $\boldsymbol{\varepsilon_i}$ = error term, $\boldsymbol{\delta_p}$ isotope ratio in precipitation and $\boldsymbol{\delta_\varepsilon}$ isotope ratio in evaporation.

Conceptually, the water balance is estimated for a pixel with a dimension of 30 m by 30 m and varying height that corresponds to the water level in the wetland (Figure 7.10). Groundwater flux, inflow and out flow were not measured, therefore these variables were constrained so that they did not contribute to the water level changes. Hence, water level in the wetland, rainfall and potential evaporation were the three variables that were considered to have some influence on the water balance in the wetlands. Using using open lake water budget model (equation7.1), equation 7.2 and the Raleigh equation (4.27) an estimated water budget (Table 7.1) was calculated for Tindama wetland and Wetland-B in the Pwalugu floodplain sites.

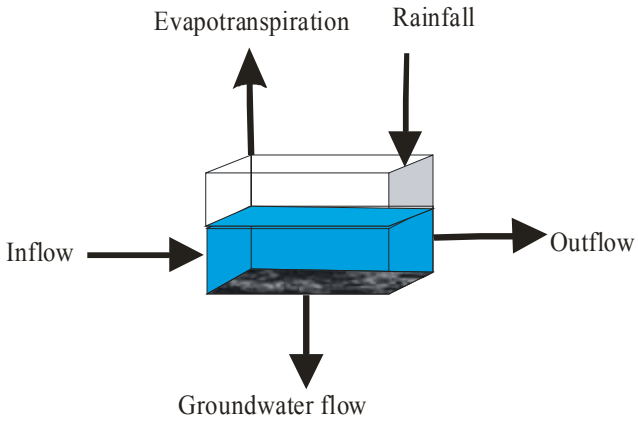

Figure 7.11 Conceptual model for water balance estimation

Table 7. 1 Water budget for the Wetland-B (Pwalugu floodplain)

Date	**Water balance P(t) - E(t) (mm)**	**Isotope Water balance $P(t)\delta_p - E(t)\delta_\varepsilon$ (mm)**	**Rayleigh equation (mm)**
20-Oct-04	-131.40	-1294.36	-88.49
20-Nov-04	-74.40	-1929.83	-128.20
20-Dec-04	-141.50	-2434.11	-152.05
20-Jan-05	-297.80	-368.03	-148.20
20-May-05	96.50	5773.61	705.16
26-Aug-05	963.90	3441.38	717.35
09-Sep-05	359.00	1968.29	249.41

Table 7.2 Water budget for the Tindama floodplain wetland

Date	Water balance P(t)-E(t) (mm)	Isotope Water balance $P(t)\delta_p$-$E(t)\delta_\varepsilon$ (mm)	Rayleigh equation (mm)
01-Sep-04	237.97	333.75	379.16
01-Oct-04	-167.46	-123.69	-271.46
01-Nov-04	-119.49	-207.98	-91.52
01-Jan-05	-174.41	-103.83	-85.05
01-Feb-05	-118.48	-133.49	-44.80
01-Mar-05	-110.00	-144.63	-56.13
01-Apr-05	-198.74	-125.05	72.02
01-Jun-05	287.06	185.70	248.98
01-Jul-05	199.49	616.57	307.76
01-Aug-05	114.06	765.33	1087.41

The water budget mirrors changes in rainfall in the Pwalugu and Tindama wetland sites (Table 7.1 and Table 7.2). The drastic change in the climatic variable (Temperature, rainfall, humidty and evaporation) influences the variation of water level in the wetland. For a given unit pixel area of 900 m^2 in the Pwalugu Wetland-B (Figure 7.10) using the Raleigh equation for August 2005, an estimated potential of 717.35 mm of water is calculated as water added to the wetland, while from November onwards to December, the evaporation increased from 128.20 mm to 152.05 mm. Using the equation 7.1 with inflow and outflow assumed to be zero (0), the loss of water from the wetland began in October 2004 with 131.40mm, this increased to 297.80mm in January 2005. A comparison was made between the Raleigh equation and isotope water balance (Figure 7.11) using regression analysis at 95% confidence level, which yielded $r = 0.84$.

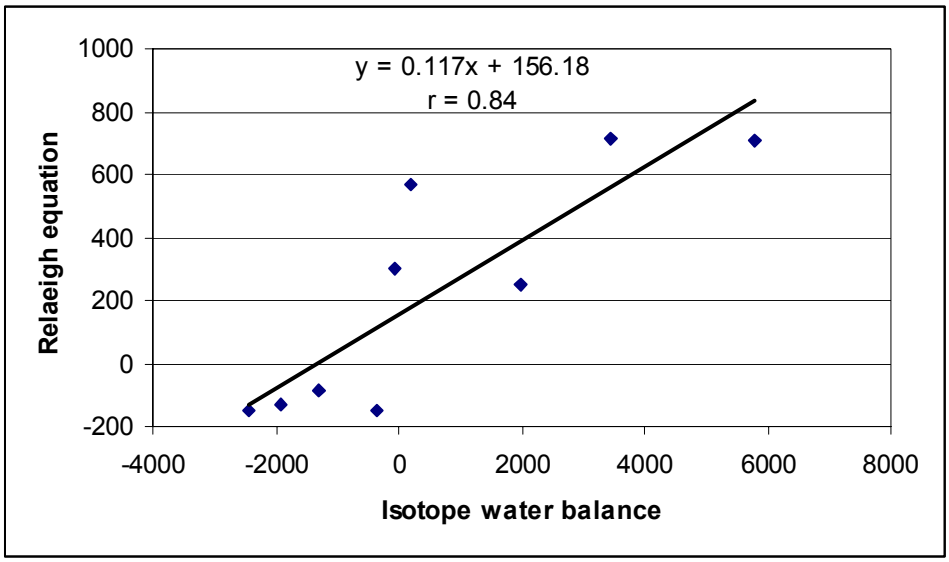

Figure 7.12 Relationships between Raleigh equation and isotope water balance in Wetland-B, Pwalugu

The approaches adopted for estimating water balance will be enhance if data on surface laterial flow and ground water recharge and discharge are collected and used. However, these approaches provide a quick way of acquiring hydrological data within the White Volta River basin for short term decision making.

7.2.5 Interaction between wetland and river flow

Stable oxygen and hydrogen isotope composition can be used to determine the contribution of old and new water to a stream (and to other hydrologic components of the catchment) during periods of high runoff, because the rain (new water) that triggers the runoff is often isotopically different from the water already in the catchment (old water). Comparison of stable isotope data of surface (wetlands and river) and sub surface water samples (piezometers) in the wetlands plotted relative to their local meteoric water line provides information on hydrological connections. The plot shows a relationship between surface water (Wetland-B) and subsurface water (piezometers PZ-1,PZ-2,PZ-3,PZ-4) on a seasonal basis (Figure 7.12), as the isotopic composition of subsurface water varies but corresponds closely in July to September 2005.

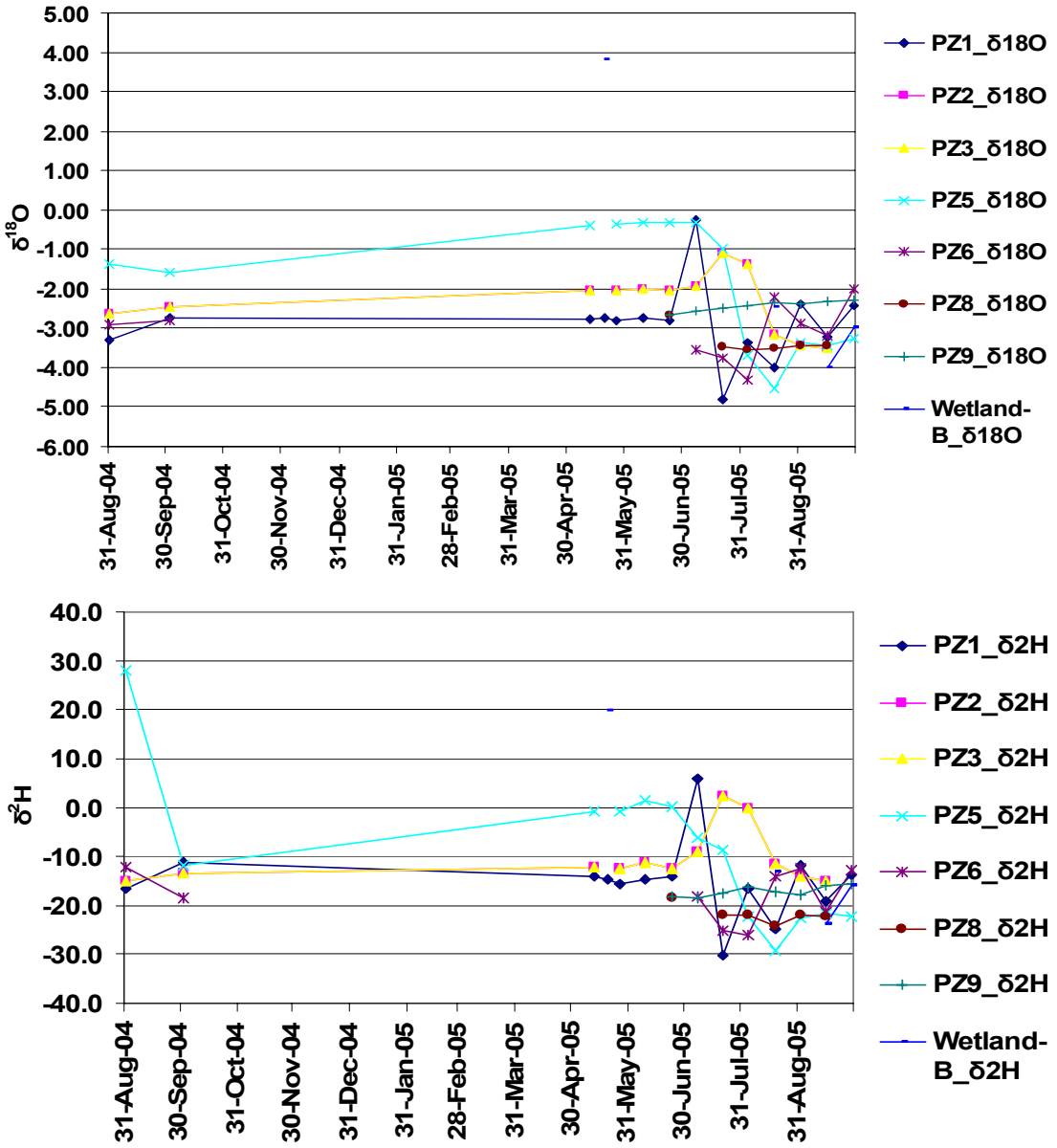

Figure 7.13 Relationship between subsurface water (piezometers) and surface water, (Wetland_B, Pwalugu) with respect to the temporal variation of $\delta^{18}O$ and $\delta^{2}H$

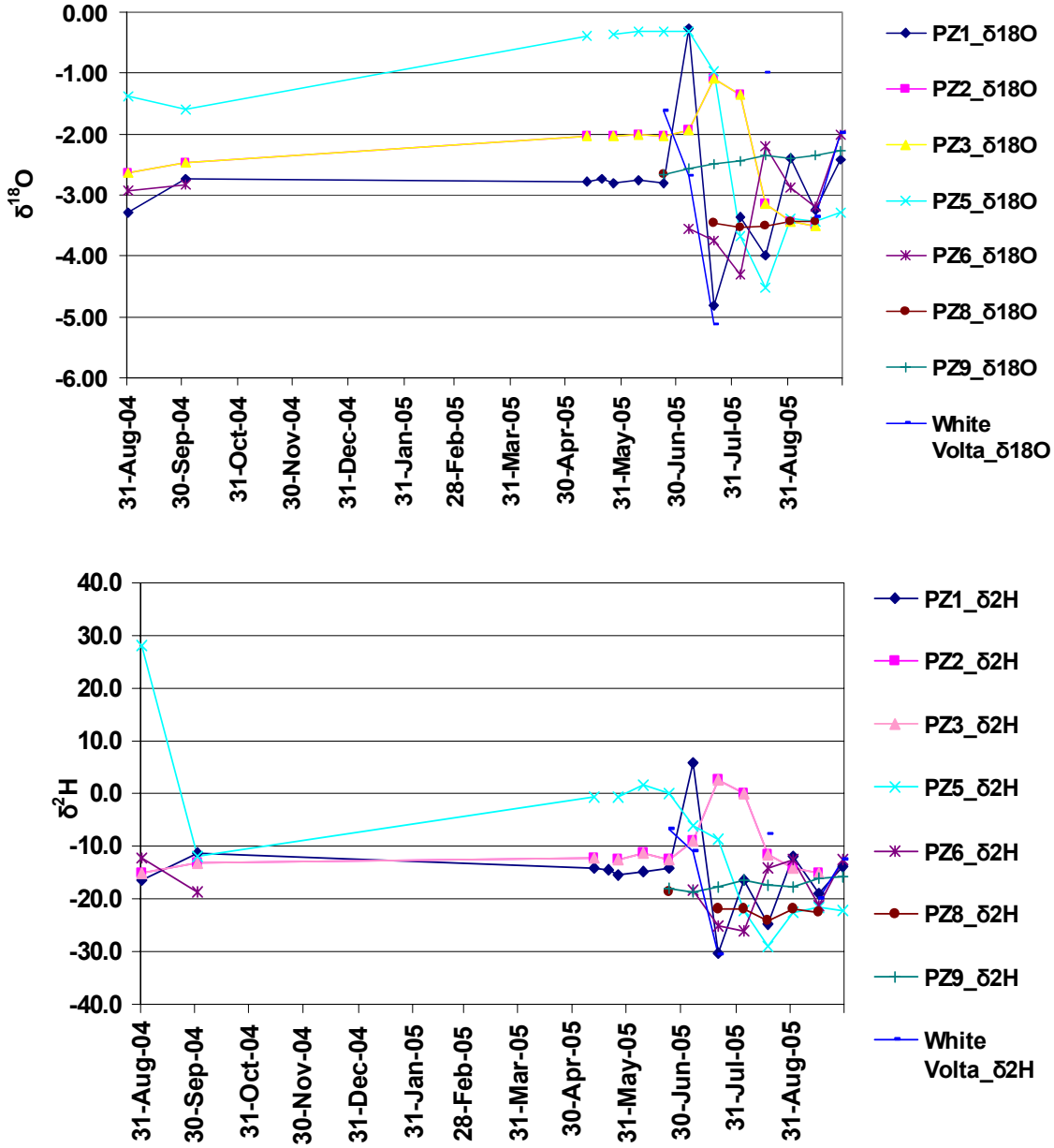

Figure 7.14 Relationship between subsurface water (piezometers) and the White Volta River with respect to the temporal variation of $\delta^{18}O$ and $\delta^{2}H$

In September 2005, at the piezometer PZ-3, PZ-5, PZ-8 and the White Volta River (Figure 7.13) the same $\delta^{18}O$ (-3.4‰) was measured, but $\delta^{2}H$ composition differed. The piezometers and river samples differed in isotope content from October onwards when the water lever was low. During this period, the isotopes composition for the White Volta were over the evaporative line (Figure 7.14), estimated at a humidity level of 25% and 75%, thus reflecting an enrichment process. This indicates that, in the dry

season, river baseflow may not be sustained by subsurface seepage from the floodplain wetlands.

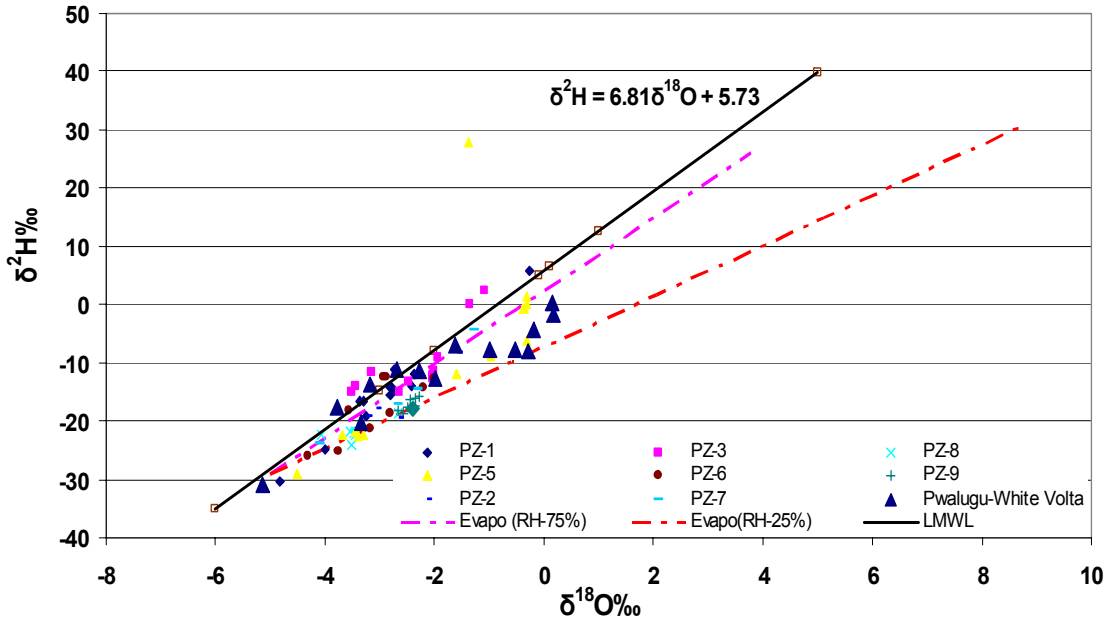

Figure 7.15 Interaction between subsurface water and White Volta River water in Pwalugu site

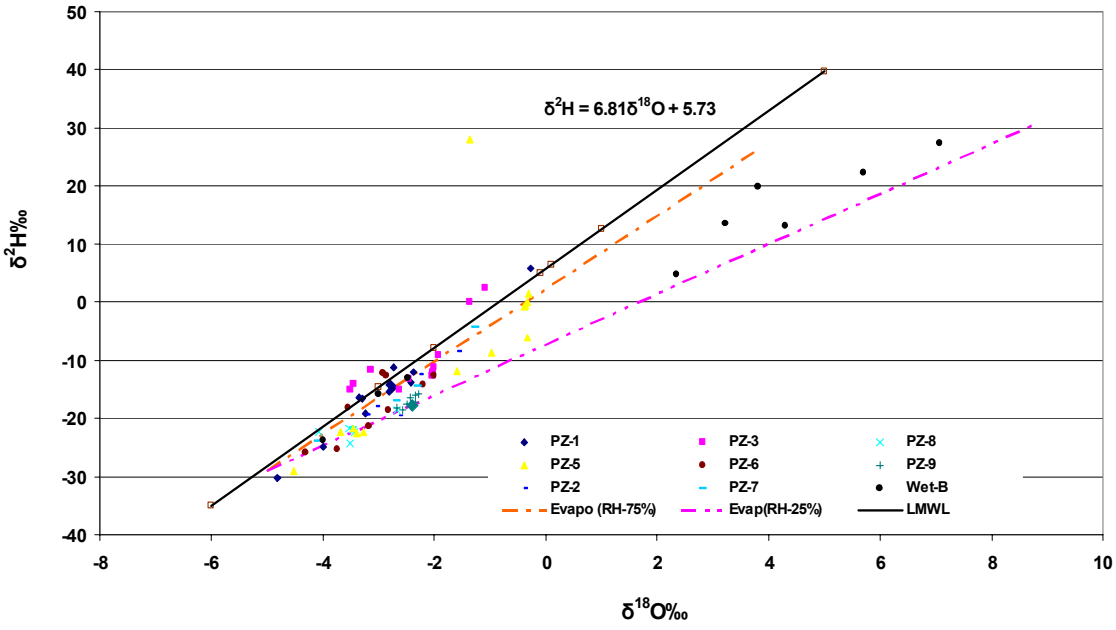

Figure 7.16 Interaction between subsurface (piezometers) and surface water in Pwalugu site

The isotopic ratios of Wetland-B and sub-surface water (piezometers) are similar. It is difficult to isolate water inflow associated with these two ratios, as in the rainy season (August 2005 to September 2005) they plot around the LMWL (Figure 7.15). Additionally, there is an indication of discrete distinct isotopic signatures that characterize water inflow, giving an idea about origin and residence time of wetland water. Therefore, the stable isotopes in the sub-surface water in Wetland-B show a relative response to rainfall input as piezometers close to the main river are always subject to occasional water-table rises. Moreover, isotopic composition of subsurface water also follows a seasonal variation pattern, but shows less fractionation compared to surface water.

8 WETLAND-RIVER FLOW INTERACTION

8.1 Introduction

Rivers interacts with the floodplain wetland in three ways: 1) through direct surface runoff, 2) through sub-surface water flow, and 3) by losing water to wetlands by seepage through the river walls. The interaction between floodplain wetlands and a river sometimes vary, over a very short time frame or distance in response to rapid rises in river stage due to storm runoff. For instance the high water level in the White Volta River as in 1994 was enough to overflow the banks and flood large areas of the floodplains and hence, a widespread surface recharge occurred. Therefore, the hydraulic connection between the White Volta River and the floodplain wetland may be direct or disconnected by the intervening unsaturated zone, with rivers losing water in the form of seepage through the walls into the floodplain wetland. Important in floodplain wetland hydrological modeling within the Upper East region is to establish the contribution of shallow well development for the sustenance of dry season irrigation. This chapter discusses processes involved in the use of PM-WIN (MODFLOW), to determine forms of interaction between the main White Volta River and the basin floodplain wetlands. It is sectioned into three main parts: 1) an overview of the model discussed in Chapter 3,2) discussion of the setting of the MODFLOW model, indicating the input data used, 3) discussion of model results and sensitivity analysis.

8.2 Background

Modeling of floodplain wetland and river interaction is both numerically and theoretically demanding and requires solving complicated numerical approximations to differential equations (Bockelmann et al. 2004; Fischer-Antze et al. 2001; Wu et al. 2000). Physical-based, process-oriented and spatially distributed models such as MIKE-SHE have seldom been applied to study wetlands in developing countries, since they are complex to operate and require a level of data that is hardly available in most developing countries (Bonell and Balek 1993). PM-WIN (MODFLOW) can simulate many of the features influencing the in-field water regime, including anisotropy and heterogeneity in hydraulic properties. The modeling of floodplain wetland river flow

interaction at the Pwalugu site was performed using PM-WIN (MODFLOW) (Chaing and Kinzelbach 1998) for the following reasons:

- MODFLOW takes account of spatial heterogeneities, vertical groundwater flow and any regional groundwater flow component.
- Leakages through heavy soils can occur at low rates and consequently become a minor component at the field scale, although the volume of leakage can be significant over the total area of the wetland.
- Irregular field boundaries and steep hydraulic gradients to the river are accommodated.
- Recharge can be distributed spatially, and recharge is assumed to be added instantaneously to the saturated zone.
- MODFLOW allows evaporation from the soil surface, hence the maximum evaporation rate is assigned to each cell when the water table equals an assigned head value and ceases below the assigned extinction depth.

Despite the above reasons, in most cases wetlands are generally incorporated in groundwater models as general head boundary nodes even though they can be used as constant heads (Restropo et al. 1998). The hydrologic regime of floodplain wetlands depends on the varying degree of flow in the main channel, making wetlands vulnerable to hydrologic changes resulting from flow regulation (Reid and Quinn 2004; Cloke at al. 2006). However, the nonlinear interactions among recharge, discharge, boundary conditions and changes in groundwater storage makes the solving of problems relating to recharge and groundwater development difficult, all the system parameters and their geographical distribution are not carefully accounted for (Sanford 2002).

8.3 Input generation

The PM-WIN (MODFLOW) model uses a finite difference method to simulate floodplain wetland and river flow interaction. The Pwalugu floodplain wetland site is represented by an array of rectangular cells, which embody the localized values of the aquifer characteristics (Figure 8.1). The area modeled covers 7.78 km^2 and comprises 8648 square cells, out of which 5693 are marked as active cells. The model for the study site is represented in two layers, and the top of the uppermost layer (Figure 8.2) corresponds to the surface of the floodplain wetland; this layer can be dried and

rewetted seasonally. The thickness of the top layer varies in thickness from 6.0 m when close to river and 26 m at the eastern boarder of the study site. The second layer below has a thickness of 10 m, specified on the basis of a geological formation that limits storage and enhances transmission of water. The spatial limits of the geological formations provided no-flow boundaries to the north and west side of the river (Figure 8.1). Flow along the southern and eastern boundaries is specified as constant head. However, during the modeling process these boundary conditions were varied between constant and variable head to achieve an optimum fit. The model is specified to enable determination of whether the wetlands contribute to or receive water from the river. This depends on the head gradient between the floodplain wetland and the river. The packages river, recharge and wetting capabilities were applied selectively during the modeling process.

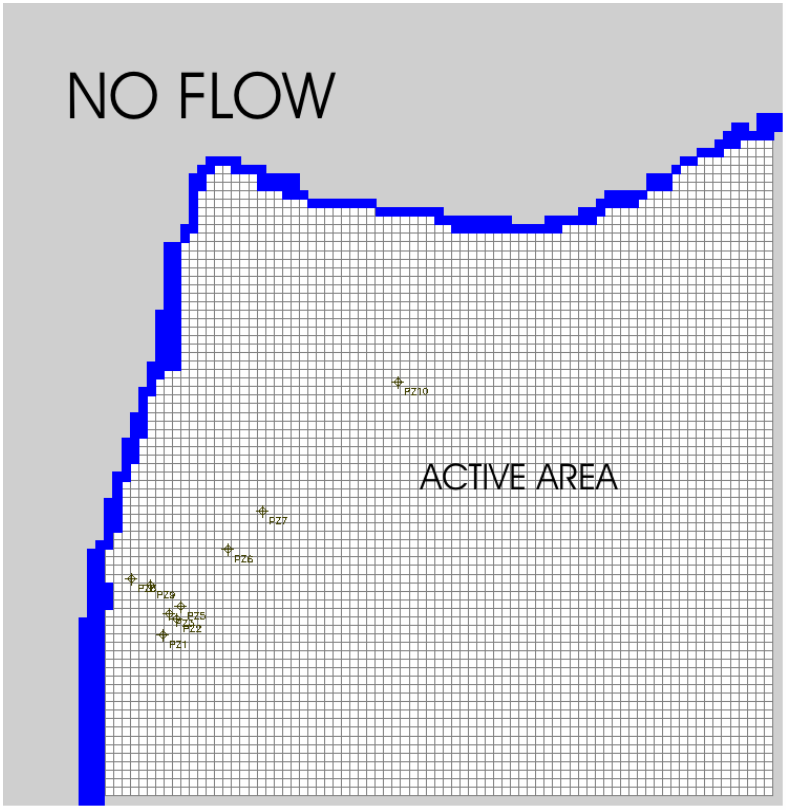

Figure 8.1 Setting of the Pwalugu floodplain wetland site

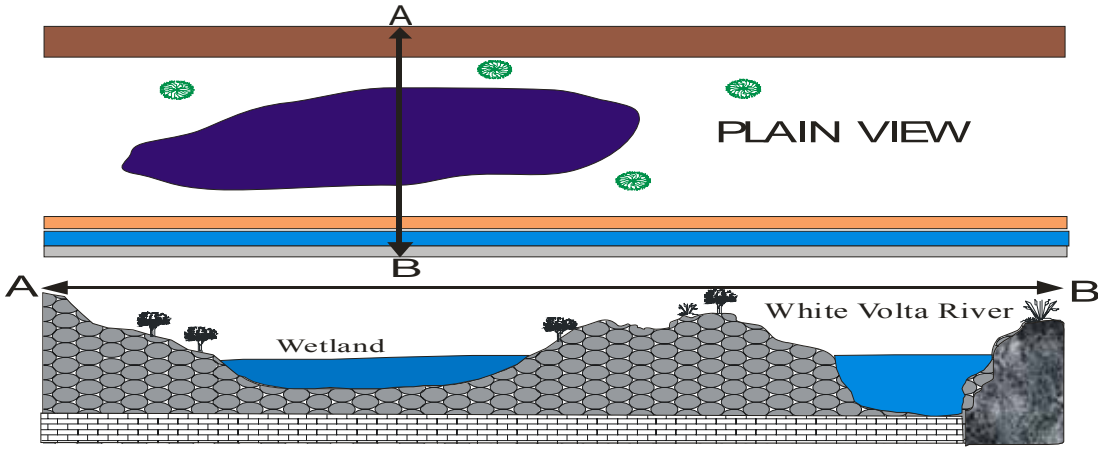

Figure 8.2 Location and transect of wetlands in the White Volta River basin

8.4 River package

The river package (Prudic 1989) was used to represent the White Volta River in the model. The White Volta River can gain from or contribute water to the floodplain wetland depending on the river stage (Figure 8.3), riverbed conductance and adjacent floodplain aquifer water levels. The river surface elevation data used were measured by the HYDRO Service of Ghana. The low level of 133.05 m was recorded in January 2004, while September 2005 had the highest reading of 140.53 m.

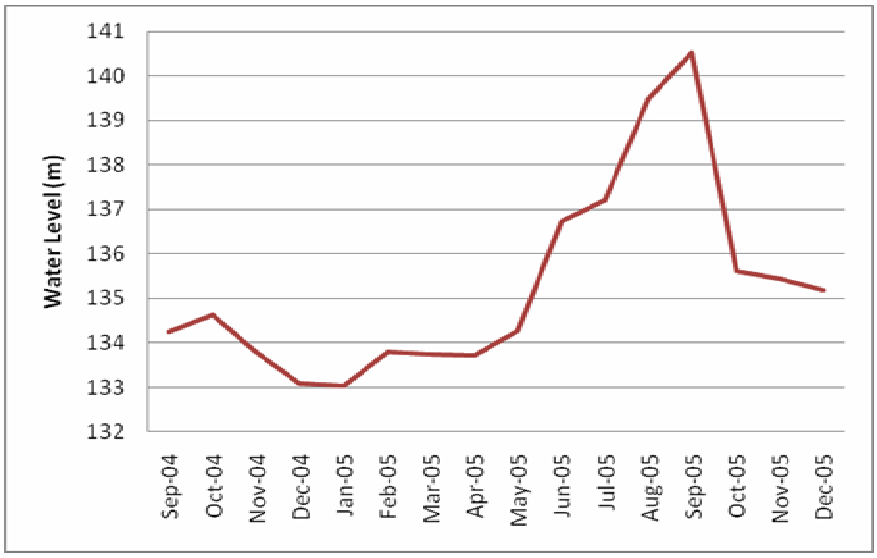

Figure 8.3 River gauge heights at Pwalugu Station

Riverbed conductance is a critical parameter in determining the amount of water seepage between the river and underlying aquifer. However, the observed

riverbed conductance in the White Volta River showed high variability, with differences between the scale at which riverbed conductance was estimated and the scale at which was applied in the model (Hayashi and Rosenberry 2002). Riverbed conductance values of between 3.09 x 10^4m/day and 3.10 x 10^4m/day were assumed and assigned using the hydraulic conductivities of the observed changing bed materials consisting of alluvial deposits, metamorphosed sedimentary and granites outcrops that mostly underlie the riverbed. Data riverbed thickness and river width were not available to justify adjustment of riverbed conductance on a river-segment basis; therefore, no calibration of riverbed conductance was made during the modeling process.

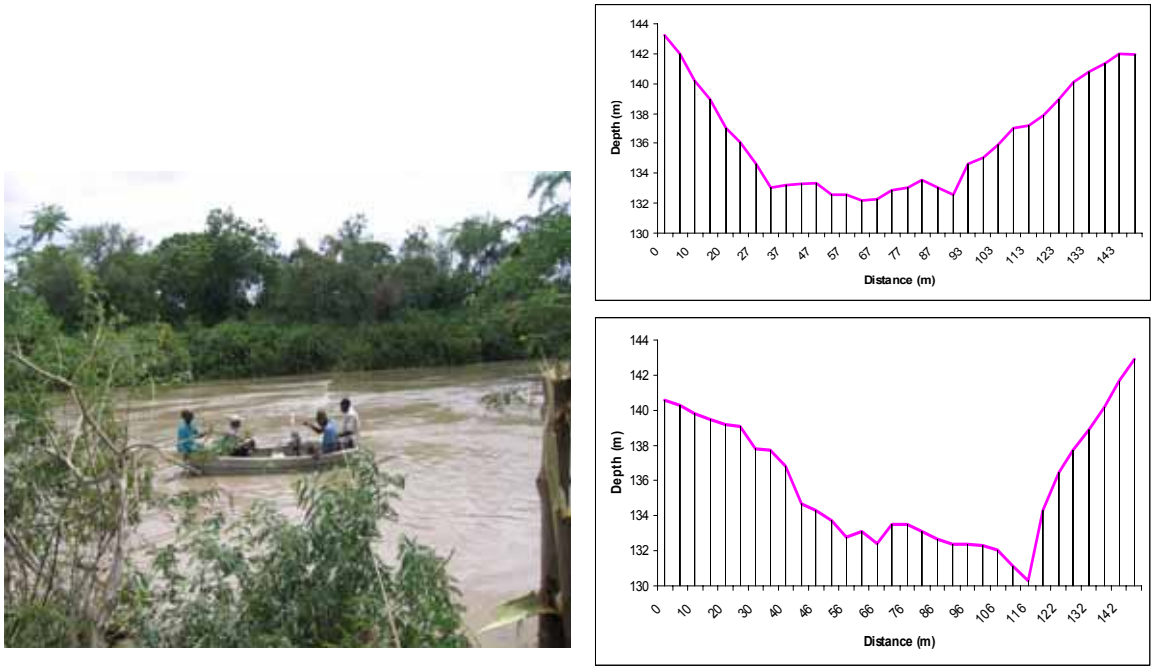

Figure 8.4 (A) Field survey of the White Volta River (Pwalugu) (B) Cross section at Pwalugu gauging station (C) cross section at 150 m upstream from Pwalugu gauging station

Digital elevation models (SRTM-DEM) for the study area and river depth survey (Figure 8.4) were used to determine the riverbed elevation. A minimum elevation of 132.5 m was approximated and used to adjust the available DEM data. The adjustment was necessary because the available SRTM-DEM measures the surface of the water level in the river channel. The resulting river profile was checked for any uphill river segment, i.e., a segment that gained elevation moving downriver. Uphill segments, typically artifacts (peaks), were flattened by replacing the riverbed elevation

with the adjacent upriver elevation. Variations in river water level measured by Hydrological Services, Ghana, were incorporated in the topographic data to derive the monthly gauge level as it relates to the topography.

The river package in MODFLOW is designed to simulate flow between surface and groundwater. To simulate the lateral flow interaction between wetland and river through the sediment deposits, an assumption about low permeability of the river bed is made to prevent leakage from the riverbed into the underlying aquifer.

8.5 Hydraulic conductivity and recharge

The vertical and horizontal hydraulic conductivity with the floodplain wetlands are not uniform, but exhibit variability in terms of depth and direction. Therefore, based on laboratory measurements and literature on the specification of the geological structure, two hydraulic conductivity layers were specified. For the top layer, due to spatial heterogeneity of vertical hydraulic conductivity, a range of 0.012 to 0.038 m/day was specified. A range of 0.12 m/day to 0.38 m/day was specified as the horizontal conductivity of the top layer. For the bottom layer, an arbitrary value of 0.09 m/day was specified for both vertical and horizontal hydraulic conductivities because of lack of information about the layer.

Recharge is limited to some extent by behavior of the sedimentary and geological system that underlies the Pwalugu floodplain wetland site. This serves as a partitioning force that controls sub-surface recharge or water movement (Fox et al. 1998). The boundary condition in the MODFLOW groundwater model is effectively represented by specifying net bottom flux of HYDRUS-1D as a recharge flux. However, for parts of the White Volta basin it is difficult to independently obtain an accurate recharge rate and distribution data. To estimate recharge for the Bongo granite aquifer in the Volta basin, Martin (2005) used the chloride mass balance, soil moisture balance and water table fluctuation methods. Martin (2005) obtained three different recharge values of 5.9%, 12.5% and 13% of the annual rainfall respectively. Apparently, recharge measurements in the field contain some amount of uncertainty; hence a variety of approaches has been used to assist researchers in estimating recharge and its distribution over geological formations. For the MODFLOW simulation, the bottom flux from the HYDRUS-1D model was specified as the net recharge (Figure 8.5) for the

Pwalugu floodplain wetland. For the entire 16 months (487 days), an estimated recharge of 444 mm obtained from HYDRUS-1D served as an input into the model. It is important to stress here that the HYDRUS-1D bottom flux is the net recharge into the subsurface; in this case, water ponding has been accounted for.

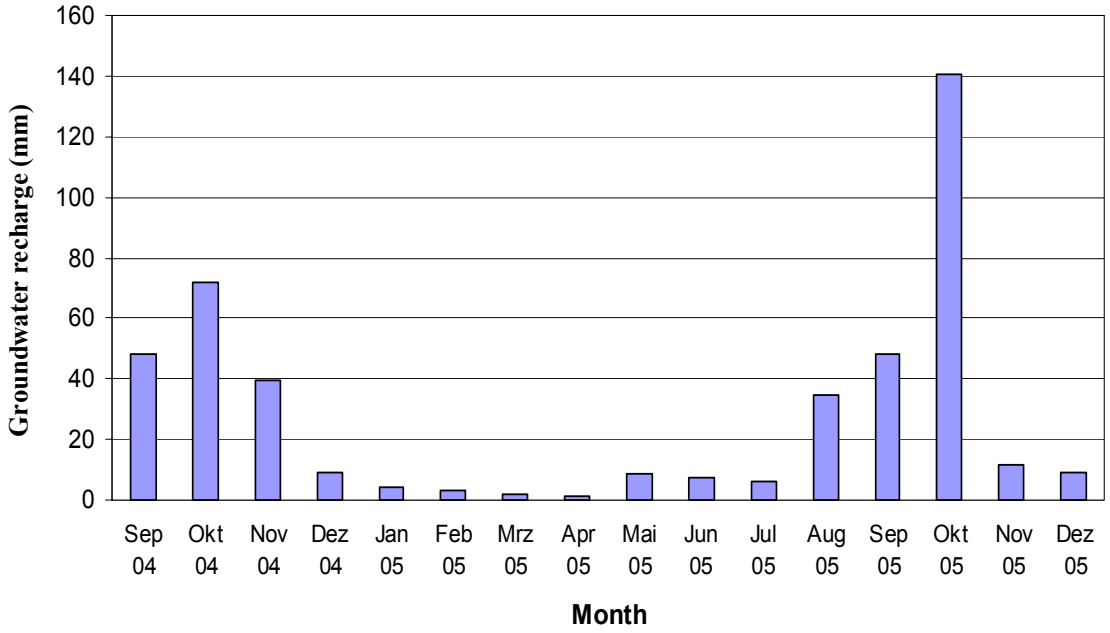

Figure 8.5 Monthly bottom fluxes from HYDRUS-1D

8.6 Floodplain wetland and river flow interaction modeling

The PM-WIN model is used to construct a two-dimensional transient model for the floodplain wetland and to quantify the temporal and spatial variation in the interaction between floodplain wetland and the White Volta River flow. The simulation of floodplain wetland and river flow interaction is important in estimating the flow and exchange of water between the wetland and rivers. An assumption made during the modeling process is that, conductivity of the riverbed is very low, thus any form of leakage from the river is a leakage into the wetland through the sub-surface. The model was run using both steady and transient mode.

The steady state flow simulation was performed to first calibrate model parameters. This was done to obtain a tolerable distribution of the initial hydraulic head. The vertical and horizontal hydraulic conductivity values of the top layer were adjusted to get good fit for conductivities of the layers. For the bottom layer, an arbitrary value

was set for both vertical and horizontal hydraulic conductivity, there was no hydro-geological information was available (Table 8.1). In addition, effective porosity, specific storage, storage coefficient and specific yield of the sub-surface were adjusted to fit the level of fluctuation occurring within the floodplain wetland. The adjustment of the conductivities and other parameters shifted the error of discrepancy between observed and modeled values to an appreciable level.

Table 8.1 Adjusted parameters for the PM-WIN model

	Top layer	Bottom layer
Vertical conductivity	0.12 - 0.38 /day	0.9 m/day
Horizontal conductivity	4 m/day	0.09 m/day
Effective porosity	0.14 – 0.25	0.25
Specific storage	0.01	0.001
Specific yield	0.07 m^3/day	0.001 m^3/day
Storage coefficient	0.01	0.001

In running the steady state model, the initial hydraulic head was assumed to be the interpolated hydraulic head of the piezometers and the river in September 2004. In addition, no recharge was specified; this gave equilibrated head values as the initial hydraulic head for the steady and transient models. This adjustment proved to be the optima for running the model. The period September to October 2004 was chosen for the calibration, as detailed hydraulic head measurements were available for this period.

The transient model was run in a time varying mode with daily time steps for 487 days. The recharge specified was the bottom flux obtained from HYDRUS-1D. Inflow and outflow at the model boundaries were varied between constant and variable head until the model results were in an acceptable range. The boundary conditions specified do not represent direct recharge, but are used in conjunction with recharge to realistically represent the sub-surface water system (Sanford 2002). In running the model in the transient mode with the wetting capabilities turned on, there was contribution of water flow from cells marked no-flow (inactive cells). In this situation, the wetting capability was removed from the modeling process. Also, the bottom layer

was disabled due to lack of data; hence it becomes a no flow boundary, thus only the top layer was used.

The result of the calibration with the hydraulic conductivities and other parameters (Table 8.1) is shown in figure 8.6 as time discharge plot from the six piezometers, for which the calculated head follows the pattern of the observed head. Water levels in the piezometers are always elevated in the rainy season and lower in the dry season, but PZ1 at the toe of the sloping part of the wetland was the last to dry. The piezometers in the Pwalugu floodplain wetland were used to represent sections of the wetlands. The simulated curve generated shows a good fit with observations especially for PZ1, PZ2, PZ3, PZ5, PZ8 and PZ9. The rises in the hydraulic heads of the simulated hydrograph are similar and follow a pattern, while the observed hydraulic head shows some differences. The variability in the observed heads is likely to be a result of heterogeneity in the sub-surface aquifer structure.

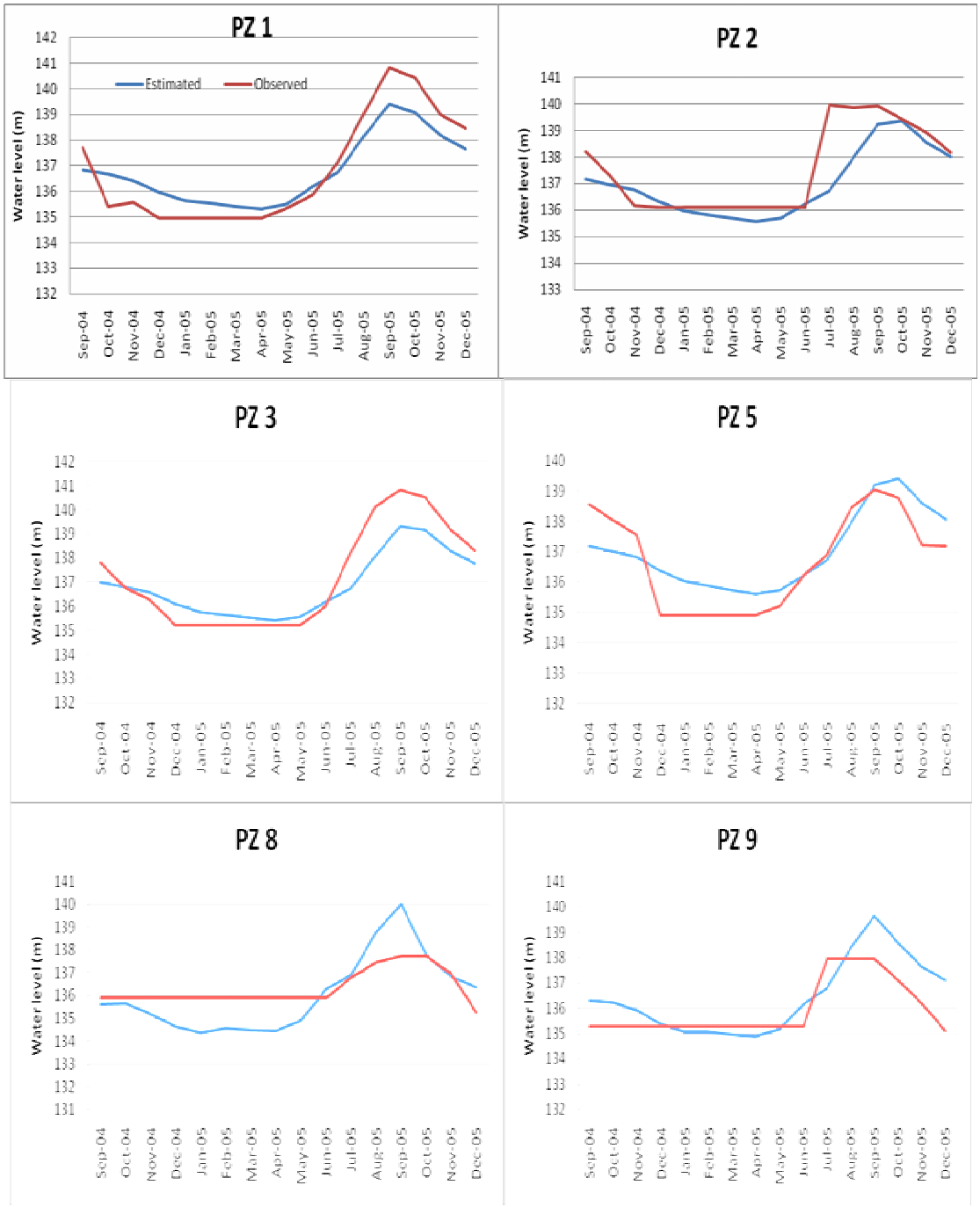

Figure 8.6 Simulated and observed heads in the Pwalugu floodplain wetland

The simulation of the sub-surface hydraulic head indicates a systematic variation relative to the White Volta River in response to changes in the rainfall pattern in the tropical savanna climatic zone. Over the months of September 2004, December 2004, March 2005, June 2005 and September 2005 (Figure 8.7) distinctive patterns of hydraulic heads were observed. For instance, the high hydraulic head simulated for September 2004 indicates that the floodplain wetland experienced a hydraulic head

between 1 and 3 m below the topographic surface. During August and September, a ponding height of 0.50 m was measured in the field. The heterogeneity of the floodplain wetland topography makes ponding uneven. In June 2005, a comparatively high hydraulic head of 4 and 6 m is simulated below the topographic surface but close to the main river course, while the further away from the river, the deeper the hydraulic heads. A bi-direction of sub-surface water flow between the White Volta River channel and the floodplain wetland system is inferred as having a temporal and spatial variation.

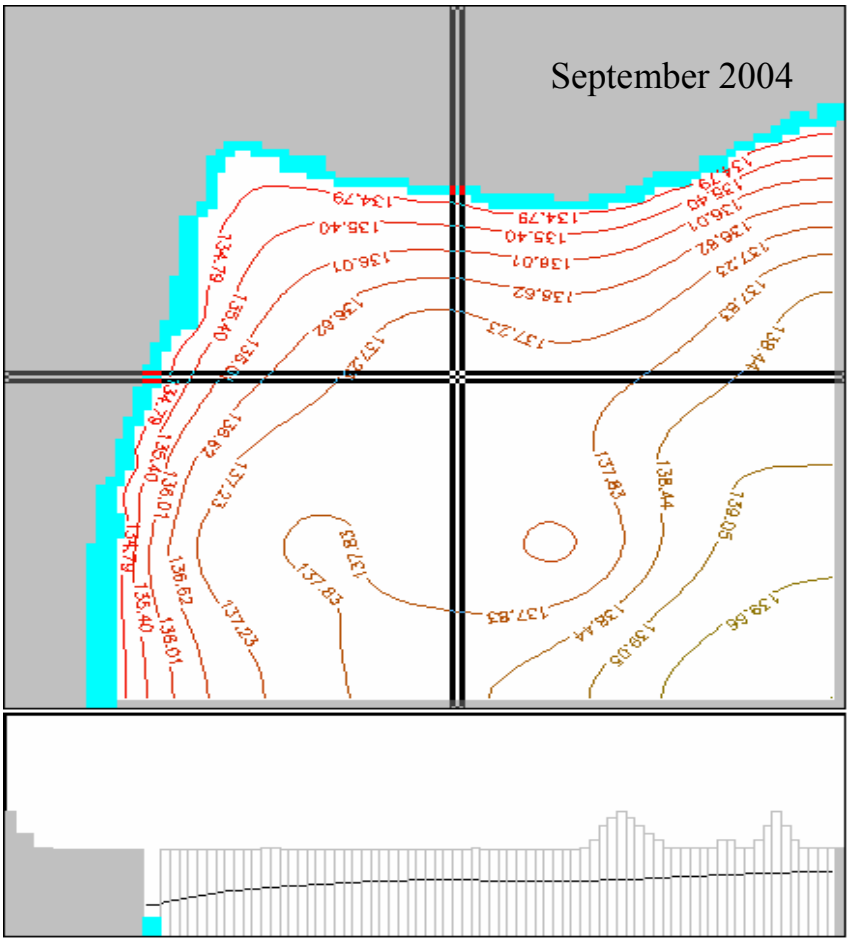

Figure 8.7 Depth of hydraulic head and cross section of floodplain wetland in September 2004, December 2004, March 2005, June 2005, and September 2005

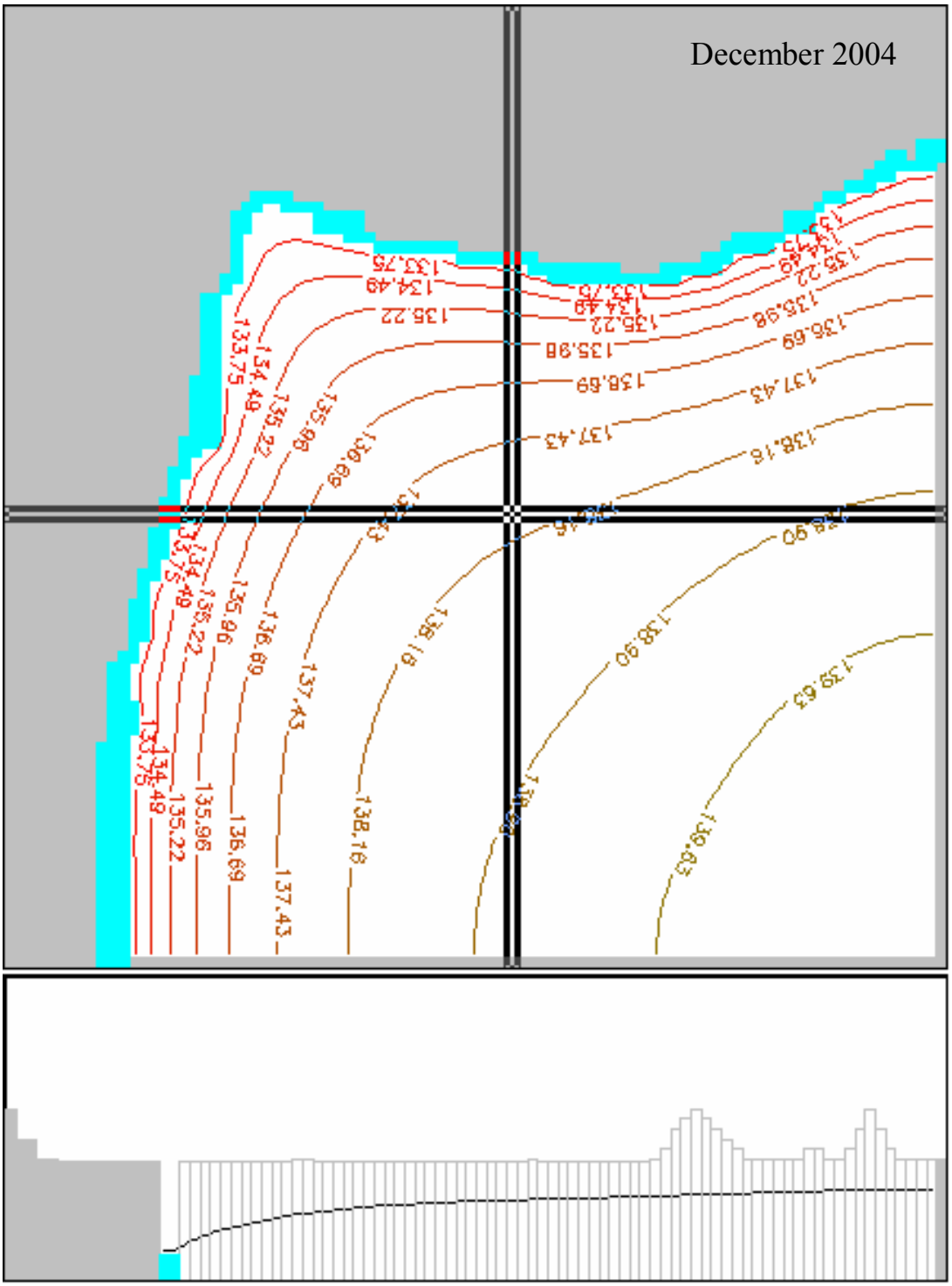

Figure 8.7 continued

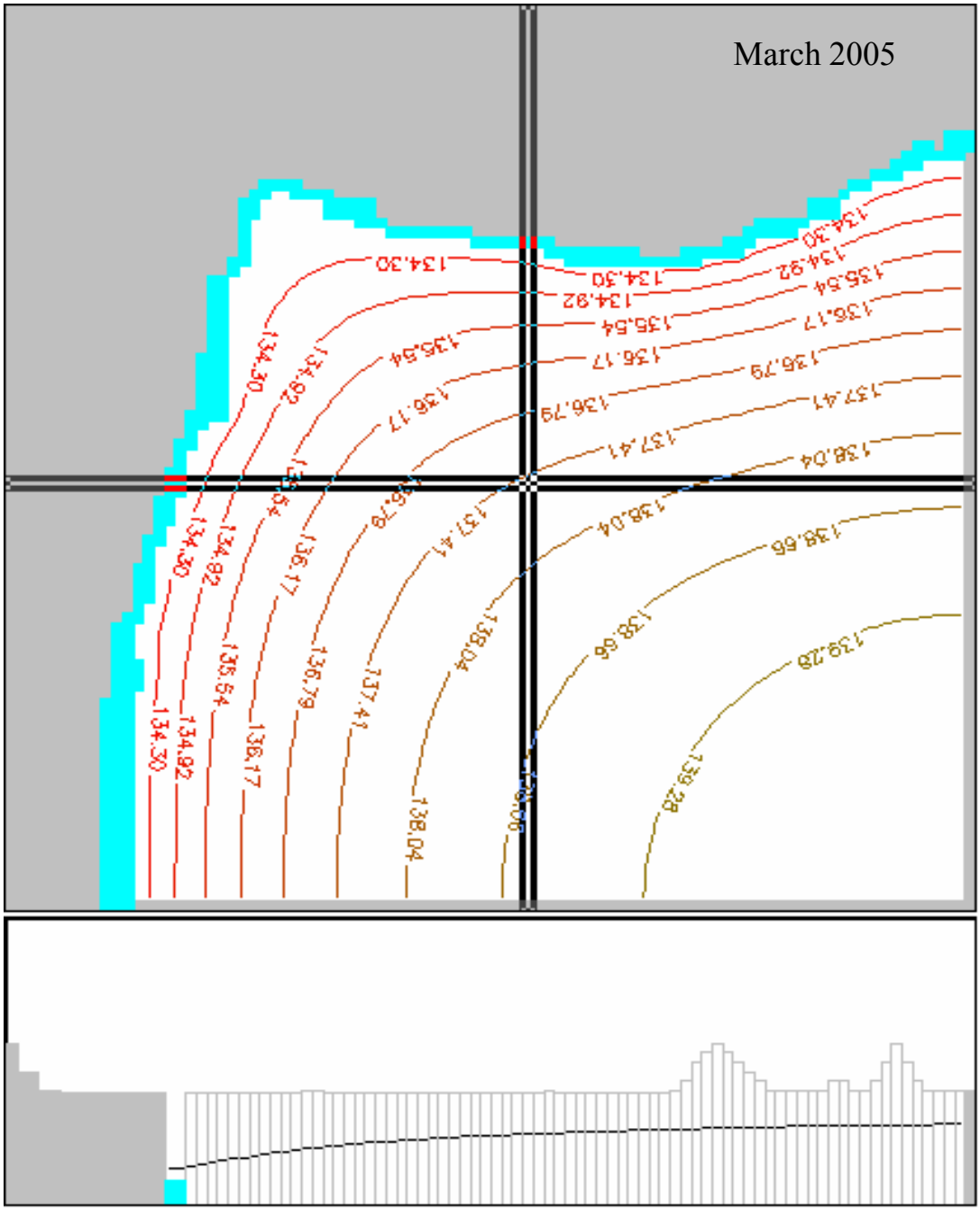

Figure 8.7 continued

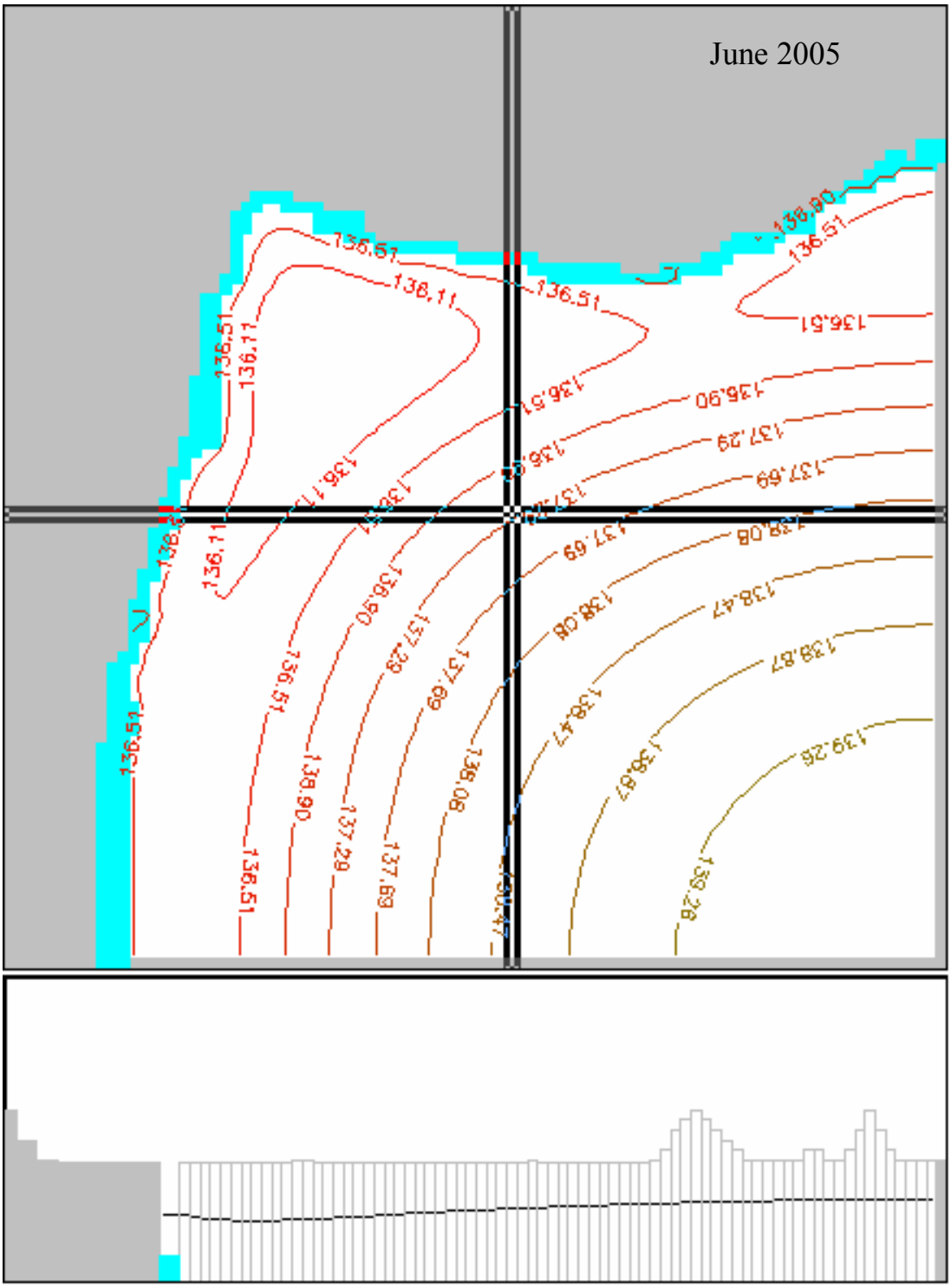

Figure 8.7 continued

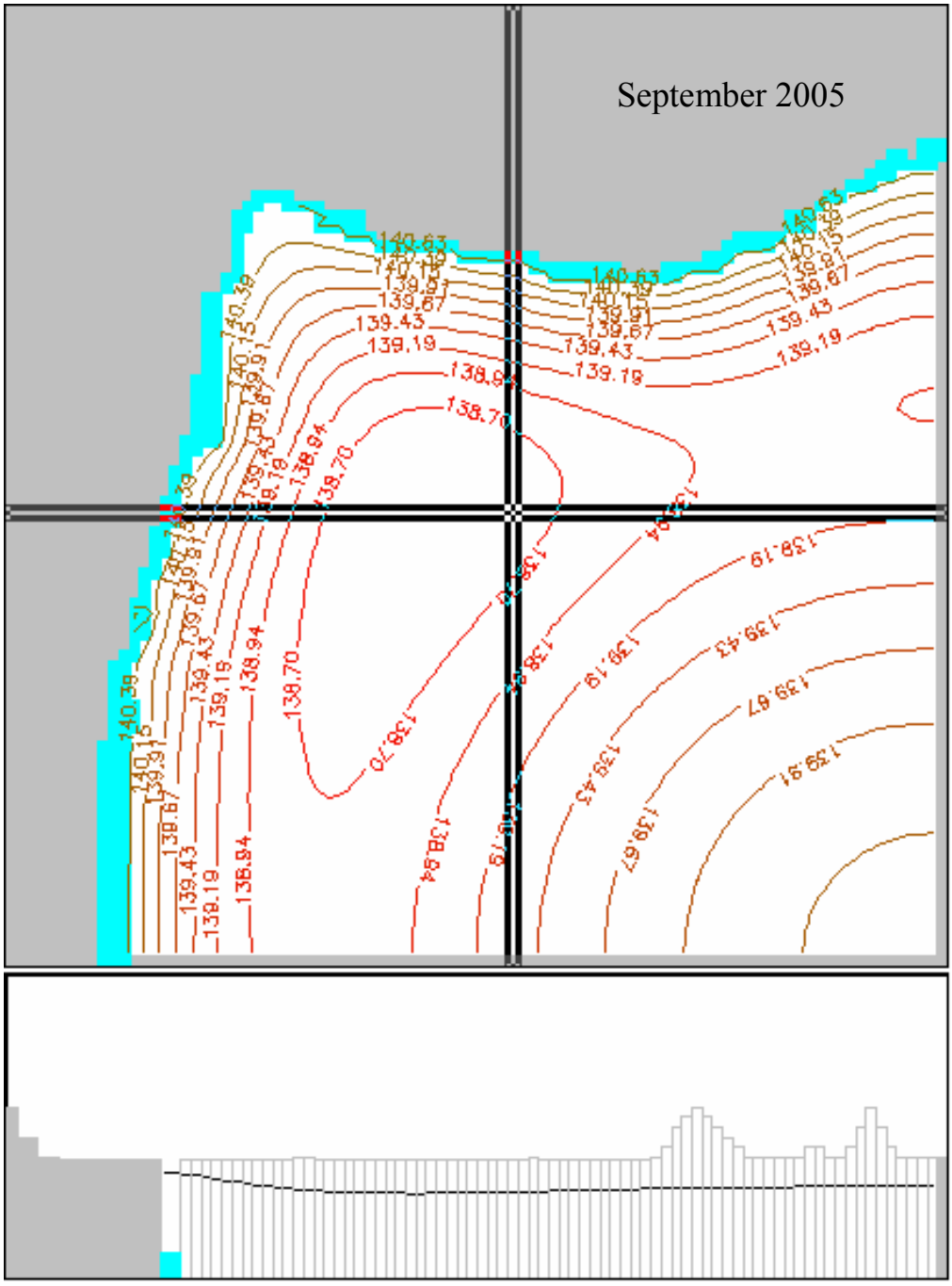

Figure 8.7 continued

Table 8.2 Model fit statistics for the transient run monthly values of observed and simulated hydraulic heads

ID	Observed (m)	Simulated (m)	R^2	Root mean square error (RMSE)	Nash and Sutcliffe (NS)	Mean absolute error (MAE)	Index of Agreement (IA)
PZ1	136.85	136.79	0.94	0.52	0.83	0.72	0.82
PZ2	137.53	137.00	0.69	0.45	0.58	1.04	0.89
PZ3	137.19	136.87	0.94	0.49	0.79	0.84	0.98
PZ5	136.74	137.04	0.71	0.33	0.67	0.78	0.93
PZ8	136.30	136.04	0.70	0.97	1.22	1.23	0.75
PZ9	135.95	136.47	0.63	0.55	0.14	1.00	0.89

The HYDRUS-1D bottom flux used as a recharge estimate resulted in a fit between the simulated hydraulic head and observed sub-surface water level fluctuation. A comparison of 6 piezometer observations and the simulated hydraulic head showed some outliers with a variance of 1.62 m with a root mean square error (RMSE) of 1.28 m and R^2 of 0.66. For instance, PZ1 and PZ3 indicated a R^2 of 0.93 between the observed and simulated hydraulic head (Figure 8.8). This level of compatibility gives indication that the model calibration needs to be improved. However, individual piezometers in the wetlands also showed differences between the observed and simulated head (Table 8.2). Additionally, PZ-1 located within the wetland and about 300 m away from the White Volta River gave a better fit (IA = 0.82, MAE = 0.72 m and RMSE = 0.52 m). PZ-8 in close proximity to the river shows a lower IA of 0.75, MAE of 1.32 m and RMSE of 1.22 m. Given the lack of spatial data, e.g., local flow pattern and hydraulic properties with depth, accurate calibration will not be feasible. In addition, detailed data on variation in the landscape, sub-surface water level fluctuation and bottom discharge will be required to develop a validated model of the accuracy required for the management of floodplain wetlands in the White Volta basin.

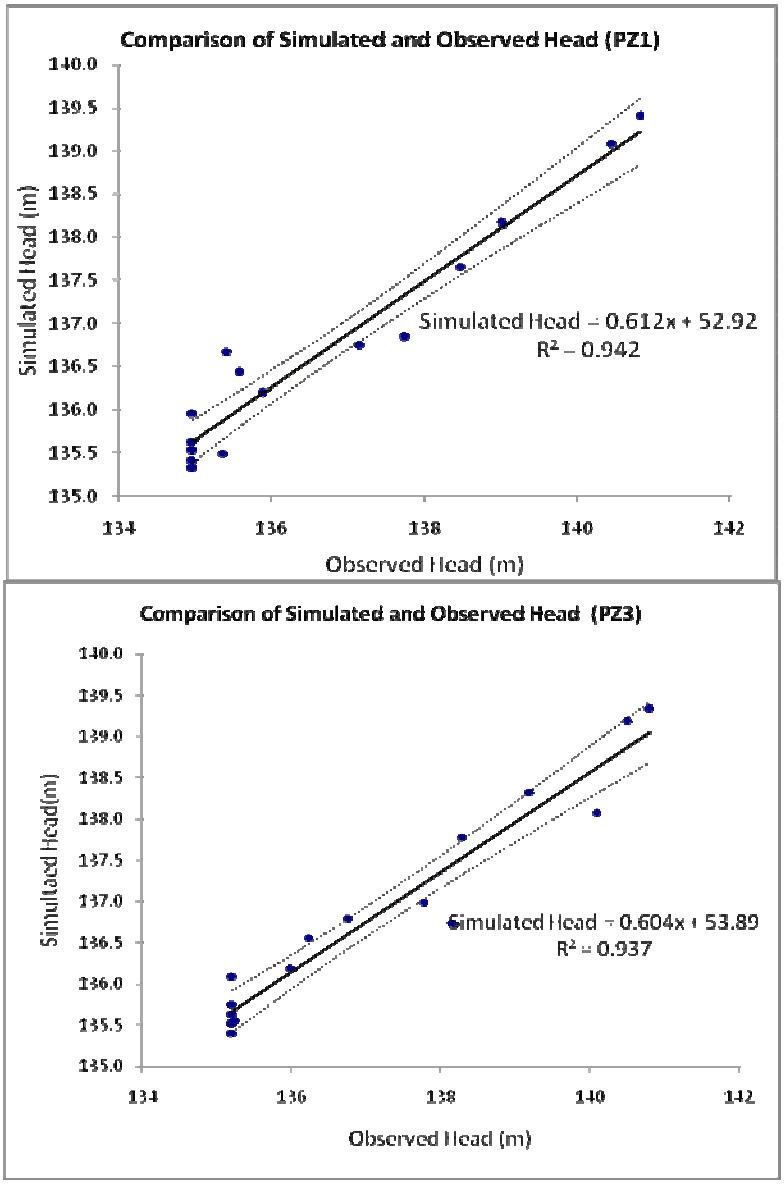

Figure 8.8 Comparison of simulated and observed heads in the Pwalugu floodplain wetland for a period of 16 months (September 2004 to December 2005). The dotted lines indicate 95% confidence interval

8.7 Mass balance

The mass balance accounts for the sources of water for recharge or discharge of a hydrologic system on monthly basis. The cumulative mass balance at the end of the run period of 16 months (487 days) for the transient model demonstrate the importance of recharge as a water balance input. The monthly recharge generated suggests a significant contribution of water from wetlands into the river. At sites that do not have any form of sub-surface influence, the form of interaction between the wetland and the White Volta River is a result overbank flow. Another important process is backwater

effect, which contributes to extensive ponding this can lead to surface water storage as noted in the Tindama floodplain wetland.

The interaction conditions vary from season to season, with March April and May showing the lowest leakage of 0.03 mm/day, 0.06 mm/day and 0.15 mm/day respectively, from the river into the floodplain, although the expectation is that floodplain wetland serves as a moisture buffer and supplies the river with water during the low season. However, in the period between July and September 2005, the recharge of the floodplain wetland aquifer causes an increase in the volume of water storage in the wetlands from 992793 m^3 to 1404853 m^3. The interaction between the wetland and the river is bidirectional with most of the flow coming out from the river (Table 8.3). These conditions persist in August and September. The leakage contribution of the floodplain wetland into the river in August was 97.28 mm, increasing to 172 mm in November as the rainfall reduced. In 2005, the contribution of the floodplain wetland to the river was 86.01 mm, while the river contributed 131.63 mm. For the period from September 2004 to December 2005, a total simulated recharge of 444 mm from HYDRUS-1D was applied to the wetland system, out of which 169.21mm leaked into the wetland from the river. Conversely, a total of 215.03 mm leaked out of the wetland system to contribute to the sustenance of the White Volta River. In this situation, floodplain wetland contributes as base flow to the White Volta River in the dry season. The total amount of water (556.75 mm) moving out of the storage in the 16 month period is only for the simulation period, and becomes depleted during the dry season. The full cycle of the dynamics of hydraulic head simulation to indicate floodplain wetland and the White Volta River interaction from September 2004 to December 2009 is show in (Figure 8.9).

Table 8.3 Cumulative mass balance

	2004	2005	Sept. 2004-Dec.2005
IN:	mm	mm	mm
Storage	36.23	61.76	171.87
River leakage	2.31	131.63	169.21
Recharge	159.67	221.11	421.64
Total In	198.21	414.50	762.72
OUT:			
Storage	141.33	338.57	556.75
River leakage	58.91	86.01	215.03
Total out	200.24	424.58	771.78
In - Out	-2.03	-10.07	-9.06

During the rainy season between June and September 2005, the water table (hydraulic head) in the Pwalugu floodplain wetlands increased from an average of 137.79 m to 139.43 m, but started declining from October 2005 where the hydraulic head was 138.38 m. The extent, depth, frequency, timing and duration of water ponding at the surface of the wetlands are important parameters controlling the extent of soil moisture for the sustenance of the river. For instance, ponded water in the Pwalugu wetland to a depth of 0.50 m as measured during fieldwork in August 2005 is the result of a complex and variable combination of groundwater upwelling and accumulation of rainfall on the saturated surface. Saturation of the entire wetland was rarely achieved in 2004, because there were frequent breaks in the rainfall pattern generating dry spells within the rainy season. In addition, the geological formation within the study area is Voltaian sandstone. This type of formation is a poor water retention system, and water stored during the rainy season is not readily transmitted to other parts of the system.

The internal conceptualization of the Pwalugu floodplain wetland was based on a semi-confined one-layer system with differing hydraulic characteristics. However, the interaction between the White Volta River and floodplain wetlands takes place in one of these three basic ways: 1) rivers gain water from inflow of groundwater through the riverbed, 2) river lose water to groundwater by outflow through the riverbed or both, or 3)river gain in some reaches and lose in others. The manner of interaction between the Pwalugu floodplain wetland and the White Volta River depends upon the processes controlling the recharge, floodplain morphology and hydraulic properties of the system. In this setup, the amount of water delivered to the water table is controlled by the

geological formation. Another issue of concern is the estimation of spatial distribution of recharge, and this can only be estimated if accurate information on the magnitude and distribution of aquifer properties is available.

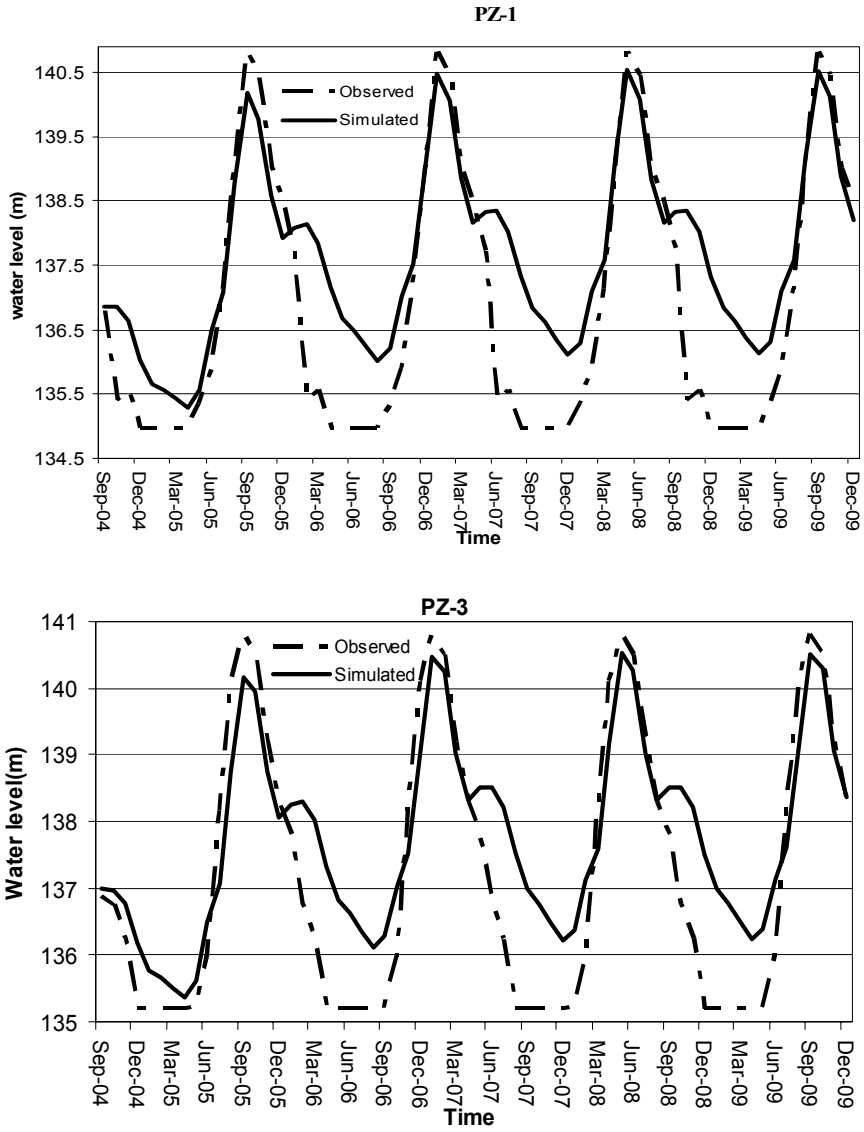

Figure 8.9 Hydraulic head simulation indicating floodplain wetland and the White Volta River interaction from September 2004 to December 2009

8.8 Uncertainty analysis

Studies have shown that in attempting to understand and to measure any hydrological process in an environmental setting, there are many different parameter sets within a chosen model structure that may be acceptable in reproducing the behaviour of that system (Feyen et al. 2004; Restrepo et al. 1998). There is seldom an "optimal" model that can generate simulated results at an acceptable limit of accuracy, rather it is more

important to consider multiple possibilities for simulating in an acceptable range (Beven 2001). To simulate results within an acceptable range, there should be sufficient interactions among components of a system, unless the detailed characteristics of these components can be isolated and calibrated independently, many representations may be equally acceptable. Therefore, searching for optimal parameter representation may not be possible, because it is statistically likely that the description of the system may be wrong. One justification for using multiple parameter sets to simulate a hydrological process stems from the fact that there are uncertainties associated with the use of models in prediction, because there are many acceptable model structures or acceptable parameter sets scattered throughout the parameter space. Diekkrüger (2003) argued that nonlinear systems are particularly sensitive to their initial and boundary condition; hence any form of dynamics in these conditions may be important in controlling the observed response. This suggests that the predictions of all the acceptable models should include an assessment of prediction uncertainty. Assessing model parameter values can be accomplished using a variety of approaches, from visual inspection of a plot of observed and predicted value to a variety of quantitative measures of goodness of fit. Uncertainty in hydrological models can stem from the fact that they are not the true reflection of the processes involved, because condition and data for running the models are not error free. There is a need to find optimum parameters that are efficient. Efficiency of parameter calibration would be enhanced, if sensitive parameters to model results can be determined.

8.9 Sensitivity analysis

Sensitivity analysis is the process of quantifying relative changes in model output in response to changes in input parameter values. This process is usually carried out after specifying, a model and its benefits include: 1) a check on the model logic and robustness of the simulation, 2) identification of the importance of specific model parameters and corresponding effort that must be invested in data acquisition for different parameters. Sensitivity analysis is carried out when initial parameterization is complete. Dimensionless and dimension scaled are the two main types of sensitivity analysis performed in MODFLOWP. These types of sensitivity analysis mentioned above have been discussed in detail in the works of Hill (1998).

8.10 Dimensionless and composite-scaled sensitivities

Dimensionless scaled sensitivities are used to compare the importance of individual observations in the estimation of a single parameter, or the importance of individual parameters in the calculation of a simulated output value (Hill 1998). In both cases, greater absolute values are associated with greater relative importance. The full weight matrix used in the two indices on the weight matrix need to be different, and scaled sensitivities are calculated as:

$$ss_{ij} = \sum_{K=1}^{ND}\left[\left(\frac{\partial y'_k}{\partial b_j}\right) b_j \omega_{ik}^{1/2}\right] \tag{8.1}$$

ss_{ij} is scaled sensitivities, y'_k is simulated value, b_j is the jth simulated parameter; $\frac{\partial y'_k}{\partial b_j}$ is the sensitivity of the simulated with respect to the jth parameter, and is evaluated at b, where $\underline{b}$ is a vector that contains the parameter value at which the sensitivities are evaluated, ω_{ik} is the weight of the ith observation and ND is the number of observations (Hill, 1998).

Composite-scaled sensitivities (css_{ij}) are calculated for each parameter using the scaled sensitivities for all observations, and indicate the total amount of information provided by the observations for the estimation of one parameter. The composite-scaled sensitivity is independent of the observed values and is calculated as:

$$css_{ij} = \left[\sum_{i=1}^{ND}\left(ss_{ij}\right)^2\Big|_{\underline{b}} / ND\right]^{1/2} \tag{8.2}$$

8.11 Dimension one-percent scaled sensitivities

While dimensionless sensitivities (dss_{ij}) are needed to compare the importance of different types of observations to the estimation of parameter values, for other purposes it is useful to have dimensional quantities such as one-percent scaled sensitivities calculated as:

$$dss_{ij} = \frac{\partial y'_i}{\partial b_j} \frac{b_j}{100} \tag{8.3}$$

One percent dimensional scaled sensitivity approximates the amount that the simulated value would change if the parameter value increased by one percent. The one-percent scaled sensitivities cannot be used to form a composite statistic, because each parameter has different units. The omission of the weighting means that the one-percent scaled sensitivities do not reflect the influence of individual observations on the regression as well as the dimensionless scaled sensitivities. This omission has an advantage, because one-percent scaled sensitivities can be calculated for any simulated quantity without having to assign the weighting.

8.12 Statistical measures of overall model fit

Model fit is evaluated by considering the magnitude of the weighted and unweighted residuals and their distribution both statistically and relative to independent variable values such as location and time (Hill 1998). The first step is generally to search the table of residuals and weighted residuals printed by MODFLOWP for the largest (in absolute value) residuals and weighted residuals. These largest residuals and weighted residuals indicate gross errors in the modeling processes. After the gross errors have been corrected, the following statistics become increasingly important.

8.13 Objective-function values

The value of the weighted least-squares objective function informally indicates model fit. It is rarely used for more formal comparisons, because its value nearly always decreases as more parameters are added, and the negative aspect of adding parameters is not reflected. The negative aspect of adding parameters is that as the data available for the estimation get spread over more parameter values the confidence with which the parameter values are estimated decreases. The standard error helps to account for this circumstance.

8.14 Calculated error variance and standard error

The commonly used indicator of the overall magnitude of weighted residuals is the calculated error variance (s^2),

$$s^2 = \frac{S(\underline{b})}{(ND + NPR - NP)} \tag{8.4}$$

where ND is the number of observations (cases), $S(\underline{b})$ is least square objective function, NPR is number of prior information values, and NP is number of estimated parameters

The square root of the calculated error variance, s, is termed the standard error of the regression and used to indicate model fit. Smaller values of both the calculated error variance and the standard error indicate a closer fit to the observations, and smaller values are preferred as long as the weighted residuals do not indicate model error. If the fit achieved by regression is consistent with the data accuracy as reflected in the weighting, the expected value of both the calculated error variance and the standard error is 1.0. Significant deviations of the calculated error variance or the standard error from 1.0 indicate that the fit is inconsistent with the weighting. For the calculated error variance, significant deviations from 1.0 are indicated if the value 1.0 falls outside a confidence interval constructed using the calculated variance.

8.15 Sensitivity results

Sensitivity analysis was performed as part of a modeling procedure to assess the usefulness of the model for decision making and the robustness of the conclusions reached from the comparison of observed and simulated conditions. The main sources of uncertainty in the model for the Pwalugu floodplain wetland site are the spatial distribution of the horizontal hydraulic conductivity, vertical hydraulic conductivity, specific storage and specific yield. While acknowledging the anisotropic nature of the aquifer deposits of the sub-surface deposit with, however, anisotropy of horizontal hydraulic conductivity (HK_1), specific storage (SS_4) and specific yield (SY_3) was assumed at the scale of interest for the aquifer parameters. This implies that uncertainty as a result of the spatial variability of the conductivity in the top layer is not accounted for in the present study. Van Leeuwen et al. (1999) showed that the variability in the

vertical conductance of a confining clay layer strongly affected the flow and shape of the capture zone. In the present study, this variability is partly accounted for by the spatial variation of the thickness of the top layer.

Sensitivity analysis was applied to horizontal hydraulic conductivity (HK_1), vertical hydraulic conductivity (VK_10), specific storage (SS_4) and specific yield (SY_3) to determine which of these parameters had the greatest effect on the simulated heads. MODFLOWP was used to generate the sensitivities by perturbing the control parameters and simulation run for 487 days on a daily time steps basis. The number of runs was 19 using 96 observations. Out of the 96 observations 30 had a residual greater or equal to zero, while the remaining 66 had residuals less than zero.

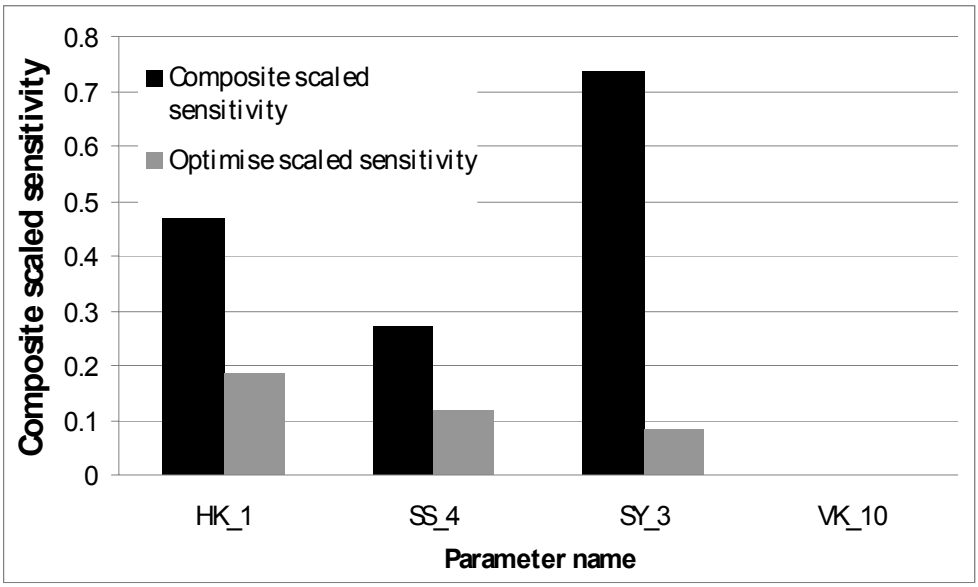

Figure 8.80 Composite scale sensitivity (horizontal hydraulic conductivity (HK_1), vertical hydraulic conductivity (VK_10), specific storage (SS_4) and specific yield (SY_3)

The composite-scaled sensitivity (Figure 8.10) indicates the relative importance of the sub-surface parameters used in the modeling processes. During the process of model calibration, HK_1, SS_4 and SY_3 were the parameters with a high level of sensitivity, thereby influencing the interaction process between floodplain wetland and White Volta River. VK_10 was insensitive to changes; hence it plays no role in the floodplain wetland-White Volta River flow interaction. After optimization, HK_1 was the most sensitive parameter, and any adjustment of HK_1 increased the amount of interaction between the wetland and the river (Figure 8.10).

Examining the one-percent scaled sensitivity (dimensional sensitivity) results (Figure 8.11) sensitivity for the selected parameters shows spatial and temporal variation.

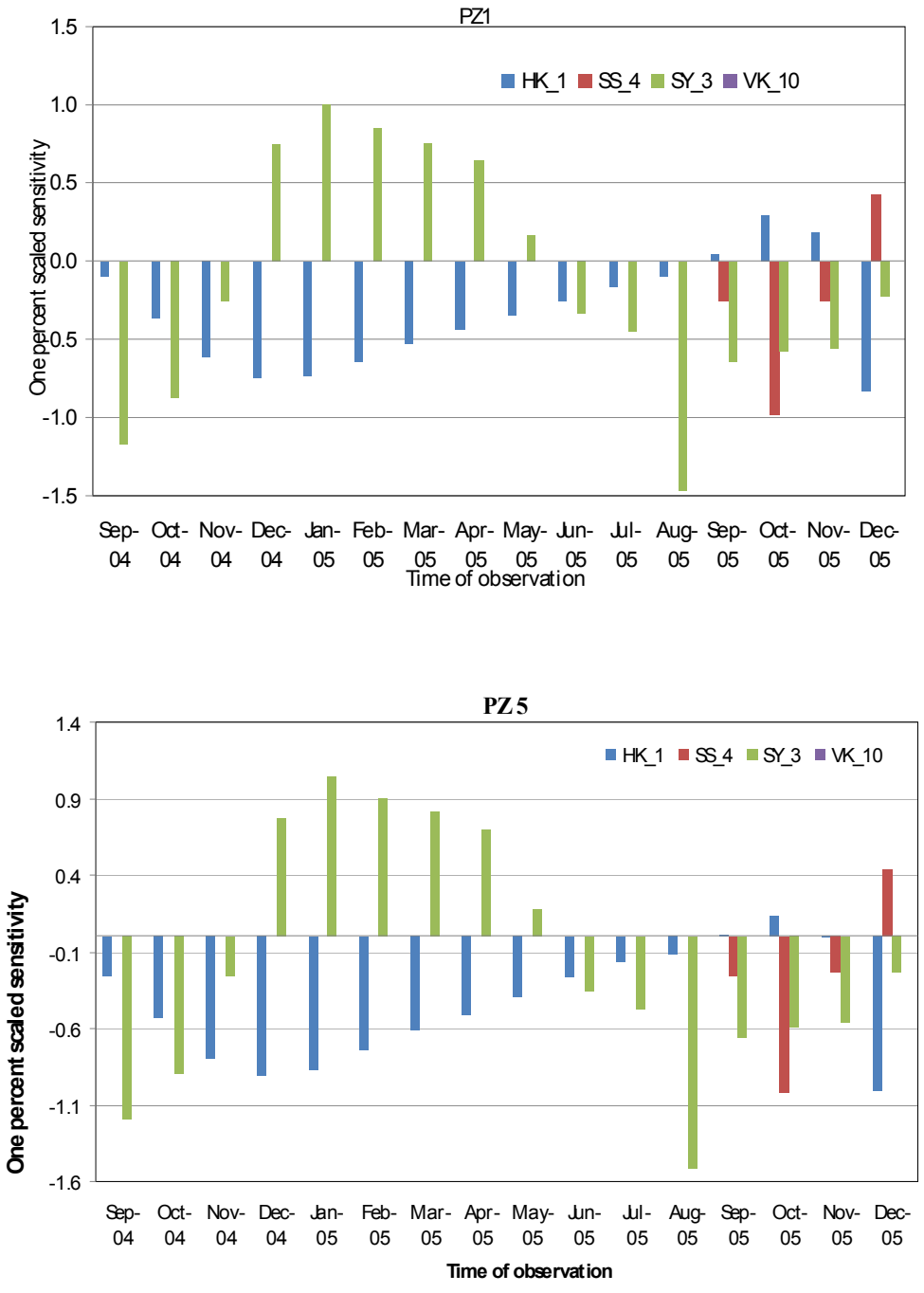

Figure 8.91 One-percent scaled sensitivity of selected hydraulic parameters used in the modeling process

Dimensional scaled sensitivity calculated for the monthly head observation compares the importance of individual parameters for the estimation of other parameters. HK_1 in the dimensional scaled sensitivities indicates high values and variation (Figure 8.11). For PZ1, from September 2004 to December 2005, HK_1 shows exceptional variations.

The sensitivity analysis assessed the effect of the distribution of the selected parameters on the sub-surface water flow in the Pwalugu wetlands. Altering of the parameter distribution resulted in an appreciable adjustment in the contribution of floodplain wetland to stream flow.

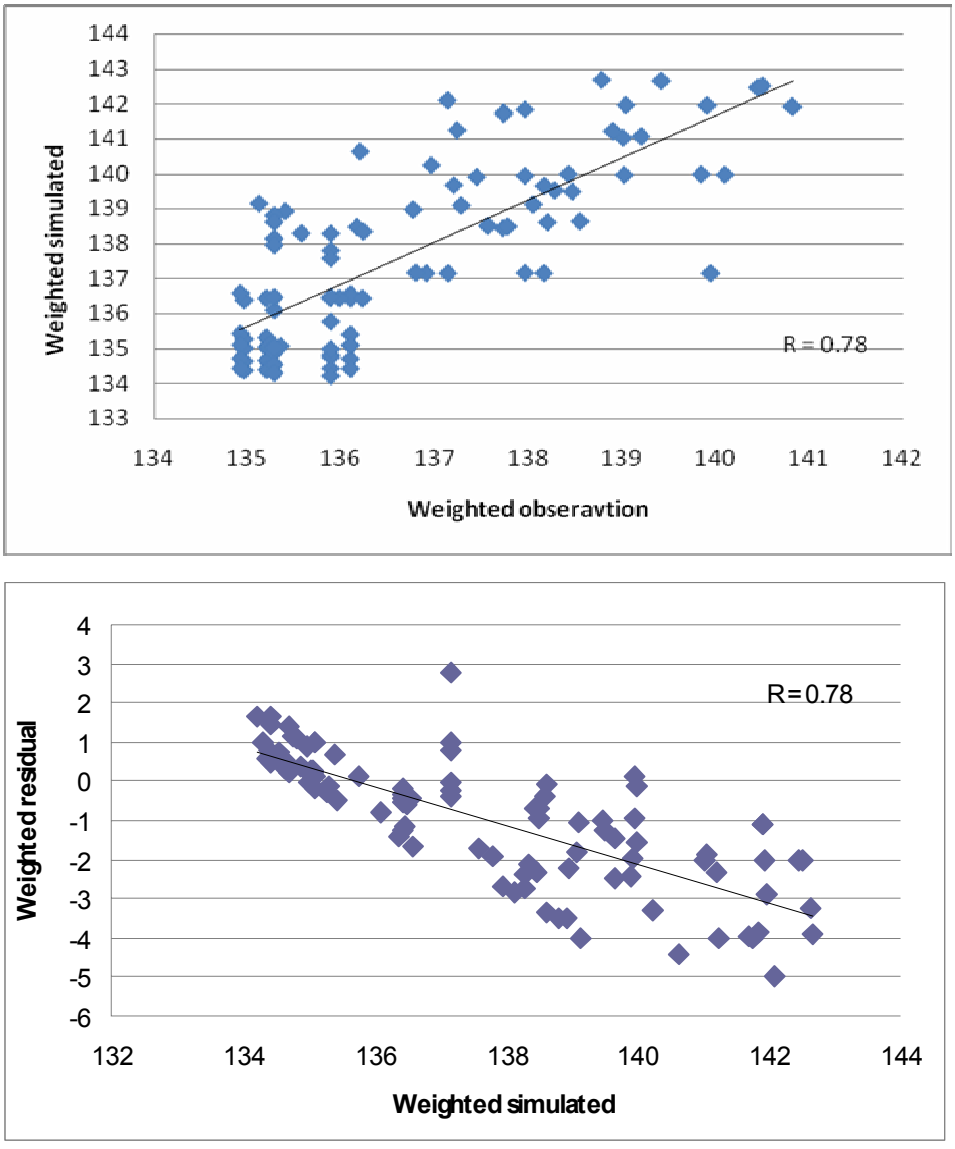

Figure 8.12 Model fit between observed and simulated hydraulic head

A correlation of 0.78 was found between the weighted residuals and weighted simulated values (Figure 8.12), although they are assumed to be independent of each other. Conversely, the model was found to have well identified parameters; however the model results were sensitive to the values of input parameters. Therefore, the application of the MODFLOW model will be more reliable for decision making.

9 SUMMARY AND CONCLUSIONS

The White Volta River catchment is experiencing climatic, hydrologic and vegetation changes. This research was conducted to examine the essential role floodplain-wetlands play in stream flow within the White Volta basin, in order to ensure good management and a sustainable level of water resource usage. This research shows that changes in floodplain-wetland characteristics have ramifications on surface water flow. Data collected for the study are derived from field measurements, field observation and laboratory analysis. Together they describe the hydro-dynamics of the floodplain wetlands and also serve as inputs for the HYDRUS-1D and MODFLOW models. This chapter summaries the research finding and presents recommendations for future research.

9.1 Floodplain-wetland mapping within the White Volta River basin

Floodplain wetlands mapping in the basin was undertaken using a combination of geographic information systems, remote sensing, and statistical techniques. In the process of wetland mapping, three (3) main stages were adopted. These stages are; extraction of hydrotopes, point sampling, and floodplain wetland extraction using logistic regression analysis. The logistic regression model assisted in analyzing the relationship between the probability of the response being a success and the explanatory variables rather than analyzing than their causal relationships.

The results of the logistic regression analysis indicate that four (4) of the predictors, Logb4, Evapo, texture, and distance are significant at $p< 0.05$. Therefore the Likelihood Ratio Chi-Square test of 454.3, computed with the Prob > $chi^2 = 0$, indicates a good model fit and none of the predictors; coefficients is likely equal to zero. Areas along the White Volta River and its tributaries have the highest probabilities of wetland occurrence. Distance played an important role in delineating probable wetland areas. That is, wetlands have a higher probability of being associated with river courses. The logistic regression results suggest that even with limited data, as in the case of Ghana, floodplain wetlands can be mapped successfully on the basis of remotely-sensed data.

9.2 Hydro-geomorphology of the White Volta River basin

The White Volta Basin is a complex system that exhibits diverse characteristics, behaviour, and evolutionary traits. Soil types found in Pwalugu and Tindama wetlands are of Kuapela and Breyanse series, which have distinct horizons and soil texture. Pwalugu and Tindama wetland soils have high clay content, with a medium to moderate sub-angular block structure. While the Kuapela soil series found in Pwalugu have few iron (Fe) concretions, these are absent in the Tindama wetland sites. Soil profiles examined in Pwalugu wetland site showed distinct colour of mottles that indicate groundwater level fluctuations. Results from the piezometer readings do not indicate total saturation of soil because during most of the year, the water table is deeper than as indicated by the gray soil colours.

Furthermore, the assessment of water movement-controlling parameters such as vertical saturated hydraulic conductivity (K_s), measured in Pwalugu and Tindama sites, show marked differences in parameter value with varying depth. In the Pwalugu wetland, K_s over the first 20 cm of depth ranged from 0.01 cm/day to 0.15 cm/day, while for the lower depth of 100 cm the conductivity ranged between 0.002 cm/day and 0.022 cm/day. In the Tindama wetland, a low conductivity averaging 0.018 cm/day was measured. The use of the inverse auger method for K_s estimation indicated little variability in the Tindama site, where values ranged between 15.57cm/day to 44.43cm/day, while Pwalugu K_s values ranged between 1.28cm/day and 96.29cm/day.

Similarly, it was evident from the HYDRUS-1 model results for Pwalugu wetland that unsaturated zone contributions to the hydrodynamic process have both temporal and spatial variation. As a case in point, the effective rainfall between July and October contributes more to the volume of water stored in the system than any other month. Additionally, the spatial variation in the volume of storage in September 2005 for Pit-1 and Pit-7 was 0.48 m^3 and 0.39 m^3 respectively. The contribution of water input to recharge sub-surface or groundwater systems shows spatial variation and is indicated in the amount of bottom water discharge in the pits. Ground water upwelling, as a result of increased water input, occurs within the months of July and October, where recharge from the unsaturated zone is high.

Vertical infiltration at Pwalugu and Tindama sites is an important process of water movement into the subsurface. Cracks of width 30mm formed on the soil surface during the dry season, and roots of plants have created pathways for preferential flow during the onset of rainfall, leading to variations in the rate of infiltration. Furthermore, infiltration in the Tindama and Pwalugu wetland sites show temporal and spatial variability. In most cases, this variability is characterized by high infiltration rates at the start of measurement but decline gradually over time, although exceptions existed during the period of water input. High infiltration rates of 2 to 4cm/min are found primarily at the fringes of the wetlands in Pwalugu where vegetation is dominant. The condition is also observed in the Tindama wetland, where rates are 0.65 to 0.9cm/min. Within a period of 150 minutes, the depth of penetration or wetting front for Pwalugu ranges between 15.4 cm to 92 cm while 16.5 cm to 38 cm was measured at the Tindama sites.

In addition, the sub-surface water fluctuation monitored at the Pwalugu wetland gave an indication of the rate of sub-surface response to water input. For instance, for a total rainfall input of 15.99cm between 11th and 16th September 2004, the response at most of the piezometers started from 20th September, 2004. The decline groundwaterrate within the wetlands also varies: areas closer to the main river experience a fast rate decline, while areas at the toe of the wetland slope are the last to experience decline. The calculated vertical hydraulic gradient (VHG) indicates upwelling(s) between June and September and draw down in the dry season between November and May. Using factor analysis, components such as water input (Rainfall or irrigation), soil potentials/antecedent soil moisture, soil structure, vegetation cover and topography, groundwater level and over bank flow of White Volta River are identified as factors influencing the hydrodynamics of the Pwalugu and Tindama wetland site.

9.3 Isotope analysis

Isotope tracers including $\delta^{18}O$ and $\delta^{2}H$ provided new insights into hydrologic processes within the basin. The concentrations of $\delta^{18}O$ and $\delta^{2}H$ in water vapor over the White Volta River Basin are influenced by the trajectory of the tropical continental (cT) from the Sahara and maritime air masses (mT) from the Atlantic Ocean, resulting in observed differences in isotopic composition of rainfall in the Pwalugu and Tindama wetland

sites, respectively. Within Pwalugu wetland catchment in June 2005, during the onset of rainfall, $\delta^{18}O$ measured -3.3‰ and δD -17.6‰. Concentrations depleted in July when the total monthly rainfall is high, with $\delta^{18}O$ measured at -4.9‰ and -28.8‰ for $\delta^{2}H$. At the Tindama wetland site, $\delta^{18}O$ measured in June is -2.1‰ and -8.1‰ for $\delta^{2}H$. For Pwalugu wetland site the local meteoric water (LWML) computed yielded a $\delta^{2}H$ excess of 8.13 and a slope of 7.67, while a $\delta^{2}H$ excess of 5.729 and a slope of 6.81 were computed for the Tindama wetland site.

To elucidate the seasonal dynamics in Pwalugu and Tindama wetlands, Pwalugu wetland-B in January is highly enriched in $\delta^{18}O$ and $\delta^{2}H$, e.g., 25‰ and 108.2‰. Tindama showed a similar trend in January 2005, with 5.4‰ of $\delta^{18}O$ and 21.3‰ of $\delta^{2}H$. During the rainy season with high rainfall input, dilution of surface water is prominent, and there is little evaporation from the system. Isotopic compositions plotted on their respective LMWL deviates and due to their low Deuterium excesses. Using the Raleigh equation, an estimated evaporative fraction of 9.62% was estimated for wetland-B in August 2005 and 5.81% in September 2005. In wetland-C, the estimated evaporative fractions for August and September 2005, were 5.9% and 8.24%t, respectively. For the Tindama wetland, in August 2004, the estimated evaporative fraction was 15.83%, while in September 2005, 16.79% was the estimated fraction, hence in August little or no evaporation occurred, thereby the water input was more than the output. Therefore, the fraction of water loss from the wetlands as evaporation ranges from 5.81 percent to 53.25 percent for wetland-B and 1.04% to 16.01% for wetland-C. In the Tindama wetland, not much evaporation was shown; it ranged from only 9.53% to 28%. Moreover, results from the Penman-Monteith potential evapotranspiration (PET) analysis and the evaporative fraction of ^{18}O (EF-$^{18}0$) suggest that the estimated water budget calculated for the wetland-B in Pwalugu mirrors the changes in rainfall. A comparison was made between the PET and EF using regression analysis. At 95 per cent confidence level, the estimated equation had an R^2 of 0.94.

Regarding surface water and subsurface water interactions, some form of relationship on seasonal basis was detected based on variation in their isotopic composition ($\delta^{18}O$ and $\delta^{2}H$), when plotted with the LMWL, they corresponding closely between July and September. The isotopic ratio of wetland-B water and sub-surface

water in the piezometers are similar and it is difficult to isolate water inflow associated with these two, due to the fact that in the rainy season, within August and September 2005 they plot around the LMWL.

9.4 Wetland river-flow interaction

The hydraulic connection between the White Volta River and floodplain wetland varies temporally and spatially because of intervening unsaturated zones. To establish the form of interaction that goes on between the main river and floodplain wetlands within the White Volta basin, PM-WIN(MODFLOW) was specified using lower boundary discharge from the HYDRUS-1D model as estimated groundwater recharge. This input quantifies the temporal and spatial variations in the interaction between floodplain wetland and stream flow. Prior to simulation, parameters were calibrated to obtain a tolerable distribution of initial hydraulic head. The calibration process reduced the error of discrepancy from -0.69 to 0. The HYDRUS-1D bottom flux used as an estimate of groundwater recharge gave a better fit between the simulated hydraulic head and observed sub-surface water level fluctuation. This level of compatibility gives indications that the model calibration needs to be improved.

The simulation of the sub-surface hydraulic head of the wetland indicates a systematic variation relative to the White Volta River in response to changes in the rainfall pattern. The interaction conditions vary from season to season with March, April, and May showing the least leakage (estimated values of 0.03mm/day, 0.06mm/day and 0.15 mm/day, respectively) from the river into the floodplain, although the expectation is that floodplain wetlands serve as a moisture buffer and supply the river with water during the low season. Nevertheless, the interaction between the wetland and the river as simulated is bidirectional. With most of the flow coming out from the river, this condition persists in the months of August and September.

9.5 Conclusions

The internal conceptualization of the floodplain wetland was based on a semi-confined two-layered system with differing hydraulic characteristics and as an integral part of the White Volta River basin. Flux of water and chemicals from and to the White Volta River reflects the position of the wetlands with respect to the different scale of the

subsurface water system. The geological controls on sub-surface water distribution, rainfall distribution and direct evapotranspiration influence the water storage in the floodplain wetlands. Therefore, understanding the importance of floodplain wetlands in relation to all controlling factors is needed for effective management of the integrated water resources in the White Volta River basin. This can be achieved by identifying characteristic, recurrent spatial and temporal patterns of water table response within the floodplain and their controlling factors.

The limitation of data on the sites studied hampered the modeling process, leading to erroneous results. Future success in understanding floodplain wetland-river flow interaction and the hydrodynamics of floodplain wetlands in the White Volta River basin will rely on continued and expanded data collection at various scales. Therefore, emphasis should be placed on the collection of high resolution data both temporally and spatially.

Understanding the hydrologic and environmental processes that define relationships between surface and sub-surface waters, the landscape connectivity of riverine system, human-induced changes and associated responses of floodplain wetlands is essential to understand the ecological effects of water resources management decisions in the basin.

There is a need to determine source, path and velocity of water flow in the subsurface of the floodplain wetlands using isotope tracers.

10 REFERENCES

Acheampong SY, Hess JW (1998) Hydrogeologic and hydrochemical ramework of the shallow groundwater system in the suthern Voltaian Sedimentary Basin of Ghana. Hydrogeol J 6(4):527-537

Adams WM (1993) Indigenous use of wetlands and sustainable development in West Africa. The Geogr J 159(2):209-218

Allen RG, Pereira LS, Raes D, Smith M (1998) Crop evapotranspiration – Guidelines for computing crop water requirements. FAO Irrigation and drainage paper 56, FAO - Food and Agriculture Organization of the United Nations, Rome

Ahvenniemi M, Ojala K, Raitala J (1998) A 15 Channel TM Classification of Bog Types In Finnish Lapland Department of Physics, University Of Oulu, Oulu, Finland

Akiti TT (1980) Etude geochimique et isotopique de quelques aquifere du Ghana. Ph.D. thesis, Universite' de Paris-Sud

Amoozegar A, Warrick AW (1986). Hydraulic conductivity of saturated soils: Field methods. In Klute A (ed.) Methods of soil analysis. Part 1. 2nd ed. Agronomy Monogr 9. ASA and SSSA, Madison, WI

Andreini M, van de Giesen N (2001) The GLOWA Volta Project. Sustainable Water Use in the Volta Basin. IHDP homepage (11/04) http://www.glowa-volta.de/publications/printed/IHDP_andreini.htm

Andriesse W (1986) Area and Distribution. In: Juo and Lowe (eds*)* The Wetlands and Rice in Sub-Saharan Africa. Proceedings of an International Conference. Ibadan, November 1985. IITA, Ibadan, Nigeria. p. 15-30

API (1996) Review of Methods to Estimate Moisture Infiltration, Recharge, and Contaminant Migration Rates in the Vadose Zone for Site Risk Assessment. API Publication No. 4643. American Petroleum Institute, Washington, DC

Augusteijn MF, Warrender CE (1998) Wetland Classification Using Optical And Radar Data And Neural Network Classification. Int J Remote Sensing 19(8):1545-1560

Atkinson RB, Perry JE, Smith E, Cairns J Jr (1993) Use of created wetland delineation and weighted averages as a component of assessment. Wetlands 13:185–193

Ayibotele NB (1999) Closing statement on the integrated Development of the Volta River Basin: 139-144. In: Gordon C and Amatekpor JK (eds) The sustainable integrated development of the Volta Basin in Ghana, Volta Basin Research Project, University of Ghana, Legon, Accra

Bagamsah TT (2005) The impact of bushfire on carbon and nutrient stocks as well as albedo in the Savanna of Northern Ghana. PhD thesis, University of Bonn, Bonn, Germany

Baghdadi N, Bernier M, Gauthier R, Neeson I (2001) Evaluation of C-Band SAR Data For Wetlands Mapping. Int J Remote Sensing 22(1):71–88

Bates P, De Roo APJ (2000) A simple raster-based model for flood inundation simulation. J Hydrol 236: 54-77

Bauer A, Black AL (1992) Organic carbon effects on available water capacity of three soil textural groups. Soil Science Society American Journal 56:248-254

Bedford BL (1996) The need to define hydrologic equivalence at the Landscape scale for freshwater wetland mitigation. Ecological Applications 6:57-68

Bennett MWA (1987) Rapid monitoring of wetland water status using density slicing. In: Proceedings of the Fourth Australasian Remote Sensing Conference; 682–691.

Beven JK (1989) Changing ideas I hydrology- the case of physically based models. J Hydrol 105:157-172

Beven JK (2000) Rainfall-Runoff Modelling: The Premier, John Wiley, UK

Beven KJ, Wood, E.F. and Murugesu, S (1988) On hydrological heterogeneity-Catchment morphology and catchment response. J Hydrol 100:353-375.

Beven KJ (1978) The hydrological response of headwater and slideslopes areas. Hydrological Sciences Bulletin 23:419-437

Bockelmann BN, Fenrich EK, Lin B, Falconer RA (2004) Development of an ecohydraulics model for stream and river restoration. Ecological Engineering 22(4-5): 227-235

Bonell M, Balek J (1993) Recent Scientific Development and Research Needs in Hydrological Processes of Humid tropics: 167-260. In: Bonell M, Hufschmidt MM, Gladwell JS (eds) Hydrology and water management in the humid Tropics: Hydrological research issues and strategies for water management. Cambridge University Press, Great Britain.

Brady NC, Weil RR (1996) The nature and properties of soil. 12 th edn, Prentice Hall, New Jersey, USA

Brady NC, Weil RR (1999). The nature and properties of soils, 12th edn, Prentice Hall, Upper Saddle River, N.J.

Bradley C, Gilvear DJ (2000) Saturated and unsaturated flow dynamics in a floodplain wetland. Hydrol Process (14):2945-2958

Bradford RB, Acreman MC (2003) Applying MODFLOW to wet grassland in-field habitats: a case study from the Pevensey Levels, UK. Hydro Earth Syst Sc 7(1), 43–55

Brian WJ (1962) Agriculture and Land Use in Ghana. OVP

Brinson MM (1993) A hydrogeomorphic classification for wetlands, Technical report WRP-DE-4, U.S. Army engineer waterways experiment station, Vicksburg, MS. NTIS No. AD A 270 053

Brown TN Johnston CA, and Cahow KR, (2003) Lateral flow routing into a wetland: field and model perspectives Geomorphology 53:11– 23.

Buckle C (1978) Landforms in Africa. Longman, London

Buttle JM (1998) Fundamentals of small catchment hydrology, In: Isotope Tracers in Catchment Hydrology, Kendall C and McDonnell JJ (eds) Elsevier, Amsterdam, 1–43

Burrough PA (1986) Principles of geographical information systems for land resources assessment. Monograph on Soils and resources Survey No. 12, Oxford Science Publications, Clarendon Press, Oxford, U.K.

Carey SK, Woo MK (2000) The Role of Soil Pipes as a Slope Runoff Mechanism subarctic Yukon, Canada, J Hydrol 233:206-222

Chiang WH, Kinzelbach W (1998) Processing MODFLOW for Windows: A Simulation System for Modelling Groundwater Flow and Pollution

Choudhury BJ, Monteith JL (1988) A four-layer model for the heat budget of homogeneous land surfaces Q J Roy Meteor Soc 114 (480):373-398

Clark I, Fritz P (1997). Environmental isotopes in Hydrogeology. Lewis Publishers. New York

Clausnitzer D, Huddleston JH (2002) Wetland Determination Of A Southeast Oregon Vernal Pool And Management Implications, Wetlands (22) 4 - December 2002

Clay A, Bradley C, Gerrard AJ, Leng MJ (2004) Using Stable Isotopes of water to infer wetland hydrological dynamics, Hydro Earth Syst Sc 8(6):1164-1173.

Cloke H, Anderson M, McDonnell JJ, Renaud J (2006) Using numerical modelling to evaluate the capillary fringe groundwater ridging hypothesis of streamflow generation. J Hydrol 316:141-162

Coplen TB, Herczeg AL, Barnes C (2000) Isotope engineering: using stable isotopes of the water molecule to solve practical problems, in Environmental Tracers in Subsurface Hydrology, by Cook P.G. and Herczeg A.L., (eds) Kluwer Academic Publishers, Boston

Congalton RG, Green K (1999) Assessing the Accuracy of Remotely Sensed Data. CRC Press Inc, Florida, USA

Compaore H (2005) The impact of savannah vegetation on the spatial and temporal variation of the actual evapotranspiration in the Volta Basin, Navrongo, Upper East Ghana. PhD thesis, University of Bonn, Bonn, Germany

Cook KH (1999) Generation of the African Easterly Jet and its role in determining West African precipitation: J Climate 12:1165–1184

Coplen TB (1993) Uses of environmental isotopes. In Regional groundwater quality, ed. W.M.Alley, pp 227-254. Van Nostrand Reinhold, New York

Cowardin LM, Carter V, Golet FC, LaRoe ET (1979) Classification Of Wetlands And Deepwater Habitats Of The United States, U.S. Department of the Interior Fish and Wildlife Service Office of Biological Services, Washington DC

Craig H (1961b) isotopic variations in meteoric waters. Sciences 133:1702-1703

Cumming IG, Van Zyl JJ (1989) Feature utility in polarimetric radar image classification. In Proceedings of IGARSS'89 (Piscataway, NJ: IEEE), pp. 1841–1846

DePaolo DJ, Conrad ME, Maher K, Gee GW (2004) Evaporation Effects on Oxygen and Hydrogen Isotopes in Deep Vadose Zone Pore Fluids at Hanford, Washington. Vadose Zone J 3:220–23

De Vaus DA (1993) Surveys in Social Research 3rd edn. Social Research Today 5 University College London, UK.

Dewey JC, Schoenholtz SH, Shepard JP, Messina MG (2006) Issues Related To Wetland Delineation Of A Texas, USA Bottomland Hardwood Forest Wetlands, 26 (2):410–429

Diekkrüger B (2003) Models - calibration, validation, sensitivity analysis (I and II). Presentation at Bonn. http://www.giub.uni-bonn.de/hrg/Poster.htm

Dingman LS (2002), Physical Hydrology, Prentice Hall, New Jersey, USA

Domenico PA (1972), Concepts and Models in Groundwater Hydrology, McGraw-Hill, New York

Dooge JCI (2003) Linear theory of hydrologic systems. EGU reprint series. European Geoscience Union, Katlenburg-Lindau, Germany, 327pp

Duguy B, Rovira P, Vallejo R (2007) Land-Use History And Fire Effects On Soil Fertility In Eastern Spain, European Journal Of Soil Science (58):83–91

Dwivedi R, Rao B, Bhattacharya S (1999) Mapping wetlands of the Sundaban Delta and it's environs using ERS-1 SAR data. Int J Remote Sens 20(11): 2235-2247

Edelfson NE, Anderson ABC (1943) The thermodynamics of Soil Moisture, Hilgardia 16, 3 1-299

Feyen L, Dessalegn AM, De Smedt F, Gebremeskel S, Atelaan O (2004) Application of a Bayesian approach to stochastic delineation of capture zones. Ground Water 42(4):542-551

Food and Agriculture Organization of the United Nations (FAO) 1999, Data on location of dams for Africa provided to WRI for PAGE Analysis. FAO Rome, Italy:

Fischer-Antze T, Stoesser T, Bates P, Olsen, NRB (2001) 3D numerical modelling of open-channel flow with submerged vegetation. J Hydraul Res 39(3):303-310

Fletcher PC, Veneman PLM, Soil Morphology as an Indicator of Seasonal High Water Tables. http://nesoil.com/properties/eshwt.htm

Fox DM, Le Bissonnais Y, Bruand A (1998) The effect of ponding depth on infiltration in crusted surface depression. Catena 32:87-100

Gat JR, Gonfiantini R (1981) Stable isotope hydrology. deuterium and oxygen-18 in the water cycle. International Atomic Energy Agency, Technical Report Series 210, Vienna

Gat JR, Mook WG, Meijer HJA, Environmental Isotopes in the Hydrological Cycle Principles and Applications VOLUME II: ATMOSPHERIC WATER, Weizmann Institute, Rehovot, Israel and Centre Isotope Research, Groningen, The Netherlands.

Gilbert JM, Warner BG, Aravena R, Davies JC, and Brook D (1999) Mixing Of Floodwaters. In Arestored Habitat Wetland In Northeastern Ontario Wetlands 19:1

Gwin SE, Kentula ME, Shaffer PW (1999) Evaluating the effects of wetland regulation through hydrogeomorphic classification and landscape profiles. Wetlands 19:477–489

Hails AJ, (ed) (1996) Wetlands, Biodiversity, and the Ramsar Convention: The Role of the Convention on Wetlands in the Conservation and Wise Use of Biodiversity. Gland, Switzerland: Ramsar Convention Bureau.

Hardly et al (1985) Recent development in erosion and sediment yield studies, Technical Document in Hydrology UNESCO, Paris

Harvey JW, Newlin JT, Krupa SL **(** 2006) Modeling decadal timescale interactions between surface water and ground water in the central Everglades, Florida, USA . J Hydro 320 (3-4): 400-420

Hay AM (1979) Sampling designs to test land-use map accuracy. Photo Eng Rem S 45(4):529–533.

Hayward D, Oguntoyinbo J (1987) Climatology of West Africa. Hutchindson, London, UK

Hayashi M, Rosenberry DO (2002) Effects of ground water exchange on the hydrology and ecology of surface water. Ground Water 40:309–316

Hess L, Melack J, Filoso S, Wang Y (1995) Delineation of inundated area and vegetation along the Amazon floodplain with the SIR-C synthetic aperture radar. IEEE T Geosci Remote 33(4):896-904

Hill MC (1998) Methods and guidelines for effective model calibration: U.S. Geological Survey Water-Resources Investigations Report 98-4005, 90p. [with application to UCODE, a computer code for universal inverse modeling, and MODFLOWP, a computer code for inverse modeling with MODFLOW

Hillel D (1998) Environmental soil physics. Academy Press, New York

Hoefs J (1987) Stable isotope geochemistry, 3rd edn. Springer-Verlag, Berlin

Hufschmidt M (1993) Water resources Management in Hydrological Processes of Humid tropics: 167-260. In: Bonell M, Hufschmidt MM, Gladwell JS (eds) Hydrology and water management in the humid tropics: Hydrological research issues and strategies for water management, Cambridge University Press, Great Britain

Hunt RJ, Walker JF, Krabbenhoft DP (1999) Characterizing Hydrology And The Importance Of Ground-Water Discharge In Natural And Constructed. Wetlands 19, No. 2 - June 1999

Jain SK, Singh RD, Jain MK, Lohani AK (2005) Delineation of Flood-Prone Areas Using Remote Sensing Techniques. Water Resour Manag 19(4):333-347

Janssen G, Hemke K (2004) Ground water models as civil engineering tools, FEM_MODFLOW, Karlovy Vary, Czech Republic

Jaramillo DF, Dekker LW, Ritsema CJ, Hendrickx (2000) Occurrence of Soil Water Repellency in Arid and Humid Climates. J Hydrol 231-232:105-111

Joris I, Feyen J (2003) Modelling water flow and seasonal soil moisture dynamics in an alluvial groundwater-fed wetland, Hydrol Earth Syst Sci, 7(1), 56-66

Jung J (2006) Regional Climate Change and the Impact on Hydrology in the Volta Basin of West Africa PhD thesis, Garmisch-Partenkirchen, Institut f¨ur Meteorologie und Klimaforschung Bereich Atmosph¨arische Umweltforschung (IMK-IFU) Forschungszentrum Karlsruhe in der Helmholtz-Gemeinschaft

Jung M, Burt TP (2004) Towards a Conceptual Model of Floodplain Water Table Response, Water Resour Res, 40: 1-13

Kasischke E, Bourgeau-Chavez L (1997) Monitoring South Florida wetlands using ERS-1 SAR imagery. Photogramm Eng Rem S 63(3): 281-291

Kasischke E, Bourgeau-Chavez L, Smith K, Romanowicz E, Richardson C (1997a) Monitoring hydropatterns in South Florida ecosystems using ERS SAR data, 3rd ERS Symposium on Space at the Service of our Environment, Florence, Italy, pp. 71-76

Kasischke E, Melack J, Dobson M (1997b) The use of imaging radars for ecological applications-a review. Remote Sen Environ 59(2):141-156

Kebede S, Travi Y, Alemayehu T, Marc V (2006) Water balance of Lake Tana and its sensitivity to fluctuations in rainfall, Blue Nile basin, Ethiopia, J Hydrol 316: 233-247

Kendall C, Caldwell EA (1998) Fundamentals of Isotope Geochemistry in Isotope Tracers in Catchment Hydrology C. Kendall and J. J. McDonnell (eds.) Elsevier Science B.V., Amsterdam. pp. 51-86

Kindscher K, Fraser A, Jakubauskas ME, Debinski DM (1998) Identifying Wetland Meadow in Grand Teton National Park using Remote Sensing and average wetland values, Wetland Ecol Manage 5: 265-273

Klute A (1986) Water retention: Laboratory methods. In: Klute A (ed) Methods of Soil Analysis, Part 1: Physical and Mineralogical Methods, Second Edition, American Society of Agronomy, Madison, WI. 635-662

Klute A, Dirkson C (1986) Hydraulic conductivity and diffusivity: Laboratory methods. In: Klute A (ed) Methods of soil analysis-Part I. American Society of Agronomy, Madison, USA.

Krasnostein AL, Oldham CE (2004) Predicting wetland water storage. Water Resour Res 40(10): W10203.1-W10203.12

Krause S, Bronstert A (2005) An advanced approach for catchment delineation and water balance modelling within wetlands and floodplains. Advances in Geosci 5: 1–5, 200

Kroes DE, Brinson MM (2004) Boccurrence Of Riverine Wetlands On Floodplains Along A Climatic Gradient, Wetlands: 24 (1):167–177

Krysanova V, Wechsung F, Arnold J, Srinivasan R, Williams J (2000) PIK Report Nr. 69 "SWIM (Soil and Water Integrated Model), User Manual".

Kushwaha S, Dwivedi R, Rao B (2000) Evaluation of various digital image processing techniques for detection of coastal wetlands using ERS-1 SAR data. Int J Rem Sens, 21(3): 565-579

Kustas WP, Choudhury BJ, Moran MS, Reginato RD Jackson RJ, Gay LW, Weaver HL (1989) Determination of sensible heat flux over sparse canopy using thermal infrared data. Agric. For. Meteorol 44: 197-216

Kustas WP, Stannard DI, Allwine KJ (1996) Variability in surface energy flux partitioning during Washita '92: resulting effects on Penman–Monteith and Priestley–Taylor parameters. Agricultural and Forest Meteorology 82: 171–193

LaBaugh JW, Winter TC, Swanson GA, Rosenberry DO et al (1996) Changes in Atmospheric Circulation Patterns Affect Midcontinent Wetlands Sensitive to Climate, Limnology and Oceanography, Vol. 41, No. 5, Freshwater Ecosystems and Climate Change in North America (Jul., 1996), pp864-870

Lillesand T, Kiefer R (2000) Remote Sensing and Image Interpretation. John Wiley & Sons, Inc., New York,

Lhomme JP, Chehbouni A, Monteny B (1994) Effective parameters for surface energy balance in heterogeneous landscape. Boundary-Layer Meterol 71:297–309

Lott RB, Hunt RJ (2001) estimating evaporation in in natural and constructed wetlands, Wetlands, 21 (4): 614–628

Loucks DP (2000) Sustainable Water Resources Management, Water Int 25(1):3-10

Lyon JG, McCarthy J (1995) Introduction to Wetlands and Environmental Applications of GIS. In: Lyon JG and McCarthy J (eds) Wetland and Environmental Applications of GIS. Boca Raton: CRC Press, Inc. New York

Majoube M (1971) Fractionnement en oxygene-18 et en deuterium entre léau et sa vapeur. J Chem Phys 197:1423-1436.

Mansell RS, Bloom SA, Sun G (2000) A model for wetland hydrology: Description and validation, Soil Sci 165:5

MArthieu R, Bariac T (1996) An isotopic study (^{2}H and ^{18}O) on water movements in clayey soils under a semiarid climate. Water Resour Res 32:779-789

Marriott S (1992) Textural analysis and modeling of a flood deposit: River Severn, UK. Earth Surf Processes 17**:**687–697

Marriott S (1996) Analysis and modeling of overbank deposits. In: Anderson, MG, Walling DE and Bates PD (eds) Floodplain Processes, Wiley, Chichester, UK, pp. 63–93.

Marron DC (1992) Floodplain storage of mine tailings in the Belle Fourche River system: a sediment budget approach. Earth Surf Processes 17**:**675–685

Martin N. (2006) Development of a water balance for the Atankwidi catchment, West Africa – A case study of groundwater recharge in a semi-arid climate. PhD thesis, University of Bonn, Bonn, Germany

Matos JE, Welty C, Packman AI (2002) Stream-Groundwater Interactions and Near-Stream Flow Systems: The Influence of Aquifer Heterogeneity and Stream Meandering on Three-dimensional Hyporheic Exchange Flows American Geophysical Union, (AGU) Fall Meeting, 887

McCarthy J, Gumbricht T (no date) Multisource rule-based contextual classification of ecoregions of the Okavango Delta, Botswana. www.globalwetlands.org

McCarthy JM, Gumbricht T, McCarthy T, Frost P, Wessels K, Seidel F (2003) Flooding Patterns of the Okavango Wetland in Botswana between 1972 and 2000 AMBIO: J Hum Environ 32:7

McDonald MG, Harbaugh AW (1988) A modular three- dimensional finite-difference ground-water flow model: U.S. Geological Survey Techniques of Water-Resources Investigations, book 6, chap. A1, 586p

Meehl GA, Stocker TF, Collins WD, Friedlingstein P, Gaye AT, et al (2007), Global Climate Projections. In: Solomon S, Qin D, Manning M, Chen Z, Marquis M, Averyt KB, Tignor M, Miller HL (eds.) Climate Change 2007: The Physical Science Basis. Contribution of Working Group I to the Fourth Assessment Report of the Intergovernmental Panel on Climate Change Cambridge University Press, Cambridge, United Kingdom and New York, NY, USA

Meijerink AMJ (1988) Data acquisition and data capture through terrain mapping units. ITC Journal 1:23-44

Meijerink AMJ, De Brouwer HAM, Mannaerts CM, Valenzuela CR (1994) Introduction to the use of Geographic Information System for Practical Hydrology, International Hydrological Programme, UNESCO and ITC. Netherlands.

Mejerink AMJ (2002) Satellite eco-hydrology-a review, Tropical Ecology 43(1):91-106

Menz G, Bethke M (2000) Regionalization of the IGBP Global Land Cover Map for Western Africa (Ghana, Togo and Benin). In: Proceedings of the 20th EARSeL-Symposium, June 2000, Dresden, 6p

Ministry Of Lands And Forestry (1999), Managing Ghana's Wetlands: A National Wetlands Conservation Strategy, Republic Of Ghana

Mitchell C (1973) Terrain Evaluation The world landscapes Terrain evaluation, Longman Group Limited, London, U.K.

Mitsch WJ, Gosselink JG (2000) Wetlands, third edn. Van Nostrand Reinhold, New York, USA

Mohanty BP, Kanwar RS, Everts CJ (1994) Comparison of Saturated Hydraulic Conductivity Measurement Methods for a Glacial-Till Soil, Soil Sci Soc Am J 58(3) May-June 672-677

Moore GK, North GW (1974) Flood inundation in the southeastern United States from aircraft and satellite imagery. Water Resour Bull 10(5):1082–1096.

Morin RH (2006) Negative correlation between porosity and hydraulic conductivity in sand-and-gravel acquifers at Cap Cod, Massachusetts, USA, J Hydrol 316:43-45

Mulligan M, Wainwright J (2004) Modelling and model building, In: Wainwright J, Mulligan M (eds) Environmetal modeling: finding simplicity in complexity. John Wiley, West Sussex, England

Nield SP, Townley LR, Barr AD (1994) A framework for quantitative analysis of Surface water–groundwater interaction: Flow geometry in a vertical section Water Resour Res, 30(8):2461–2476

Novitski RP (1979) Hydrologic characteristics of Wisconsin's wetlands and their influence on floods, stream flow, and sediment. In: Greeson PE, Clark JR and Clark JE (eds) Wetland Functions and Values: the State of our Understanding. American Water Resources Association, Minneapolis, MN, USA, pp377–388

Nyarko BK, Diekrüger B, Rodgers C (2006) Modeling floodplain extent in the White Volta Basin: an application of the lisflood FP model, poster presented at the EGU General Assembly 2006, 02-07 April 2006–Vienna, Austria

O'loughlin EM (1986) Prediction of surface Saturation zones in natural catchments by topographic analysis. Water Resour Res 22:794-804.

Ozesmi SL, Bauer ME (2002) Satellite Remote Sensing of Wetlands, Wetlands Ecology and Manage 10:381-402

Park EJ, Smucker AJM (2005) Erosive Strengths of Concentric Regions within Soil Macroaggregates, Soil Sci Soc Am J 69:1912-1921

Peixoto JP, Oort AH (1992): Physics of Climate; American Institute of Physics (AIP), New York

Philip JR (1957) The theory of Infiltration: 4. Sorptivity and Algebraic Infiltration Equations. Soil Science 84:257-264

Philip JR (1991), Horizontal Redistribution with Capillary Hysteresis. Water Resour Res 27(7):1459-1469

Philip JR (1969) A Linearization Technique for the Study of Infiltration. In: Water in the Unsaturated Zone, IASH/AIHS - Unesco.

Poage MA, Chamberlain CP (2001) empirical relationship between elevation and the stable isotope composition of precipitation and surface waters: consideration for studies of Paleoelevation change. Am J Sci 301:1-15.

Poaini KA, Johnson WC (1993) Potential effect of climatic change on semi-permanent Priare wetland. Climate Change, 24(3):213-232

Poiani KA, Carter J, Swanson W, Winter TCGA. (1996.) Climate Change and Northern Prairie Wetlands: Simulations of Long-Term Dynamics Limnology and Oceanography, Freshwater Ecosystems and Climate Change in North America, 41(5):871-881

Pope K, Rejmankova E, Paris J, Woodruff R (1997). Detecting seasonal flooding cycles in marshes of the Yucatan Peninsula with SIR-C polarimetric radar imagery. Remote Sensing of the Environment, 59: 157-166

Pope K, Rey-Benayas J, Paris J (1994). Radar remote sensing of forest and wetland ecosystems in the Central American tropics. Rem Sens Environ 48(2):205-219

Prudic DE (1989), Documentation of a computer program to simulate stream-aquifer relations using a modular, finite-difference, ground-water flow model: U.S. Geological Survey Open-File Report 88-729,113

Radcliffe ED, Rasmussen TC (2002). Soil water Movement, In Warrick, AW (edt) Soil Physics Companion. CRC Press, USA, pp85-126

Rao BRM, Dwivedi RS, Kushwaha SPS, Bhattacharya SN, Anand JB, Dasgupta S (1999). Monitoring the spatial extent of coastal wetlands using ERS-1 SAR data. Int J Rem Sens, 20(13):2509-2517

Ravi V, Williams JR, Burden DS (1998) Estimation of Infiltration Rate in the Vadose Zone: Compilation of Simple Mathematical Models Volume I, U.S. ENVIRONMENTAL PROTECTION AGENCY EPA/600/R-97/128a

Restrepo JI, Montoya AM, Obeysekera J (1998) A wetland simulation module for the MODFLOW ground water model, Ground Water 36(5):764-770

Reid MA, Quinn GP (2004) Hydrologic regime and microphyte assemblages in temporary floodplain wetlands; implications for detecting responses to environmental water allocations. Wetlands 24:586-599

Riekerk H, Korhnak LV (2000) The Hydrology of Cypress Wetlands in Florida Pine Flatwoods. Wetlands 20(3):448-460

Ross PJ (1990) Efficient Numerical Methods for Infiltration Using Richards' Equation Water Resour Res 26(2):279-290

Sanford W (2002) Recharge and groundwater models: an overview. Hydrogeological Journal 10:110-120

Scanlon BR, Goldsmith RS (1997) Field study of spatial variability in unsaturated flow beneath and adjacent to playas Water Resour Res. 33(10):2239–2252

Schultz GA (2000) Potential of Modern Data Types for Future Water Resources Management, Water Int 25(1):96-109

Shaw G, Wheeler D (1985) Statistical Techniques in Geographical Analysis John Wiley, New York.

Smith L (1997). Satellite remote sensing of river inundation area, stage, and discharge: a review. Hydro Process 11:1427-1439.

Sokol J, Pultz TJ, Bulzgis V (no date) Monitoring Wetland Hydrology In Atlantic Canada Using Multi-Temporal And Multi-Beam RADARSAT Data

Souch C, Grimmond CSB, Wolfe CP (1998) Evapotranspiration rates from wetlands with different disturbance histories: Indiana Dunes National Lakeshore. Wetlands Vol. 18, No. 2 - June 1998

South Africa National Water Act 36 of 1998

Steele NM, Winne JC, Redmond R (1998) Estimation and Mapping of Misclassification Probabilities for Thematic Land Cover Maps. Rem Sens Environ 66:192-202

Stephens DB (1996) Vadose Zone Hydrology. CRC Press, Inc. Boca Raton, FL.

Storm B, Jogensen GH, Styczen M (1987) Simulation of Water flow and soil erosion processes with distributed physically-based modeling system. In: Forest Hydrology and Watershed Management. Proc. Vancouver Symp, August 1987. Int'l Assoc of Hydrol Sci Publ 167:595-608

Sun GH, Riekerk H, Commerford NB (1998a) Modeling the fores hydrology of wetland-upland ecosystems in Florida. J.Am. Water Res. Assoc 34: 827-841

Swartzendruber D (1997) Exact Mathematical Derivation Of A Two-Term Infiltration Equation Water Resour Res. 33(3):491–496

Thompson JR, Polet G (2000). Hydrology and Land use in a Sahelian Floodplain Wetland. Wetlands 20(4):639-659

Tiner RW (2003) Geographically Isolated Wetlands Of The United States. Wetlands 23:494–516

Tobias CR, Harvey JW, Anderson IC (2001) Quantifying Groundwater Discharge through Fringing Wetlands to Estuaries: Seasonal Variability, Methods Comparison, and Implications for Wetland-Estuary Exchange, Limnology and Oceanography 46(3):604-615

Töyra J, Pietroniro A, Martz LW, Prowse TD (2002) A Multi-Sensor Approach To Wetland Flood Monitoring. Hydrol Process 16:1569–1581

Trepel M, Kluge W (2004) WETTRANS: a flow-path-oriented decision-support system for the assessment of water and nitrogen exchange in riparian peat lands, Hydrol Process 18:357–371

UNESCO (1971) Flood Studies: An international guide for collection and processing of data, UNESCO, France

U.S. EPA. (1998) National Water Quality Inventory 1998 Report to Congress. Office of Water, Washington, DC. EPA 841-S-00-001

Van de Giesen N (2001): Characterization of West African shallow flood plains with L- and C-Band radar. IAHS Publication 267: Remote Sensing and Hydrology 2000: 365-367 IAHS Press

Vepraska MJ (2001) Morphological features of seasonally reduced soils, In Richardson JL, Vepraskas MJ (eds) Wetland Soils: Genesis, Hydrology, Landscape and Classification, Lewis publishers, New York

Vizy EK, Cook KH (2002) Development and application of a mesoscale climate model for the tropics: Influence of sea surface temperature anomalies on theWest African monsoon; J Geophysical Res- Atmosph 107: ACL – 2 1–21.

Von der Heyden CJ, New MG (2003) The role of a dambo in the hydrology of a catchment and river network downstream. Hydro Earth Sys Sci 7(3):339-357

Wang XF, Yakir D (2000) Using stable isotopes of water in evapotranspiration studies Hydrol Process 14:1407-1421

Wegner T, Boyle DP, Lees MJ, Wheater HS, Gupta HV, Sorooshian, (2001) A framework for development and application of Hydrological Models. Hydro Earth Sys Sci 5(1):13-26

Wesley PJ, Warinner J, Reedy M (1992) Application of the Green-Ampt Infiltration Equation to Watershed Modeling, Water Resour Bull 28(3-2):623-635

Wildenschild D, Hopmans JW, Simunek J (2001) Flow rate dependence of soil hydraulic characteristics. Soils Sci Soc Am J 65:35-48

Wood J (1996) The Geomorphological Characterization of Digital Elevation Models, Ph.D. Dissertation, Department of Geography, University of Leicester, Leicester, UK

Wroblicky GJ, Campana ME,Valett HM, Dahm CN (1998) Seasonal variation in surface-subsurface water exchange and lateral hyporheic area of two stream-aquifer systems. Water Resour Res 34(3):317–328

Wu W, Rodi W, Wenka T (2000) 3D numerical modelling of flow and sediment transport in open channels. J Hydrau Eng, 126(1):4-15

Young PC (2001) Database mechanistic modeling and validation of rainfall-flow processes. In: Anderson MG, Bates PD (eds) Model validation perspectives in hydrological sciences. John Wiley, Chichester.

Zzaslavsky D, Sinai G (1981) Surface hydrology; I Explanation of phenomena, II. Distribution of raindrops, III Causes of lateral flow, IV. Flow in slope layered soil V. In-surface transient flow. Proc Am Soc Civil Engrs J Hydraulics Div. HY1: 1-93

11 APPENDICES

Appendix A

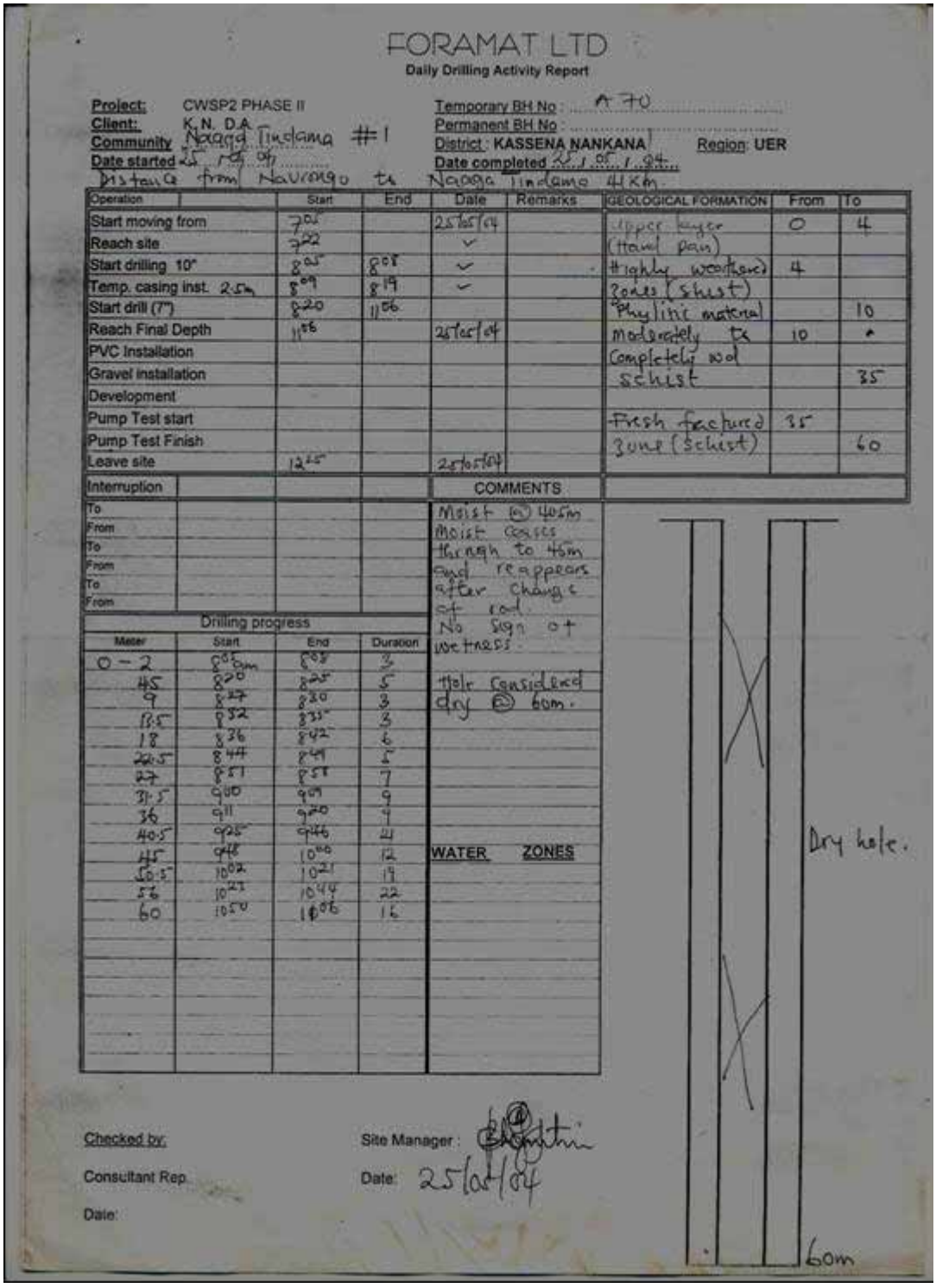

FORAMAT LTD

Daily Drilling Activity Report

Project: CWSP2 PHASE II
Client: K.N. D.A.
Community: Naaga Tindamo #1
Date started: 25/05/04
Distance from Nauroago to Naaga Tindamo 41Km

Temporary BH No: A70
Permanent BH No:
District: KASSENA NANKANA Region: UER
Date completed: 25/05/04

Operation	Start	End	Date	Remarks
Start moving from	7[0]2		25/05/04	
Reach site	7[2]2		✓	
Start drilling 10"	8[0]5	8[0]8	✓	
Temp. casing inst. 2.5m	8[0]9	8[1]9	✓	
Start drill (7")	8[2]0	11[0]6		
Reach Final Depth	11[5]6		25/05/04	
PVC Installation				
Gravel installation				
Development				
Pump Test start				
Pump Test Finish				
Leave site	12[2]5		25/05/04	

GEOLOGICAL FORMATION	From	To
Upper layer (Hard pan)	0	4
Highly weathered zones (schist)	4	
Phyllitic material		10
Moderately to Completely wd schist	10	35
Fresh fractured zone (schist)	35	60

Interruption			
To			
From			
To			
From			
To			
From			

COMMENTS

Moist @ 40Sm
Moist ceases through to 45m and reappears after change of rod.
No sign of wetness.
Hole considered dry @ 60m.

Drilling progress

Meter	Start	End	Duration
0 - 2	8[0]5am	8[0]8	3
4[5]	8[2]0	8[2]5	5
9	8[2]7	8[3]0	3
13[.]5	8[3]2	8[3]5	3
18	8[3]6	8[4]2	6
20[.]5	8[4]4	8[4]9	5
27	8[5]1	8[5]8	7
31[.]5	9[0]0	9[0]9	9
36	9[1]1	9[2]0	9
40[.]5	9[2]5	9[3]6	11
45	9[4]8	10[0]0	12
50[.]5	10[0]2	10[2]1	19
56	10[2]2	10[4]4	22
60	10[5]0	11[0]6	16

WATER ZONES

Dry hole.

60m

Checked by:
Consultant Rep
Date:

Site Manager:
Date: 25/05/04

Appendix A continued

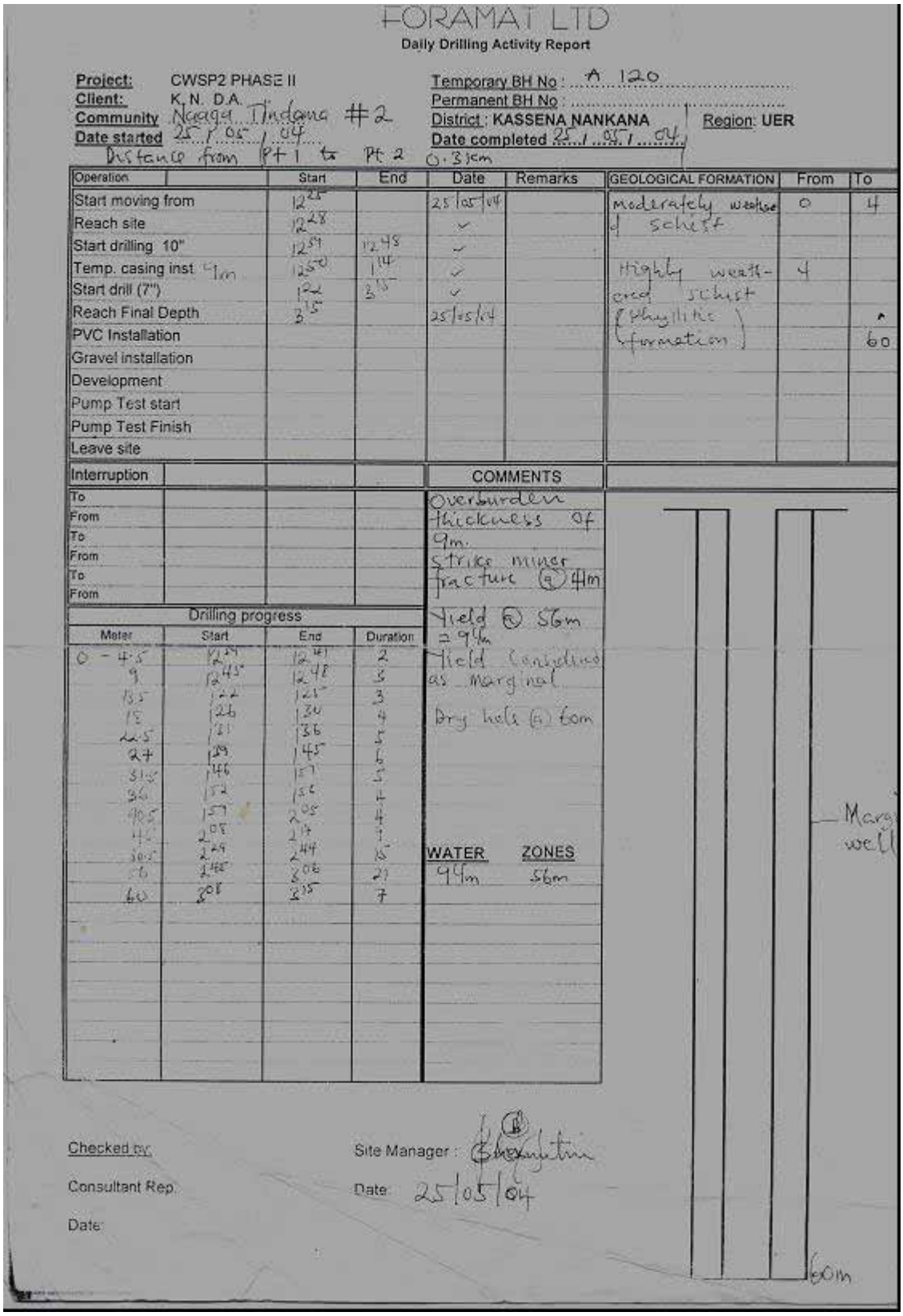

FORAMAT LTD

Daily Drilling Activity Report

Project: CWSP2 PHASE II
Client: K. N. D.A.
Community Ngaga Tindana #2
Date started 25/05/04
Distance from Pt 1 to Pt 2 0.31cm

Temporary BH No: A 120
Permanent BH No:
District: KASSENA NANKANA
Date completed 25/05/04
Region: UER

Operation	Start	End	Date	Remarks
Start moving from	12[25]		25/05/04	
Reach site	12[28]		✓	
Start drilling 10"	12[59]	12[48]	✓	
Temp. casing inst 4.1m	12[50]	1[14]	✓	
Start drill (7")	1[22]	3[15]	✓	
Reach Final Depth	3[35]		25/05/04	
PVC Installation				
Gravel installation				
Development				
Pump Test start				
Pump Test Finish				
Leave site				

GEOLOGICAL FORMATION	From	To
Moderately weathered schist	0	4
Highly weathered schist (phyllitic formation)	4	60

Interruption			
To			
From			
To			
From			
To			
From			

COMMENTS

Overburden thickness of 9m.
Strike minor fracture @ 4m
Yield @ 56m = 9½m
Yield considered as marginal
Dry hole @ 6om

Drilling progress

Meter	Start	End	Duration
0 - 4.5	12[29]	12[41]	2
9	12[45]	12[48]	3
13.5	1[22]	1[25]	3
18	1[26]	1[30]	4
22.5	1[31]	1[36]	5
27	1[39]	1[45]	6
31.5	1[46]	1[51]	5
36	1[52]	1[56]	4
40.5	1[57]	2[02]	5
45	2[08]	2[17]	9
49.5	2[29]	2[44]	15
54	2[45]	3[06]	21
60	3[08]	3[15]	7

WATER ZONES
9½m 56m

Marg well

60m

Checked by:
Consultant Rep.
Date:

Site Manager: [signature]
Date 25/05/04

Appendix B

Correlation Matrix of soil Parameters in Pwalugu wetland sites												
	% Org M.	% C.E.C	Ks cm/day	B. Den g/cm3	Moist. Cont	Total Porosity	Effective Porosity	Sand	Clay	Wilt Pt. 1500KPa	Field Cap 33KPa	Sat. Cond. cm/day
% Org M.	1.000											
%C.E.C	0.683	1.000										
Ks cm/day	0.110	-0.160	1.000									
B. Den g/cm3	-0.474	-0.246	-0.209	1.000								
Moist. Cont	0.009	-0.263	0.216	-0.353	1.000							
Total Porosity	0.438	0.189	0.221	-0.998	0.390	1.000						
Effective Porosity	0.304	0.407	-0.065	-0.349	-0.753	0.312	1.000					
Sand	-0.532	-0.631	0.034	0.350	-0.180	-0.322	-0.044	1.000				
Clay	0.605	0.677	0.029	-0.320	0.150	0.291	0.053	-0.661	1.000			
Wilt Pt. 1500KPa	0.622	0.678	0.034	-0.336	0.162	0.306	0.052	-0.676	0.999	1.000		
Field Cap 33KPa	0.628	0.681	0.010	-0.389	0.228	0.360	0.021	-0.888	0.916	0.928	1.000	
Sat. Cond. cm/day	-0.254	-0.353	0.162	0.235	-0.287	-0.221	0.138	0.706	-0.672	-0.689	-0.802	1.000

Appendix B continued

Correlation Matrix of soil Parameters in Tindama wetland sites												
	% Org M.	%C.E.C	Ks (cm/day)	B. Den g/cm3	Moist. Cont	Total Porosity	Effective Porosity	Sand %	Clay %	1500 kPa Wilt Pt.	33 kPa Field Cap	Sat. Cond. (cm/day)
OrgM	1.000											
%C.E.C	0.259	1.000										
Ks(cm/day)	-0.366	0.337	1.000									
B. Den g/cm3	-0.015	-0.292	-0.789	1.000								
Moist.Cont	-0.073	0.164	0.614	-0.922	1.000							
Total Porosity	0.015	0.292	0.789	-1.000	0.922	1.000						
Effective Porosity	0.159	0.400	0.787	-0.755	0.443	0.755	1.000					
Sand %	-0.385	-0.226	-0.104	0.431	-0.447	-0.431	-0.242	1.000				
Clay %	0.115	0.201	0.241	-0.353	0.369	0.353	0.192	-0.672	1.000			
1500 kPa Wilt Pt.	0.126	0.205	0.241	-0.355	0.369	0.355	0.196	-0.672	-	1.000		
33 kPa Field Cap	0.214	0.229	0.235	-0.411	0.422	0.411	0.238	-0.815	0.960	0.964	1.000	
Sat. Cond. (cm/day)	-0.030	-0.155	-0.190	0.232	-0.286	-0.232	-0.052	0.552	- 0.811	-0.824	-0.865	1.000

ACKNOWLEDGEMENTS

I wish to express my heartfelt thanks to my parents, brother, sister, uncles, aunties and other relatives for assisting me to pursue this course, and fulfilling their Godly duties towards me.

In the very first place, I would like to thank Prof. Dr. Nick Van de Giessen for heeding to my cry and giving me the opportunity and the support to join PhD programme here in ZEF. My heartfelt gratitude goes to Professor B. Diekkrüger (Geography Institute, University of Bonn) and Prof. Dr. Barbara Reichert (Geology Institute, University of Bonn) for guiding and supervising this study. I most gratefully acknowledge the immense contribution of Dr. Charles Rodgers (ZEF) for the time and guidance he provided during the entire period of this research. Special thanks to Dr. Manske (Coordinator, PhD program), Mrs Zabel and administration of the PhD Program of the Center for Development Research (ZEF), GLOWA-VOLTA project, University of Bonn and to the sponsors of this research German Ministry of Education and Research (BMBF).

I also gratefully acknowledge the enormous support given by the Isotope Hydrology Section of, International Atomic Energy Agency (IAEA), Vienna for assisting and given me the grant to analyse my water samples. I greatly acknowledge the support of Professor P. Vlek (Director, Center for Development Research (ZEF), Bonn), and his administration staff, Volker Merx, Sabine Aengenendt-Baer, and Miryam Buttenhoff for providing the necessary resources for this research. Many thanks to Dr. Nicola Martin for her advice and support in working with Isotopes. I am also grafetful to Frau Margaret Jend for reading and correcting my drafts. Special thanks to Stephan Klose, Sabastien of the IMPETUS group, Dr Matthias Braun and the entire ZFL staff and all those who contributed in several ways to make my stay in Germany (Bonn) successful. I wish to extend my appreciation to my office mate Kirsten Kienzler for making life less boring and the encouragement she gave me during tough times. My thanks goes to the queen mothers of Sirigu (Irite Eguavoen) and Dano (Katrin Zitzmann) for the German translation of my abstract. I will also like to say thank you to my friends (Adelina, Daniela, Steffi, Jean Prerrie, Tia, Sefakor, Msaferi Markrius, Msaferi Kasina, Maruf, and the Friday Badminton group) for making me enjoy the social life in Bonn.

I would also like to express my sincere gratitude to my field workers in Pwalugu and Tindama most especially the driver of GLOWA-VOLTA project in Ghana, Eli, Kwasi, Ben, Salisu and the late Acquah. Finally I am also grateful to Dr Annabel Akosua Ankrah (Radiology Dept, Korle Teaching Hospital, Accra) for her encouragement, prayers, and support during the final stages of my thesis writing.